The effect of Type and Concentration of Surfactant on Stability and Rheological properties of Explosive Emulsions

by

NSENDA NGENDA TSHILUMBU

Dissertation submitted in fulfilment of the requirements for the degree
MASTER OF TECHNOLOGY
Chemical Engineering

in the Faculty of Engineering
at the Cape Peninsula University of Technology

Cape Peninsula
University of Technology

THE EFFECT OF TYPE AND CONCENTRATION OF SURFACTANT ON STABILITY AND RHEOLOGICAL PROPERTIES OF EXPLOSIVE EMULSIONS

by

NSENDA NGENDA TSHILUMBU
B Sc (Metallurgical Engineering)

Dissertation submitted in fulfilment of the requirements for the degree

Master of Technology: Chemical Engineering

in the Faculty of Engineering

at the Cape Peninsula University of Technology

Supervisor: Prof. I. Masalova

Cape Town
Date submitted May 2009

DECLARATION

I, NSENDA NGENDA TSHILUMBU, declare that the contents of this dissertation represent my own unaided work, and that the dissertation has not previously been submitted for academic examination towards any qualification. Furthermore, it represents my own opinions and not necessarily those of the Cape Peninsula University of Technology.

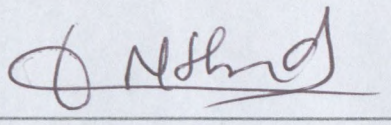

Signed

25/05/2009

Date

ABSTRACT

This study investigated water-in-oil (W/O) super-concentrated emulsions used as pumpable explosives. The aqueous phase of the emulsions is a supersaturated nitrate salt solution (at room temperature), with a volume fraction usually greater than 0.8. Aqueous phase droplets are deformed by packing and contact with neighbouring droplets. Compounds of this kind are thermodynamically unstable and their instability is related to the coarsening of emulsions (droplet coalescence) and phase transition (crystallisation) in the dispersed phase. However, it was demonstrated that the dominating mechanism is slow crystallisation inside the super-cooled droplets. The main goal of this thesis therefore concerned a phenomenological study of the dependence of type and concentration of surfactant, as well as the ageing processes, on the rheological properties of these emulsions.

The bulk rheological measurements were carried out using a rotational dynamic rheometer MCR 300 (Paar Physica). Samples of different types of surfactant (*Pibsa-MEA*, *Pibsa-UREA*, *Pibsa-IMIDE, SMO* and *SMO/Pibsa-MEA*) and different concentrations of surfactants were studied. The results of the measurements include the flow and viscoelastic properties of the materials. The rheological parameters have been correlated with the kinetics of structural changes during ageing as a function of emulsion formulation content.

The emulsions under study were non-Newtonian liquids. It was demonstrated that different surfactant types yield different interfacial properties. In fact, both the interfacial tension and the interfacial elastic modulus were found to decrease according to the sequence MEA-UREA-MEA/SMO-IMIDE-SMO. It was established that the surfactant type and surfactant concentration affected the bulk rheological properties of explosive emulsions. Indeed, both the elastic modulus and the yield stress as function of surfactant type decreased in the following order: MEA-IMIDE-UREA-MEA/SMO, whereas they also decreased as the surfactant concentration increased. However the sensitivity of the rheological parameters to the type or concentration of surfactant was found to decrease as the droplet size increased. Moreover, the changes in rheological parameters were more strongly expressed than any changes in interfacial tension. This last finding is considered as rather important. It seems reasonable to assume that it provides proof of an active role of a surfactant not only as a compound responsible for the interfacial tension, but also creating additional sources of elasticity.

The research indicated that, in the linear regime, the dimensionless elastic moduli do not collapse on a single master curve. Indeed, other factors such as electrolyte concentration, phase ratio, surfactant concentration and the nature of the external phase being kept constant, IMIDE-based emulsions, for example, showed very high dimensionless elastic moduli compared to other Pibsa-based emulsions. This serves to confirm that the physical interaction between interface layers of different droplets and a droplet surface layer with the matter of a droplet does play a key role in generating additional sources of elasticity in the system. Moreover, the increase in surfactant concentration does not affect the intrinsic elasticity of the droplet (the capillary pressure); it decreases only the magnitude of the additional elasticity.

The rheological parameters of emulsion explosives are sensitive to the ageing process. It was shown by different methods that ageing leads to emulsion-to-suspension transition. This affected the rheological properties in such a way that solid-like behaviour became increasingly evident. Both the storage modulus and the yield stress measured in the downward-sweeping shear rate mode increased with time. The dependencies of all the characteristic rheological parameters on ageing were investigated. Qualitative (optical microscope) and quantitative (X-ray diffraction analysis) investigations of the crystallisation process showed that ageing leads to slow crystallisation within the super-cooled aqueous droplets. In this sense, the observed emulsion-to-suspension transition was a direct consequence of the phase transition. The kinetics of this transition are described by the Johnson-Mehl-Avrami-Kolomogorov (JMAK) equation and correlated with the evolution of the rheological properties of the dispersion. A general correlation between the kinetics of crystallisation and the evolution of the rheological properties of these emulsions has been identified and evaluated for the whole family of Pibsa-based surfactants used in this study.

ACKNOWLEDGEMENTS

I wish to thank:

- African Explosives Limited (AEL) for the financial support towards this research and for permission to publish the results of the study for my dissertation. Opinions expressed in the thesis and the conclusions arrived at are those of the author, and are not necessarily to be attributed to the African Explosives Limited (AEL),

- Lake International for providing samples of surfactants and oils,

- The Cape Peninsula University of Technology, as well as the Institute of Material Science and Technology at the Cape Peninsula University of Technology, for the utilisation of their Laboratories,

- Dr Ernest Ferg for the realisation of the X-ray diffraction experiments.

- Prof. Rainer Haldenwang for useful remarks and comments.

- My sincere thanks are due to my supervisor, Prof. I. Masalova, who guided my first steps into the field of rheology and enabled me to develop my skills in research.

Nsenda Ngenda Tshilumbu

DEDICATION

This work is dedicated to

- The Lord Jesus Christ, the cornerstone of any major construction and source of all grace

- My wife, Yvette Tshilumbu, for her spiritual and moral support, especially during difficult times

- My children, Benedict Ntumba, Ans Tshilumbu, Deborah Odia, Henoc Kalonji and Stars Mubeneshay

- My deceased parents

- My brother and sisters

TABLE OF CONTENTS

LIST OF FIGURES

LIST OF TABLES

GLOSSARY

This part of the Dissertation provides definitions of terms and expressions relating to the measurement of rheological properties in liquid based systems (emulsion, suspension, etc.) published by National Institute of Standards and Technology in "Guide to Rheological Nomenclature" by V.A. Hackey and C.F. Ferraris, 2001, Special Publication 949. Definitions are generally consistent with nomenclature published by the American Concrete Institute (AIC), the British Standard Institute (BSI), the International Union of Pure and Applied Chemistry (IUPAC) and the Society of Rheology (Hackley & Ferraris, 2001).

Terms	Definition
Coalescence	Spontaneous joining of smaller droplets in an emulsion system to form larger ones.
Crystallinity	The ratio between the mass of the crystalline region and the total mass of the solid.
Elastic	A conservative property in which part of the mechanical energy used to produce deformation is stored in the material and recovered on release of stress.
Elastic modulus	A modulus of a body that obeys Hook's law.
Emulsion	Two immiscible liquids (usually oil and water), with one of the liquids dispersed as small spherical droplets in the other.
Flow	Continuous increasing deformation of a material body under the action of finite forces. When the forces are removed, the strain does not eventually return to zero, then flow has occurred.
Flow curve	A graphical representation of the behaviour of flowing materials in which shear stress is related to shear rate.

Modulus	The quotient of stress and strain where the type of stress and strain is defined by the type of deformation employed.
Rheology	The science of deformation and flow of matter.
Shear	The relative movement of parallel adjacent layers
Shear modulus	The ratio of shear stress to its corresponding shear strain.
Shear rate	The rate of change of shear strain with time. For liquids, the shear rate, rather than strain, is generally used in describing flow.
Shear strain	The relative in-plane displacement of two parallel layers.
Shear strain	The relative in-plane displacement of two parallel layers in a material body divided by their separation distance.
Shear stress	The component of stress that causes successive parallel layers of a material body to move in their own planes (i.e. the plane of shear), relative to each other.
Shear-thinning	A decrease in viscosity with increasing shear rate during steady shear flow.
Steady shear flow	Condition under which a fluid is sheared continuously in one direction during the duration of a rheometric experiment.
Storage modulus	The quotient of the part of the stress in phase with the strain divided by the strain under sinusoidal conditions.

Surfactant	An amphiphilic (amphipathic) molecule that has a hydrophilic head group (polar region), which has a high affinity for water, and a lipophilic tail group (non-polar Region), which has a high affinity for oil
Viscoelastic	A time-dependent property in which a material under stress produces both a viscous and an elastic response.
Yield stress	A critical shear stress value below which an ideal plastic or viscoplastic material behaves like a solid (i.e. will not flow). Once the yield stress is exceeded, a plastic material yields (deforms plastically) while a viscoplastic material flows like liquid.

NOMENCLATURE

Symbol	Description	Unit
A	interfacial area	m^2
a_c	area occupied by the surfactant headgroup	
C	solute concentration	g/l
C_{el}	electrolyte concentration	g/l
CMC	critical micelle concentration	%
C_S	solubility	g/l
D or d	diameter of droplet (particle)	m
dA	increase in contact area	J/m^2
dG	increase in free energy of the system	J/m^2
d_S	diameter of solid particles	m
E^s	total surface energy	J/m^2
F	free energy	J
f_a^*	adhesion force between droplets	N
G'	storage modulus	Pa
G"	loss modulus	Pa
G^s	surface free enthalpy	J/m^2
h	film thickness	nm
HLB	hydrophile-lipophile balance	-
H^s	surface enthalpy	J/m^2
I	scattered intensity.	-
I_{am}	diffraction intensity of the most nearly amorphous sample	-
I_{cry}	diffraction intensity of the most crystalline sample	-
I_{ii}	diffraction intensity with an unknown crystallinity	-
K	equilibrium constant	-
lc	the chain length of the tail	Á
M	total mass	kg
M	mass	kg
M_{am}	mass of the amorphous region	kg
Mcr	mass of the crystalline region	kg
n	Avrami exponent	-
n_i	excess surfactant concentration at the surface	-

P	pressure	Pa
Pc	critical packing parameter of the surfactant	-
R_{32}	surface-volume mean drop radius	m
S(8)	solubility of the solute in the continuous phase for a droplet with infinite curvature (a planar interface)	g/l
S(r)	solubility of the solute when contained in spherical droplet of radius r	
S^s	surface entropy	J/m^2
T	absolute temperature	K
t	time	s
t_{inh}	time scale of inherent processes in material	s
T_{obs}	characteristic time of observation	s
T_c	Congelation point	K.
T_c	congelation temperature	K
T_d	crystallisation temperature of dispersed phase	K.
T_d	crystallisation temperature of the dispersed phase: fudge point	K
T_{hn}	homogeneous nucleation temperature	K
V_D	volume of emulsion droplets	m^3
V_E	total volume of the emulsion	m^3
V_m	molar volume of the solute	m^3/mol
Xcr	relative crystallinity	-
$\Delta_{ad} F$	free adhesion energy	J
Δp	drop in pressure	Pa
Γ	surface excess concentration	$mole/m^2$
Γ_8	surface excess concentration when the surface is completely saturated with solute	$mole/m^2$
ε	elasticity of the interface	N/m
ϕ	dispersed phase volume fraction	%
ϕ^*	volume fraction that corresponds to the hexagonal close packing of undistorted spheres	%
ϕ_c	volume fraction at which the modulus G' collapses to zero	%
ϕ_{eff}	effective volume fraction	%
ϕ_m	dispersed mass fraction	%
ϕ_S	volume fraction of solids in suspo-emulsion	%
γ	shear strain	%
ν	volume of the hydrophobic tail	$Å^3$

π	surface pressure	N/m^2
θ	characteristic time	week
ρ_c	density of the continuous phase	Kg/m^3
ρ_{Dph}	density of the dispersed phase	Kg/m^3
σ	interfacial tension	N/m
τ	shear stress	Pa
τ_y	yield stress	Pa
ω	angular frequency	Hz

Subscripts

Abbreviations	Explanation
am	amorphous
AN	ammonium nitrate
c	continuous phase
Cr	crystalline
Dph or d	dispersed phase
Oph	oil phase

CHAPTER 1
INTRODUCTION

The subject of this study is highly concentrated (super-concentrated) water-in-oil (W/O) emulsions used as pumpable explosives. Such emulsions comprise a rather special class of colloids. In contrast to standard emulsions and suspensions, the concentration of the dispersed phase in highly concentrated explosive emulsions exceeds the limit of the closest packing of regular spheres (app. 74 %) that is possible due to the "compressed" state of droplets which have a polyhedron shape. The aqueous phase is an oversaturated (overcooled) nitrate salt solution at room temperature, comprising less than 20 % water by mass. Compounds of this kind are thermodynamically unstable and their instability is related to the coarsening of emulsions (droplet coalescence) and phase transition (crystallisation) in the dispersed phase.

Currently, there is considerable interest in highly concentrated emulsions (HCE) due to both their practical applications (as pharmaceuticals, food products, crude oil recovery, mining, polymer blends, biological liquids, explosives and so on) and the variety of rheological effects that are observed in flow and deformations of emulsions (Barnes, 1994; Malkin, Masalova, Slatter & Wilson, 2004a).

Bulk emulsion explosives are progressively penetrating the underground mining market and are replacing packaged explosives for reasons of improved safety, more efficient logistics, high rates of detonation and reduced overall blasting costs (Bampfield & Cooper, 1988). However, these emulsions are subject to transport-induced structural decomposition caused by high speed pumping as well as by ageing. Uncontrolled crystallisation can lead to emulsion breakdown and/or reduction in flow ability and detonation sensitivity (Thomas & Halou, 2003). Considerable effort has been devoted to the improvement of the emulsion stability by explosives manufacturers, but most of the data are proprietary. For the most part the discussions describe only a few of the improvements claimed, in particular those where a chemical effect is assigned to the stabilising system (Becher, 1988). The flow characteristics (rheology) are of considerable importance from both the fundamental and the applied point of view:

- The main shortcoming in the field of the present-day state of knowledge of rheological properties of highly concentrated water-in-oil emulsions is the absence of systematic

experimental data, especially concerning the correlation of the evolution of rheological characteristics with the kinetics of structural changes.

- At the present, there is no quick method to relate the formulation of an explosive emulsion to three areas, namely pumpability, stability and detonation sensitivity of the emulsion.

The majority of publications, both theoretical and experimental, are devoted to emulsions with the concentration of the dispersed phase less than approximately 74 % by volume, which corresponds to the limit of close packing of homogeneous spherical droplets. Models predicting rheological properties of such emulsions were proposed by Princen (1983; 1985), Princen and Kiss (1986a; 1986b), Palierne (1990), Madiedo and Gallegos (1997) and Pal (1996b; 2001). Model predictions that allow one to correlate rheological (viscoelastic) properties with the structure of emulsions (primarily polymer blends) were proposed by Bousmina (1999); Yu, Bousmina, Grmela, Palierne and Zhow (2002a). The theoretical model was also developed for the non-linear domain of viscoelastic behaviour in emulsions (Yu, Bousmina, Grmela & Zhow, 2002b).

Meanwhile, the current interest in studies of the rheological properties of emulsions has been focused on highly concentrated emulsions as well with the content of the dispersed phase exceeding close packing. Viscoelastic properties of such emulsions were measured (Pons, Solans, Stebe, Erra & Ravey, 1992a; Pons, Erra, Solans, Ravey & Stebe, 1992b; Pons, Solans & Tadros, 1995) and treated in the frames of the simplest Maxwellian relaxation mode. The model of flow of such emulsions was also proposed by Schwartz and Princen (1987). The concentration dependence of viscoelastic properties of highly concentrated emulsions was discussed on the basis of Princen's theory, by Ponton, Clement & Grossiord (2001). There was also a series of publications devoted to highly concentrated water in oil (W/O) emulsions where the continuous phase used was fluorinated oil and non-ionic fluorinated surfactant was based on diethylene glycol. It was shown that such highly concentrated (up to 94 %) emulsions behave in a solid-like manner (Langenfield, Schmitt & Stebe, 1999).

Theoretical analysis predicts the main solid-like properties of such emulsions; their elastic modulus and yield stress (Babak, Langenfeld, Fa & Stebe, 2001). Phase behaviour and structure of similar systems were studied by Rocca and Stebe (2000). One of the interesting problems discussed in many publications of this type is the role of droplet size. The principal papers devoted to modelling these systems do not distinguish between highly concentrated

emulsions and foams (Princen, 1985; Princen & Kiss 1989).The most significant result of these publications is the predication of the dependence of elastic modules, G, on the size of droplets, D, and volume fraction, ϕ. The theory states that the elastic modules, as well as the yield stress, should be proportional to the reciprocal diameter of the droplets. However, recent experimental data on highly concentrated water in oil emulsions used as pumpable explosives (dispersed aqueous droplets supersaturated in salts, water comprising less than 20 % by mass) showed serious differences from foams. The elastic modulus was found to be proportional to D^{-2} while the Newtonian viscosity was proportional to D^{-1} (Malkin *et al.*, 2004a; Masalova & Malkin, 2007a; 2007c, 2008).

Of all the experimental studies on the rheology of highly concentrated emulsion explosives reviewed, very few considered time effects and the correlation of steady-state properties of the emulsions (as measured by rotational instruments) with prediction of their stability and behaviour. Only a few studies are known and have been published concerning the correlation of direct observation of the structural process (crystallisation) during ageing of the emulsion explosives with changes of their rheological properties during storage (Kharatiyan, 2005; Masalova, Malkin, Ferg, Taylor, Kharatiyan & Haldenwang, 2006; Masalova & Malkin; 2007b). This presents a significant problem, because only an understanding of the nature of the structural process within the emulsions under investigation would enable one to track the evolution of the rheological properties, which determines their application value.

This study continues the above theme in the search for answers to the following questions:

- How does the emulsion content (type and concentration of surfactant) affect the physical structure (structure and strength of the interface, thin oil film network) and rheological properties?
- How does ageing affect the structure (shape, size of the crystals, and the degree of crystallinity) and rheological properties of highly concentrated emulsion explosives?
- How does the emulsion content (type and concentration of surfactant) affect the evolution of physical structure (kinetic of crystallisation process) and rheological properties (kinetic of changing of characteristic rheological parameters) during ageing?

The overall aim of this study was to determine how the type and concentration of surfactant affect the physical structure (thin oil film network, and the structure at the interface oil-water) of a fresh explosive emulsion and the structural stability of these

emulsions with time in the context of the evolution of rheological properties and structure during ageing.

The specific objectives were:

- To investigate the rheological bulk properties of fresh explosive emulsions as a function of type and concentration of surfactant for different droplet sizes.
- To investigate the structure (shape and size of crystals, and the degree of crystallinity) and rheological properties of highly concentrated explosive emulsions as a function of time (ageing) for different surfactant types and concentrations.
- To investigate the evolution of physical structure (kinetic of crystallisation process) and rheological properties (kinetic of changing of characteristic rheological parameters) during ageing as a function of type and concentration of surfactant, for different droplet sizes.
- To evaluate, the newly developed model, the rheology-kinetics of crystallisation.

To answer these questions, and achieve the overall aim of the study, the following methodologies were adopted:

1. Rheological investigations

The rheological experimental methods were based on measuring the rheological properties of emulsions. They were obtained by using a Rotational Rheometer MCR-300 Paar-Physica, Germany. The wide ranges of shear rates (from app. 10^{-6} to 10^{3} s^{-1}) and shear stresses available for investigation allows one to obtain characteristics of rheological properties over a very wide range. This instrument can also operate over the wide range of frequencies from 10^{-3} up to 10^{2} Hz. In this oscillating mode of deformations, the dynamic modules are measured as a function of frequency. In addition, the amplitude of deformations can vary between 0.01 % and 100 %. Instrument measurements are supported with modern software, which includes many applied programs.

Rheological investigations included:

- Flow curve and amplitude sweep of fresh explosive emulsions as functions of type and concentration of surfactant for different droplet sizes.
- Flow curve and amplitude sweep of aged explosive emulsions as functions of type and concentration of surfactant for different droplet sizes.
- Determination of the characteristic rheological parameters in order to use

them for the evaluation of a newly developed model of the structural evolution during ageing (rheology-kinetic of crystallization model).

- Correlation of the characteristic rheological parameters with emulsion formulation and ageing period.

2. Optical and spectroscopic methods included:

2.1 Optical observations:

The optical analysis was conducted to use visual observations for the analysis of structural changes of the materials at different emulsion formulation content and for the analysis of size and shape of crystals during ageing. The analysis was carried out with a Leica optical microscope equipped with a digital camera, at a magnification of 500 times.

Optical methods were also used to obtain the dispersed phase particle size distribution. This was done using the Malvern Mastersizer 2000 technique. This method is based on measuring the angle distribution of the He-Ne laser light scattered by particles.

2.2 Spectroscopic methods:

X-ray diffraction pattern analysis was performed to follow the structural changes quantitatively in terms of degree of crystallinity of emulsion with ageing. The relative crystallinity of the material was analysed on a Brucker D8 X-ray powder diffractometer with Cu-K_a radiation. The configuration of the device allows for the analysis of uneven samples in particular slurries or emulsions without causing any shifts of the respective diffracted peaks.

The following emulsion formulations were used in this study:

- 3 different droplet sizes: 10, 12, and 15μm.
- 4 types of surfactant: *Pibsa-MEA*, *Pibsa-IMIDE*, *Pibsa-UREA*, *SMO*, and one mixture *SMO/Pibsa-MEA* (1:10).
- 2 different concentrations for each surfactant 8 % and 14 % by mass in the oil phase.
- 2 different types of oil: Mosspar and Shellsol.

All the samples under investigation were tested weekly for a period of 36 weeks at 30 $°C$.

The findings of this study will benefit a wide range of industries, ranging from mining, explosives, pharmaceutical, cosmetics, food industries, etc., which use highly concentrated

emulsions, either as a mode of transportation or a process ingredient due to the need for product storage. The main thrust of this study lies with the explosives industries, where both long-term storage and pipeline pumping are economically viable options.

The experimental results obtained in the study will allow an understanding of the kinetic process taking place in the evolution of structure of multi-component systems (highly concentrated emulsions), and provides a basis for predicting pipeline transport characteristics.

The thesis is subdivided into the following chapters:

- Chapter 1 serves as an introduction to this thesis.
- Chapter 2 is a presentation of the relevant literature pertaining to the study. It covers relevant literature on theoretical rheological fundamentals of high internal phase ratio emulsions, as well as the relevant experimental work.
- Chapter 3 provides a comprehensive description of the methods of experimentation, procedures used in the analysis of the results, and the inherent discussions pertaining to the experimental findings.
- Chapter 4 presents the summary of the thesis. It offers an overview of the research thesis. Conclusions drawn from the experimental results are also presented.

CHAPTER 2
THEORY AND LITERATURE REVIEW

This chapter presents the relevant fundamental rheological theory and literature pertaining to the stability of high internal phase ratio emulsion explosives. The relevant fundamentals of emulsion stability are discussed with greater emphasis on the stability of high internal phase ratio emulsions, particularly high internal phase ratio emulsion explosives. The theory of the basic rheological properties of viscoelastic materials is also presented. This includes the applicable flow models for pseudo-plastics fluids. The dependence of surfactant type, surfactant concentration, and the effect of the ageing processes in emulsions on the rheological properties of such emulsions are also discussed in detail.

This chapter covers relevant theoretical aspects associated with the stability of emulsions and the flow of non-Newtonian fluids, and the following topics are presented:

- definition of emulsions
- general consideration of emulsion stability
- factors determining emulsion stability
- surfactant and interfacial properties
- stability of high internal phase emulsion explosives
- definition of rheology
- general classifications of flow behaviour
- general description of viscoelastic behaviour
- rheology of emulsions, with emphasis on high internal phase emulsions, particularly high-internal phase emulsion explosives
- dependence of surfactant type, surfactant concentration and ageing processes on the rheology of high internal phase emulsions, particularly high-internal phase emulsion explosives.

2.1 General definitions of emulsions

An emulsion is a mixture of two immiscible liquids, one of which is dispersed in the continuous phase of the other, typically created by rupturing droplets down to colloidal sizes through mixing. To inhibit recombination or coalescence, a surfactant which is concentrated at the interfaces must be added to create short-ranged interfacial repulsion between the droplets (Becher, 1965; Mason, Lacasse, Grest, Levine, Bibette & Weitz, 1997). For an appropriate surfactant, a quantity much less than the mass of the liquids is often sufficient to make this interfacial repulsion strong enough to render the emulsion kinetically stable against

coalescence and de-mixing. This kinetic stability differentiates emulsions from thermodynamically stable micro-emulsions which form spontaneously without mixing when the proper proportions of certain fluids and surfactants are placed in contact (Mason *et al.*, 1997).

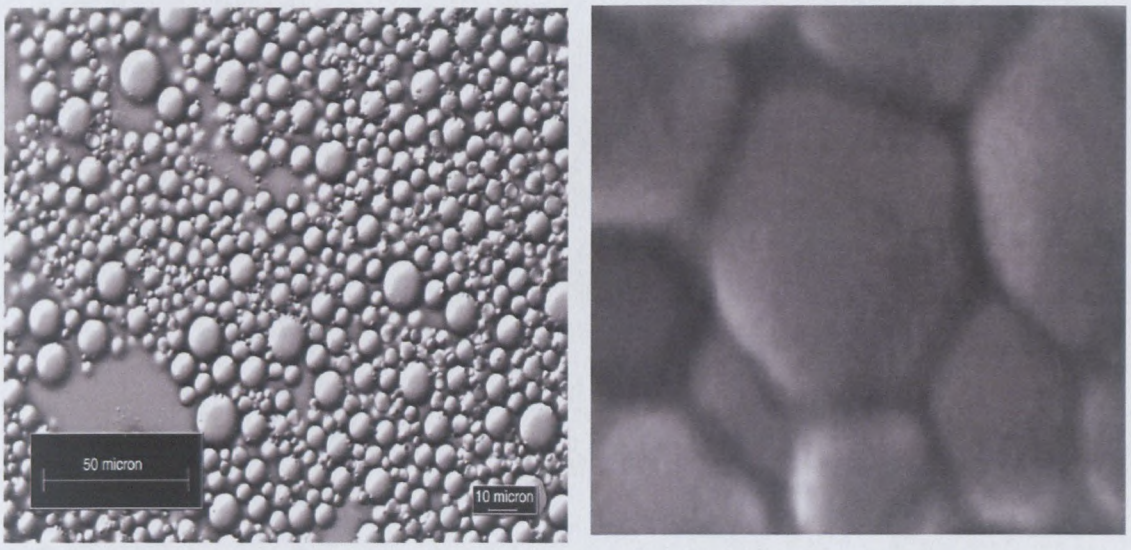

(a) (b)

Figure 2.1: Microscopic images of a dilute emulsion (a) and a highly concentrated emulsion (b).

(Adapted from: (a) McClements, 2005:3; (b) Masalova & Malkin, 2007a:3)

Emulsions can be conveniently classified according to the distribution of the oil and aqueous phases. A system consisting of oil droplets dispersed in an aqueous phase is called an oil-in-water, or O/W, or direct emulsion. A system which consists of the water droplets dispersed in an oil phase is called a water-in-oil or W/O, or inverse emulsion. The substance that makes up the droplets in an emulsion is referred to as the dispersed or internal phase, whereas the substance that makes up the surrounding liquid is called the continuous or external phase. It is also possible to prepare multiple emulsions of the oil-in-water-in-oil (O/W/O) or water-in-oil-in-water (W/O/W) type (Dickinson & McClements, 1995; McClements, 1999; 2005). For example, a W/O/W emulsion consists of water droplets dispersed within larger oil droplets, which themselves are dispersed in an aqueous continuous phase (McClements, 1999; 2005).

The process of converting two separate immiscible liquids into an emulsion, or of reducing the size of the droplets in a pre-existing emulsion, is known as homogenisation.

It is possible to form an emulsion by homogenising pure oil and pure water together, but the two phases rapidly separate into a system consisting of a layer of oil (lower density) on top of layer of water (higher density). This is because droplets tend to merge with their neighbours when they collide with them, which eventually leads to complete phase separation. The driving force for this process is the fact that contact between water and oil molecules is energetically unfavourable (Israelachvili, 1992), so that emulsions are thermodynamically unstable systems. It is possible to form emulsions that are kinetically stable (metastable) (Atkins, 1994) for a reasonable period of time (a few days, weeks, months, or years) by including substances known as emulsifiers and/or thickening agents prior to homogenisation. Emulsifiers are surface-active molecules, which adsorb to the surface of freshly formed droplets during homogenisation, forming a protective membrane, which prevents the droplets from coming together close enough to aggregate. Most emulsifiers are amphiphilic molecules. Thickening agents are ingredients that are used to increase the viscosity of the continuous phase of emulsions, and they enhance emulsion stability by retarding the movement of the droplets. A stabiliser is any ingredient that can be used to enhance the stability of an emulsion and may therefore be either an emulsifier or a thickening agent (McClements, 1999).

Most emulsions are much more complex than the simple three-component (oil, water and emulsifier) systems. The aqueous phase may contain a variety of water-soluble ingredients. The oil phase usually consists of a complex mixture of oil-soluble components. The interfacial region may contain a mixture of various surface-active components. In addition, these components may form various types of structural entities in the oil, water, or interfacial region (McClements, 1999).

Knowledge of the concentration of droplets is important because the droplet concentration influences the appearance, texture, stability and cost (in terms of concentration of the dispersed phase and, therefore, surfactant) of emulsion-based products. The concentration of droplets in an emulsion is usually described in terms of the dispersed phase volume fraction (ϕ), which is equal to the total volume of the emulsion droplets (V_{DPh}) divided by the total volume of the emulsion (V_E):

$$\phi = \frac{V_{Dph}}{V_E}$$ **Equation 2.1**

In some situations, it is more convenient to express the composition of an emulsion in terms of the dispersed phase mass fraction (C), which is related to the volume fraction by the following equation:

$$C = \frac{\phi\rho_{Dph}}{\phi\rho_{Dph} + (1-\phi)\rho_c}, \qquad \textbf{Equation 2.2}$$

where ρ_c and ρ_{DPh} are the densities of the continuous and dispersed phases, respectively. When the densities of the two phases are equal, the mass fraction is equivalent to the volume fraction. The dispersed-phase volume fraction of an emulsion is often known because the concentrations of the ingredients used to prepare it are carefully controlled (Mc Clements, 1999).

It is generally accepted that the volume fraction of the dispersed phase in a reasonably stable emulsion can be increased relatively easily up to a certain critical value, above which the emulsion tends to break or invert (Becher, 1965). In the case of an ordered, monodispersed emulsion, Ostwald's phase volume theory (Mason *et al.*, 1997) indicates that this point is reached at, or is close to ϕ^*= 0.7405, i.e., the volume fraction that corresponds to the hexagonal close packing of undistorted spheres. For randomly packed monodispersed spheres, ϕ^* = 0.64. As the dispersed phase volume fraction is increased above the critical volume fraction ϕ^*, the structure can not be described as a system of uncompressed monodispersed spheres. Polyhedral distorsion must occur (Figure 2.1).

Emulsion explosives are high-internal-phase water-in-oil emulsions of a concentrated solution of nitrate salts in water emulsified into an oil base. In general, commercial explosives consist of an intimate mixture of condensed oxidizer, almost invariably the nitrate salts of ammonia, sodium and calcium, which are mixed with a fuel and other additives. The purpose of the latter is to control the rheology and to provide the correct reactivity, physical form, and density to ensure reliable detonation. It is also the most technically sophisticated, as it must meet requirements of shelf life, resistance to handling, immunity to changes in temperature, etc. (Becher, 1988).

Emulsion explosives are also characterised by a number of unusual scientific features. Their detonation capabilities, and particularly their high velocities of detonation, depend on maintaining a very intimately mixed, all-liquid system. In practice, this requires droplet sizes of the order of 1μm. Since water is an effective detonation inhibitor, the desired sensitivities

are achieved by controlling water levels in the formulation. Finally, the requirements of redox stoechiometry create a situation that can be resolved only by the use of a large volume of supersaturated (and therefore metastable) salt solution, dispersed in a small volume of hydrocarbon oil. As in most other industrial explosives, ammonium nitrate is the major ingredient: about 70 % by mass of the overall composition. The dispersed aqueous phase, which constitutes over 90 % by weight of the liquid fraction and generally contains other salts, such as sodium and calcium nitrates, is emulsified into 7 to 10 % of an oil or oil/wax phase. Additional solid ingredients (generally less than 15 % by mass) include glass or plastic micro bubbles, aluminium powder as an energetic fuel, and some quantities of particulate salts. A variety of other ingredients, e.g., sensitiser, may be added to perform specific functions (Becher, 1988).

The structure of an emulsion explosive is directly relevant to its rheology, stability and detonation properties. As the dispersed phase volume fraction is typically 88 to 94 % by mass, the structure cannot be described as a system of uncompressed monodispersed spheres. The polyhedral distortion must occur. Tetrakaidecahedron packing (8 contact points at lower dispersed-phase volumes, 14 at high dispersed-phase volumes) was shown to be more efficient for high dispersed-phase volumes (Lissant *et al.,* 1974). Lissant, Peace, Wu and Maykhan (1974) proposed that the free drop interface contacts the film, separating the droplets at a finite angle, which is a function of the dispersed phase volume. This contact angle may approach zero for thick films, or have a finite value, which may be quite large, for thin films. This angle, however, is fixed by molecular forces across the film. This forces the droplet into complex non-spherical shape. Kirby (1983) has developed a semi-empirical theory of the geometry of emulsion explosives which describes this in terms of the radius of curvature of the pockets of the oil phase at the corners between droplets, the thickness of the film separating droplets, and the plateau angle. The latter was assumed to vary as the inverse third power of the film thickness, this being obtained by considering the van der Waals forces in the bilayer. The film separating the droplets may be extremely thin – down to the thickness of two back-to-back interlocking C_{16} monounsaturated chains, depending on the oil used to form the emulsion (Becher, 1988).

To serve as a complete description of emulsions, a theory must be able to explain and predict all aspects of emulsion formation, stability, and type; the influence of environmental factors such as temperature and pressure; the role of emulsifiers and stabilisers and their chemical structures; the role of the chemical structures of the immiscible phases; and the

effects of additives in each phase. This is a highly complex problem, as illustrated by the fact that, even though a vast amount of experimental data relating to each of these questions is available, no generally applicable theory has yet been developed.

2.2 General consideration of emulsion stability

An emulsion (metastable system) tends to revert back to the thermodynamically most stable state of the system, which consist of a layer of oil on top of a layer of water.

2.2.1 Different mechanisms of instability

According to Myers (1992), four terms commonly encountered in emulsion science and technologies, relating to stability, are breaking, coalescence, creaming/sedimentation, and flocculation. Although they are sometimes used almost interchangeably, these terms, in fact, are quite distinct in meaning as far as the condition of an emulsion is concerned. Coalescence, for example, refers to the joining of two (or more) drops to form a single drop of greater volume, but a smaller interfacial area (Figure 2.2a). Such a process is obviously energetically favourable in almost all cases. Although coalescence will result in significant microscopic changes in the condition of the dispersed phase (e.g., changes in average particle size and distribution), it may not immediately result in a macroscopically apparent alteration of the system. The breaking of an emulsion (Figure 2.2b) refers to a process in which a gross separation of the two phases occurs. The process is a macroscopically apparent consequence of the microscopic process of drop coalescence. In such an event, the identity of individual drops is lost, along with the physical and chemical properties of the emulsion. Such a process obviously represents a true loss in the stability of the emulsion. (Myers, 1992).

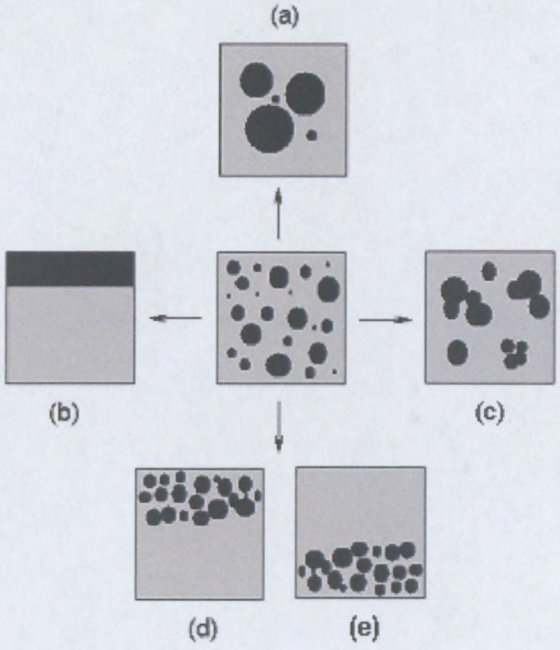

Figure 2.2: The ultimate fates of emulsions related to colloidal stability: (a) coalescence; (b) breaking; (c) flocculation; (d) creaming; (e) sedimentation

(Adapted from Myers, 1992: 213)

Flocculation refers to the mutual attachment of individual emulsion drops to form flocs or loose assemblies of particles in which the identity of each is maintained (Figure 2.2c), a condition that clearly differentiates it from the action of coalescence. Flocculation can be, in many cases, a reversible process, overcome by the input of much less energy than was required in the original emulsification process. Finally, creaming and sedimentation are both forms of gravitational separation. Creaming describes the upward movements of droplets due to the fact that they have a lower density than the surrounding liquid (Figure 2.2d) while sedimentation describes the downward movement of droplets due to the difference in the density of the two phases. The rate of creaming/sedimentation will be dependent on the physical characteristics of the system, especially the viscosity of the continuous phase. It does not necessarily represent a change in the dispersed state of the system; however, and it can often be reversed with minimal energy input. Obviously, flocculation and creaming/sedimentation represent conditions in which drops "touch" but do not combine to form a single unit. The key to understanding the true stability of emulsions, then, lies on the line separating the process of flocculation and coalescence. (Myers 1992).

In addition to the mechanical action and interfacial potential energy considerations that will act to reduce the degree of dispersion of an emulsion, other considerations act to limit the stability of emulsions. One such factor affecting long-term stability is the phenomenon commonly termed "Ostwald ripening". Ostwald ripening occurs because the solubility of the material in a spherical droplet increases as the size of the droplet decreases (Dickinson, 1992):

$$S(r) = S(\infty)\exp\left(\frac{2\sigma V_m}{RTr}\right), \qquad \textbf{Equation 2.3}$$

where V_m is the molar volume of the solute, σ is the interfacial tension, $S(\infty)$ is the solubility of the solute in the continuous phase for a droplet with infinite curvature (a planar interface), and S(r) is the solubility of the solute when contained in a spherical droplet of radius r. The increase in solubility with decreasing droplet size means that there is a higher concentration of solubilised material around a small droplet than around a larger one. The solubilised molecules therefore move from the smaller droplets to the larger droplets because of this concentration gradient. Once steady state has been achieved, the rate of Ostwald ripening is given by (Kabalnov & Shchukin, 1992):

$$\frac{d\langle r\rangle^3}{dt} = \frac{8\sigma V_m S(\infty) D}{9RT}, \qquad \textbf{Equation 2.4}$$

where D is the translation diffusion coefficient of the solute through the continuous phase. This equation indicates that the change in droplet size with time becomes more rapid as the equilibrium solubility of the molecules in the continuous phase increases (McClements, 1999).

Myers (1992) stressed that, to obtain a useful emulsion with any long-term persistence, it is necessary to include a third component that served some "magical" purpose and imparted the required degree of stability. Such additives include simple inorganic electrolytes; natural resins and other macromolecular compounds; finely divided, insoluble solid particles that locate themselves at the interface between the two phases; and amphiphilic or surface active materials that are soluble in one or both phases and significantly alter the interfacial characteristics of the system.

2.2.2 Different mechanisms of stabilisation

Early theories of emulsion stability recognised the importance of additives such as surfactants, polymers and particles to the processes of emulsion preparation; the type of emulsion produced; and the overall stability of the final system. However, it was not until the work of Langmuir and Harkins (Harkins, 1952) that a reasonably sound theoretical picture began to evolve. Based on studies of a monolayer of surfactant at interfaces, the concept of a rigid multilayer film of adsorbed material imparting stability was discarded in favour of the idea of oriented monomolecular films in which each portion of the adsorbed molecules showed a strong preference for association with one of the two liquid phases. As a result, it became possible to schematically represent the emulsion droplets as shown in Figure 2.3 (Myers, 1992).

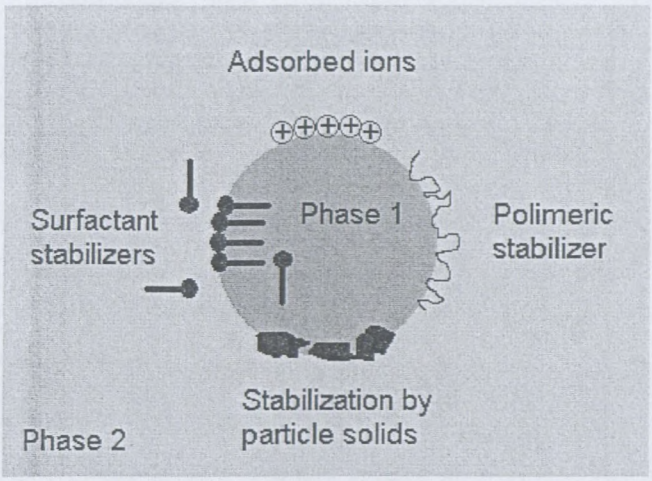

Figure 2.3: Various possible mechanisms of emulsion stabilisation

(Adapted from Myers, 1992: 218)

2.2.3 Molecular basis of an interface

An interface is a narrow region that separates two condensed phases. Atoms or molecules at an interface will generally have higher potential energy than those in the bulk of a material. Their location at the interface means that they will experience a net force due to the nearest neighbour interactions significantly different from those in the bulk (Myers, 1992). Thus, an expenditure of energy is needed to increase the interfacial area. The reversible work at constant pressure and temperature required to increase the contact area between

two immiscible liquids is given by the increase in free energy of the system; this work is proportional to the increase of the surface area (Adamson, 1997; McClements, 1999):

$$dW = dG = \sigma dA \qquad \textbf{Equation 2.5}$$

$$\sigma = \left(\frac{\delta G}{\delta A}\right)_{T,P} \qquad \textbf{Equation 2.6}$$

dG: Increase in free energy of the system

dA: Increase in contact area

σ: Constant of proportionality called interfacial tension. The interfacial tension is a physical characteristic of an interface, which is determined by the imbalance of molecular forces across an interface: The greater the interfacial tension, the greater the imbalance of forces (Israelachvili, 1992; McClements, 1999). The interfacial tension is referred to as interfacial free energy per unit area or force per unit length.

2.2.4 Formation, stability of an interface and the interfacial tension

The change in free energy when a molecule is brought from the interior of the phase to the interface is determined by changes in the interaction energies of the molecules involved, as well as by various entropy effects.

$$G^S = \sigma = H^S - TS^S \qquad \textbf{Equation 2.7}$$

Often, and as a good approximation, H^S and the surface energy E^S are not distinguished, so Equation 2.6 can be seen in the form (Adamson, 1997):

$$G^S = \sigma = E^S - TS^S \qquad \textbf{Equation 2.8}$$

E^S: The total surface energy; It is generally larger than the interfacial tension and is frequently the more informative of the two quantities, or, at least, is more easily related to molecular models (Adamson, 1997). It characterises the interaction energy between the molecules present at the interface.

S^S: The surface entropy per unit area of surface. The thermal energy associated with the entropy has a disorganising influence, inducing a continual motion of molecules (translation, rotation and vibration) that opposes molecular interaction energy. The entropy effect associated with the interface is mainly due to the fact that a molecule, when located at an interface, is confined to a region which is considerably smaller than the volume it would occupy in a bulk liquid and its molecular rotation is restricted. Both of these effects are entropically unfavourable.

Because of the thermal energy, fluctuations at the interface tend to take place to cause the latter to be in a very turbulent state; wave-like behaviour of the interface may occur, which will tend to merge the two phases (Adamson, 1997; McClements, 1999).

$$\left(\frac{\delta G^S}{\delta T}\right)_P = \frac{d\sigma}{dT} = -S^S \qquad \text{Equation 2.9}$$

- If $\sigma > 0$ ($E^S > TS^S$), a thin, stable interface will form because the strong repulsions between the molecules present at the interface is greater than the dispersive forces. The interactions between the different types of molecules are highly unfavourable and the interfacial region is relatively thin because the protrusion of a molecule from one phase into another involves a large expenditure of energy (Adamson, 1997).
- If $\sigma < 0$ ($E^S < TS^S$), the two liquids are miscible and the interfacial region disappears altogether: the fluctuations will lead to a complete dispersion of one phase into another.
- If $\sigma = 0$ ($E^S = TS^S$), an unstable interface is formed; the liquids are partially miscible. The fluctuation forces will lead to a partial dispersion of one phase into another and the interfacial region increases in thickness. In this case, the interface tends to exhibit undulations and molecules will be twisting and turning continually, as well as moving in and out of the interfacial region (Adamson, 1997).

A general prerequisite for the existence of a stable interface between two phases is that the free energy of formation of the interface be positive. Where the interfacial tension is negative or zero, fluctuations would lead to partial or complete dispersion of one phase into another system (the thickness and mobility of the interfacial region are therefore governed by a balance between the interaction energies and the thermal energy of the system (Adamson, 1997; Israelachvili, 1992; McClements, 1999).

2.2.5 Curvature and orientation at an interface

2.2.5.1 Orientation at an interface

An important characteristic of an interface is that it is directional. Properties vary differently, both along and perpendicular to the interface. To be incorporated at an interface, some molecules must be in a specific orientation (McClements, 1999). Unsymmetrical molecules will be oriented at an interface so that their mutual interaction energy will be at maximum. A somewhat more quantitative development along this subject was given by Langmuir in what

he termed the principle of independent surface action. He proposed that, qualitatively, one could suppose each part of a molecule to possess local surface free energy. One can employ this principle to decide how surface-active molecules should be oriented (Adamson, 1997).

2.2.5.2 Effect of curvature

The majority of surfaces and interfaces found in emulsions are curved rather than planar. The curvature of an interface alters its characteristics in a number of ways (McClements, 2005).

Droplets tend to be spherical because this shape minimises the energetically unfavourable contact area between oil and water molecules (this shape gives the smaller surface for a given volume). At equilibrium, the pressure within the droplet is larger than that outside and can be related to the interfacial tension and radius of the droplets, using the Laplace-equation:

$$\Delta p = \frac{2\sigma}{r}$$ **Equation 2.10**

Δp: The drop in pressure across a curved interface

r: radius of the droplet

This equation indicates that the pressure difference across the interface of an emulsion droplet increases as the interfacial tension increases or the size of the droplet decreases.

Droplets become non-spherical when they experience an external force that is large enough to overcome the Laplace pressure (e.g. gravity, centrifugal forces or mechanical agitation). The Laplace equation emphasises that the magnitude of the force needed to deform a droplet decreases as the interfacial tension decreases or the radius increases. This accounts for the ease with which the relatively large droplets in highly concentrated emulsions are deformed into polygons (McClements, 1999; 2005).

For any curvature, the general form of the Young-Laplace equation is given by:

$$\Delta p = \sigma\left(\frac{1}{r_1} - \frac{1}{r_2}\right)$$ **Equation 2.11**

r_1 and r_2 are the principal radii of curvature.

2.2.6 Surfactant

2.2.6.1 Definition

A surfactant is an amphiphilic (amphipathic) molecule that has a hydrophilic head group (polar region), which has a high affinity for water, and a lipophilic tail group (non-polar region), which has a high affinity for oil (Becher, 1988; McClements, 1999).

2.2.6.2 Molecular characteristic

The formula RX can represent a surfactant, where X represents the hydrophilic head group and R the lipophilic tail (Dickson & McClements, 1995; McClements, 1999). The characteristics of a particular surfactant depend on the nature of its head and tail groups. The head group may be anionic, cationic, zwitter-ionic, or non-ionic (Myers, 1992). The tail group usually consists of one or more hydrocarbon chains, having between 10 and 20 carbon atoms per chain (McClements, 1999). Surfactant chains may be saturated or unsaturated, linear or branched, aliphatic and/or aromatic.

2.2.6.3 Functional properties

The dual character of a surfactant is responsible for the phenomenon of surface activity and spontaneous aggregation in solution (McClements, 1999; 2005). Owing to their tendency to become adsorbed at the polar/non-polar interface, in order to satisfy their double affinity, they are often called surface active agents. As a class, these substances can be called association colloids, the name indicating their tendency to aggregate spontaneously in solution to form a variety of thermodynamically stable structures known as association colloids (e.g. micelles, bi-layers, vesicles, and reverse micelles). These structures are adopted because they minimise the unfavourable contact area between the non-polar tails of the surfactant molecules and water (McClements, 1999; 2005).

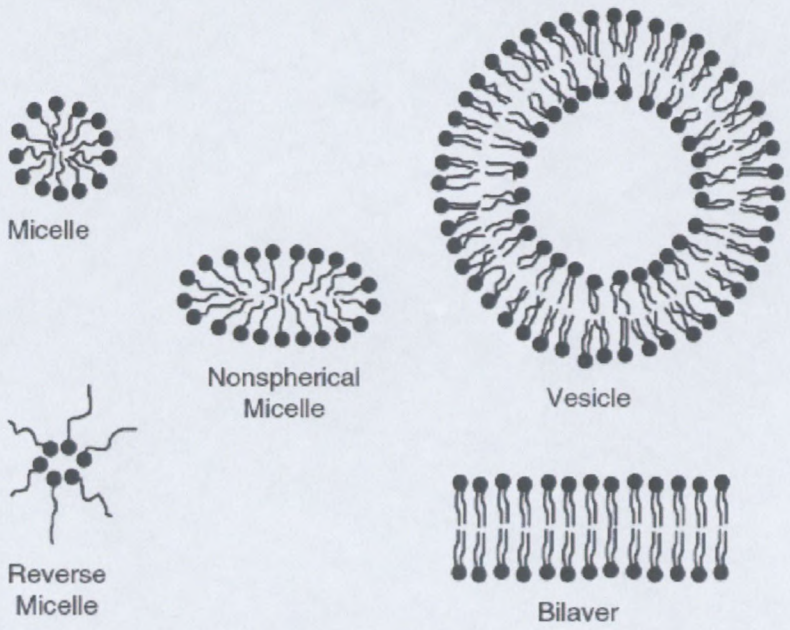

Figure 2.4: Some typical structures formed due to the self-association of surfactant molecules at relatively low surfactant concentrations. At higher surfactant concentrations, many different kinds of liquid crystalline phases may form.

(Adapted from McClements, 2005: 31).

The properties of surfactant molecules dispersed as monomers are different from those in colloidal associations. For example, surfactant monomers are amphiphilic and have a high level of surface activity, whereas micelles have little surface activity. Consequently, the interfacial tension decreases when surfactants are monomers, whereas it remains fairly constant in the presence of micelles (McClements, 1999).

A surfactant forms micelles or reverse micelles in a solution when its concentration exceeds some critical level, known as the critical micelle concentration or CMC (Myers, 1992; McClements, 2005). Below the CMC, the surfactant molecules are dispersed, predominantly as monomers, but once the CMC is exceeded, any additional surfactant molecules form micelles, and the monomer concentration remains fairly constant (Hiemenz & Rajagopalan, 1997). It is worth mentioning that when surfactant is added to a solution above the CMC, the number of micelles, rather than the size or shape of the individual micelles, tends to increase (although this may not be true at high surfactant concentrations) (Israelachvili, 1992; McClements, 2005; Michaels, 2006) .

There is an abrupt change in the physicochemical properties of a surfactant solution when the CMC is exceeded, for example in surface tension, electrical conductivity, turbidity, and osmotic pressure (Figure 2.5) (Rosen, 1978; Hiemenz & Rajagopalan, 1997; McClements, 2005).

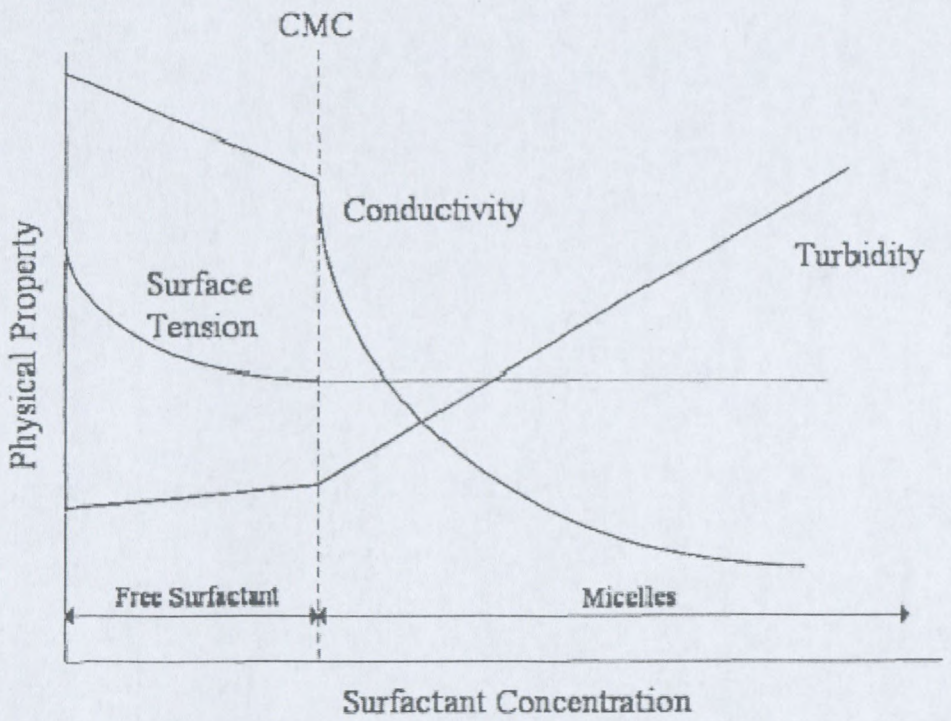

Figure 2.5: Important manifestations of micelle formation: abrupt changes in solution conductivity, a discontinuity in the surface tension vs concentration curve and a sudden increase in solution turbidity.

(Adapted from Michaels, 2006: 18)

Micelles have highly dynamic structures because they are only held together by physical interactions that are relatively weak, compared to the thermal energy of the system (Israelachvili, 1992; McClements, 2005). Despite the highly dynamic nature of their structure, surfactant micelles have a fairly well-defined average size and shape governed by geometric and energetic considerations. It is unreasonable to assume that surfactant molecules pack into a micelle in such an orderly manner as to produce a smooth, perfectly uniform surface structure. If it were possible to photograph a micelle with ultra-high-speed film, thereby freezing the motion of the molecules, the picture would probably show an irregular molecular

cluster more closely resembling a sweet gum seed than a golf ball (Figure 2.6) (Michaels, 2006).

Figure 2.6: Irregular surface of micelle compared to smooth uniform surface

(Adapted from Michaels, 2006: 20)

Micelles are in dynamic equilibrium with individual surfactant molecule monomers that are constantly being exchanged between the bulk and the micelles. Additionally, micelles themselves are continuously dissoluting and reforming (Michaels, 2006). Two relaxation processes are involved in micellar solutions. The first one is the fast relaxation process with relaxation time τ_1 (generally in the order of microseconds), which is associated with the fast exchange of monomers between micelles and the surrounding bulk phase (Figure 2.7). The second relaxation time τ_2 (usually in the order of milliseconds) is attributed to the micelle formation and dissociation process (Michaels, 2006).

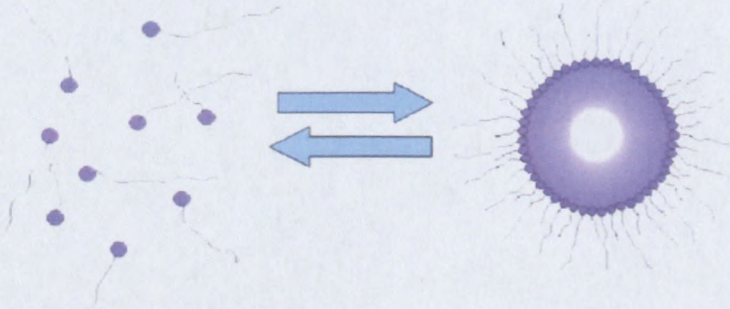

Figure 2.7: Equilibrium of surfactant monomers and reverse micelles in solution

(Adapted from Michaels, 2006: 21)

2.2.6.4 Surfactant classification

Surfactants can be classified according to their physical properties or functionalities.
The following is the most common classification and is based on the nature of the hydrophilic group (Michaels, 2006).

Anionic: surface-active portion exhibits a negative charge

Cationic: surface-active portion exhibits a positive charge

Non-ionic: surface-active portion exhibits no charge

Zwitter-ionic: surface-active portion contains both negative and positive functional groups

- **Bancroft's rule.**

One of the first empirical rules developed to describe the type of emulsion that could be stabilised by a given surfactant was proposed by Bancroft (McClements, 2005). Bancroft's rule states that the phase in which the surfactant is most soluble will form the continuous phase of an emulsion. Hence, a water soluble surfactant should stabilise O/W emulsions, whereas an oil-soluble surfactant should stabilise W/O emulsions. It has recently been highlighted that the solubility should be determined by the total surfactant concentration (monomers + micelles) in a phase, not just the monomers (McClements, 2005).

Bancroft's rule is a useful empirical method of determining the type of emulsion that a surfactant will potentially stabilise (O/W or W/O); however, it provides little insight into the relationship between the molecular structure of a surfactant and the long-term stability of the emulsions formed.

- **Hydrophile-Lipophile Balance (HLB)**

The HLB concept is a semi-empirical method that is widely used for classifying surfactants (Bergenstahl, 1997). The hydrophile-lipophile balance is described by a number that gives an indication of the relative affinity of a surfactant molecule for the oil and aqueous phases (Becher, 1983). Each surfactant is assigned a HLB number according to its chemical structure. A molecule with a high HLB number has a high ratio of hydrophilic groups to lipophilic groups, and vice versa. The HLB number of a surfactant can be calculated from knowledge of the number and type of hydrophilic and lipophilic groups it contains, or it can be estimated from experimental measurements of its cloud point (Shinoda & Friberg, 1986). A widely used semi-empirical method of calculating the HLB number of a surfactant is as follows (Davis, 1994):

HLB = 7 + Σ (hydrophilic group numbers) – Σ (lipophilic group numbers) **Equation 2.12**

Table 2.1 lists the ranges of HLB numbers that have proved most useful for various applications.

Table 2.1: HLB ranges and their general area of application
(Adapted from Michaels, 2006: 25)

Range	Application
3 – 10	Water-in-Oil emulsions (W/O)
7 –11	Wetting
11 – 18	Oil-in Water emulsions (O/W)
3 – 15	Detergency
15 – 18	Solubilisation

- **Molecular geometry and the Phase Inversion Temperature**

The molecular geometry of surfactants plays an important role in the micellisation process; therefore, it is essential to understand how surfactants pack. Two opposing forces control the self-association process: hydrocarbon/water interactions that favour aggregation (i.e., pulling surfactant molecules out of the aqueous environment), and head group interactions that work in the opposite manner. These two contributions can be considered an attractive interfacial tension term due to hydrocarbon tails and a repulsion term depending on the nature of the hydrophilic group. More recently, the revision and quantification of the basic idea resulted in the concept that aggregation of surfactants is controlled by a balanced molecular geometry (McClements, 2005; Michaels, 2006). In brief, the geometric treatment separates the overall free energy of micellisation into three critical geometric terms:

(1) a_o - the area occupied by the head group

(2) ν - the volume of the hydrophobic tail

(3) l_c - the chain length of the tail

$$P_C = \frac{\nu}{a_o l_c} \qquad \textbf{Equation 2.13}$$

The dimensionless value of P_c is a useful quantity since it allows the prediction of aggregate shape and size. When surfactant molecules associate with each other, they tend to form a monolayer that has a curvature that allows the most efficient packing of the molecules. At

this optimum curvature, the monolayer has its lowest free energy, and any deviation from this curvature requires the expenditure of free energy. The optimum curvature (H_0) of a monolayer depends on the packing parameter of the surfactant: for p = 1, a monolayer with zero curvature ($H_0 = 0$) is preferred; for p < 1, the optimum curvature is convex ($H_0 < 0$); and, for p > 1 the optimum curvature is concave ($H_0 > 0$) (Figure 2.8).

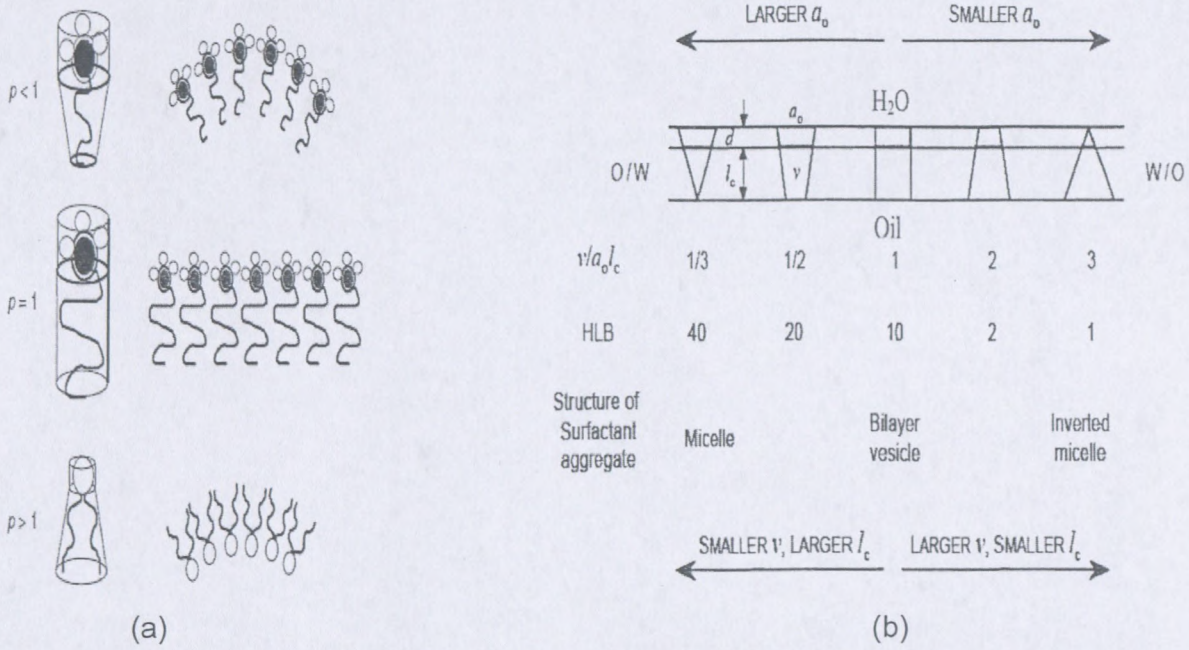

Figure 2.8: Effect of molecular geometry and system conditions on packing parameter

[Adapted from (a): Mc Clements, 1999:40; (b): Michaels, 2006:29]

The packing parameter is also useful because it accounts for the temperature dependence of the physicochemical properties of surfactant solutions and of emulsions (Kabalnov & Wennerstrom, 1996). The temperature at which a surfactant solution converts from a micellar to a reverse-micellar system or an O/W emulsion changes to a W/O emulsion is known as the PIT (Phase Inversion Temperature) (Shinoda & Kunieda, 1983; Shinoda & Friberg, 1986).

2.2.7 Thermodynamic of adsorption

2.2.7.1 Affinity of a surfactant molecule for an interface

The affinity of a surfactant molecule for an interface can be described by its adsorption efficiency and its surface activity. The adsorption efficiency is a measure of the minimum amount of surfactant required to saturate an interface. The surface activity is a measure of the maximum decrease in interfacial tension achievable when an interface is completely saturated; it is a measure of the ability of a molecule to accumulate at an interface (McClements, 1999; 2005). Adsorption efficiencies and surface activities depend on the molecular structure of the surfactant, as well as the prevailing environmental conditions (Dickinson, 1992; McClements, 1999).

2.2.7.2 Definition of surface excess concentration

The accumulation of surfactant molecules at an interface is characterised by the surface excess concentration

$$\Gamma = \frac{n_i}{A}, \qquad \text{Equation 2.14}$$

where A is the surface area and n_i is the excess surfactant concentration at the surface. It corresponds to the total amount of surfactant present in the system, minus that which would be present if the surfactant were not surface-active (McClements, 1999; 2005).

The surface excess concentration is often identified with an experimentally measurable parameter called the surface load, which is the amount of surfactant adsorbed to the surface of emulsion droplets per unit area of interface (McClements, 1999; 2005).

2.2.7.3 Surface pressure and reduction of interfacial tension

The ability of surfactant molecules to shield direct interactions between two immiscible liquids is governed by their optimum packing at the interface, which depends on their molecular geometry. When the curvature of an interface is equal to the optimum curvature of a surfactant monolayer, i.e., optimum packing is possible, the interfacial tension is extra low because the direct interactions between the oil and water molecules are effectively eliminated. On the other hand, when the curvature of an interface is not at its optimum, the interfacial tension increases because some of the oil molecules are exposed to the polar

regions of the surfactant or some water molecules come into contact with the hydrophobic part of the surfactant (McClements, 1999; 2005).

A quantitative prediction of the surface or interfacial tension produced by a given concentration of surfactant can most conveniently be made using an equation of state of the monolayer (McClements, 2005). In such equations, surface tension lowering is expressed in terms of the surface pressure, π, defined as

$$\pi = \sigma^0 - \sigma \qquad \text{Equation 2.15}$$

σ^0: the interfacial tension of the pure oil-water interface

σ: the interfacial tension in the presence of the surfactant (Hiemenz, 1986; McClements, 1999).

2.2.7.4 Relationship between adsorbed and bulk solute concentrations

There are two different thermodynamic approaches that have been developed to describe this relationship: the Langmuir adsorption isotherm and the Gibbs adsorption isotherm (Hunter, 1993; Hiemenz & Rajagopalan, 1997). These approaches are based on a thermodynamic analysis of the adsorption process, assuming that the adsorption-desorption of solutes at the surface is reversible, and that solute-solute interactions do not occur in the bulk solution or at the surface.

The Langmuir adsorption isotherm is useful for relating the amount of solute present at a surface to the concentration and surface activity of the solute in the bulk solution:

$$\theta = \frac{\Gamma}{\Gamma_\infty} = \frac{c / c_{1/2}}{1 + c / c_{1/2}} \quad , \qquad \text{Equation 2.16}$$

where θ is the fraction of adsorption sites that are occupied, Γ_8 is the surface excess concentration when the surface is completely saturated with solute, and $c_{1/2}$ is the solute concentration in the bulk solution where $\theta = 1/2$. The equilibrium constant for adsorption ($K = 1/c_{1/2}$) provides a good measure for the surface activity or binding affinity of an emulsifier: the greater $1/c_{1/2}$ the higher the binding affinity. The surface activity of a molecule is related to the free energy of adsorption by the following equation:

$$K = \frac{1}{c_{1/2}} = \exp\left(-\frac{\Delta G_{ads}}{RT}\right) \quad , \qquad \text{Equation 2.17}$$

where ΔG_{ads} corresponds to the free energy change associated with exchanging a solvent molecule with a solute molecule at the surface.

There is equilibrium between surfactant molecules at the interface and those in the bulk liquid. As the concentration in the bulk liquid is increased, so does their concentration at the interface. The presence of the surfactant molecules at the interface shields the unfavourable contact within oil and water molecules and therefore reduces the tension. The relationship between the decrease in interfacial tension with surfactant concentration and the amount of surfactant present at the surface is known as the Gibbs isotherm equation.

For a dilute solution (McClements, 1999):

$$\Gamma = -\frac{1}{RT}\left[\frac{d\sigma}{d\ln c}\right] = \frac{1}{RT}\left[\frac{d\pi}{d\ln c}\right] \quad \text{for non-ionic surfactants} \qquad \textbf{Equation 2.18}$$

$$\Gamma = -\frac{1}{2RT}\left[\frac{d\sigma}{d\ln c}\right] = \frac{1}{RT}\left[\frac{d\pi}{d\ln c}\right] \quad \text{for ionic surfactants} \qquad \textbf{Equation 2.19}$$

c: the concentration of surfactant in the bulk solution

Γ: the surface excess concentration; the slope of the curve of the interfacial tension versus the logarithm of concentration.

σ: the interfacial tension

π: surface pressure

The Gibbs adsorption isotherm can also be presented in the following form:

$$\pi = pRT\int_0^c \Gamma(c)d\ln c \qquad \textbf{Equation 2.20}$$

p = -1 for non ionic surfactant; p = -1/2 for ionic surfactant.

Insertion of the Langmuir adsorption isotherm into the above Equation 2.20 and expressing the surface excess concentration in units of mass per unit area rather than moles per unit area gives

$$\pi = \left(\frac{pRT}{M}\right)\Gamma_\infty \ln\left(1+\frac{c}{c_{1/2}}\right) \qquad \textbf{Equation 2.21}$$

A typical plot of surface tension against the logarithm of concentration is shown in

Figure 2.9.

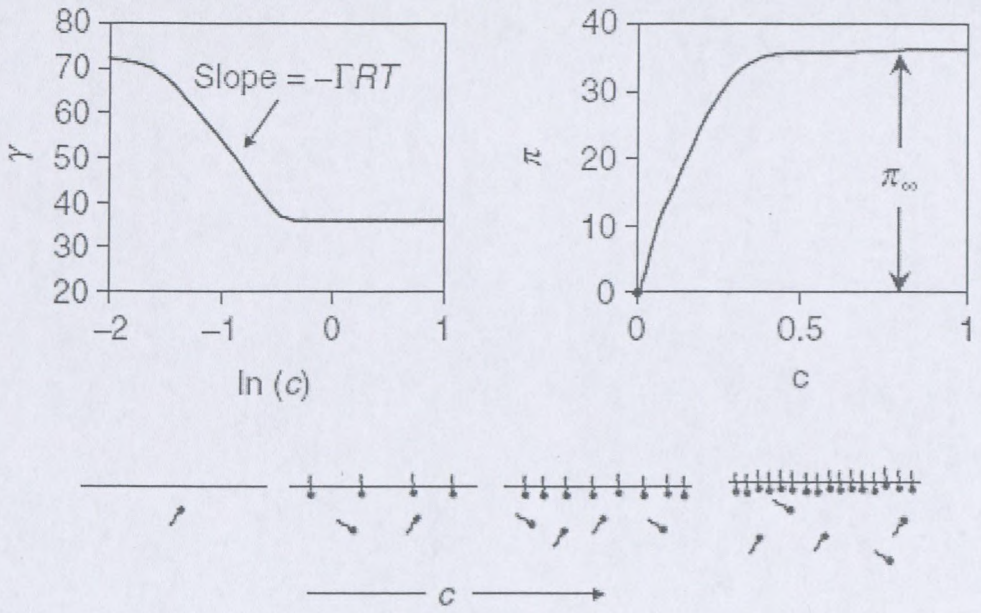

Figure 2.9: Interfacial tension as a function of surfactant concentration in the bulk solution

(Adapted from McClements, 2005: 7)

2.2.8 Interfacial film and emulsion stability

As discussed by Myers (1992), the effectiveness of any adsorbed film of surface-active materials in retarding the inevitable movement of emulsified systems toward a minimum in total energy may be considered in at least three contexts. The adsorbed molecules can:

- reduce the potential energy of the dispersed system by lowering the interfacial tension
- erect a rigid or highly viscous barrier at the interface that is capable of preventing or retarding the coalescence of droplets that collide as a result of random Brownian motion, thermal convection, or mechanical agitation
- in cases where the adsorbed molecules carry an electric charge, impart that charge to the surface of droplets, resulting in the formation of an electrical double layer that lessens the frequency and effectiveness of close droplet approach and contact leading to droplet growth.

While it may be tempting to attribute emulsion stability to the existence of low interfacial tension, it is generally felt nowadays (Myers, 1992; McClements, 1999) that interfacial

tension effects are less important to overall long-term emulsion stability than are the effects of the nature of the interfacial film. The ability of the interfacial film to withstand the pressures of droplet contacts (its tenacity), its properties as a barrier to the passage of dispersed phase into the continuous phase (to limit Ostwald ripening), and its ability to erect a physical or electrical barrier to droplet contact appears to be the major characteristics determining the ultimate stability of an emulsion (Myers, 1992).

Any discussion of the stability of emulsions must be concerned not only with the mechanism of stabilisation but also with the time frame of the stability requirements and the conditions of treatment concerned (Myers, 1992). The rates of degradation of emulsions vary immensely, and it is not possible to define a single number that can be used as a measure of acceptable or unacceptable persistence. In any emulsion, especially one that is unstabilised or only very poorly stabilised; the degradation or breaking process will involve the coalescence of droplets brought together by the action of Brownian motion, convection currents and other random disturbances. Their stability can be measured in the order of seconds or minutes. In the presence of gentle agitation (stirring) the process may be accelerated, while more vigorous stirring may result in the occurrence of a competitive process of coalescence and new droplet formation. Therefore, such moderate agitation may result in the development of a steady state or equilibrium particle size distribution that will be highly dependent on the rate of agitation, the concentration of the dispersed phase, particle size distribution, and the conditions of disturbance under which it is examined (Myers, 1992).

Emulsions that contain more effective stabilising additives may be stable for hours, days, or months. In such systems, the action of random or induced motion and droplet collision will continue, but the interfacial layers will possess sufficient strength and rigidity to prevent coalescence in most cases. When emulsion creaming (or sedimentation) occurs, additional pressures are applied to the interfacial area. At extreme pressures, as in the process of centrifugation, or in the case of highly concentrated emulsions, the drops deform into the shape of polyhedra. As a polyhedron necessarily has a larger area than a sphere of equal volume, this process stretches the layer of emulsifying agent and may lead to its rupture (Myers, 1992).

2.2.9 Stability of explosive emulsions

Explosive emulsions are highly internal phase water-in-oil emulsions. The aqueous phase is a supersaturated nitrate salt solution (at room temperature), with a volume fraction usually greater than 0.8. Aqueous phase droplets are deformed by packing and contact with neighbouring droplets.

The instability mechanisms of explosive emulsions mainly involve droplet coalescence and crystallisation of a supercooled salt solution forming the droplets of the dispersed phase (White, Henderson & Perriman, 2004). Recent experimental data (Malkin *et al.*, 2004a, Masalova *et al.*, 2006; Masalova & Malkin, 2007b) demonstrated that explosive emulsions do not flocculate, aggregate or cream because of the close packing of the droplets. On the other hand, direct measurements of droplet size distribution during the process of multiple-month ageing showed that there were no essential changes in the droplet size distribution or in the average value of size dimensions prior to the crystallisation process (Kharatiyan, 2005; Masalova *et al.*, 2006; Masalova & Malkin, 2007b). This means that the ageing of highly concentrated water-in-oil emulsions of the liquid explosive type is directly related to the crystallisation of the supersaturated aqueous salt solution forming the droplets of the dispersed phase. It should be realised that crystals are not necessarily confined to their original droplet size and shape, but can break through the films separating droplets (Becher, 1988; Kharatiyan, 2005; Masalova *et al.*, 2006; Masalova & Malkin, 2007b).

It is worth noting that uncontrolled crystallisation can lead to emulsion breakdown and reduction in detonation sensitivity of the emulsion's explosive composition (Thomas & Halou, 2003).

The crystallisation process can be considered as:

- Initiation of crystallinity of the dispersed phase of the emulsion which depends strongly on the purity of ammonium nitrate (Becher, 1988; Ashok & Neilson, 1991) and could depend on the interaction between the ammonium nitrate solution and the surfactant head group (Ganguly, Krishna, Bhasu, Mathews, Adiseshaiah & Kurma, 1992; Ashok & Neilson, 1991).
- Penetration of the crystallinity throughout the substance: could depend strongly on micelle concentration (White, Henderson & Hawley, 2004) and/or on the strength of the interface (Kharatiyan, 2005; White, Reynolds, Hawley & Perriman, 2005).

2.2.9.1 Factors affecting the crystallisation process

The crystallisation of emulsified aqueous solutions in explosive emulsions is governed by several factors, the important ones being:

- Electrolyte concentration (Ganguly *et al.*, 1992).
- Impurities in the electrolyte: dust (Becher, 1988), ions (Ashok & Neilson, 1991).
- Physicochemical characteristics of the surfactant (Ganguly *et al.*, 1992; White *et al.*, 2004).
- Surfactant concentration (Ganguly *et al.*, 1992; White *et al.*, 2004).
- Droplet size distribution (Kharatiyan, 2005; Masalova *et al.*, 2006; Masalova & Malkin, 2007b).
- Dispersed phase volume fraction (Kharatiyan, 2005; Masalova *et al.*, 2006; Masalova & Malkin, 2007b).
- Oil type (White *et al.*, 2005).

2.2.9.2 Effect of droplet size and dispersed phase volume fraction

The crystallinity penetration process is sensitive to the emulsion particle size and to the dispersed phase volume fraction. Experimental data demonstrated that the crystallinity penetration process in explosive emulsions increase with increase in droplet size or increase in the concentration of the dispersed phase (Kharatiyan, 2005; Masalova *et al.*, 2006; Masalova & Malkin, 2007b).

2.2.9.3 Effect of ammonium nitrate purity and concentration

- **Effect of ammonium nitrate concentration**

Ammonium nitrate (AN) holds a unique position in the properties of salts in very concentrated aqueous solutions, because of the striking similarity of the NH_4^+ ion to the water molecule concerning mass, partial molar volume, bond angles and atomic distance. NH_4^+ and H_2O form hydrogen bonds of about the same strength and the electrostatic forces exerted on their nearest neighbours are likely to be the same (Bengtsson, Frostemark & Holmberg, 1994). On the one hand, when increasing the AN concentration in an aqueous solution, there is a decrease in the ammonium nitrate ion-water and nitrate ion-water coordination (Walker, Lawrence, Neilson & Cooper, 1989; Bengtsson *et al.*, 1994) and the hydration shell moves closer in at higher concentrations (Walker *et al.*, 1989). At concentrations greater than 60 % by mass, there is evidence which demonstrates a direct interaction between the NH_4^+ and NO_3^- (Ashok & Neilson, 1991; Bengtsson *et al.*, 1994). The increased tendency to NH_4^+...

NO_3^- ion-pair formation with decreasing water content in the system NH_4NO_3-H_2O increases the equilibrium crystallisation temperature of the solution. On the other hand, an increase in AN concentration can improve the stability against the crystallisation process through its influence on the amount of surfactant adsorbed at the interface and/or on the micelle size and its aggregation number (Reynolds, Gilbert & White, 2001). For example, the amount of surfactant adsorbed at the water/oil interface appears to be less than a monolayer (area per surfactant molecule of 230 A^2 for the acid amide head group) while the same head group at the ammonium nitrate/oil interface form a close-packed monolayer of surfactant (area per surfactant molecule of 83-140 A^2) (Reynolds, Mc Gillivray, Gilbert, Holt, Henderson & White, 2003).

- **Effect of impurities in ammonium nitrate solution**

Stabilisation of concentrated aqueous ammonium nitrate solutions often involves the addition of other species such as ions or molecules (Ashok & Neilson, 1991) or surfactant head group (Ganguly *et al.*, 1992). The mechanism by which such stabilisation can take place and that by which the solution becomes unstable depends on the structure of the solution and how it can be altered (Ashok & Neilson, 1991; Ganguly *et al.*, 1992). For example, the effect of the addition of Ca^{2+} to AN is to increase the separation distance between NH_4^+ and NO_3^- ions. On a qualitative level, the presence of doubly charged Ca^{2+} ions which can strongly coordinate with NO_3^- brings about the separation of the counter-ions. This result shows the inhibiting role of Ca^{2+} on the chemical kinetics of concentrated AN solutions (Ashok & Neilson, 1991).

It is worth mentioning that any presence of dust will accelerate the crystallisation process by inducing heterogeneous nucleation. Large droplets have an increased chance of containing a heterogeneous nucleus, and therefore higher crystallisation probability (Becher, 1988).

2.2.9.4 Effect of type and concentration of surfactant

- **Effect of surfactant type**

The nature of the surfactant has a large influence on the freezing behaviour and on surfactant-electrolyte interactions in the case of concentrated emulsions with dissolved electrolytes in an aqueous phase (Ganguly *et al.*, 1992). As pointed out by Ganguly *et al.* (1992), experimental results obtained from different techniques displayed strong correlations and led the authors to believe that there is a large interdependence between molecular-level behaviour and bulk properties: the strong surfactant-electrolyte interaction could give rise to more stable emulsions. Laughlin and Brown (1978) have attempted a classification of polar

groups with respect to whether or not they are operative hydrophilic groups in relation to surfactant behaviour. Laughlin and Brown (1978) have also examined possible relationships between surfactant behaviour and two independent criteria of polarity, i.e. dipole moment and hydrogen-bonding thermodynamics. They state that the phase behaviour of a surfactant is a function of its total structure, which includes the lipophilic group, the hydrophilic group and the proximate groups. The proximate groups include the counter-ions (solute) as well as the hydration sphere.

- **Effect of surfactant concentration**

The freezing behaviour of emulsified aqueous solutions is sensitive to the surfactant concentration (Ganguly *et al.*, 1992; White *et al.*, 2004; 2005).

Below the CMC, the surfactant concentration mainly affects the surfactant-electrolyte interaction and the strength of the interface. As the surfactant concentration in the bulk liquid increases, so does the concentration at the interface. Therefore the surfactant-electrolyte interactions increase (Ganguly *et al.*, 1992). Furthermore, because of the increase in surfactant concentration at the interface, the latter becomes more complex but not necessarily more resistant (White *et al.*, 2005). The emulsions which are more stable to shear or to ageing are those with the most complex interface, but in which the interface is not very thick and/or lumpy (White *et al.*, 2005). The elasticity of the interface could act as an inhibitor preventing the crystallisation in one of the micron-scale aqueous droplets to propagate through the rest of the emulsion, crystallising all droplets (White *et al.*, 2005).

Above the CMC, depending on the type of surfactant, the penetration of crystallinity throughout the substance could be strongly dependent on micelle concentration. Indeed, explosive emulsions produced by using polyisobutylene-based surfactants are highly stabilised by a significant number of surfactant rich reverse micelles a few nanometres in diameter in the oil phase (White *et al.*, 2004; 2005). The hypothesis in the proposal, that crystallisation was triggered by changes in the monolayer at the aqueous oil interface, thereby allowing contact between the contents of different droplets, seems untrue (White *et al.*, 2004). It is the reverse micelles that prevent such contacts by an unknown mechanism. The highly unstable emulsions are those in which the reverse micelle concentration is very small (White *et al.*, 2004).

It is worth mentioning that the propagation of crystallisation from one micron-scale aqueous droplets in emulsion explosives are stabilised by a surfactant monolayer or multilayer at the aqueous oil interface and/or by spherical reverse micelles in the oil phase. The relative contribution of the strength of the interface and the reverse micelle to the inhibition of propagation of crystallinity is strongly dependent on surfactant type (White *et al.*, 2005).

2.2.9.5 Stability of Pibsa-based and SMO-based emulsions

Sorbitan monooleate (SMO) is the historical emulsifier used by the explosive industry. Its lower cost and wide availability make it the emulsifier of choice for mild conditions and short sleep time (time of the explosive emulsion residence in a borehole before blasting) applications (Thomas & Halou, 2003).

Better performing emulsifiers were developed to make emulsion explosives which can be used in more severe applications. These more active emulsifiers were derived mostly from carboxylic acylating agents. Anhydride derivatives obtained by reacting an olefin, more specifically polyisobutene (PIB), with an unsaturated anhydride can be used as such or after further modification, most of the time by an amine or a hydroxylamine. Polyisobutene succinic anhydrides (PIBSA) and PIBSA reacted with amine are commercial examples of such emulsifiers used in the explosive industry (Reynolds *et al.*, 2003).

In PIBSA-based emulsions, most of the surfactant is in the form of reverse micelles in the oil phase, and dissolved in the oil phase (~ 95 %). Rather less occurs as a monolayer at a flat aqueous/oil interface, with a very small amount in the form of micron-scale surfactant aggregate (White *et al.*, 2004; Reynolds, Gilbert & White, 2000; Reynolds *et al.*, 2001). Both the film quality of the monolayer (interfacial area per molecule, called footprint, and film thickness) and the reverse micelle structure (shape, size and water content) depend on the nature of the head group, the tail length, the polydispersiveness in tail length and head group and on ionic strength; they are independent of surfactant concentration (Reynolds *et al.*, 2000; 2003). The molecular area is determined partly by PIB coil size and partly, for larger head groups, by the requirement that the whole head group has contact with the aqueous phase. In a general case, the head group will prefer a much tighter packing, but this is impossible because the major interactions are based on the size of the tail. The highest molecular weight PIBSA is least flexible, with poorest coverage (Reynolds *et al.*, 2003).

White *et al.* (2004) pointed out that the stability against crystallisation of the emulsion stabilised by Pibsa-MEA, SMO or the mixture SMO/Pibsa-MEA could be determined by reverse micelles, rather than by the strength of the interface. According to the authors, both lowering SMO content in SMO-based emulsions or increasing SMO content in emulsions prepared with the mixture SMO/Pibsa-MEA (for the same total surfactant concentration) render them susceptible to crystallisation. The SANS results showed that, in both cases, the aqueous oil/interface was invariant, both in the thickness of the monolayer and the footprint of the adsorbed surfactant molecules. Only reverse micelle concentration decreased – more or less in step with total surfactant concentration (White *et al.*, 2004). On the other hand, Ganguly *et al.* (1992) pointed out that emulsion stability could be controlled primarily by the surfactant-electrolyte interactions. According to the authors, the high stability of Pibsa-MEA emulsions, compared to SMO/Pibsa-MEA-based emulsions, or SMO/Pibsa-MEA emulsions compared to SMO-based emulsions, primarily could be attributable to the much stronger MEA-ammonium nitrate interaction, compared to the SMO-ammonium nitrate interaction (Ganguly *et al.*, 1992). Indeed, the surfactant head groups in the two surfactants have a moderate-to-strong hydrogen-bonding tendency, although the polar group in MEA could have a much stronger interaction compared to that of the corresponding groups in SMO. This is because, according to Laughlin's classification, the hydroxyl group just misses being operative, while the amino group is operative (Ganguly *et al.*, 1992). The cumulative effect of hydroxyl groups and the carbonyl group could account for the surfactant properties of SMO. MEA, however, contains amino, carboxyl and hydroxyl groups which could render it a more effective surfactant (Ganguly *et al.*, 1992). Moreover, with SMO the only type of interaction possible is the hydrogen-bonding type while, in the case of Pibsa-MEA, in addition to this type of interaction, there exists the possibility of electrostatic-type interaction (Ganguly *et al.*, 1992; Reynolds *et al.*, 2001). Pibsa-MEA has been shown to confer additional stability provided by steric and electrostatic forces in the thin film between the adjacent droplets (Ganguly *et al.*, 1992).

2.2.9.6 Degree of crystallinity

Kakudo and Kasai (1972) describe the principle of measuring crystallinity of semi-crystalline materials. The principle relies on the fact that the total intensity of the diffracted scattering of a body of fixed mass should be constant when the incident X-ray intensity is constant, irrespective of the steric structure of the atoms in the bulk of the body. This implies that the integral diffracted intensity will be constant, irrespective of the ratios of crystalline to amorphous regions in the scattered body. If the structures of the crystalline region and the

amorphous regions are clearly distinguishable and the interferences between the scattering of the two regions can be ignored, the total scattering can be divided into the crystalline scattered (I_{cr}) region and the amorphous scattered (I_{am}) region.

Crystallinity (X_{Cr}) is defined in terms of the total mass (M) and the respective masses of the crystalline (M_{cr}) and amorphous (M_{am}) regions, by

$$X_{Cr} = \frac{M_{cr}}{(M_{cr} + M_{am})}. \qquad \textbf{Equation 2.22}$$

The ratios of the scattering densities of the X-rays from the amorphous and crystalline regions of a material are nearly equal to the ratio of the masses of the two types of regions as long as the compositions of the two regions are of the same material. Hence, the crystallinity of the material can be determined from the ratio of the total scattering intensities of the two regions.

If the diffraction intensity of the material with an unknown crystallinity has the value of I_u and the corresponding intensities of the most crystalline and most nearly amorphous samples of the same material over the wide range of angles are I_{cry} and I_{am} respectively, the relative crystallinity (X_{Cr}) can be determined by

$$X_{Cr} = \frac{(I_u - I_{am})_j}{(I_{cry} - I_{am})_j}. \qquad \textbf{Equation 2.23}$$

This principle can be used to determine the relative crystallinity from the intensity differences of the fully crystalline and amorphous phases of the room temperature explosive emulsion.

Transformations involving crystal nucleation and crystal growth processes can be modelled using the Johnson-Mehl-Avrami-Kolmogorov (JMAK) equation:

$$X(t) = 1 - \exp\left[-\left(\frac{t}{\theta}\right)^n\right], \qquad \textbf{Equation 2.24}$$

where X(t) is a fraction of material that has crystallised at time t under isothermal conditions, Θ is a characteristic time constant corresponding to a approximately 63 % crystallinity, and n is the Avrami exponent that depends on the dimensionality of crystal growth and on the

nucleation mechanism (Walter, Gross, Evans-Lutterdodt, Brown, Oh, Merchant & Naresh, 2000; Celli, Zanotto & Avramov, 2003).

Considerable effort has been devoted to the improvement of emulsion stability by explosives manufacturers, but most of the data unfortunately are proprietary. The above discussion describes only a few of the improvements claimed, in particular those where a chemical or physical effect is assigned to the stabilising system.

2.3 Rheology of emulsions

Rheology is usually defined as the science of deformation and flow of matter. According to Fredrickson (1964), "the goal of rheology is to predict the force system necessary to cause a given deformation or flow in a body, or conversely, to predict of the deformation or flow resulting from the application of a given force system to a body". Its techniques can be used to study the structure of emulsions ranging in consistency from fluids to solids. The application of a force to a fluid produces flow. When this force is removed the fluid does not return to its original state – it undergoes irreversible deformation. The response of a solid to an applied force depends on whether it shows elastic or plastic behaviour. An elastic solid undergoes deformation but it does not flow. When the force is removed it returns to its original state, thereby exhibiting reversible deformation. A plastic solid behaves in a similar way, provided the applied force does not exceed a critical value. If this critical value is exceeded, however, it flows as a fluid. When the applied force is removed it does not return completely to its original state (Malkin, 1994).

2.3.1 Flow properties

Very dilute emulsions behave like simple liquids and exhibit Newtonian flow. In more concentrated systems, droplets interact with one another and show viscoelastic behaviour: i.e., they have rheological properties that are partly viscous and partly elastic (Sherman, 1968; Dickinson, 1992).

Non-ideality may manifest itself in a number of different ways; for example, the viscosity of a liquid may depend on the shear rate and/or the time over which the shear stress is applied, or the fluid may exhibit some elastic as well as viscous properties (Macosko, 1994; Tung & Paulson, 1995).

2.3.1.1 Shear-rate-dependent non-ideal liquids

In an ideal liquid, the viscosity is independent of shear rate and the length of time the liquid is sheared (i.e., the ratio of the shear stress to the shear rate does not depend on shear rate or time) (Figure 2.10).

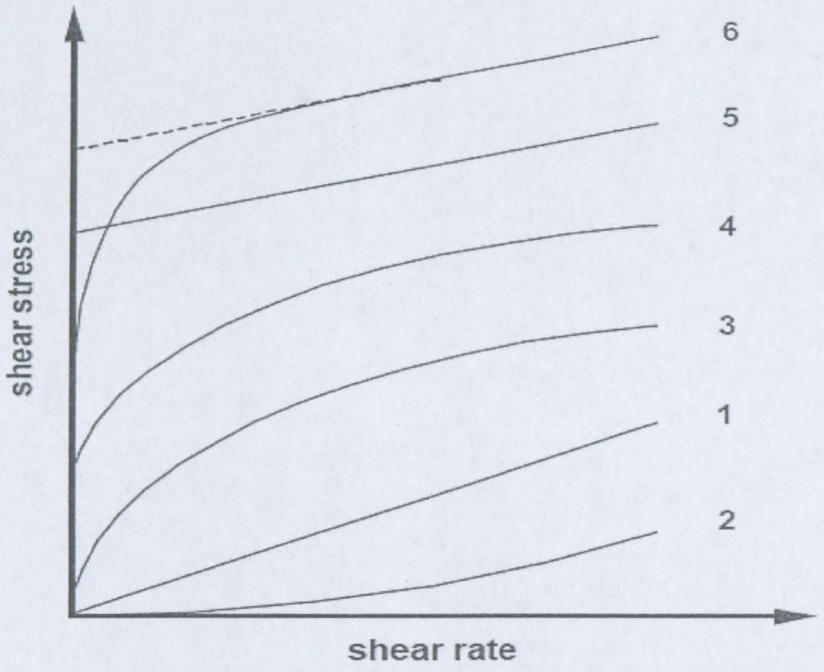

Figure 2.10: Comparison of the flow behaviour of ideal and non-ideal liquids – Shear stress versus shear rate

(Adapted from Becher, 1988)

The viscosity of an emulsion may increase or decrease when the shear rate is increased, rather than remaining constant, as for a Newtonian liquid (Figure 2.10). In these systems, the viscosity at a particular shear rate is referred to as the apparent viscosity. The dependence of the apparent viscosity on shear rate means that it is crucial to stipulate the shear rate used to carry out the measurements when reporting data (McClements, 1999).

According to "Guide of Rheological Nomenclature" (Hackley & Ferraris, 2001), the following classification system covers the six most frequently encountered flow types as illustrated in the accompanying graph (Figure 2.10):

1. *Newtonian*. Differential viscosity and coefficient of viscosity are constant with shear rate (Figure 2.10).

2. *Shear thickening*. Differential viscosity and coefficient of viscosity increase continuously with shear rate (Figure 2.10).
3. *Shear thinning (pseudoplastic)*. Differential viscosity and coefficient of viscosity decrease continuously with shear rate. No yield value (Figure 2.10).
4. *Shear thinning (pseudoplastic) with yield response*. Differential viscosity and coefficient of viscosity decrease continuously with shear rate once the yield stress has been exceeded (Figure 2.10).
5. *Bingham plastic (ideal)*. Obeys the Bingham relation ideally. Above the Bingham yield stress, the differential viscosity is constant, while the coefficient of viscosity decreases continuously to some limiting value at infinite shear rate (Figure 2.10).
6. *Bingham plastic (non-ideal)*. Above the apparent yield stress, the coefficient of viscosity decreases continuously, while the differential viscosity approaches a constant value with shear rate (Figure 2.10).

A number of emulsions exhibit rheological behaviour known as plasticity (Sherman 1968; 1970; Tung & Paulson, 1995). A plastic material has elastic properties below a certain applied stress, known as the yield stress, but flows like a fluid when this stress is exceeded. Above the yield stress, the fluid exhibits non-Newtonian behaviour (e.g., pseudoplastic, dilatant, thixotropic, or rheopectic). The material also exhibits non-ideal elastic behaviour below the yield stress (e.g., the yield point may not be sharply defined; instead, the stress may increase dramatically, but not instantaneously, when the shear rate is increased) (Figure 2.10). This would occur if the material did not begin to flow at all at a particular stress, but experienced a gradual breakdown of the network structure over a range of stresses (Sherman, 1968).

2.3.1.2 Factors influencing rheological behaviour

When interpreting rheological data for emulsions, it should be appreciated that many factors other than the phenomenological effects may exert some effect. All the factors involved are influenced by the chemical nature, and other properties, of the ingredients used in preparing the emulsions (Sherman, 1968). Some of the most important factors associated with emulsion ingredients which influence rheological behaviour are (Sherman, 1968):

1. Internal phase
    a. Volume concentration;
    b. Viscosity; deformation of droplets in shear;

c. Droplet size, and droplet size distribution, technique used to prepare emulsions; interfacial tension between the two liquid phases;
d. Chemical constitution.

2. Continuous phase
   a. Viscosity and other rheological properties;
   b. Chemical constitution;
   c. Electrolyte concentration in the polar medium.
3. Emulsifying agent
   a. Chemical constitution;
   b. Concentration and solubility in internal and continuous phases;
   c. Thickness of film adsorbed around droplets.
4. Additional stabilising agents

Highly concentrated emulsions are classified as high internal phase ratio emulsions (or simply HIPRE emulsions) and the dispersed phase droplets are arranged in a closely packed hexagonal configuration (i.e. far beyond the close packing limit of spherical ordered monodispersed droplets of 74 %). This closely packed configuration and the profound hydrodynamic interaction between neighbouring droplets, induce mechanical interference between the droplets, thus prohibiting their free movement. In such systems, extensive aggregation or flocculation of the dispersed phase droplets occur, which results in a stable, weak, gel-like, particulate network (Jager-Lézer, Tranchant, Alard, Vu, Tchoreloff & Grossiord, 1998; Partal, Guerrero, Berjano & Gallegos, 1997).

High internal phase ratio emulsion systems exhibit a plastic-like response to shear deformations: for small deformations, they resist the shear elastically, with the stress being linearly proportional to the strain; however, for large enough deformations, they flow, offering comparatively much less additional resistance (Webber, 1999; Masalova, Malkin, Slatter & Wilson, 2003a). Grassi, Lapasin and Pricl (1996) mentioned that the plastic behaviour is generally ascribed to the existence of three-dimensional network under limiting shear conditions (i.e. $\gamma \rightarrow 0$). The shear-dependent behaviour just described is typical of weak gel systems (many polymer solutions and dispersed systems), for which the application of large or continuously increasing deformations leads to the progressive breakdown of their networks into smaller clusters (Grassi *et al.*, 1996) leading to a strong decrease in viscosity and permitting the flow of the system (Manca, Lapsin, Partal & Gallegos, 2001). Since nearly all practical applications of emulsions require their transport, it is important to understand

how their flow behaviour is influenced by the surfactant type and concentration and the properties of the constituent droplets, such as their packing, their degree of deformation, their radius and their volume fraction.

As was pointed out by Mason, Bibette and Weitz (1996), the flow properties of compressed, elastic emulsions can be broadly divided into two categories: yielding and steady shear flow. The change from a linear to non-linear stress-strain relationship can be crudely characterised by a yield stress, which marks the significant departure of the microscopic droplet structure from its initial, unsheared configuration. For shear stresses higher than the yield stress, the emulsion flows irreversibly, creating a residual deformation, after the stress has been removed, which cannot be attributed to the equilibrium dissipation of fluctuations. During steady shear flow, the strain rate dependence of the additional viscous stress above the yield stress reflects the interplay of dissipative mechanisms like fluid flow and droplet rearrangements, with storage mechanisms like deformation. Thus the flow properties of the compressed emulsions depend sensitively on the packing and the deformation of the droplets, and on their intrinsic elasticity.

The flow properties of polydispersed emulsions have been extensively investigated in a comprehensive set of experiments using well-controlled samples (Princen & Kiss, 1986b; 1989; Khan & Armstrong, 1987). The flow properties of emulsions have also been investigated theoretically (Princen, 1983) and through simulation (Reinelt & Kraynik, 1989; 1990). Models predicting rheological properties of emulsions were also proposed by Palierne (1990); Madiedo and Gallegos (1997); and Pal (1997; 2001). However, this work was focused on idealised emulsions that were perfectly monodispersed or/and perfectly ordered.

At the limit of the very high volume fraction, the emulsion is composed of a network of thin films, and its stability under shear is determined entirely by the mechanical stability of the intersection of these films at the plateau borders; three continuous phase films which meet at an edge must be separated by 120° angles, and four films which meet at a corner must meet at tetrahedral angles (Thomson, 1887).

2.3.1.3 Flow properties of explosive emulsions

Emulsion explosives show many of the same features as those of more conventional W/O emulsions provided it is remembered that at temperatures below the crystallisation temperature of the dispersed phase (T_d) the shear imparted by a viscometer can often cause crystallisation. This results in appreciable quantities of the solid phase being presented in the measuring region and erratic results are obtained. Also, if waxes are employed as part of the continuous phase, the rheological properties of the emulsion will change at or about the congelation point of the wax (T_c). We shall deal mostly with the effects observed at processing or delivery temperatures which are usually above T_d or T_c. (Becher, 1988).

A typical shear rate viscosity curve for an emulsion explosive at temperature above T_d or T_c is shown in Figure 2.11, from which it can be seen that these materials generally behave as pseudoplastic liquids with upper and lower Newtonian region (Utracki, 1980).

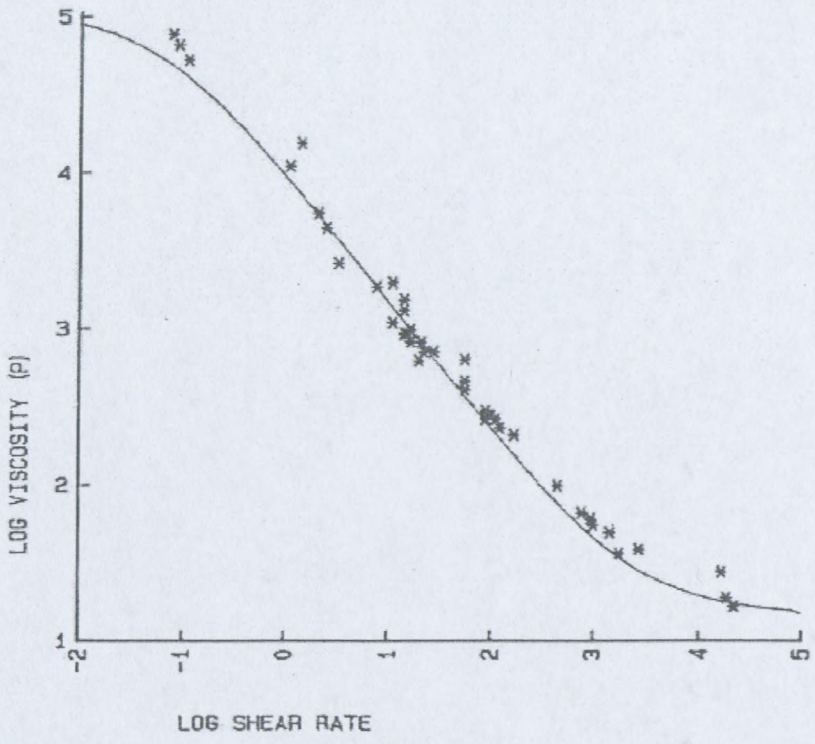

Figure 2.11: Viscosity of emulsion explosives (Utracki, 1980)

(Adapted from Becher, 1988)

Recently Masalova and Malkin (2005; 2007c), Malkin and Masalova (2007) and Kharatiyan (2005) have emphasised the presence of an inflection point on the flow curve of explosive emulsion suggesting two competing processes taking place in the shearing of an emulsion. One of them dominates at low shear rates and leads to an increase in viscosity, while the other prevails at high shear rates, resulting in typical shear thinning behaviour. According to some direct optical observations, the following model was proposed. In the low shear rate domain, drops maintain their shape and flow proceeds as larger particles rolling over smaller ones until a critical shear stress ("second yield stress") is reached. When t = "second yield stress", the drops will more strongly deform and arrange in "trains", thus causing more uniform "inner shear layers" of the oil phase, which triggers the shear thinning behaviour. The plastic deformation of droplets occurs and then results in a catastrophic suppression of the Reynolds mechanism of dilatancy. In addition, the yield stress was found to be proportional to D^{-2}, while Newtonian viscosity is proportional to D^{-1}. In the low shear rate domain, emulsion explosives are rheopectic materials (a slow increase of viscosity at constant shear rate was observed).

2.3.1.4 Effect of surfactant type and concentration

There are no published data on the behaviour of the surfactant film in the high-internal-phase systems such as emulsion explosives. It may be speculated that, since both distortion of droplet shape and shearing of the inter-droplet layer must be involved, for the systems to flow, there would be an effect due to surfactant changes. Indeed, in a quantitative way this can be observed, e.g., oxazoline and amine surfactants tend to give lower viscosity emulsions than do sorbitan derivatives, but little systematic work has been done on this (Becher, 1988).

There is a further mechanism by which a surfactant in this system can affect the rheology. Bampfield and Cooper (1988) have shown that certain polymeric surfactants dramatically increase the viscosity of emulsion explosives, while at the same time making them rubbery. It is possible that such materials operate through bridging between the droplets, giving some structure to the emulsion.

2.3.2 Viscoelastic properties

Malkin (1994) marked that rheological behaviour related to viscoelasticity is the most relevant for the description of a majority of real materials. In general, viscoelasticity is a combination

(or superposition) of characteristic properties for liquids (viscous dissipative losses) and solids (storage of elastic energy). Therefore, a general definition of viscoelastic materials includes two components – elastic potential and intensity of dissipative losses. Viscoelastic behaviour can be considered as a delayed development of stresses and deformations in time, and this delay must not be confused with inertial effects also characterised by a specific lag time.

The time of observation of the viscoelastic processes is very important. The dimensionless criterion called the Deborah Number, De, was introduced to be a measure of a ratio between characteristic time of observation, t_{obs}, and the time scale of inherent processes in material, t_{inh}. The Deborah Number is especially important for viscoelastic phenomena because they always proceed in time. Since the time interval is very wide, it must encounter a situation when the Deborah Number is of the order of 1 (Malkin, 1994).

There are three fundamental experiments, which are treated as reflections of viscoelastic behaviour of a matter:

- Creep – delayed development of deformations under the action of constant force (or stress)
- Relaxation – slow delay of stresses at preserving constant deformation
- Periodic oscillations – harmonic changing of stresses or deformations with relative shift of deformation in relation to stress.

In oscillatory shear, the evolution of the linear viscoelastic functions in the frequency range between 10^{-2} and 10^{2} rad/s, for highly concentrated emulsions, is characterised by the appearance of a minimum in the loss modulus at intermediate frequencies and a "plateau region" in the storage modulus (G'>>G") (Franco, Guerrero & Gallegos, 1995; Franco, Berjano & Gallegos, 1997; Tadros, 1994; Kharatiyan, 2005).

2.3.2.1 Viscoelasticity and microstructural parameters

Some attempts at correlating rheology and microstructural parameters may be found in the literature. An early study based on a model of a foam-like structure valid for monodispersed foams and highly concentrated emulsions was carried out by Princen (1983), who derived an expression that related the elastic shear modulus, G', to the interfacial tension, s, the volume fraction of the dispersed phase, ϕ, and a characteristic size of the unit cell, represented by

the surface-volume mean radius of undistorted spheres, $R_{3,2}$. Princen and Kiss (1986a) extended this treatment to obtain, experimentally, an equation for the small-strain elastic shear modulus for real polydispersed emulsions:

$$G = a\frac{\sigma}{R_{3,2}}\phi^{1/3}(\phi - \phi^*), \qquad \text{Equation 2.25}$$

where a and $\phi*$ are dimensionless constants, although their values may depend slightly on the thickness of the aqueous films located between the oil droplets and droplet size distribution (DSD). The latter constant is thought to be related to the volume fraction of close-packed undistorted droplets (Bengoechea, Cordobés & Guerrero, 2006). Thus, it has been shown that the elastic modulus of a concentrated emulsion is proportional to the interfacial tension, σ, and inversely proportional to the droplet radius, R.

As the thickness of the films separating individual droplets was negligible in the case of the emulsions investigated by Princen and Kiss (1986a; 1989), the above equations are valid for emulsions with negligible interdroplet film thickness. According to Princen (1983), the effect of a finite film thickness can be taken into account by using the effective volume fraction (ϕ_{eff}) of the dispersed phase (instead of the true volume fraction ϕ) in the above equations. The relationship between (ϕ_{eff}) and ϕ is given by (Princen & Kiss, 1986a)

$$\phi_{eff}^{-1/3} = \phi^{-1/3} - 1.105\frac{h}{D}, \qquad \text{Equation 2.26}$$

where h is the film thickness and D is the average droplet diameter.

According to this model, the considerable elasticity of the concentrated emulsions exists only because the repulsive droplets have been compressed by an external osmotic pressure Π, and thus concentrated to a sufficiently large droplet volume fraction $\phi > \phi*$, which permits the storage of interfacial elastic shear energy (Dimitrova & Leal-Calderon, 2004). Indeed, two droplets forced together will begin to deform before their interfaces actually touch, due to the intrinsic repulsive interactions between them. Thus, emulsions minimise their total free energy by reducing the repulsion (which may have a different origin) at the expense of creating some additional surface area by deforming the droplet interfaces. The necessary work to deform the droplets is done through the application (by any means) of an external osmotic pressure, π, and the excess surface area of the droplets determines the equilibrium of elastic energy stored at a given osmotic pressure. Provided the droplets are compressed by an osmotic pressure, additional excess surface area created by a perturbative shear deformation determines the elastic shear modulus, G'(ϕ) (Dimitrova & Leal-Calderon, 2004).

Some authors have successfully used this equation to correlate structural and rheological parameters for emulsions stabilised by low molecular weight surfactants (Princen & Kiss, 1986b; Pons *et al.*, 1995; Sánchez, Berjano, Brito, Guerrero & Gallegos, 1998) or polymeric surfactants (Perrin, 2000). Working on monodispersed concentrated emulsions of dodecane stabilised by sodium dodecyl sulphate (SDS), Mason *et al.* (1997) have observed a sharp increase of the elasticity at $\phi*$ and have shown that the elastic modulus of the concentrated emulsion could be rescaled by σ /R, in agreement with Princen's model. Nevertheless, they obtained a universal master curve for the evolution of G′ versus ϕ that obeyed the following relationship:

$$G' \propto \phi\left(\phi - \phi^*\right), \qquad \textbf{Equation 2.27}$$

where $\phi*$ is the close-packing volume fraction that has a value of 0.64 for randomly packed monodispersed spheres. Therefore, the elasticity is governed by the Laplace pressure, $2s/R_{32}$ of the droplets, in agreement with Princen's model. Their work has provided incontestable proof for the original work by Princen, who first predicted the scaling of the G' with the capillary pressure, σ/R (σ being the interfacial tension and R being the drop radius). Moreover, the scaling with σ/R confirms that the elasticity of compressed monodispersed emulsions depends only on the packing geometry of the droplets (Dimitrova & Leal-Calderon, 2004). However, the increase of the elastic modulus was slower than originally predicted by Princen. By means of numerical simulations of shearing of soft spheres, Lacasse, Grest and Levine (1996) showed that this quasi-linear rise of G′ with ϕ was due to the positional disorder of the droplets. Indeed, due to disorder, under an affine deformation, droplets depart randomly from affine motion and thus relax some of the imposed deformation, leading to a smaller elasticity than that predicted for ordered systems and in good agreement with Mason's experimental results.

Some authors have recently tried to use the scaling procedure reported by Mason *et al.* (1997) for protein-stabilised oil-in-water emulsions (Dimitrova & Leal-Calderon 2001; 2004; Bressy, Hebraud, Schmitt & Bibette, 2003), water-in-oil emulsions stabilised by non-ionic polymeric and non-ionic low molecular weight surfactants (Malkin *et al.*, 2004a; Masalova & Malkin, 2007a; 2007c; Alvarez, Mougel, Baravian, Calton, Marchal, Stébé & Choplin, 2006; Lee, 2006). However, the elastic modulus was much higher than that predicted by Princen's model or Mason's law. Thus, an additional source of elasticity should be considered.

2.3.2.2 Additional sources of elasticity: Effect of surfactant type and concentration

- **Interfacial dilatational and shear elasticity**

In all studies cited above, it was implicitly supposed that the interfacial tension does not change with the application of the perturbative strain, due to the rapid relaxation or the surfactant layers. This corresponds to the case of deformation/strain applied at zero frequency. In fact, at non-zero frequency, the local variation of the interfacial tension (interfacial elasticity) will also contribute to the overall elasticity, and the stored elastic energy can be higher than at rest (zero frequency) (Dimitrova & Leal-Calderon, 2004).

Lacasse *et al.* (1996) performed Monte Carlo simulations aimed at predicting the dependence of the elastic shear modulus on the volume fraction. Their simulations provide a physical insight into the origin of the behaviour of the shear modulus of emulsions: The energy of deformation per facet (film) formed between two neighbouring droplets is not Hookean; i.e., the droplets do not relax instantaneously.

Hemar, Hocquart & Lequeux (1995) also considered the visco-elasticity of emulsions and showed that both dilatational and shear elasticity of the stabilising amphiphilic layer contribute to the emulsion's overall elasticity. The contribution is pronounced differently for the dilatational and shear case, being, as expected, a function of the frequency of the deformation. Evidently, interfacial layers will produce an experimentally observable effect only if their relaxation time is comparable (or higher) to the inverse frequency applied in the conventional mechanical rheometers. Generally, the frequencies at which the elastic shear modulus of an emulsion is determined are of the order of 1 Hz. The relaxation time of surfactant monolayers is of the order of milliseconds (or even less), therefore, no surface elasticity effects are detectable for a low molecular weight surfactant under typical experimental conditions. The elasticity of the polymeric layers is generally much higher than the elasticity of the low molecular weight surfactants and, since the polymeric layers can store energy themselves, it is reasonable to expect this effect to influence the bulk (3D) rheology of emulsions (Dimitrova & Leal-Calderon, 2004).

Buzza and Cates (1994) have shown that the free energy change, δF, of a piece of interface whose area, A, is increased by δA, obeys:

$$\frac{\delta F}{A} = \sigma\left(\frac{\delta A}{A}\right) + \frac{1}{2}\varepsilon\left(\frac{\delta A}{A}\right)^2 \quad , \qquad \textbf{Equation 2.28}$$

where ε is the elasticity of the layer, which can be formally defined in different ways.

For a static strain (zero frequency) one has $F \propto G\alpha^2$, where $G = G' (\omega = 0) \propto \sigma/R$. This arises purely from the first term on the right-hand side in Equation (2.28). At non-zero frequency, the local variation of the interfacial tension will also contribute, and the stored elastic energy can be higher than in equilibrium (zero frequency). Note that the term 'non-zero frequency' always should be considered in conjunction with the characteristic relaxation time of the surfactant layer stabilising the emulsion. A different approach was adopted by Hemar *et al.* (1995). They suggested scaling rules for *G'* in the case of concentrated emulsions stabilised by layers with dilatational viscosity or shear elasticity. The scaling with the capillary pressure on the non-deformed droplets is preserved, but the viscoelastic nature of the interfacial layers leads in both cases to an increase in G', i.e. $G' (\omega > 0) > G' (\omega = 0)$.

Dimitrova and Leal-Calderon (2004) have studied the oscillatory shear behaviour of protein-stabilised HIPRÉs of small droplet size (mean radius about 0.25 μm). Their data do not support the shear modulus equation of Princen and Kiss. The values of $G'/(\sigma/R)$ exhibited by their protein-stabilised emulsions were substantially larger than the ones obtained for equivalent emulsions stabilised by low molecular weight surfactants. They found that the protein layer adsorbed at the surface of the droplets contributes to the emulsion's overall elasticity.

Hemar and Horne (2000) measured the dynamic rheological properties (storage and loss moduli) of protein-stabilised HIPRÉs over a ϕ range of 0.68-0.89. The Sauter mean radius of the droplets was approximately 10 μm. Their data supported the shear modulus equation of Princen and Kiss (1983; 1986a).

The rheological behaviour of soya bean oil emulsions stabilised by sodium caseinate (0.1 and 0.7 % sodium caseinate) was studied by Bressy *et al.* (2003). While having a very low interfacial tension (σ = 0.1 mN/m and 0.3 mN/m; D =1 μm and 6 μm), these emulsions, when concentrated up to an oil volume fraction of 64 %, have very high elasticity. It is 30 times higher than those usually observed for surfactant-stabilised emulsions. This high elasticity originates from the interfacial shear elasticity of the bilayer interface. The elastic shear modulus can be rescaled by 1/R but not by σ/R, as predicted by Mason *et al.* (1997). So, sodium caseinate-stabilised droplets can be regarded as droplets coated with a solid shell (Bressy *et al.*, 2003). An opposite result was observed on hexadecane-in-water emulsions

stabilised by casein (Dimitrova & Leal-Calderon, 2004). This is probably due to the high value of the interfacial tension (14.5 mN/m) which might hide the other possible origins of the elasticity or individual pure casein used by Dimitrova and Leal-Calderon (2004), which does not have the same interfacial characteristics as the caseinate aggregates used in Bressy's work (Bressy *et al.*, 2003).

Highly concentrated oil-in-water (O/W) emulsions stabilised by means of gluten and soya protein isolate (SPI) at low pH have been characterised by means of linear dynamic viscoelasticity (Bengoechea *et al.*, 2006). It should be noted that, in general, the values obtained for SPI-based emulsions were much higher than those shown for gluten-based emulsions. This effect should be attributed to a difference in the values of the interfacial tension (Bengoechea *et al.*, 2006). The Mason model of elasticity of compressed emulsions has been used to correlate viscoelastic and microstructural parameters, giving adequate fitting but underestimating the elastic properties obtained for the highest concentration of gluten. According to the authors, these deviations can be explained in terms of an enhancement of the elastic network formed in the aqueous phase in which the glutenin fraction must play an important role.

- **Pair interaction potential energy**

From a general point of view, the elasticity of concentrated dispersions was closely related to the pair interaction potential energy (Quemada & Berli, 2002). On the other hand, in the case of emulsions concentrated above the critical random packing volume fraction, the elasticity is related to the interfacial energy of deformed droplets (Princen & Kiss, 1986a). Nevertheless, this local elasticity is transmitted at the sample scale through the interaction potential between droplets (Alvarez, Mougel, Bravian, Caton, Marchal, Stébé & Choplin, 2006).

Some authors pointed out the importance of the nature of the interaction potential between droplets, which depends on the surfactant type and concentration:

- If the inter-droplet potential energy is purely repulsive for all ranges of $\phi > \phi*$, i.e. the inter-droplet pair energy does not present any inflection point (Figure 12a), the elasticity is related only to the interfacial energy of deformed droplets. Indeed, Alvarez *et al.* (2006) stated that the use of ionic surfactants makes electrostatic repulsion forces dominant. In this case, the elasticity is only determined by the interfacial tension of deformed droplets. Buzza and Cates (1994) have found that, for oil-in-water emulsions stabilised with ionic surfactants, double-layer forces between the charged oil drops had a significant effect on the osmotic pressure, up to a factor of

three or four for the experimentally achievable conditions of small emulsion drops and low ionic strength in the continuous water phase (for example, undeformed drop radius R ~ 1 μm, σ = 0.01 mN/m). But the double layer force contribution to G (ϕ) for this small-drop, low ionic strength emulsion has been found negligible.

- If the potential pair energy presents any inflection point associated with the very short-range attractions, the overall elasticity of the system is determined not only by the interfacial properties; the interaction potential between droplets can also play an important role (Figure 2.12b). Indeed, Alvarez *et al.* (2006) stated that, in the case of non-ionic surfactants, because there is no electrostatic charge on the surface of droplets, the dominant behaviour of the system could be due to van der Waals forces. According to these authors, this could explain the dependence $G' \propto D^{-2}$ showed by their experimental results. Quintero, Noïk, Dalmazzone and Grossiord (2008) corroborated that it would seem that Princen's model could be invalid for very high volume fractions (ϕ > 90 %), i.e. $h \rightarrow 0$; for such volume fractions stabilised by a non-ionic surfactant, another correlation would be necessary, taking into account the van der Waals attraction between the close droplets.

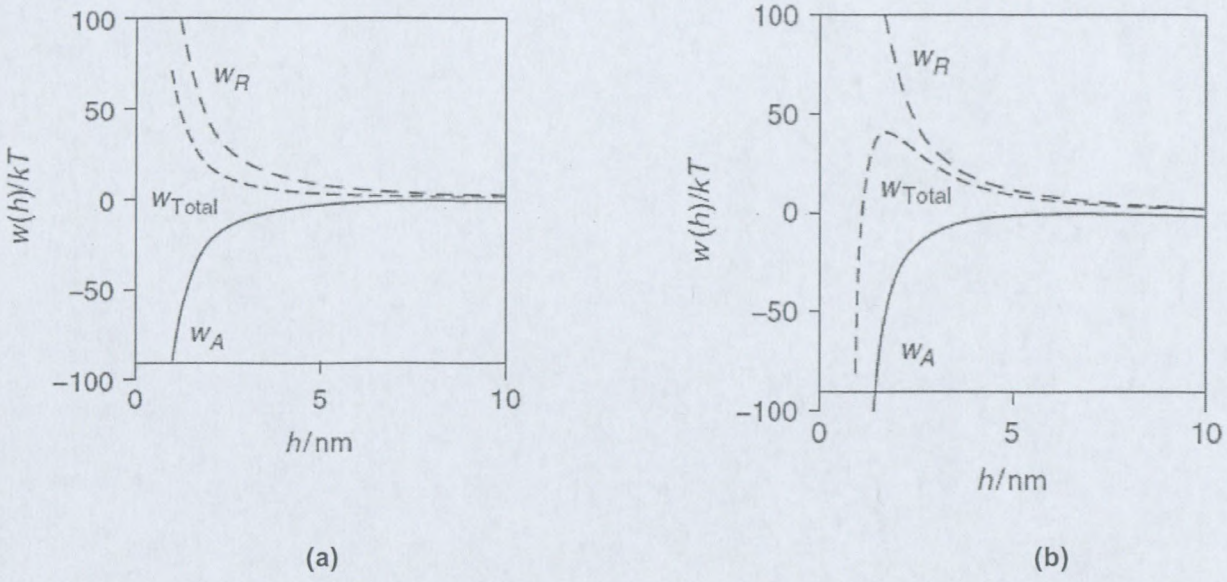

Figure 2.12: The overall interaction of a pair of emulsion droplets depends on the relative magnitude and range of any attractive and repulsive interactions. The overall interaction may be repulsive (a) or attractive at some separations and repulsive at others (b)

(Adapted from McClements, 2005:3)

Malkin *et al.* (2004a) and Masalova and Malkin (2007a; 2007c) have studied the dependence of the elastic modulus on the average droplet size and on the volume fraction of highly concentrated water-in-oil emulsion stabilised by Pibsa-based surfactants (non-ionic polymeric surfactants) in the presence of a high concentration of micelles. The expected dependence of the elastic modulus on the reciprocal diameter, as proposed in some theoretical models (Princen & Kiss, 1986; Babak *et al.*, 2001; Pal, 2002b) and observed by several authors (see, e.g., Aronson & Petko, 1993; Pons *et al.*, 1992b; Langenfield, Schmitt & Stébé, 1999), did not correspond to their experimental data, whereas the dependence of the elastic modulus on D^{-2} is really linear, i.e., emulsions exhibited relatively high values of the elastic modulus in comparison to Princen's model.

Alvarez *et al.* (2006) confirmed the dependence $G' \propto D^{-2}$ on a highly concentrated water-in-oil emulsion stabilised by sorbitan monooleate, a non-ionic non-polymeric surfactant, in the presence of a high concentration of micelles. Another interesting experimental observation from Alvarez *et al.* (2006) is the divergence of G' when ϕ approaches 1. This divergence,, again, is not taken into account in Princen's model.

Lee (2006) has studied the dependence of the storage modulus and the yield stress with the average droplet size of a highly concentrated water-in-oil emulsion (ϕ = 0.89; 2.5-24 μm; surfactant/oil = 0.19) stabilised by a non-ionic surfactant, SMO, in concentration well above the CMC. He found the dependence $\tau_y \propto D^{-1.35}$.

Pal (2006) has studied the oscillatory shear behaviour of a series of O/W emulsions ($0.7855 < \phi < 0.9402$; d = 1.28 and 1.95 μm; continuous phase: de-ionized water) stabilised by a non-ionic surfactant, octylphenol ethoxylate, in a concentration well above the CMC. The Princen and Kiss equation described the storage modulus data very well when $\phi = 0.93$; at higher values the experimental data fell above the predicted values.

Quintero *et al.* (2008) studied water-in-oil type emulsions formed during the crude oil production process in the presence of natural non-ionic surfactants, asphaltenes and resins ($0.7 < \phi < 0.8$; d = 5 μm). They found that elasticity was determined by the surface energy, as predicted in Princen's model.

2.3.2.3 Effect of micelle concentration: adhesive emulsions

In the presence of micelles in the oily phase, adhesive forces are generated due to the non-compensated osmotic (depletion) pressure exerted by micelles on the emulsion droplets because of the impossibility of the micelles to penetrate into the narrow gap between the droplets (Figure 2.13) (Babak & Stébé, 2002). This attraction is purely entropic, and depends on the parameters characterising the micellar solution of the continuous phase in the emulsion (micellar concentration, size, shape, electric charge, etc.)

As has been shown by Aronson and Princen (1980a; 1980b), when increasing the surfactant or electrolyte concentrations, the oil-in-water emulsions stabilised by ionic surfactants (e.g., alkyl sulphates, alkyl carboxylates) presents adhesive properties. Adhesive properties are also observed in the case of highly concentrated water-in-oil emulsions stabilized by non-ionic surfactants (Aronson & Petko, 1993; Leal-Calderon, Gerhardi, Espert, Brossard, Alard, Tranchant, Stora & Bibette, 1996), as well as in the presence of non-adsorbing polymers in the continuous liquid phase (Perrin, 2000). This adhesiveness is characterised by a critical dependence of the functional properties of emulsions on the surfactant C_s and electrolyte C_{el} concentrations, temperature T and on the droplet radius R (Aronson & Princen, 1980a; Aronson & Petko, 1993). Beginning with some threshold values of these parameters, the droplets become adhesive and form remarkably high contact angles (sometimes as large as ~65°) (Babak & Stébé, 2002). This means that the latter properties sharply increase, beginning by some critical value of C_{el}, C_s, T, or R.

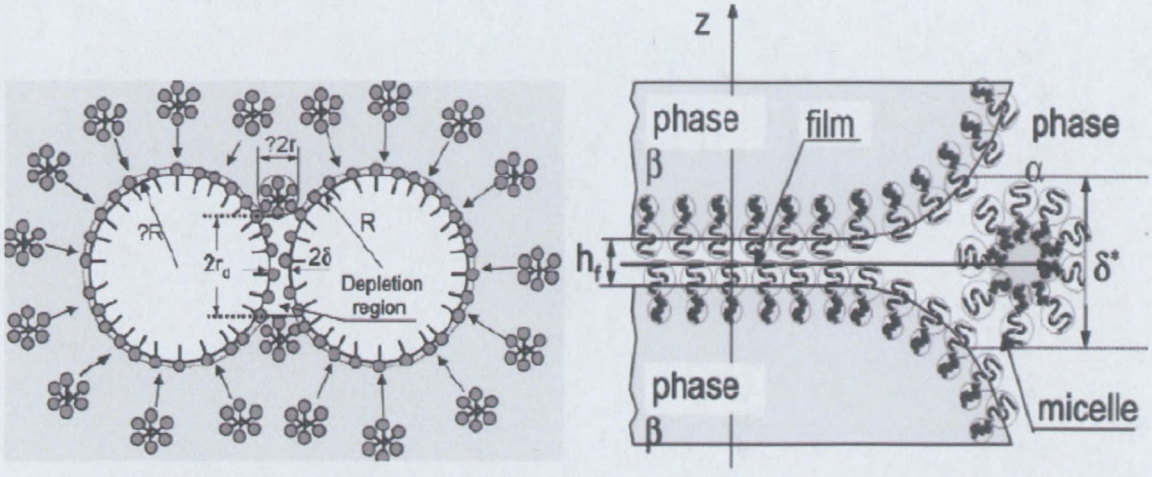

Figure 2.13: Schematic illustrating the mechanism of depletion attraction between two emulsion droplets

(Adapted from Babak *et al.*, 2002:6)

As pointed out by Babak and Stébé (2002), the attraction between liquid droplets is responsible for the viscoelastic properties of gel-emulsions. According to the authors, the Princen model describes the observed experimental dependence G' ~ σ/R correctly, although it does not rely on the proportionality of G' to the capillary pressure P_c in the droplets, which is also proportional to the ratio σ/R. These emulsions exhibit a yield stress proportional to the adhesion force f_a^* that is characteristic of a plastic solid. According to the theory of adhesion of fluid particles, f_a^* is proportional to free adhesion energy between the interfaces in thin emulsion films, $\Delta_{ad}F$, and, consequently, there is proportionality between τ_y and $\Delta_{ad}F$.

2.3.3 Rheological properties of high internal phase suspo-emulsions

After an emulsion has been prepared, changes occur which lead to a deterioration in rheological properties. In all applications of highly concentrated emulsions, two principal characteristics determine their properties: their rheological properties in a newly prepared state ("fresh" material) and the stability of these properties in time during their storage (ageing). Storage is important because highly concentrated emulsions consist of incompatible components, and from the thermo-dynamical position are unstable, with a tendency for coalescence and phase separation. In the case of emulsion explosives, the aqueous phase is a supersaturated nitrate salt solution (at room temperature) and therefore the instability is mostly derived from the crystallisation of the meta-stable aqueous phase. Thus, during the ageing process, the two-phase samples will transform to multiphase dispersions, the substances consisting of two phases (droplets and crystals) dispersed within a continuum of a third phase. Being transformed into particle suspensions (crystals) in viscoelastic media (emulsion) the studied samples can exhibit interesting rheological properties (Pal, 2000b; Marcovich, Reboredo, Kenny & Aranguren, 2004; Harzallah & Dupuis, 2003).

In such a system, the emulsion acts as the continuous phase, while the solid crystals act as the dispersed phase. During storage, slow morphological changes of these crystals take place, from the multi-crystalline form of a drop toward a better-defined single crystal. The remaining droplets in the absence of the heterogeneous nuclei can be supercooled down to the homogeneous nucleation temperature, T_{hn} (K):

$$T_{nh} = k\,(T_d + 273), \qquad \textbf{Equation 2. 29}$$

where k = 0.82±0.02, and T_{hn} = -3 ^{0}C to 11 ^{0}C, T_d is a fudge point. If the emulsion explosive system is carefully cooled to $T_{hn} < T < T_c$, the system can be described in terms of the rheology of a partially crystallised oil phase, which primarily depends on the rigidity of the matrix, the wax content in the oil phase, but not on the size and/or concentration of the dispersed water droplets. If the material is sheared, the aqueous phase will crystallise, leading to eventual solidification of the emulsion explosive.

While a significant amount of published literature exists on the rheology of suspensions (Jeffrey & Acrivos, 1976; Metzner & Whitlock, 1958; Michaels & Bolger, 1962) and emulsions (Langenfeld *et al.*, 1999; Pons *et al.*, 1995; Bower, Gallegos, Macley & Madiedo, 1999; Princen, 1983; 1985; Princen & Kiss, 1986b; Jager-Lézer *et al.*, 1998; Malkin *et al.*, 2004a), little work has been reported on the rheology of high internal phase suspo-emulsions. However, from studies conducted by Pal (1990) and Yuhua, Pal and Masilyah (1991), the following conclusions can be drawn pertaining to the rheology of suspo-emulsions:

- At lower volume fractions of the solids, i.e. $\phi_s < 0.1$, the size of the solid particles exerts little effect on the rheology of emulsion systems. However, at $\phi_s > 0.1$, the solid particle size effect is more pronounced, and the smaller the size the larger the size effect.
- Addition of solids to emulsion systems leads to bimodal size suspo-emulsion systems with higher viscosities than the parent monomodal emulsion systems.
- The emulsion system acts as a continuous phase towards the solids, when the solids are much larger than the emulsion droplets, i.e. when the size ratio of solids to droplets $\frac{d_s}{d} > 3$. In such systems, the Barnea and Mazrahi (1973) equation can be used to describe the viscosity of the suspo-emulsion relative to that of solid-free emulsions, provided the shape of the solid particles is spherical and $\phi_s \leq 0.04$.
- In general, suspo-emulsions always have higher viscosities than solid-free emulsions at the same total concentration of the dispersed phase (Hugelshofer, Windhab & Wang, 2000; Hiemenz & Rajagopalan, 1997).
- The effect of solid shape on the viscosity decreases as the shear stress increases, and that the more the solid shape deviates from that of sphere, the higher is the viscosity of the suspensions (Bampfield & Cooper, 1988; Pal *et al.*, 1990; Yuhua, Pal & Masliyah, 1991; Utracki, 1980).

2.4 Summary

Emulsion explosives are highly internal phase water-in-oil emulsions. The aqueous phase is a supersaturated nitrate salt solution (at room temperature), with a volume fraction usually greater than 0.8. Aqueous phase droplets are deformed by packing and contact with neighbouring droplets.

Despite being comprised solely of liquids, emulsions consisting of highly concentrated droplets can possess a striking shear rigidity that is characteristic of an elastic solid, which sensitively affects their flow properties (Dimitrova & Leal-Calderon, 2004; Masson *et al.*,1997). Since nearly all practical applications of emulsions require their transport, it is important to understand how different formulation factors affect

- The emulsion elasticity in a newly prepared state ("fresh" materials) and
- Their structural stability with time in the context of the evolution of rheological properties and structure during ageing.

Some attempts in correlating rheology and microstructural parameters may be found in the literature. An early study based on a model of a foam-like structure valid for monodispersed foams and highly concentrated emulsions has been carried out by Princen (1983). According to this model the considerable elasticity of the concentrated emulsions exists only because the repulsive droplets are deformable and thus can store the interfacial elastic shear energy (Dimitrova & Leal-Caledron, 2004; Mason *et al.*, 1997). Therefore the elasticity is governed by the Laplace pressure, $2\sigma/R_{32}$, of the droplets. Some authors have successfully used this equation to correlate structural and rheological parameters for emulsions stabilised by low molecular weight surfactants (Princen & Kiss1986b; Pons *et al.*, 1995; Sanchez *et al.*, 1998) or polymeric surfactants (Perrin, 2000).

Some authors have recently tried to use the scaling procedure reported by Mason and co-workers for protein-stabilised oil-in-water emulsions (Dimitrova & Leal-Calderon, 2001; 2004; Bressy *et al.*, 2003), for non-ionic polymeric-based water-in-oil emulsions (Malkin *et al.*, 2004a; Masalova & Malkin, 2007a; 2007c) and for non-ionic low molecular weight-based water-in-oil emulsions (Alvarez *et al.*, 2006; Lee, 2006). However, the elastic modulus was much higher than that predicted by Princen's model or Mason's law. Thus an additional source of elasticity should be considered.

Hemar *et al.* (1995) and Buzza and Cates (1994) have shown that both the dilatational and the shear elasticity of the stabilising amphiphilic layer contribute to the emulsion's overall elasticity. The contribution is pronounced differently for the dilatational and shear case, being a function of the frequency of the deformation. Bressy *et al.* (2003) pointed out that, while the interfacial tension is very low the interfacial shear elasticity can become the main source of elasticity. According to the authors, the elastic shear modulus in this case can be rescaled by 1/R but not by σ/R, as predicted by Mason *et al.* (1997).

Some authors pointed out the importance of the nature of the interaction potential between droplets, which depends on surfactant type and concentration:

- If the inter-droplet potential energy is purely repulsive for all ranges of $\phi > \phi*$, the elasticity is related only to the interfacial energy of the deformed droplets (Alvarez *et al.*, 2006; Dimitrova & Leal-Caledron., 2004; Perrin, 2000). Indeed. Alvarez *et al.* (2006) stated that the use of ionic surfactants makes electrostatic repulsion forces dominant. In this case, the elasticity is only determined by the interfacial tension of the deformed droplets. Buzza and Cates (1994) have found that, for oil-in-water emulsions stabilised with ionic surfactants, double-layer forces between the charged oil drops have a significant effect on the osmotic pressure. However, the study of the contribution of double-layer forces to G (ϕ) have been found to be negligible.
- If the potential pair energy presents any inflection point associated with the very short-range attractions, the overall elasticity of the system is determined not only by the interfacial properties; the interaction potential between droplets can also play an important role. Indeed, Alvarez *et al.* (2006) stated that, in the case of non-ionic surfactants, because there is no electrostatic charge on the surface of droplets, the dominant behaviour of the system could be due to van der Waals forces. According to the authors, this could explain the dependence $G' \propto D^{-2}$ showed by their experimental results. Quintero *et al.* (2008) corroborated that it would seem that Princen's model could be invalid for very high volume fractions (ϕ > 90 %), i.e. $h \rightarrow 0$; for such volume fractions stabilised by a non-ionic surfactant, another correlation would be necessary, taking into account the van der Waals attraction between the close droplets.

Malkin *et al.* (2004a) and Masalova and Malkin. (2007a; 2007c) have studied the dependence of the elastic modulus on the average droplet size and on the volume fraction of highly concentrated water-in-oil emulsions stabilised by Pibsa-based surfactants (non-ionic polymeric surfactants) in the presence of a high concentration of micelles. The expected

dependence of the elastic modulus on the reciprocal diameter, as proposed in some theoretical models (Princen & Kiss, 1986a; Babak *et al.*, 2001; Pal, 2002) and observed by several authors (see, e.g., Aronson and Petko, 1993; Pons *et al.*, 1992b; Langenfield *et al.*, 1999), did not correspond to their experimental data, whereas the dependence of the elastic modulus on D^{-2} was really linear, i.e., emulsions exhibited relatively high values of the elastic modulus in comparison with the Princen model.

.

Lee (2006) studied the dependence of the storage modulus and the yield stress with the average droplet size of a highly concentrated water-in-oil emulsion (ϕ = 0.89; 2.5 - 24 μm; surfactant/oil = 0.19) stabilised by a non-ionic surfactant, SMO, in concentrations well above the CMC. He found the dependence $\tau_y \propto D^{-1.35}$.

Pal (2006) studied the oscillatory shear behaviour of a series of O/W emulsions ($0.7855 < \phi < 0.9402$; d = 1.28 and 1.95 μm; continuous phase: de-ionized water) stabilised by a non-ionic surfactant, octylphenol ethoxylate, in concentrations well above the CMC. The Princen and Kiss equation described the storage modulus data very well when ϕ = 0.93; at higher values the experimental data fell above the predicted values.

After an emulsion has been prepared, changes occur which lead to a deterioration in rheological properties. In the case of emulsion explosives, the instability mostly derives from the crystallisation of the meta-stable aqueous phase. Thus, during the ageing process, the two-phase samples will transform into multiphase dispersions, the substances consisting of two phases (droplets and crystals) dispersed within a continuum of a third phase.

The freezing behaviour of emulsified aqueous solutions seems to be strongly dependent on the chemical structure of the surfactant and its possible influence on surfactant-electrolyte interactions (Ganguly *et al.*, 1992) and on the strength of the interface (White *et al.*, 2005). The emulsions which are expected to be more stable to shear at low surfactant concentrations are those with the more intense surfactant-electrolyte interactions (Ganguly *et al.*, 1992) and/or the most complex interface, but in which the interface is not very thick and lumpy. The latter could act as an inhibitor preventing the crystallisation in one of the micron scale aqueous droplets to propagate through the rest of the emulsion, crystallising all droplets (White *et al.*, 2005).

Above the CMC, depending on the type of surfactant, the penetration of crystallinity throughout the substance could be strongly dependent on micelle concentration (White *et al.*, 2004). Indeed, explosive emulsions produced by using polyisobutylene-based surfactants are highly stabilised by a significant number of surfactant-rich reverse micelles a few nanometres in diameter in the oil phase. The hypothesis in the proposal that crystallisation was triggered by changes in the monolayer at the aqueous oil interface allowing contact between the contents of different droplets seems untrue. It is the reverse micelles that prevent such contacts by an unknown mechanism. The highly unstable emulsions are those in which the reverse micelle concentration is very small (White *et al.*, 2004).

2.5 Research issues identified

The main shortcoming in the present-day state of knowledge of rheological properties of highly concentrated inverse phase emulsions is the absence of systematic experimental data, especially concerning

- the effect of the oil phase composition (type and concentration of surfactant) on the rheology of fresh emulsion explosives
- the slow evolution of emulsion properties with different types and concentrations of emulsifiers, as a result of ageing, leading to delicate structural rearrangements of a colloid system.

It must also be mentioned that, among the numerous published works devoted to emulsions, only a limited number touch on emulsions of the type which is the subject of this project, i.e. emulsions in which the dispersed phase is formed by supercooled water solutions of inorganic salts. Meanwhile, the metastable nature of this phase creates new and very promising features for these types of systems.

The interest in such highly concentrated emulsions is great because they have numerous potential technological applications in cosmetics, mining, oil recovery and explosives. In all these applications, two principal characteristics of highly concentrated emulsions determine their properties, their rheological properties in a newly prepared state ("fresh" materials) and the stability of these properties over time during their storage. Storage is important because highly concentrated emulsions are unstable, with a tendency to coalescence and phases to separate. The results from studies of the rheological properties of highly concentrated emulsions are rather rarely published, though some interesting exceptions are known.

Very little is known and published concerning the correlation of direct observations of structural processes in the ageing of emulsions with changes of their rheological properties. This presents a significant problem because only an understanding of the structural processes of emulsions will enable us follow the evolution of the rheological properties, which determines their application value.

The main objective of this study was to determine how the surfactant type and concentration affects the structural stability of highly concentrated water-in-oil emulsion explosives over time in the context of the evolution of rheological properties and structure during ageing.

CHAPTER 3
RESULTS AND DISCUSSION

3.1 Introduction

This chapter is devoted to the interpretation of experimental results of an investigation of the rheological properties of highly concentrated water-in-oil emulsions and the kinetics of the crystallisation process of the aqueous phase of an emulsion with ageing. The results of the measurements include:

- Flow properties
- Viscoelastic properties
- X-ray diffraction patent analysis
- Optical observations

The main goal of this work, however, was to correlate rheological parameters of emulsion explosives with the kinetics of the crystallisation process of the emulsion's aqueous phase with ageing, in order to estimate the stability of the emulsion with ageing by a measured constant, namely yield stress. Emulsion formulations with four different surfactant types, each of them used in two different concentrations, were investigated. Samples of fresh emulsions were investigated by all the above-mentioned methods. All tests were repeated weekly over a period of 36 weeks under the same experimental conditions.

3.2 Materials

Samples were provided by Lake International Technologies as surfactants dissolved in hydrocarbon-based oils at various concentrations. Four surfactants were used for this study; they are known here as Pibsa-MEA, Pibsa-IMIDE, Pibsa-UREA, and SMO. The first three are derivatives of Polyisobtylene succinic anhydride (Pibsa). So, they belong to the same type of chemical compounds, though with different end groups, and they can be treated as oligomers, while SMO (a sorbitan ester) is a monomeric product. Mixtures of Pibsa-MEA and SMO (taken in the ratio 10:1) were used in some cases. When originally synthesised, the surfactants were dissolved or dispersed in Parprol 32, paraffinic petroleum oil with no additives. Further dilution with other hydrocarbon-based oils was used to achieve the desired concentration and viscosity.

Two oils besides Parprol 32 where used in this study; here they are named Shellsol 2325, and Mosspar-H.

3.2.1 Surfactants

The hydrophobic moiety for the three Pibsa derivatives is the polyisobutylene group, with an approximate relative molecular mass of 1050; the hydrophilic moiety is the modified succinic anhydride group, with an approximate relative molecular mass of 150. Thus the hydrophilic-lipophilic balance (HLB) lies heavily towards lipophilicity (i.e. hydrophobicity), and the surfactants are soluble in hydrocarbon oils, but insoluble in water. For the SMO, the hydrophobic moiety is an oleic group with an approximate relative molecular mass of 280. The hydrophilic moiety is the sorbitan group with a relative molecular mass of 160. Thus the balance is also towards lipophilicity.

3.2.1.1 Pibsa-MEA

This, described by Lake as Pibsa (i.e. polyisobutylene succinic anhydride) of molecular weight 1048, reacted approx 1:1 with monoethanolamine to an uncondensed amide/acid head group, as shown in Figure 3.1.

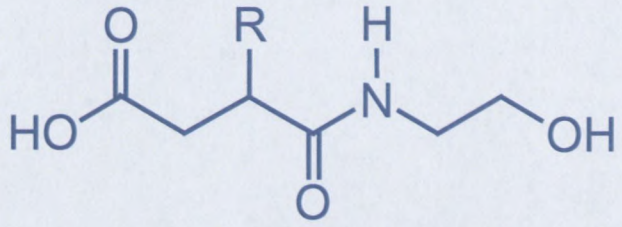

Figure 3.1: Structure of Pibsa-MEA

The R indicates polyisobutylene, the repeat unit of which is $-C(CH_3)_2-CH_2-$ i.e. a chain of carbon atoms with two methyl side groups attached to every second one. To give a molecular weight of 1048, there would have to be about 19 repeat units in the chain. If these are contained in a single chain, the length would be 38 carbon atoms with an additional 38 in the methyl side groups (the chain may be attached to the carbon atom adjacent to the carboxylic acid group, rather than the one adjacent to the amide group as shown). The overall molecular weight will be about 1109. The HLB number is not known precisely, but will be low (< 4). One of the possible conformations of Pibsa-MEA surfactants is shown in Figure 3.2.

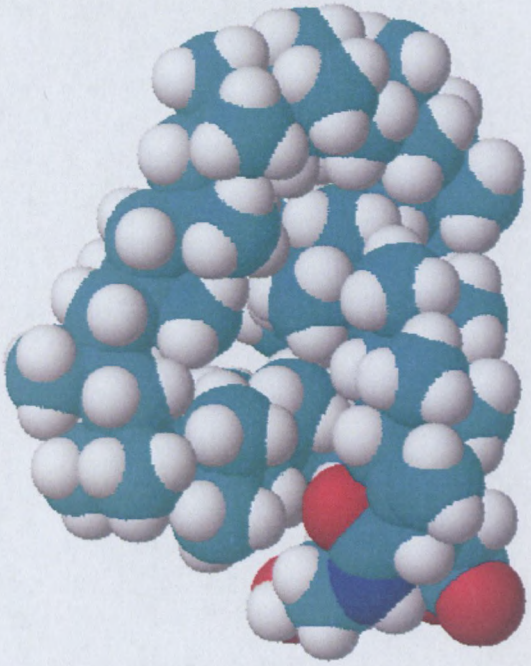

Oxygen – red
Nitrogen – blue
Carbon – light blue
Hydrogen - white

Figure 3.2: 3-D VIEW of one of the possible conformations of Pibsa-MEA

3.2.1.2 Pibsa-IMIDE

Pibsa-IMIDE is described by Lake as Pibsa-MEA condensed to an N-substituted pyrrolidinedione (succinimide) structure, as shown below in Figure 3.3.

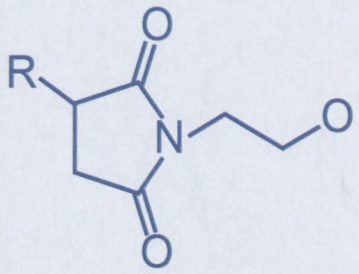

Figure 3.3: Structure of Pibsa-IMIDE of one of the possible conformations of Pibsa-MEA

The overall molecular weight will be 1091, the HLB number will be low (< 4). One of the possible conformations of the Pibsa-IMIDE surfactant is shown in Figure 3.4.

Oxygen – red
Nitrogen – blue
Carbon – light blue
Hydrogen - white

Figure 3.4: 3-D VIEW of one of the possible conformations of Pibsa-IMIDE

3.2.1.3 Pibsa-UREA

Pibsa-UREA is adduct of Pibsa and urea, with a head group structure as shown in Figure 3.5

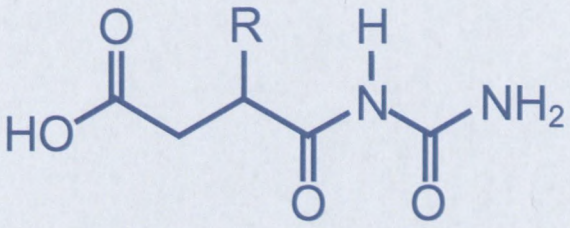

Figure 3.5: Structure of Pibsa-UREA

The overall molecular weight is about 1109, and the HLB number will be low (< 4). One of the possible conformations of Pibsa-UREA surfactant is shown in Figure 3.6.

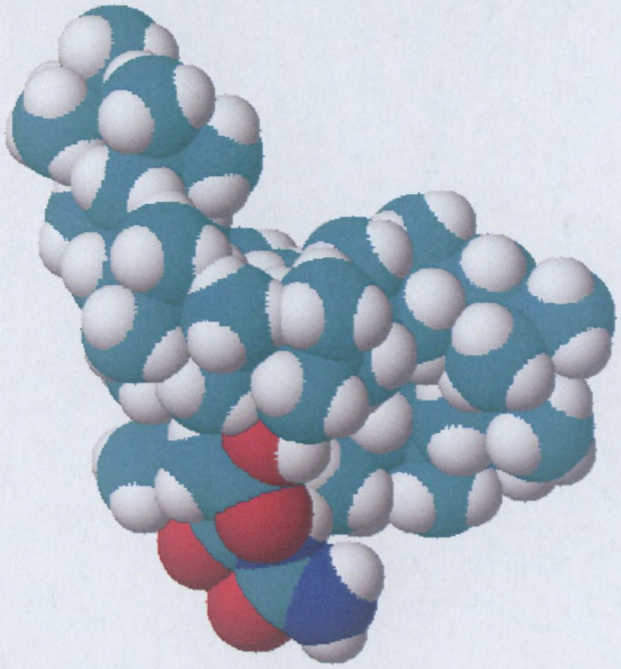

Oxygen – red
Nitrogen – blue
Carbon – light blue
Hydrogen - white

Figure 3.6: 3-D VIEW of one of the possible conformations of Pibsa-UREA

3.2.1.4 Sorbitan MonoOleate (SMO)

This is an ester formed between sorbitan and oleic acid (oleic acid is a C18 fatty acid with a single *cis* double bond, written as C18:1). The structure of SMO is given below in Figure 3.7.

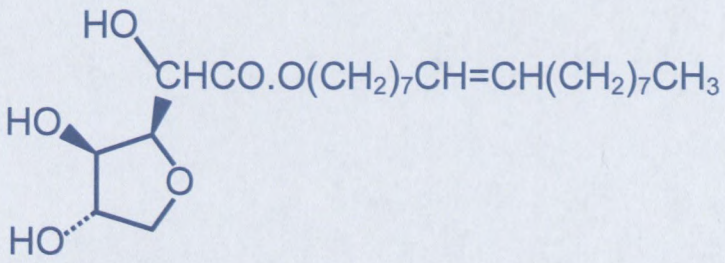

Figure 3.7: Structure of SMO

The molecular weight of sorbitan monooleate is 428, with the HLB number about 4.3. Commercial SMO is often known by its trade name Span®80.

3.2.1.5 Summary of surfactant properties

The properties described above are summarised in Table 3.1

Table 3.1: Summary of surfactant properties

Name	Relative molecular mass	HLB number
Pibsa-MEA	1109	Low (<4)
Pibsa-IMIDE	1091	Low (<4)
Pibsa-UREA	1109	Low (<4)
SMO	428	4.3

3.2.2 Fuel oils

The surfactants used for this study were originally dissolved at high concentrations in Parprol 32. Fuel oils used for dilution to the required concentration were Mosspar-H and Shellsol 2325. The properties of these materials are given in Table 3.2.

Table 3.2: Properties of fuel oils

	Parprol 32	Mosspar H	Shellsol 2325
Manufacturer	Engen Chemicals	PetroSA	Shell Chemicals
Manufacturer's description	Solvent dewaxed light paraffinic distillate	Isoparaffinic solvent	Wide cut mixture of paraffins, cycloparaffins and aromatics… high flash, slow evaporating type of hydrocarbon solvent
Boiling range, °C		290 - 300	220 - 250
iso-paraffins, %	70	80-90	60
n-paraffins, %		1-10	
Cycloparaffins, %	26	10-15	21
Aromatics, %	4	< 0.1 typical)	19
Density 20°C, kg m^{-3}	866 or 874	790 – 820 (792 typical)	812
Density 22°C, kg m^{-3} (measured)	863	794	800
Viscosity 40°C, cSt	28 – 33	2.5	< 7
Viscosity 30°C, mPa.s (measured)	42.9	2.9	1.7
Refractive index, n_{20}^{D} (measured)	1.478	1.443	1.451

The internal phase was formed by an oversaturated aqueous solution of ammonium nitrate (AN).

For the preparation of the emulsions, the granulated AN was added to the distilled water at 80° C. The concentration of AN in the aqueous solution was kept at 80-wt %. The equilibrium crystallisation temperature (fudge point) of the solution with the chosen concentration of AN was app. 63° C. The density of the solution was about 1.4 to 1.5 g/l. For all emulsion formulations, the concentration of the aqueous phase was kept at 85 % by volume.

3.2.3 Preparation of the emulsion samples

To manufacture emulsion samples, the Hobart mixer was used and the following instructions were applied:

- Transfer the fuel phase into the preheated bowl. Allow 5 minutes for the fuel phase to heat up.
- Switch "on" the mixer at speed 1.
- Slowly transfer the oxidiser solution into the bowl by running the solution into the bowl by means of a spatula.
- Ensure that an emulsion is formed.
- Continue adding the entire oxidiser solution. Stop the mixer and switch to speed 2.Then run the mixer at speed 2 for a further 2 minutes.
- Stop the mixer and switch to speed 3.
- Cover the mixing bowl with plastic or the aluminium cover to stop the emulsion from splashing.
- Let the mixer run at speed 3 until the required viscosity is reached.

Continuous sampling procedure

- Small samples were taken from speed 3 every 2.5 mins till 30 mins. This procedure was repeated for all formulations.
- Samples were then taken for measurement of droplet size distributions, using the Malvern Matersizer.
- Droplet sizes with similar size distributions were then selected and made into batches.

3.2.4 Matrix of samples

The manufactured emulsion samples can be divided into the following groups:

(a) Materials with the same surfactant concentration and oil type, but different surfactant types.

(b) Materials with the same surfactant type and oil type, but of varying surfactant concentration.

(c) Materials with the same surfactant type and concentration, but different oil types

(a) **Table 3.3: Samples with different surfactant types**

% Oxidiser (AN)	Fuel oil	% surfactant	d, μm	Surfactant type
80	Mosspar-H	8	10	Pibsa-MEA
				Pibsa-IMIDE
				Pibsa-UREA
				SMO/Pibsa-MEA
				SMO
			12	Pibsa-MEA
				Pibsa-IMIDE
				Pibsa-UREA
				SMO/Pibsa-MEA
			15	Pibsa-MEA
				Pibsa-IMIDE
				Pibsa-UREA
				SMO/Pibsa MEA
		14	10	Pibsa-MEA
				Pibsa-IMIDE
				Pibsa-UREA
				SMO/Pibsa-MEA
				SMO
			12	Pibsa-MEA
				Pibsa-IMIDE
				Pibsa-UREA
				SMO/Pibsa-MEA
			15	Pibsa-MEA

(b) **Table 3.4: Samples with different surfactant concentrations**

% Oxidiser (AN)	Fuel oil	Surfactant type	d, μm	% Surfactant
80	Mosspar-H	Pibsa-MEA	10	8
				14
			12	8
				14
		Pibsa-IMIDE	10	8
				14
			12	10
				14
		Pibsa-UREA	10	8
				14
			12	8
				14
		SMO/Pibsa-MEA	10	8
				14
			12	8
				14
		SMO	10	8
				14
			12	8
				14

(c) **Table 3.5: Samples with different oil types**

% Oxidiser (AN)	Surfactant type	% Surfactant	d, μm	Fuel oil
80	Pibsa-IMIDE	8	10	Mosspar-H
				Shellsol 2325
			12	Mosspar-H
				Shellsol 2325
			15	Mosspar-H
				Shellsol 2325
		14	10	Mosspar-H
				Shellsol 2325
			12	Mosspar-H
				Shellsol 2325

3.3 Instrumentation

Optical microscopy, rheological analysis and X-ray diffraction were performed to characterise the different concentrated emulsions.

3.3.1 Microscopy

The observations were carried out on the samples under investigation with an optical microscope ('Leica') equipped with a digital camera, at a magnification of x 500.

3.3.2 Rheological analysis

All bulk rheological measurements were carried out with the use of a rotational dynamic rheometer MCR 300 (Paar Physica). The geometry of the measuring unit was a "bob-in-cup" (coaxial cylinder with conical base to the bob) with a sandblasted bob surface. The bob diameter was 27 mm and the gap distance between cup and bob was 1 mm. The experiments were conducted in the following regimes of deformation:

- Steady state flow measuring flow curves (shear stress versus shear rate);
- Oscillatory measurements for measuring amplitude dependence of the (storage and loss) components of the dynamic modules.

All experiments were carried out at 30°C.

3.3.3 X-ray diffraction patent analysis

The relative crystallinity of the material was analysed in a Brucker D8 X-ray power diffractometer with Cu radiation. The diffractometer was fitted with a primary parallel beam monochromator (Goebel Mirror). The scintillation detector was fitted with a standard solar slit and a 0.6 mm receiving slit.

3.4 Experimental investigation

3.4.1 Microscopic observation of concentrated emulsions

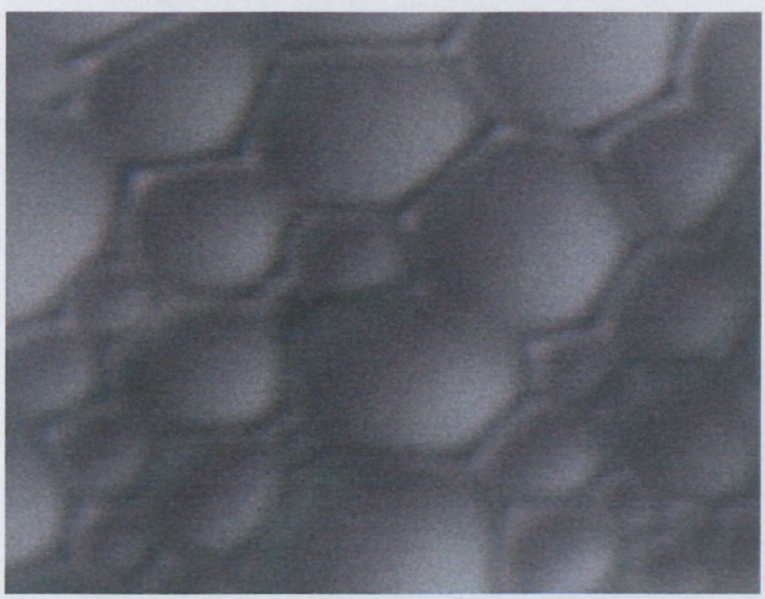

Figure 3.8: Microscopic image depicting the emulsion with 8 % Pibsa-IMIDE for d = 15 μm (500 times magnification)

The analysis showed that the samples that were studied were polydispersed. The drops were deformed by packing into polyhedral structures and by contact with neighbouring droplets. They were separated by a thin film of continuous phase (see Figure 3.8).

3.4.2 Rheological Behaviour of Highly Concentrated Emulsion

In this section, typical rheological properties of highly concentrated water-in-oil emulsions will be discussed.

3.4.2.1 Viscoelastic properties - Amplitude sweep

The oscillation amplitude was selected as a variable and the frequency kept constant in the amplitude sweep test. The frequency was 1 Hz and the strain was controlled between 0.1 and 200 %. The corresponding storage modulus, which reflects the elasticity of the emulsion, and the loss modulus, which reflects the dissipation, was measured as a function of strain.

Figure 3.9 shows the evolution of the storage (G'), and loss (G") moduli according to the increase of strain amplitude.

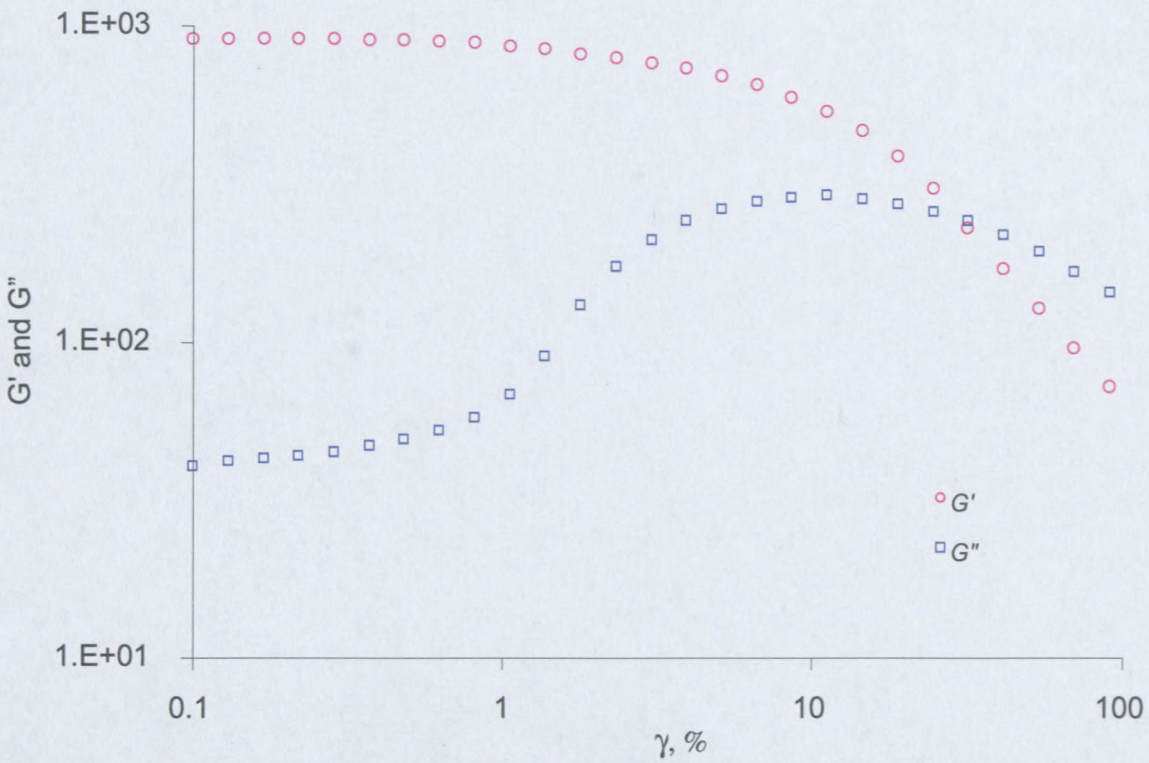

Figure 3.9: Typical amplitude sweep for highly concentrated explosive emulsion (8 % IMIDE-Mosspar, 10 μm)

For the material, the elastic modulus G' was greater than the viscous modulus G" over the entire range of applied strain, indicating the predominantly elastic behaviour of the material with G'/G" >> 10 in all cases, at low test strains. As can be seen, the storage modulus was independent of strain amplitude up to some critical deformation (approximately 9 %), a zone of constant response (plateau region) indicating an unaltered structure not disturbed by shear. It was related only to the equilibrium microscopic structure, forces, and inherent dissipation of fluctuations (Bird, Armstrong & Hassager, 1987). In this linear region the particles were crowded and could not move freely past one another, which defined the elastic domain. At higher deformations, the values of the storage modulus decreased with a deformation increase, the applied strain being sufficient to allow the particles to move past one another and inducing a transition to the viscous domain. Above the critical shear stress value, emulsions lose their viscoelasticity and become a fluid. This stress is known as yield stress. The peak in loss modulus also confirms and elucidates the transition from elastic to viscous region. From an empirical point of view, the existence of a loss modulus maximum means a transition phenomenon in most cases, whatever its nature. From a microstructural point of view, this peak probably means that the dissipation of energy is maximal when the droplets are deformed and flattened enough to allow flow despite the crowding (Jager-Lézer *et al.*, 1998; Ponton *et al.*, 2001)

The length of the plateau of the elastic modulus is an indication of the structure flexibility to deformation and the drop of modulus is related to the break-down of the solid structure.

The storage modulus was obtained from the linear region of the storage modulus by extrapolation of the curve to zero deformation.

3.4.2.2 Flow properties

The shear rate was controlled in the decreasing regime of deformation over a range of 10^{-6} to 200 s^{-1}. Figure 3.10 represents a typical flow curve.

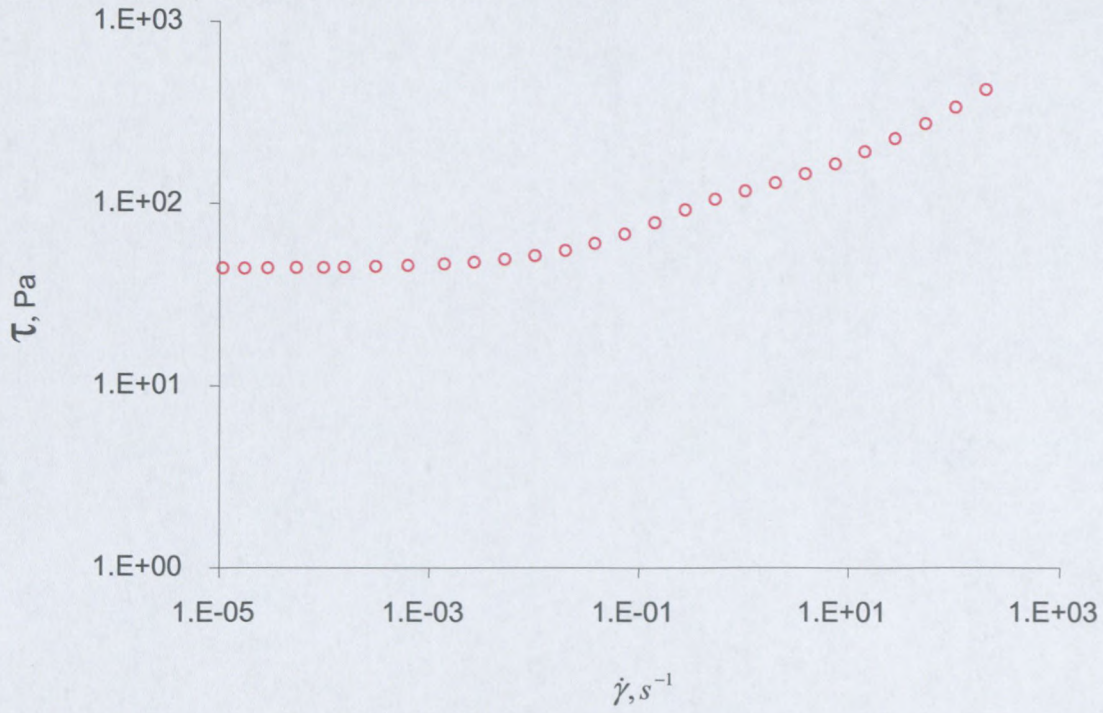

Figure 3.10: Typical flow curve for highly concentrated emulsion explosives (8 % IMIDE-Mosspar, 10 μm)

The flow curve shows an inflection point at some specific value of shear stress as pointed out earlier (Masalova & Malkin 2005; 2007c; Malkin & Masalova 2007; Kharatiyan, 2005). According to these authors, two competing processes occur in the shearing of an explosive emulsion. One of them dominates at low shear rates and leads to an increase in viscosity, while the other prevails at high shear rates, resulting in typical shear thinning behaviour. According to the authors, drops maintain their shape in the low shear rate domain and flow proceeds as larger particles rolling over smaller ones until a critical shear stress ("second yield stress") is reached. When $\tau \geq$"second yield stress" the drops will more strongly deform and arrange in "trains", thus causing more uniform "inner shear layers" of the oil phase, which triggers the shear thinning behaviour. The plastic deformation of droplets occurs and then results in a catastrophic suppression of the Reynolds mechanism of dilatancy. Therefore one can conclude that, below the first yield stress, the elasticity is dominated by the resistance to the rolling rather than the resistance to the deformation.

3.4.3 Effect of surfactant type on rheological properties of explosive emulsions

The basic idea of this section was the clearing up of the role of a surfactant in the rheological properties of a higly concentrated emulsion with an oversaturated (overcooled) internal phase. Two starting arguments had to be discussed. On one hand, the samples used had the same dispersed phase volume fraction, the droplet size distributions were analogous in all cases (see section 3.4.3). Bearing in mind the basic conception of the Princen-Mason model of highly concentrated emulsions, any difference in rheological properties of the samples prepared with different surfactant types should be expected to originate only from differences in interfacial tensions. However, the study of the effect of droplet size on rheological properties of explosive emulsions stabilised by Pibsa-based surfactants (Malkin *et al.*, 2004a; Masalova & Malkin, 2007a; 2007c) has shown that the expected dependence of the elastic modulus on the reciprocal diameter did not correspond to the experimental data. The emulsions exhibited relatively high values of the elastic modulus in comparison to Princen's model. Therefore, additional sources of elasticity does exist in Pibsa-based explosives emulsions. The role of the surfactant's nature might be richer than could be expected from the basic model.

The volume fraction of the dispersed phase was fixed at 85 % for all samples. The droplet size distributions of samples used in this section are given below.

3.4.3.1 Droplet size distribution

The droplet size distribution in all samples was measured using the Malvern Mastersizer 2000 technique. The particular procedure is based on sample dispersion under software control and the measurement of angle dependence of the intensity of scattering of a collimated He-Ne laser beam. Particle size in the range from 0.02 to 2000 μm can be measured by this means; this range is much wider than the droplet size distribution of the real samples used in this work, however. The particle size distribution calculations are based on the rigorous Mie theory and the use of the standard software applied to the instrument. The sample was diluted in the oil of the continuous phase just before the measurements were taken. The results are shown below, in Figures 3.11 to 3.14 and Tables 3.6 to 3.8.

- **Particle size distribution (d = 10 μm)**

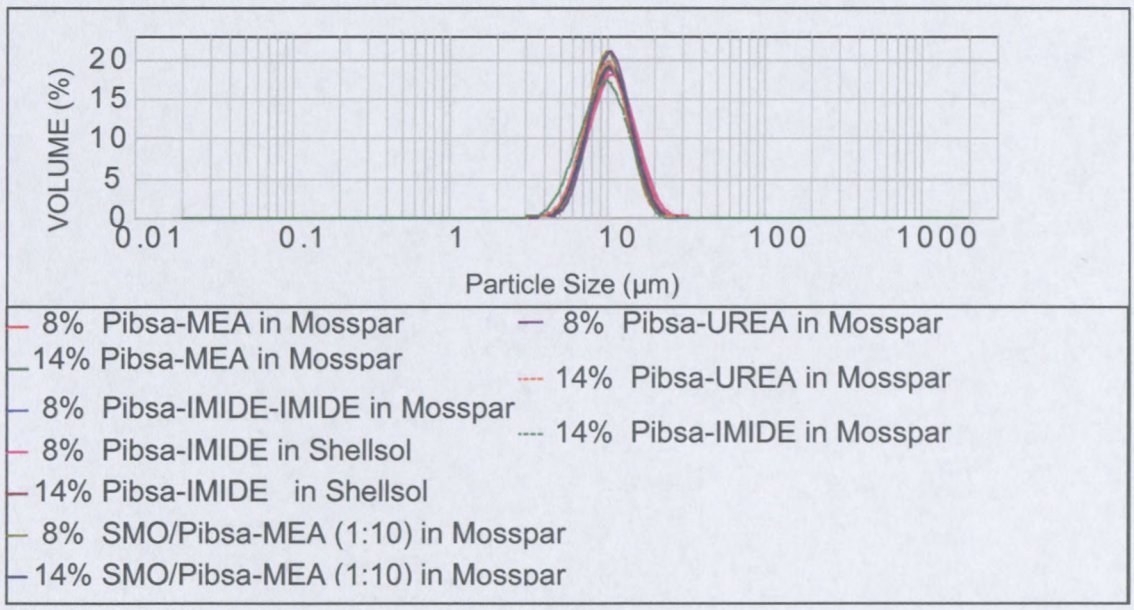

Figure 3.11: Histogram of drop size distribution of the emulsion for different PIBSA-based surfactant types and the SMO/Pibsa-MEA mixture (d = 10 μm)

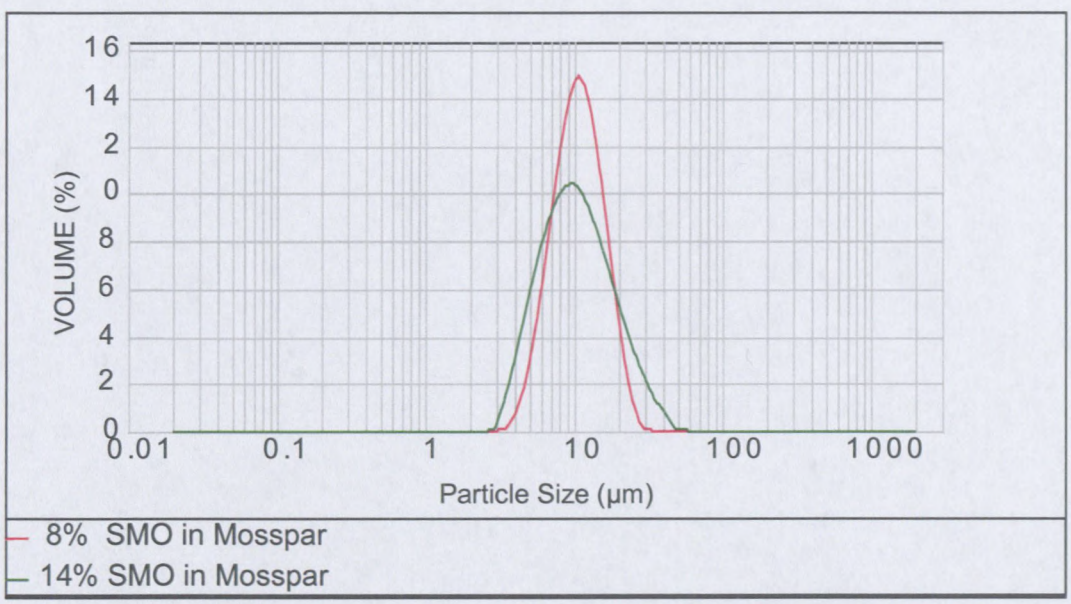

Figure 3.12: Histogram of drop size distribution of the emulsion for different concentrations of SMO (d = 10 μm)

Table 3.6: Drop sizes of the emulsion with different surfactant types with droplet size 10 μm

Surfactant type	% Surfactant	$d_{0.1}$ (μm)	$d_{0.5}$ (μm)	$d_{0.9}$(μm)	D[3,2]
Pibsa-MEA	8	7.1	10.7	15.9	10.1
	14	6.8	10.2	14.9	9.6
Pibsa-IMIDE	8	6.7	10.1	15.1	9.6
	14	6.1	9.6	14.8	9
Pibsa-UREA	8	7.3	10.5	15.1	10.1
	14	6.6	9.9	14.4	9.4
SMO/Pibsa-MEA	8	7	10.1	14.4	9.7
	14	6.9	10.4	15.4	9.9
SMO	8	5.8	10	17.2	9.2
	14	5.1	10	21.8	8.9

It is clear from the above results that all samples for which the PIBSA-based surfactants were used, as well as the one for which the SMO/Pibsa-MEA mixture was used, had similar droplet sizes and droplet size distributions. However, the sample for which pure SMO was used had a markedly different particle size distribution, and therefore that sample was not included in the rheological investigation.

- **Particle size distribution (d=12 μm).**

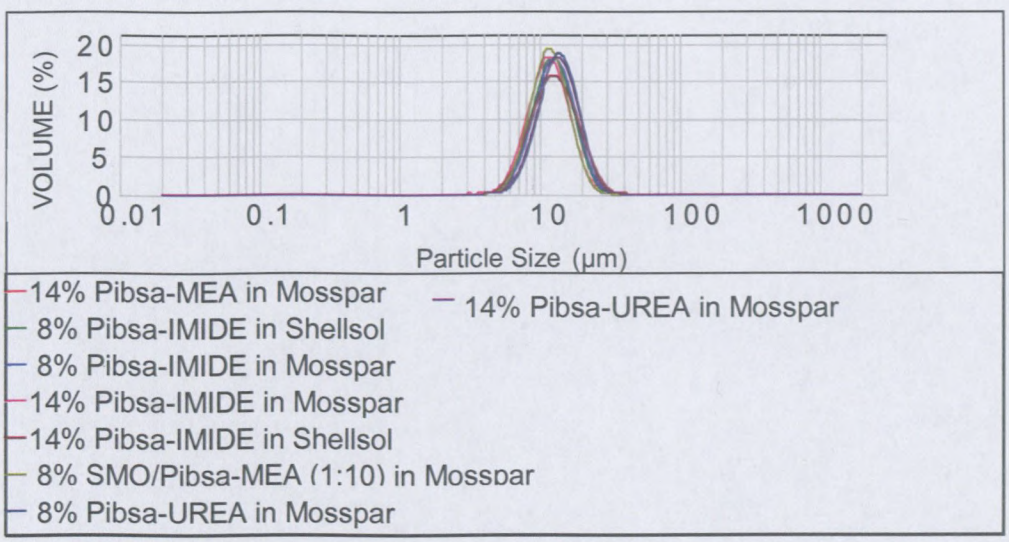

Figure 3.13: Histogram of drop size distribution of the emulsion for different types of surfactant (d = 12 μm)

Table 3.7: Drop sizes of the emulsion with different surfactant types with droplet size 12 μm

Type of surfactant	% Surfactant	$d_{0.1}$ (μm)	$d_{0.5}$ (μm)	$d_{0.9}$(μm)	D[3,2]
Pibsa-MEA	8	8.5	12.5	19.6	12.3
	14	7.8	11.9	17.7	11.5
Pibsa-IMIDE	8	8.2	12.7	19.2	12
	14	7.5	11.6	17.4	10.9
	8	8.1	12.4	18.6	11.7
	14	7.8	12.7	20.5	11.9
Pibsa-UREA	8	8.9	13.6	20.2	12.9
	14	8.7	13.5	20.3	12.7
SMO/Pibsa-MEA	8	7.9	11.7	17.3	11.2
	14	-	-	-	-

It is clear that all the samples had a similar droplet size and droplet size distribution

- **Particle size distribution (d = 15 μm).**

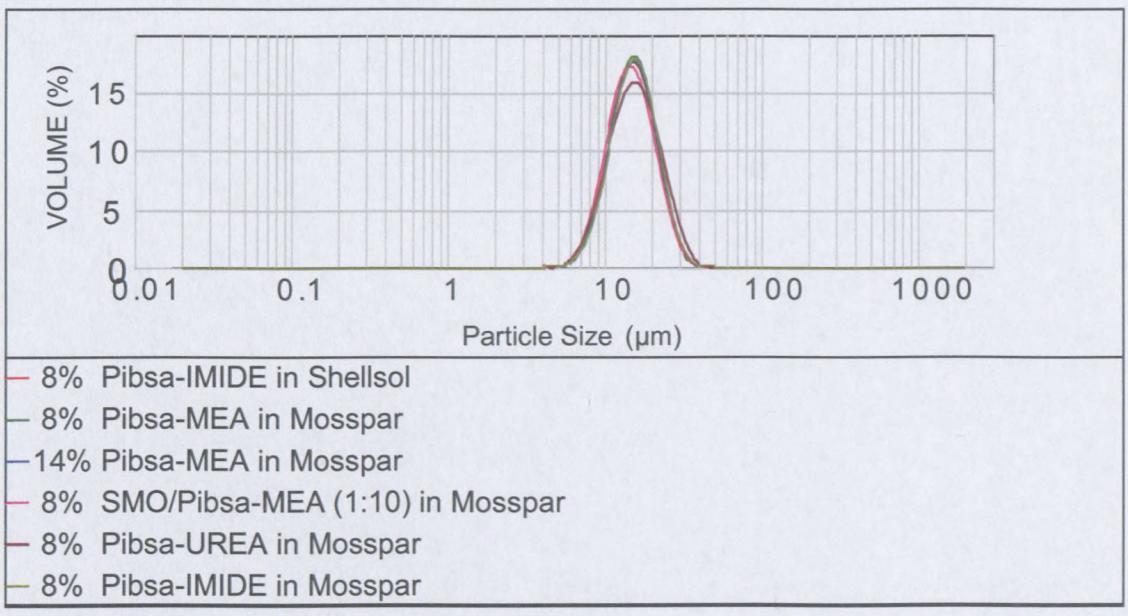

Figure 3.14: Histogram of drop size distribution of the emulsion for different types of surfactant (d = 15 μm)

Table 3.8: Drop sizes of the emulsion with different surfactant types with droplet size 15 μm

Type of surfactant	% Surfactant	$D_{0.1}$ (μm)	$d_{0.5}$ (μm)	$d_{0.9}$(μm)	D[3,2]
Pibsa-MEA	8	9.8	15.2	22.4	14.3
	14	9.6	15.2	23.1	14.2
Pibsa-IMIDE	8	9.2	14.7	22.6	13.7
Pibsa-UREA	8	9.4	15.4	24.6	14.3
SMO/Pibsa-MEA	8	9.3	14.5	22.5	13.7

It is clear that all the samples had the same droplet size and droplet size distribution

3.4.3.2 The effect of surfactant type on viscoelastic properties

The oscillation amplitude was selected as the variable and the frequency was kept constant in the amplitude sweep test. The frequency was 1 Hz and the strain was controlled between 0.1 and 200 %. The corresponding storage modulus, relating to the elastic portion of the sample, and the loss modulus, the viscous portion of the sample, was measured as a function of strain. Figures 3.15 to 3.19 show the evolution of the storage (G') modulus according to the increase of strain amplitude as a function of surfactant type for two different surfactant concentrations and three different droplet sizes.

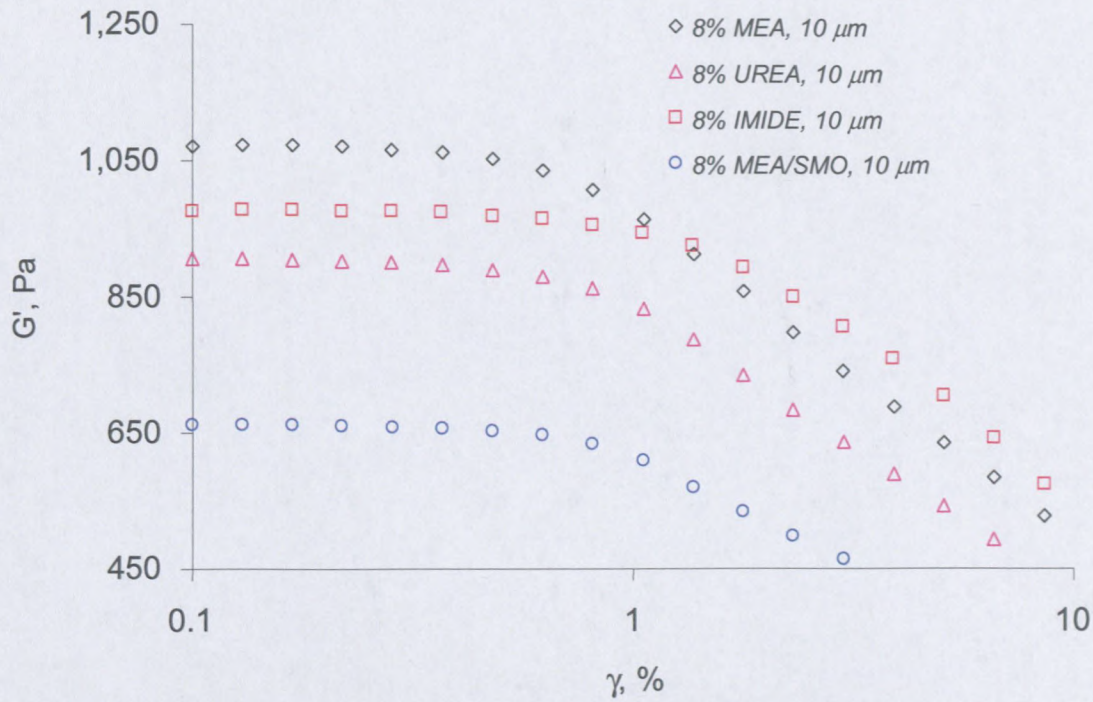

Figure 3.15: Effect of type of surfactant on viscoelastic properties (d = 10 μm, 8 % surfactant in Mosspar)

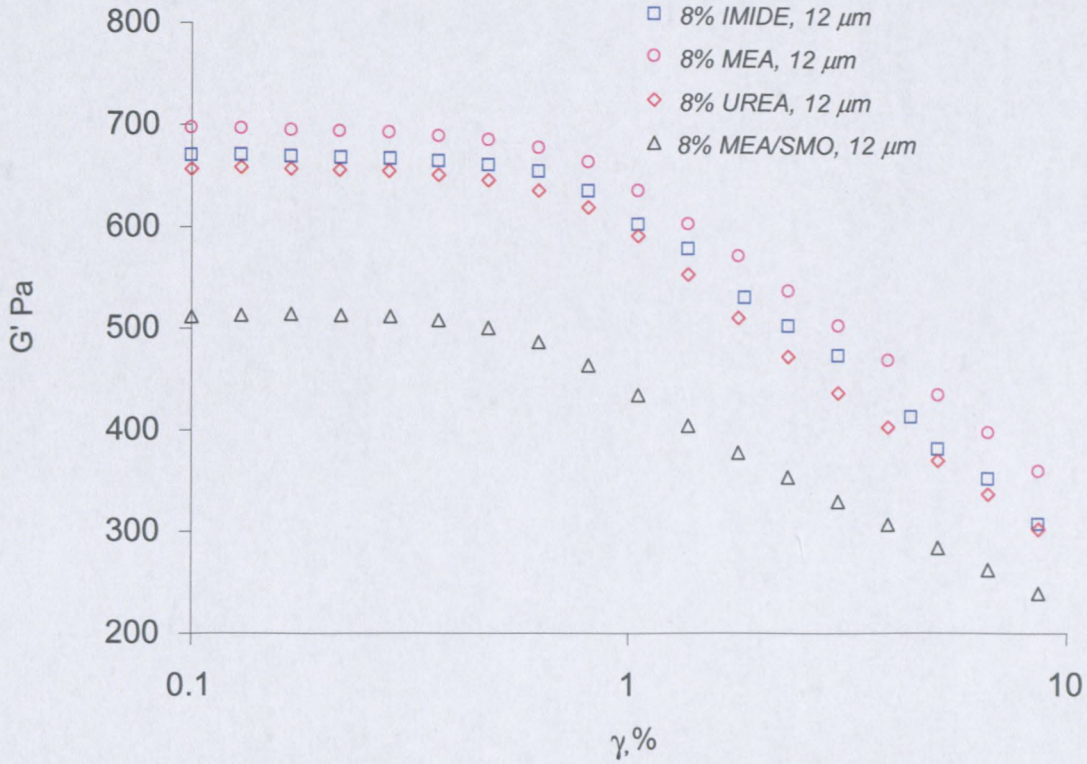

Figure 3.16: Effect of type of surfactant on viscoelastic properties (d = 12 μm, 8 % surfactant in Mosspar)

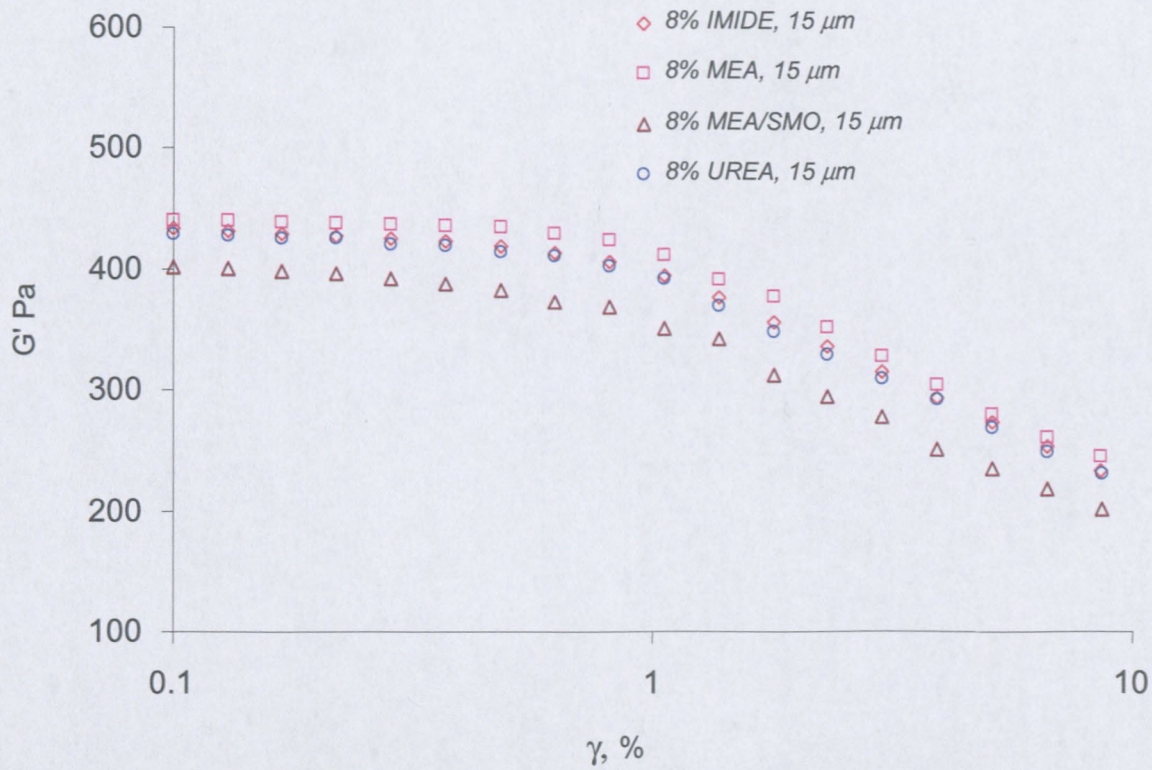

Figure 3.17: Effect of type of surfactant on viscoelastic properties (d = 15 μm, 8 % surfactant in Mosspar)

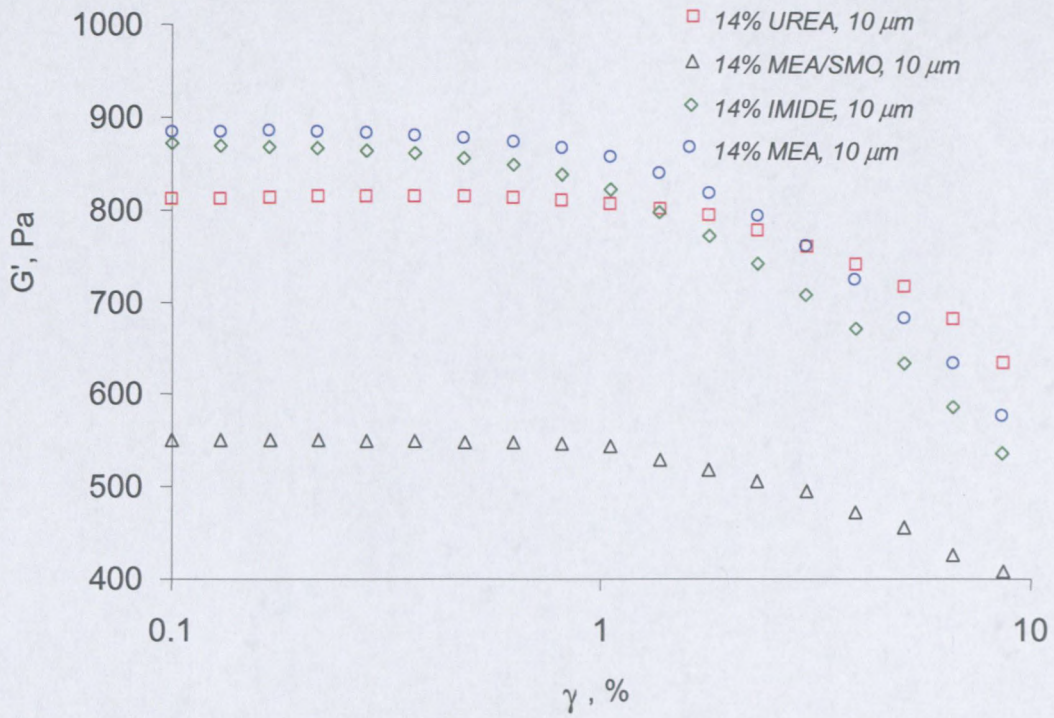

Figure 3.18: Effect of type of surfactant on viscoelastic properties (d = 10 μm, 14 % surfactant in Mosspar)

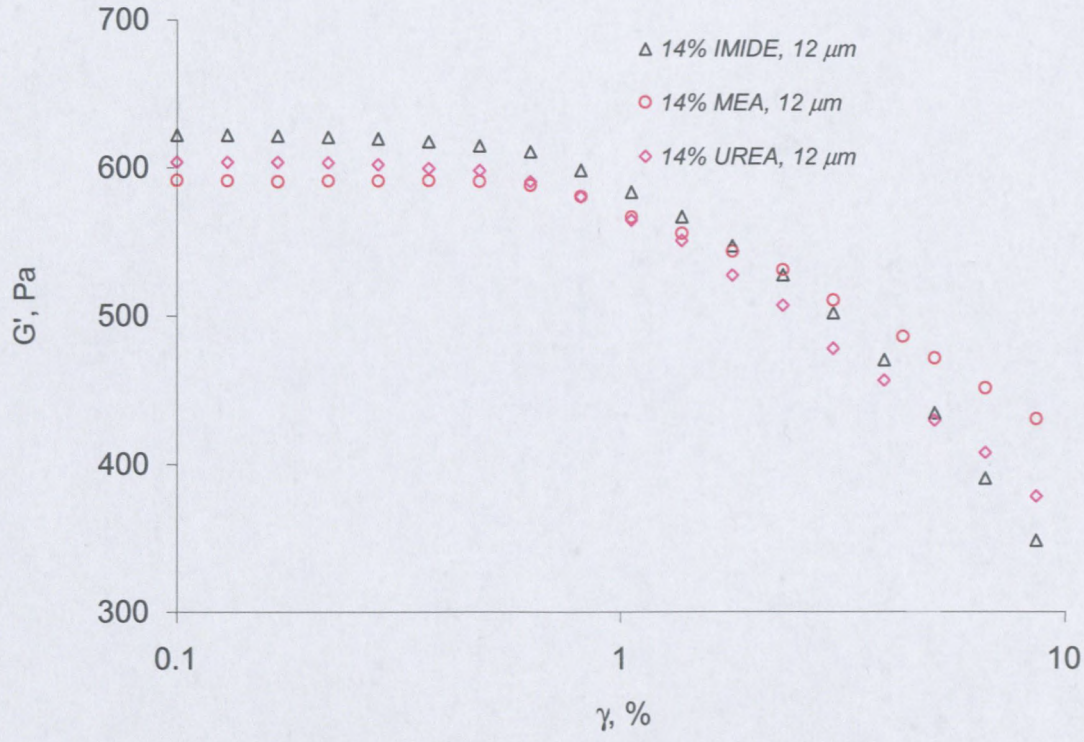

Figure 3.19: Effect of type of surfactant on viscoelastic properties (d=12 μm, 14% surfactant in Mosspar)

The effects of surfactant type on the storage modulus associated with the linear region, for all surfactant concentrations, are listed in Table 3.9

Table 3.9: Storage modulus values for all emulsions with different surfactant types determined by amplitude sweep experiment

d, μm	Pibsa-MEA	Pibsa-IMIDE	Pibsa-UREA	SMO/Pibsa-MEA
G', Pa; 8 % surfactant				
10	1012	948	911	661
12	696.5	669.5	656.4	511.4
15	439.3	433.1	428.5	401.3
G', Pa; 14 % surfactant				
10	884	868.9	809.8	550
12	630.5	622.2	603	-

From the above it is clear that the measured values of *G'* depend on the type of surfactant:

- The nature of the surfactant does influence the elasticity of highly concentrated explosive emulsions. Without a doubt, the elastic modulus decreases according to the sequence MEA-IMIDE-UREA-MEA/SMO. However, the sensitivity is less pronounced for bigger droplets.
- The influence is especially evident in the transition from oligomeric surfactants to the mixture [low molecular weight surfactant (SMO)/ oligomeric surfactant]. In this transition the changes in the storage modulus (see Table 3.9) are much more strongly expressed than the changes in the interfacial tension (see Table 3.10). Indeed, for the same total surfactant, the addition of SMO in low concentration (1:10) to Pibsa-MEA lowers the elastic modulus much more than it does the interfacial tension. The rather close values of the interfacial elastic modulus (see Table 3.10) cannot explain this observation. We consider the last fact as rather important. It seems reasonable to accept it as a proof of an active role of a surfactant not only as a compound responsible for the interfacial tension, but also as creating additional sources of elasticity by means of physical interaction between interface layers of different droplets and a surface layer with the matter of droplet.

It is more instructive to plot the data in the $G'/(\sigma/R)$ - γ coordinates, σ being the interfacial tension, and R being the mean drop radius. This type of plot provides the possibility of

comparing the results, with exclusion of the effects of particle size and interfacial tension (Dimitrova & Leal-Caledron, 2004). By doing this, one can easily detect the presence of any additional source of elasticity in the system (see Figure 3. 21).

3.4.3.3 Interfacial properties: Interfacial tension and Interfacial elasticity

The dynamic interfacial tension and interfacial moduli were determined using a PAT 1 tensiometer supplied by Sinterface Technologies, Berlin, Germany. The basic principles of the operation of this instrument is that the Young-Laplace equation is fitted to the profile of an image of a droplet in the more dense phase suspended in the less dense phase from a capillary. The Young-Laplace equation balances the interfacial tension against gravity, with the interfacial tension tending to reduce the interfacial area and gravity tending to increase it by extending the droplet. This balance leads to certain practical considerations concerning the capillary diameter and the droplet volume. For example, if the droplet volume is too low, the interfacial tension dominates and the droplet assumes a spherical shape from which the interfacial tension cannot be extracted. If the droplet volume is too high, gravity dominates and the droplet detaches from the capillary. A droplet volume of 3 mm^3 with a capillary outer diameter of 1.97 mm was used for the samples considered here.

Except for SMO, the interfacial tension quoted was measured after 15,000 seconds, by which time a reasonably constant value had been reached. For SMO, the droplet tended to detach from the capillary, and the experiment could only be sustained for one hour.

For the Fourier algorithm to be applicable, and for measurements made at different frequencies to be comparable, the interfacial tension should be constant. In practice this criterion should not change appreciably for the duration of the oscillation experiment.

The range of frequencies used was also a matter of judgment and trial and error. The Fourier software requires at least two cycles, preferably more, so the low frequency limit depends in part on the rate at which the material properties are changing over time, and in part on how long the operator is prepared to wait for a data point. But the magnitude of the complex interfacial modulus, and therefore the amplitude of the oscillating interfacial tension, must increase with increasing frequency. This means that the lower the frequency, the lower the oscillation amplitude, and the less easily the oscillating interfacial tension can be distinguished from the mean interfacial tension. Thus the low frequency limit also depends on the material properties and the resolution of the instrument. The high frequency limit depends

on the response time of the mechanical components of the instrument, and on the sampling rate, since the Fourier algorithm requires a minimum number of points per cycle.

It was found that a frequency range of 0.01 Hz to 1 Hz could be used for most samples, although, in cases where the interfacial moduli were low, the results at the higher and lower frequencies may have large uncertainties associated with them. The frequencies used were 0.01 Hz, 0.02 Hz, 0.05 Hz, 0.1 Hz, 0.2 Hz, 0.5 Hz and 1.0 Hz for a nominal strain of 7.5 %. In the results section of this study, a table of moduli at 0.1 Hz is given, as data at this frequency were the most reliable.

- **Determination of surfactant CMC**

The CMC is given by the concentration at which there is an abrupt change in the slope of the curve of concentration plotted against interfacial tension. Below the critical micelle concentration, the surfactant interfacial excess concentration, Γ, is given by Equation 2.1 (see section 2.2.7), which is derived from the Gibbs adsorption isotherm (McClements, 1999; 2005). Thus the CMC can be obtained from a plot of interfacial tension against the natural logarithm of the surfactant bulk concentration. If the condition of saturation adsorption is achieved, the plot of concentration against the natural logarithm of the interfacial tension will be linear.

The interfacial tension was determined using the Krüss K100 tensiometer, supplied by Krüss Gmbh, Germany. This was used in preference to the PAT1 because Equation 3.1 requires the equilibrium interfacial tension, which is arrived at more rapidly with the K100.

The principle of operation of the K100 is straightforward. About 15 cm^3 ammonium nitrate solution is placed in a clean 70 mm diameter glass dish. A hydrophilic platinum (Wilhelmy) plate is suspended vertically from a sensitive force transducer with its lower edge penetrating the surface of the ammonium nitrate solution. About 50 cm^3 of the oil phase are added, so that the plate is wholly submerged. The interfacial tension is given by Equation 3.1.

$$\sigma = \frac{F}{2(L_P + T_P)\cos\alpha} \quad , \qquad \textbf{Equation 3.1}$$

where F is the vertical force acting on the plate, after a correction for the plate's buoyancy has been made, W_p and T_p represent the plate length and thickness respectively, and α is the contact angle. Since the plate is hydrophilic, the contact angle is taken as zero.

Surfactant solutions were made up by successive dilution. After each dilution, the solution was split and the interfacial tension measurement was taken using one part, the other part being used for the next dilution. All experiments were conducted at 30°C.

Figure 3.20 shows an example of a plot of interfacial tension against the natural logarithm of the surfactant bulk concentration for the PIBSA-MEA surfactant in Mosspar.

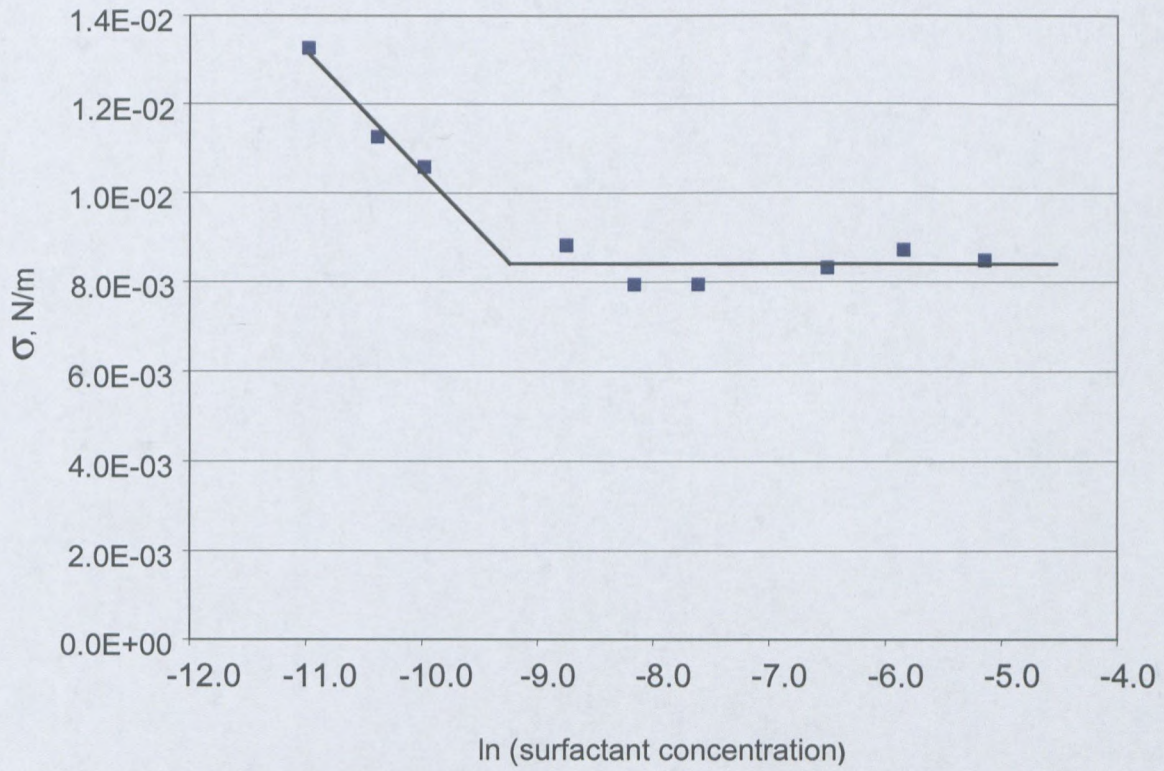

Figure 3.20: interfacial tension against ln (surfactant concentration) for the system Pibsa-MEA / Mosspar / 40 % ammonium nitrate

Results of interfacial tension, interfacial elastic modulus and CMC readings for different surfactant types and concentrations are summarised in Table 3.10.

Table 3.10: Interfacial tension, interfacial elastic modulus and CMC for different PIBSA-based surfactants and SMO

Surfactant type	% Surfactant	σ, mN/m	E', mN/m	CMC, %
Pibsa-MEA	8	7.7	2.9	$1.5.10^{-2}$
	14	7.5	3	
Pibsa-IMIDE	8	3.5	1.1	$6.2.10^{-2}$
	14	3.6	1.2	
Pibsa-UREA	8	6.4	2.9	$1.7.10^{-2}$
	14	6.5	2.7	
SMO/Pibsa-MEA	8	5.1	2.1	-
	14	4.9	2	
SMO	8	1.9	0.3	$2.3.10^{-2}$
	14	1.8	0.3	

The following can be noted from Table 3.10:

- The total amount of surfactant used in this work is far in excess of the amount adsorbed at the oil/water interface, even for the lowest surfactant concentration. This provides the evidence for the presence of reverse micelles in the oily phase. The reverse micelle shape is expected to be spherical, with a mean radius or an aggregation number depending on the surfactant head group (White *et al.*, 2004; Reynolds *et al.*, 2000; 2001; Shen & Duhamel, 2008). It is worth mentioning that Pibsa-based reverse micelles present in the oily phase of explosive emulsions contain ammonium nitrate in their core (Reynolds *et al.*, 2000; 2001) and that the associative strength (aptitude to induce self-assembly of surfactant molecules) originates from hydrogen-bondings between the surfactant head group and the ammonium nitrate solution (Ganguly *et al.*, 1992; Shen & Duhamel, 2008).
- The onset of micellation of Pibsa-MEA, Pibsa-UREA and Pibsa-IMIDE occurs at 1.5 % (99 μM), 1.7 % (112 μM) and 6.2 % (409 μM), respectively. These critical micelle concentrations are small compared to that of AOT, i.e. sodium bis(2-ethyl-1-hexyl) sulfo-succinate (~1000 μM), suggesting that Pibsa-based surfactants aggregate at low concentrations, as was observed earlier with other succinimide dispersants (Vipper *et al.*, 1968; Shen & Duhamel, 2008). Since, for Pibsa-based surfactants, a lower CMC is a reflection of both a high associative strength and a strong anchor of the polar head group onto the interface (Shen & Duhamel, 2008), it seems reasonable to assume that the AN-surfactant interaction is following the trend MEA-UREA-IMIDE. This hypothesis can be supported by the fact that both the associative

strength and the binding energy at the interface are governed by the hydrogen bondings between the surfactant head core and the ammonium nitrate.

- Among the four surfactants, Pibsa-IMIDE or SMO, which have no secondary amine in their polar head core, exhibit the highest CMC values. This result suggests that the micellation of a Pibsa-based surfactant is favoured by the presence of secondary amines in the polar core of the surfactant, as was observed earlier with other succinimide dispersants (Shen & Duhamel, 2008). The high CMC value associated with IMIDE compared to SMO could suggest a high associative strength of SMO reverse micelles.

The last fact is considered as rather important. It seems reasonable to assume it to be the proof of the increase of AN-surfactant interaction with the presence of secondary amines (because, as we said, a high CMC value is a reflection of a weak anchor of the polar head group onto the interface). Indeed, the surfactant head groups in all the surfactants used in this study have a moderate-to-strong hydrogen-bonding tendency, although the polar group in MEA or UREA might have a much stronger interaction compared to that of the corresponding groups in SMO or IMIDE. This is because the presence of secondary amines increases the hydrogen-bonding strength of the surfactant which, in turn, improves its efficiency at binding onto the interface (Shen & Duhamel, 2008). According to Laughlin's classification, the hydroxyl group just misses being operative in hydrogen bondings while the amino group is operative (Ganguly *et al.*, 1992). The cumulative effect of hydroxyl groups and the carbonyl groups could account for the surfactant properties of SMO and IMIDE. MEA or UREA, however, contains amino, carboxyl and hydroxyl groups which could render them more effective surfactants. Moreover, with SMO the only type of interaction possible is the hydrogen-bonding type, while in the case of MEA, in addition to this type of interaction, there exists the possibility of an electrostatic-type of interaction (Ganguly *et al.*, 1992; Reynolds *et al.*, 2001). The chemical structures of IMIDE and UREA head groups (see sub-sections 3.2.1.2 and 3.2.1.3) suggest that, with IMIDE, the only interaction might be the hydrogen bondings, while UREA, which has many groups similar to those present in MEA, the electrostatic type of interaction is also possible.

From the above, it seems reasonable to assume that the AN-surfactant interaction follows the trend MEA > UREA > SMO > IMIDE.

- Neither the interfacial tension nor the dilatational elastic modulus is sensitive to the surfactant concentration. This is probably due to the fact that the total amount of

surfactant is far in excess of the amount adsorbed at the oil/water interface. However, the reverse micelle concentration is expected to increase with increase in surfactant concentration while the non-dependence of reverse micelle size (aggregation number) from this factor is also expected (McClements, 1999; 2005; Reynolds *et al.*, 2000; 2001; Shen & Duhamel, 2008).

- Different surfactant types yield different interfacial properties. Both the interfacial tension and the interfacial elastic modulus decrease according to the following sequence MEA-UREA-MEA/SMO-IMIDE-SMO.

The above suggests a similarity of trend, among the three Pibsa-based surfactants, between the AN-surfactant interaction (MEA-UREA-SMO/MEA-IMIDE) and the interfacial properties (MEA-UREA-SMO/MEA-IMIDE). This similarity of trend could be an indication that any effect of Pibsa-based surfactants on interfacial tension values or on the interfacial dilatational elastic modulus primarily can be attributable to the intensity of surfactant-ammonium nitrate interaction (because, as we said, all Pibsa-based surfactants have the same hydrophobic tail). A high level of surfactant-ammonium nitrate interaction could generate a high interfacial elasticity (strength of the interface).

The lowest values of interfacial properties associated with SMO were expected, since SMO is a low molecular weight surfactant. Indeed, the lowest value of the interfacial tension shown by SMO is due to the high efficiency of packing of molecules of this surfactant at the interface (because there is no steric congestion) allowing the adsorption of a large amount of surfactant onto the interface (McClement, 1999; 2005; Myers, 1992). On the other hand, as pointed out by Dimitrova & Leal-Calderon (2004), the relaxation time of low molecular weight surfactant monolayers is of the order of milliseconds (or even less) and interfacial layers can produce an experimentally observable surface elasticity effect only if their relaxation time is comparable (or higher) to the inverse frequency applied in the conventional mechanical rheometers. Since the applied frequency in the current study was 1 Hz, no significant surface elasticity could be detected for SMO.

A comparison between Table 3.9 and Table 3.10 shows that, except for IMIDE-based emulsions, the bulk elasticity of Pibsa-based emulsions follows the same trend as the interfacial elasticity (interfacial tension or interfacial dilatational elasticity). This could be an indication of the high impact of interfacial elasticity on the bulk elasticity of emulsions prepared with MEA, UREA or the mixture MEA/SMO.

The plot of the storage modulus data in the G'/(σ/R) - γ coordinates is shown below in Figure 3. 21.

3.4.3.4 Scaling of Elastic modulus by Laplace pressure

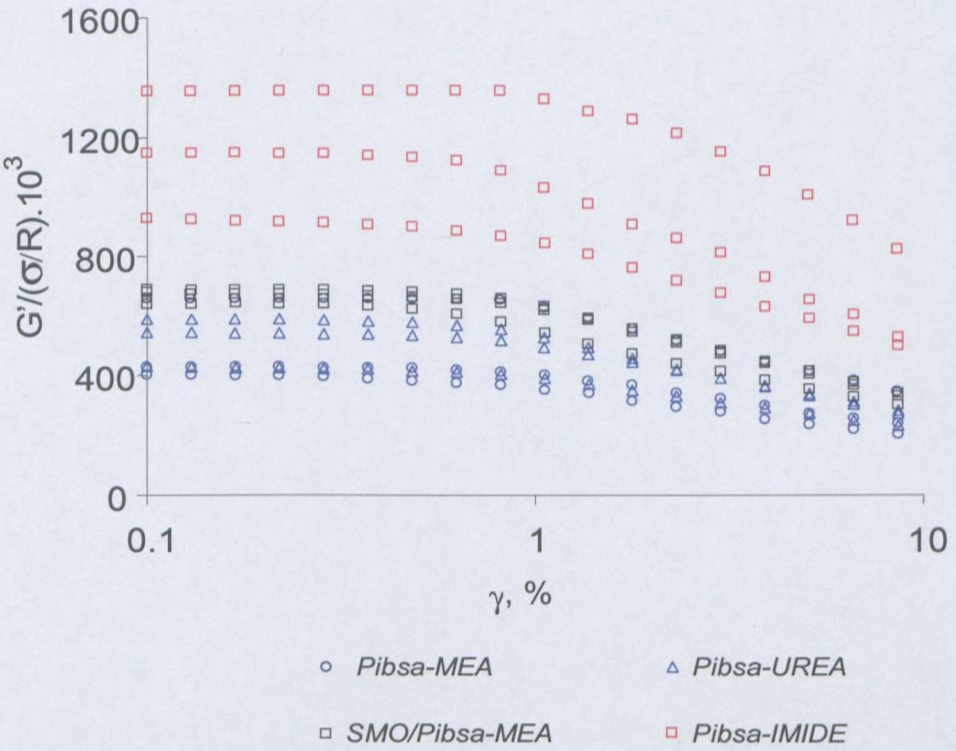

Figure 3.21: Effect of surfactant type on the dimensionless elastic modulus

The effect of surfactant type on the dimensionless elastic modulus of emulsion explosives is quite evident from Figure 3.21, above:

- This shows that the scaled elastic moduli G'/(σ/R) obtained for emulsions stabilised by different surfactant types do not collapse on a single master curve. Thus, additional sources of elasticity exist in the system.
- The dimensionless elastic moduli emphasise the considerable difference between W/O emulsions prepared with Pibsa-IMIDE and W/O emulsions stabilised with other Pibsa-based surfactants. Indeed other factors such as electrolyte concentration, phase ratio, surfactant concentration and the nature of the external phase being kept constant, IMIDE-based emulsions show very high dimensionless elastic moduli compared to other Pibsa-based emulsions. Therefore the observed differences have to be attributed primarily to the different chemical structures of the surfactant head group and their influence on the surfactant-electrolyte interactions. This fact can be

considered as rather important. It can be used as proof of the most active role of Pibsa-IMIDE as a compound creating additional sources of elasticity by means of the physical interaction between interface layers of different droplets and/or a droplet surface layer with the matter of a droplet.

The effect of surfactant type on the dimensionless elastic modulus can be accounted for on the basis of the balance between van der Waals attraction and repulsive forces (DLVO theory):

- On the one hand, because of the non-ionic character of Pibsa-based surfactants used in this work, the dominant interaction energy between droplets could be due to van der Waals attraction (Alvarez *et al.*, 2006; Bibette, Leal-Calderon & Poulin, 1999; Baravian, Mougel & Alvarez, 2006; Quintero *et al.*, 2008). The latter could act as a source of additional elasticity (Alvarez *et al.*, 2006; Baravian *et al.*, 2006; Quintero *et al.*, 2008). Moreover, because of the presence of ions (NH_4^+, NO_3^-) within the aqueous droplets, an additional attractive potential energy could be generated in the thin film between droplets. Indeed, ion-fluctuation gives rise to attraction between adjacent micro droplets, similar to the van der Waals interaction between neutral atoms (Sheng & Tsao, 2004; Tsao, Sheng & Chen, 2002). This electrostatic attraction is not sensitive to the ion concentration and consists of contributions from various induced multipole-multipole interactions, including dipole-dipole, dipole-quadrupole, dipole-octupole, and quadrupole-quadrupole interactions (Sheng & Tsao, 2004). Tsao *et al.* (2002) pointed out that the fluctuation-driven attraction is so strong at short distance that it may dominate over the Coulomb repulsion between like-charged droplets.
- On the other hand, because of its strong tendency to form hydrogen bonds, the ammonium ion (NH_4^+) interacts with the surfactant head group to form hydrogen bonded species, whereas the nitrate ion (NO_3^-) is less involved (Ganguly *et al.*, 1992). Thus, on a qualitative level, the AN-surfactant interaction is expected to increase the separation distance between NH_4^+ and NO_3^- ions (Ashok & Neilson, 1991; Ganguly *et al.*, 1992). The charge separation could give rise to electrostatic repulsion between adjacent droplets, similar to the repulsions between permanent dipoles. In fact, the surfactant head group pulls the NH_4^+ more strongly than the nitrate ion, and so a dipole could be formed as a result of different micro-dipoles induced inside the droplet. The higher the surfactant-AN attraction, the higher might be the dipole moment. Thus, the dipole moment of the droplet could follow the same trend as the surfactant-electrolyte interaction (MEA-UREA-MEA/SMO-IMIDE-SMO). It is worth

mentioning that the contribution of the positive pair potential energy to the overall elasticity has been found to be negligible (Alvarez *et al.*, 2006; Buzza *et al.*, 1994).

According to the above references we can assume that the appearance of electrostatic repulsive forces could affect the negative pair potential energy between adjacent droplets. An increase in the positive potential pair energy could reduce the impact of van der Waals attraction as an additional source of elasticity, and consequently the overall elasticity. Accordingly, the balance of repulsive forces-attractive forces could be one of the major factors which could determine the magnitude of the additional elasticity of explosive emulsions.

From the above we can assume that:

- The effect of positive pair potential energy on the overall pair potential energy in the thin film could be less pronounced in the case of IMIDE compared to other Pibsa-based surfactants. Thus the strong deviation of the IMIDE-scaled elastic modulus in comparison with other surfactants could be an indication of the highest impact of van der Waals forces as an additional source of elasticity to the overall elasticity of the system. This hypothesis could be supported by the high instability of IMIDE-based emulsions, compared to other Pibsa-based surfactants (see section 3.4.6).

- The addition of SMO to Pibsa-MEA could reduce the impact of positive pair potential in the thin film between droplets. Indeed the dimensionless elastic moduli corresponding to the mixture MEA/SMO is markedly higher than the ones associated with Pibsa-MEA, no matter what the droplet size is. This could be due to the fact that the replacement of some MEA surfactant by SMO is expected to reduce the degree of charge separation inside the droplet because the surfactant-electrolyte interaction is more intense in the case of MEA, compared to SMO (Ganguly *et al.*, 1992). This hypothesis, once again, could be supported by the very high stability of MEA-based emulsions, compared to MEA/SMO-based emulsions (see section 3.4.6).

From the above analysis one can conclude that the differences in elasticity shown by different surfactant types used in this study could result from the combination of interfacial elasticity (interfacial tension and interfacial dilatational modulus) and the attractive pair potential energy (van der Waals attraction, ion-fluctuation attraction) as an additional source of elasticity. Due to their different influence on surfactant-electrolyte interactions, different surfactant types induce different interfacial properties and could induce a different balance of

repulsive forces-attractive forces in the thin film between droplets; therefore, different contributions of additional elasticity.

3.4.3.5 The effect of surfactant type on flow properties

Flow curves of the emulsion with different types of surfactant for three droplet sizes and two surfactant concentrations are shown in Figures 3.22 to 3.26.

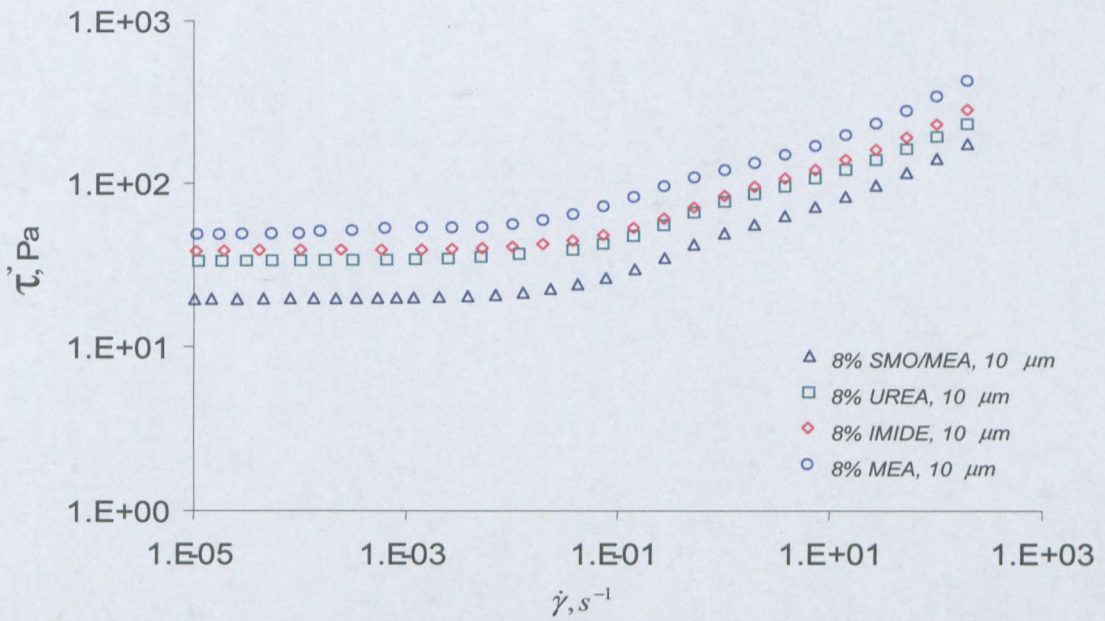

Figure 3.22: Effect of surfactant type on flow properties (d = 10 μm, 8 % surfactant in Mosspar)

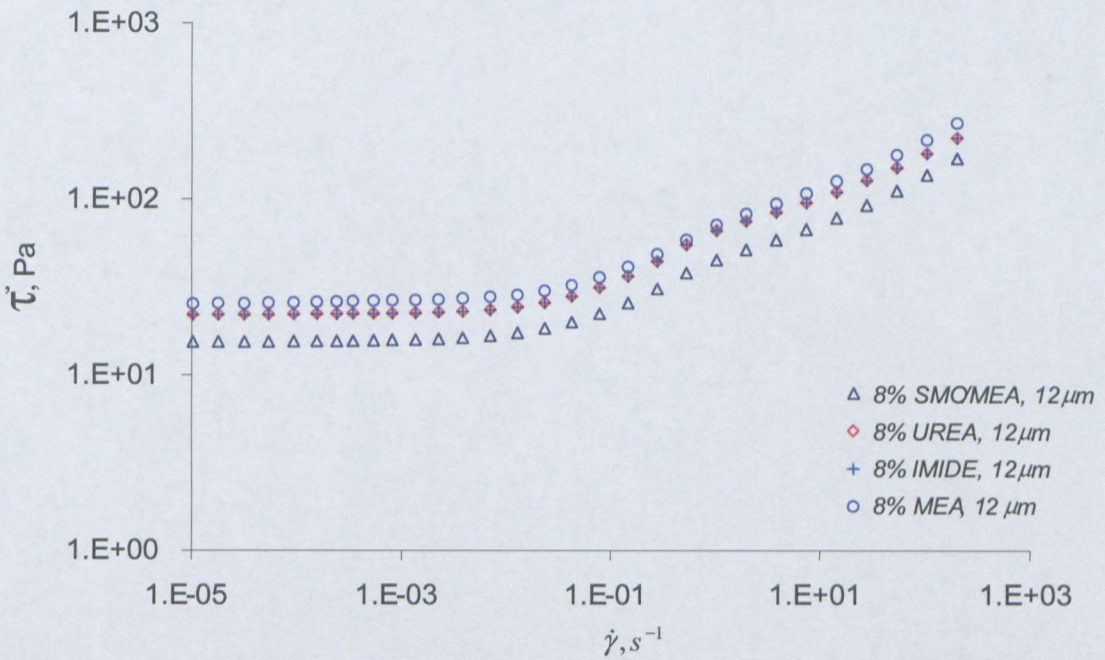

Figure 3.23: Effect of surfactant type on flow properties (d = 12 μm, 8 % surfactant in Mosspar)

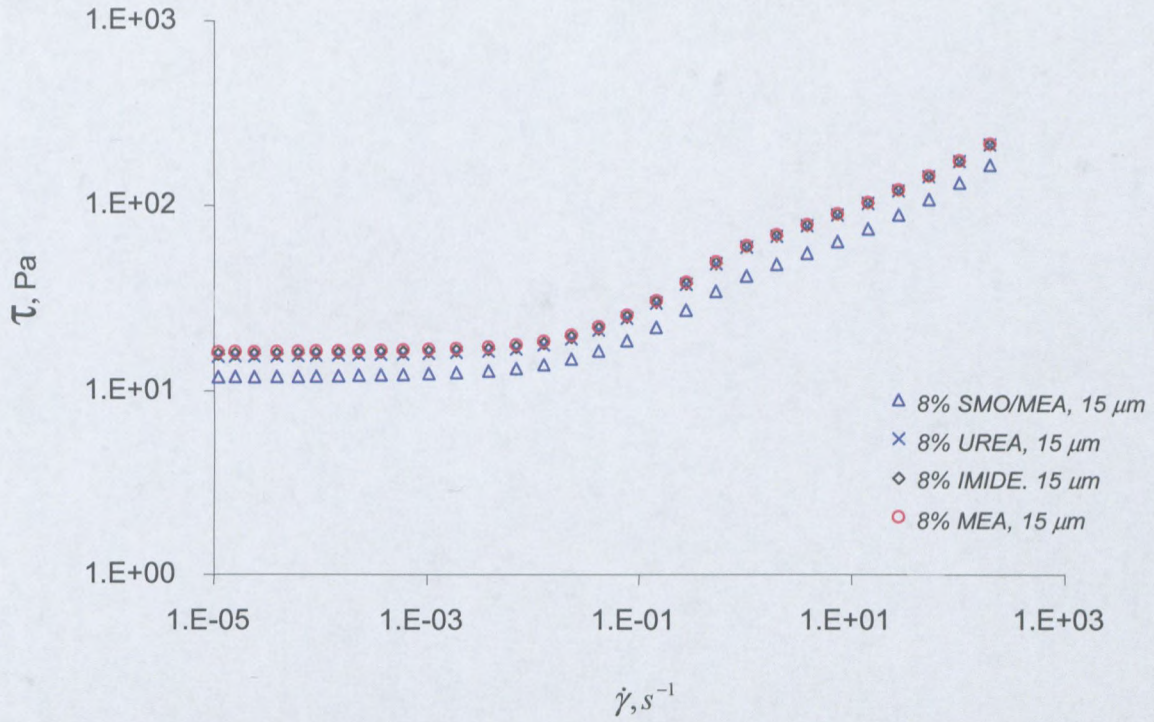

Figure 3.24: Effect of surfactant type on flow properties (d = 15 μm, 8 % surfactant in Mosspar)

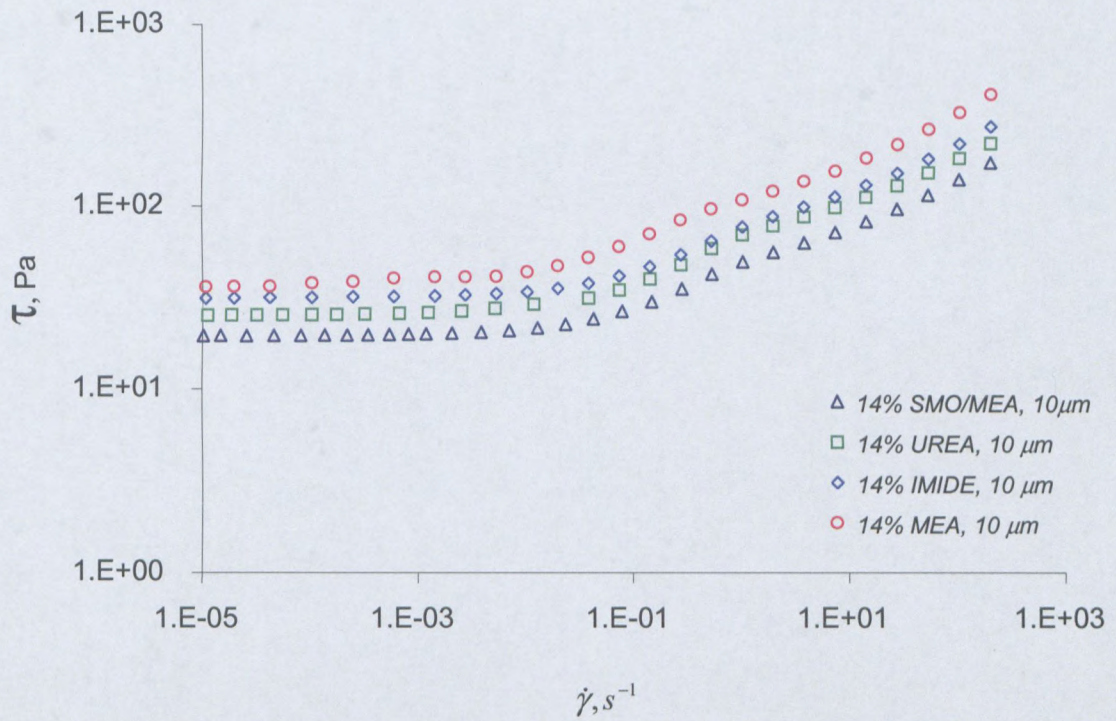

Figure 3.25: Effect of surfactant type on flow properties (d = 10 μm, 14 % surfactant in Mosspar)

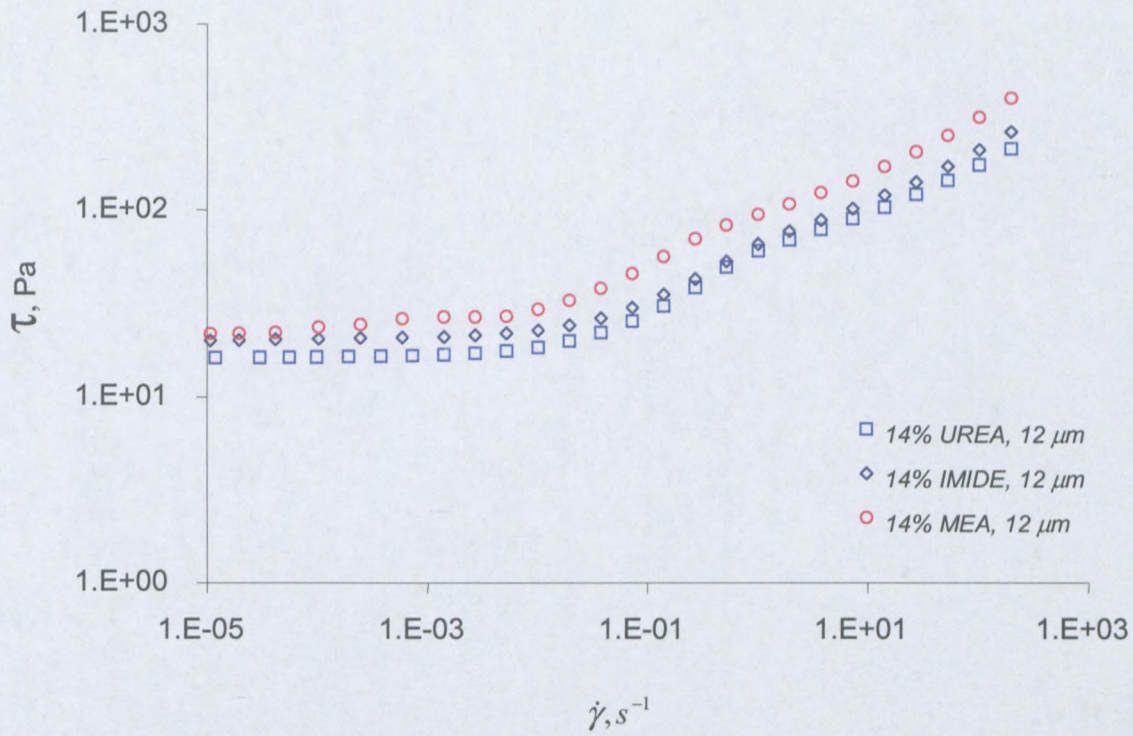

Figure 3.26: Effect of surfactant type on flow properties (d =12 μm, 14 % surfactant in Mosspar)

The effect of the type of surfactant on the yield stress for all surfactant concentrations, are listed in Table 3.11.

Table 3.11: Yield stress values determined from FC for different types of surfactant

d, μm	PIBSA-MEA	PIBSA-IMIDE	PIBSA-UREA	SMO/PIBSA-MEA
τ_y, Pa; 8 % surfactant				
10	41.9	37.4	35.6	22.6
12	24.8	21.9	21.9	15.4
15	16	15.7	15.3	11.6
τ_y, Pa; 14 % surfactant				
10	34.5	30.5	24.6	18.2
12	20.5	19.3	16	-

It can be seen clearly that the type of surfactant affects the yield stress of emulsion explosives and reveal the same trend as the elastic modulus.

3.4.4 Effect of surfactant concentration on rheological properties of explosive emulsions

The volume fraction of the dispersed phase was fixed at 85 % for all samples. The droplet sizes and droplet size distributions used in this section are given below in Figures 3.27 to 3.35 and Tables 3.12 to 3.20. Both surfactant concentrations used in this section (8 % and 14 %) were well above the CMC (see Table 3.10).

3.4.4.1 Droplet size distribution

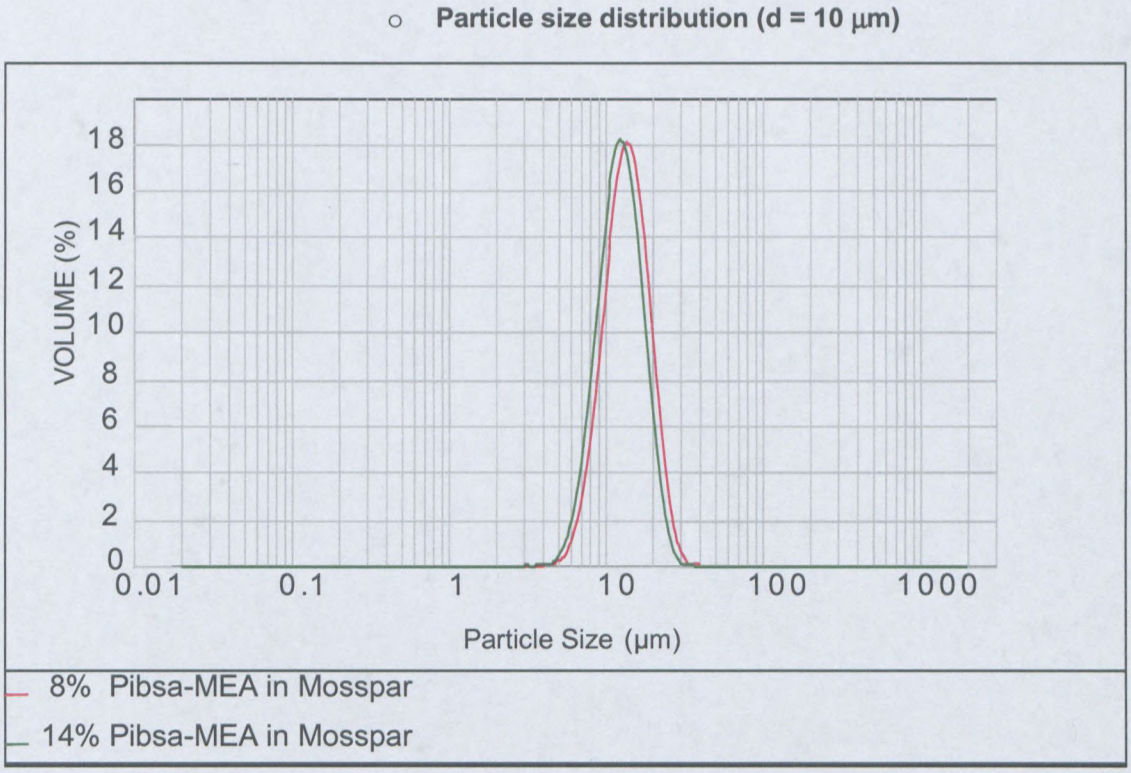

Figure 3.27: Histogram of drop size distribution of the emulsion for different Pibsa-MEA concentrations in Mosspar

Table 3.12: Under sizes of the emulsion at different Pibsa-Mea concentrations in Mosspar with droplet size 10 µm

% Surfactant	$d_{0.1}$ (µm)	$d_{0.5}$ (µm)	$d_{0.9}$(µm)	D[3,2]
8	7.1	10.7	15.9	10.1
14	6.8	10.2	14.9	9.6

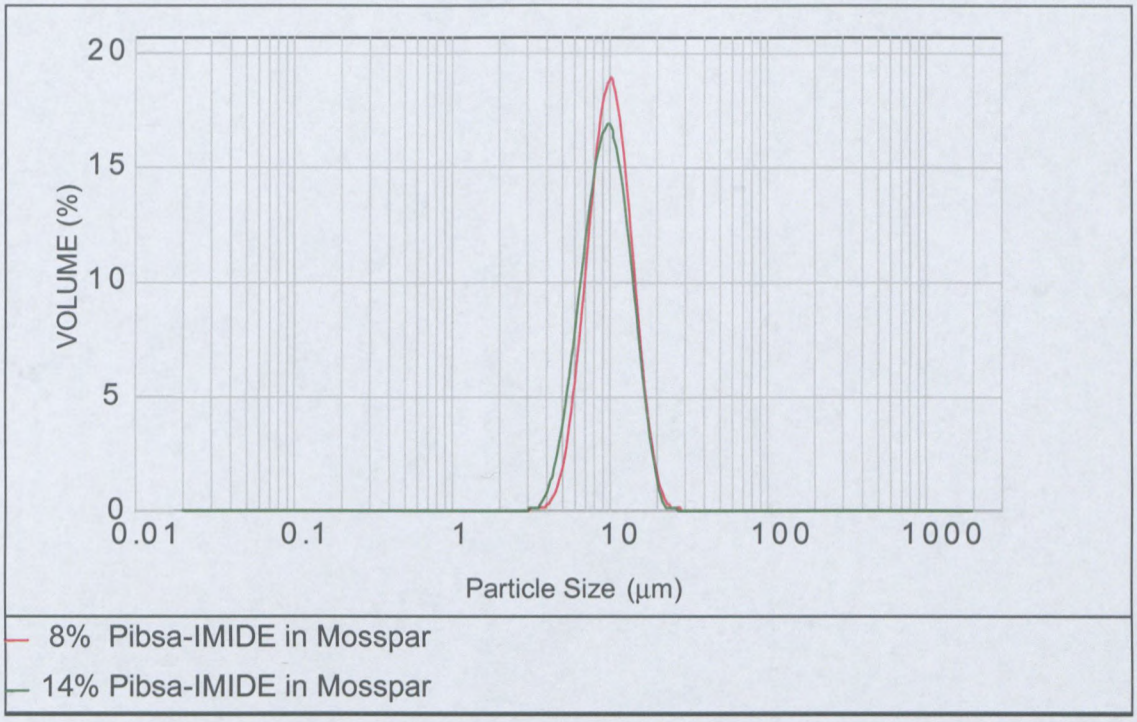

Figure 3.28: Histogram of drop size distribution of the emulsion for different Pibsa-IMIDE concentrations in Mosspar

Table 3.13: Under sizes of the emulsion at different Pibsa-IMIDE concentrations in Mosspar with droplet size 10 µm.

% Surfactant	$d_{0.1}$ (µm)	$d_{0.5}$ (µm)	$d_{0.9}$(µm)	D[3,2]
8	6.7	10.1	15.1	9.6
14	6.1	9.6	14.8	9

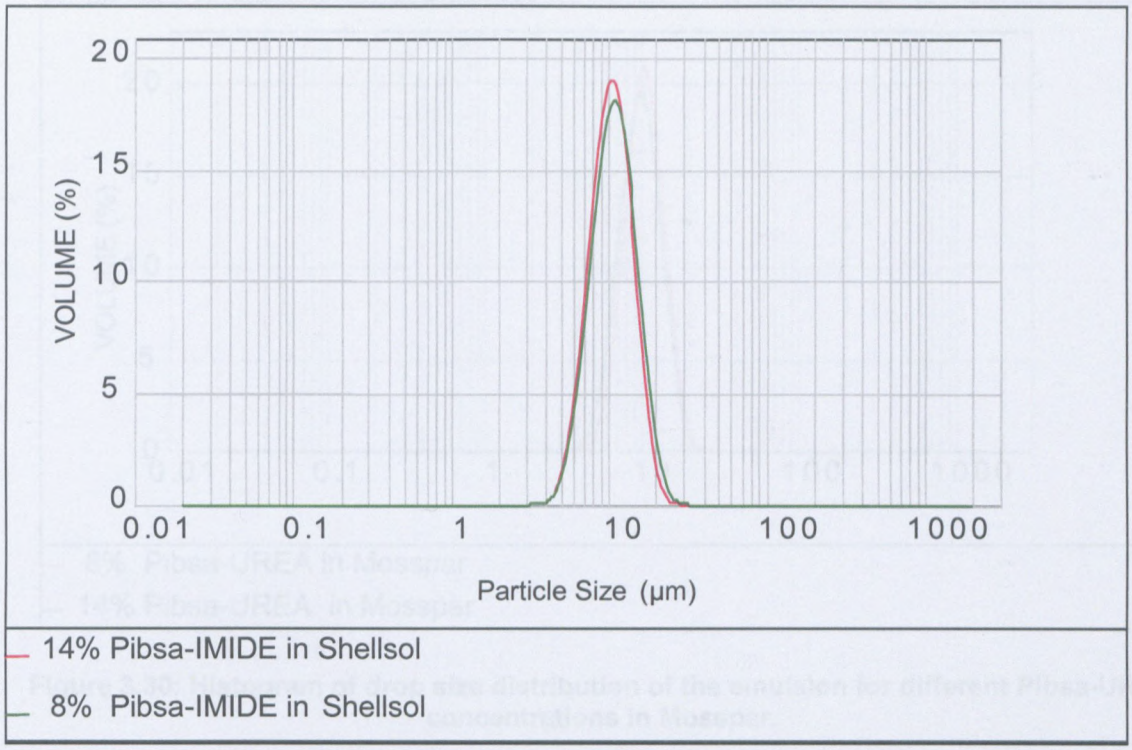

Figure 3.29: Histogram of drop size distribution of the emulsion for different Pibsa-IMIDE concentrations in Shellsol

Table 3.14: Under sizes of the emulsion at different Pibsa-IMIDE concentrations in Shellsol with droplet size10 µm

% Surfactant	$d_{0.1}$ (µm)	$d_{0.5}$ (µm)	$d_{0.9}$(µm)	D[3,2]
8	7.1	10.9	16.5	10.3
14	6.9	10.4	15.4	9.9

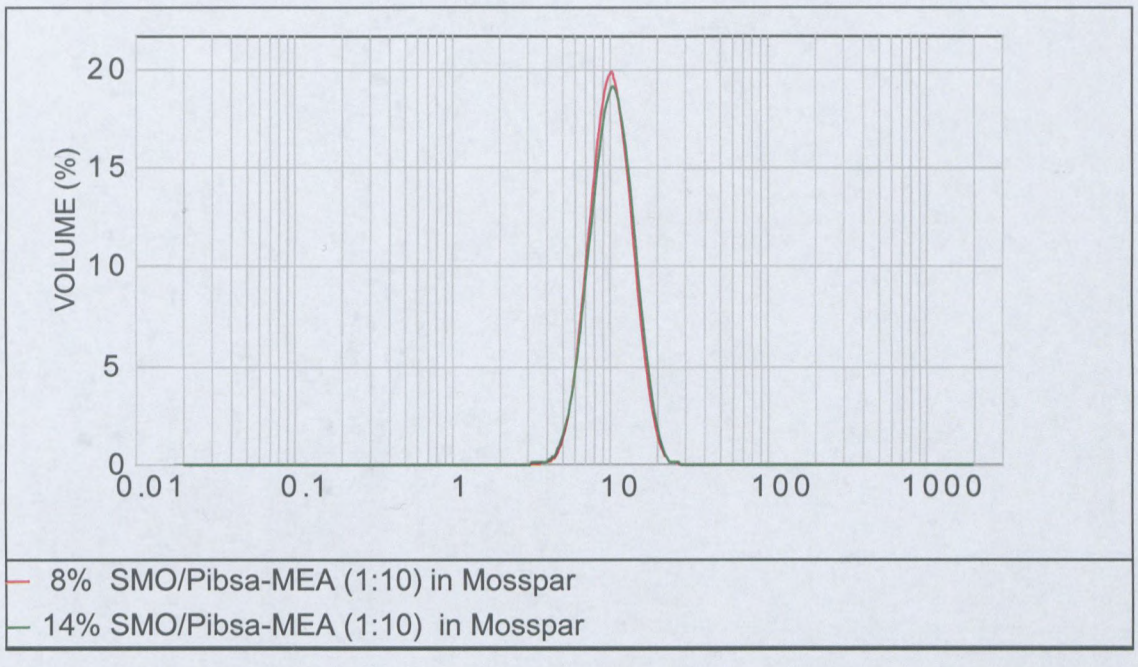

Figure 3.31: Histogram of drop size distribution of the emulsion for different SMO/Pibsa-MEA in Mosspar

Table 3.16: Under sizes of the emulsion at different SMO/Pibsa-MEA concentrations in Shellsol with droplet size 10 μm

% Surfactant	$d_{0.1}$ (μm)	$d_{0.5}$ (μm)	$d_{0.9}$(μm)	D[3,2]
8	7	10.1	14.4	9.7
14	6.9	10.4	15.4	9.9

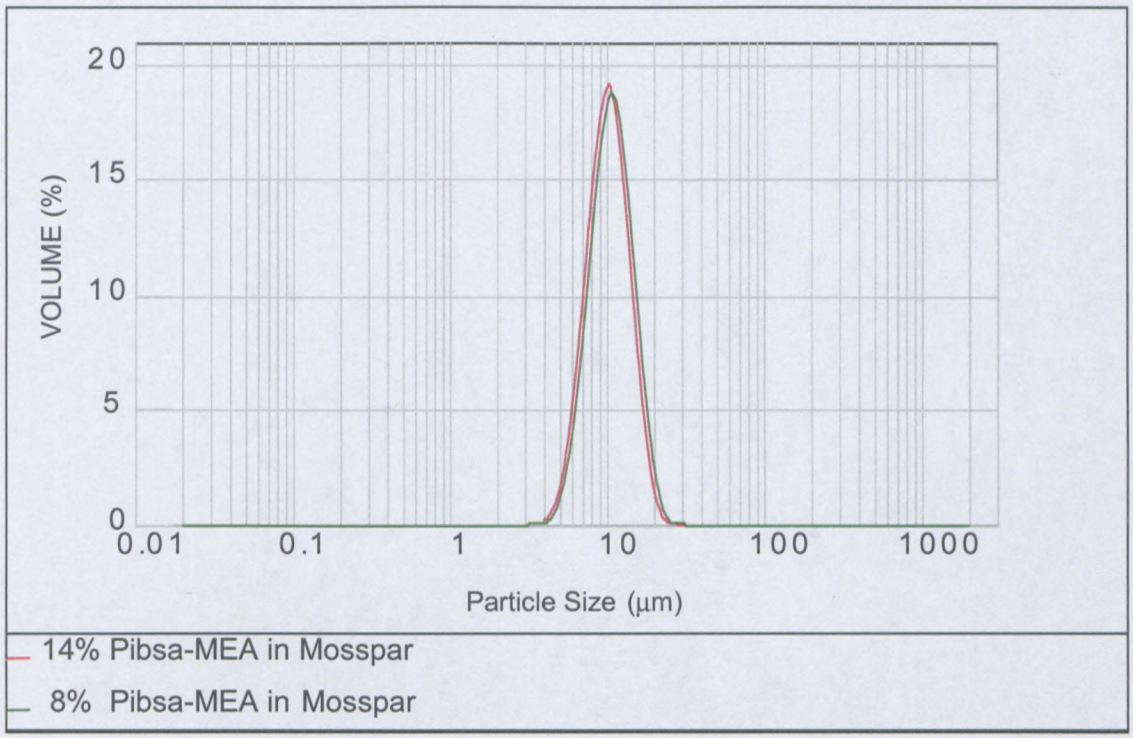

Figure 3.32: Histogram of drop size distribution of the emulsion for different Pibsa-MEA concentrations in Mosspar.

Table 3.17: Under sizes of the emulsion at different Pibsa-MEA concentrations in Mosspar with droplet size 12 μm

% Surfactant	$d_{0.1}$ (μm)	$d_{0.5}$ (μm)	$d_{0.9}$(μm)	D[3,2]
8	8.5	12.5	19.6	12.3
14	7.8	11.9	17.7	11.5

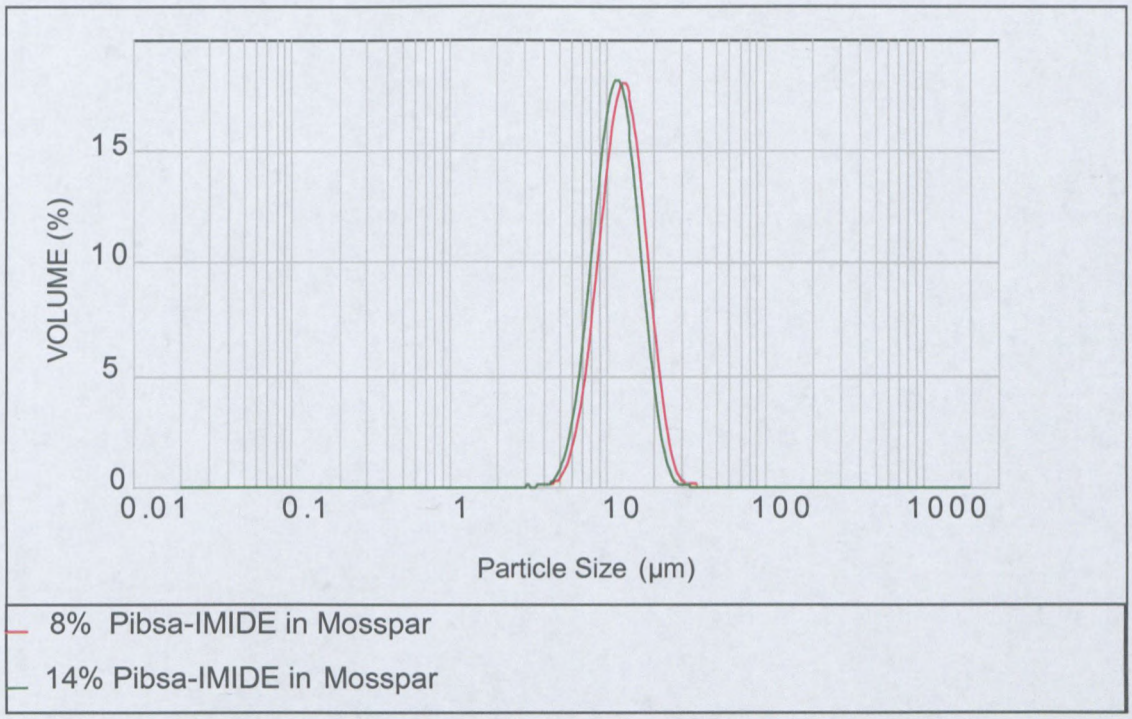

Figure 3.33: Histogram of drop size distribution of the emulsion for different Pibsa-IMIDE in Mosspar

Table 3.18: Under sizes of the emulsion at different Pibsa-IMIDE concentrations in Mosspar with droplet size 12 µm

% Surfactant	$d_{0.1}$ (µm)	$d_{0.5}$ (µm)	$d_{0.9}$(µm)	D[3,2]
8	8.2	12.7	19.2	12
14	7.5	11.6	17.4	11.9

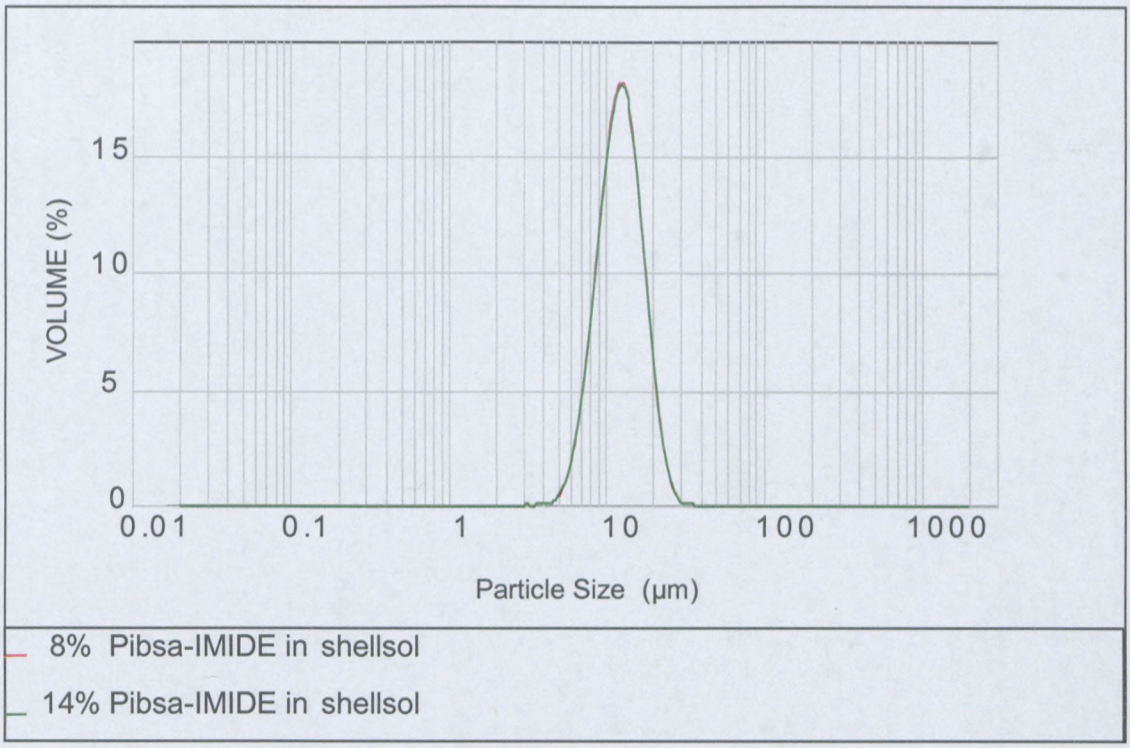

Figure 3.34: Histogram of drop size distribution of the emulsion for different Pibsa-IMIDE in Shellsol

Table 3.19: Under sizes of the emulsion at different Pibsa-IMIDE concentrations in Shellsol with droplet size 12 µm

% Surfactant	$d_{0.1}$ (µm)	$d_{0.5}$ (µm)	$d_{0.9}$(µm)	D[3,2]
8	8.1	12.4	18.6	11.7
14	7.8	12.7	20.5	11.9

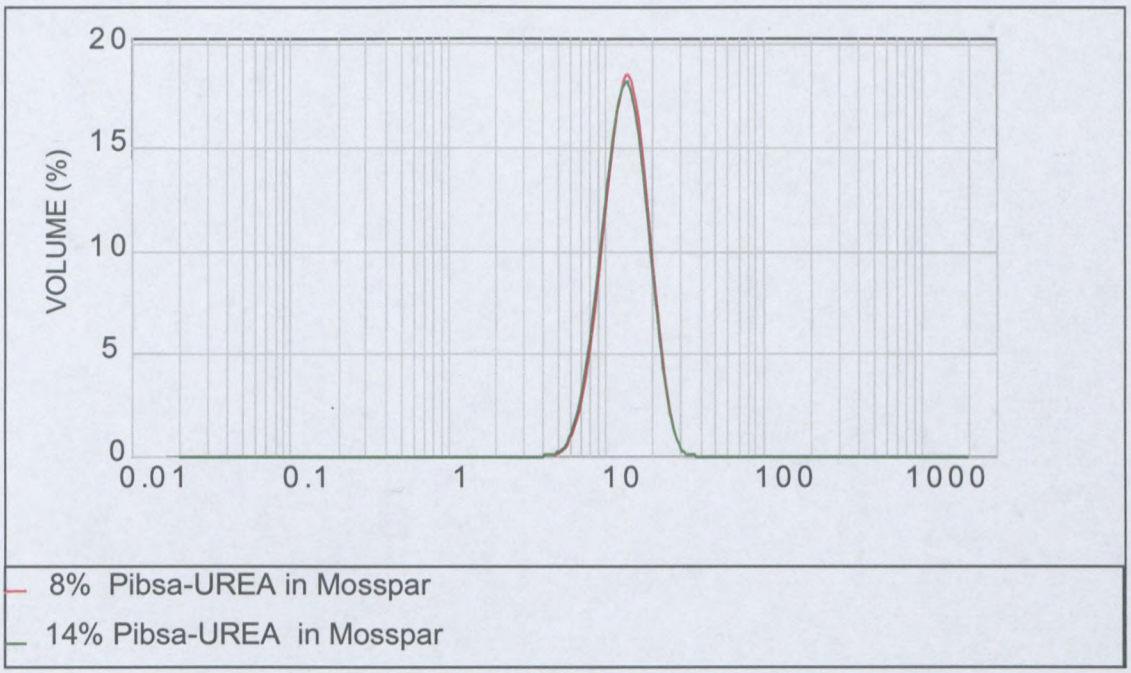

Figure 3.35: Histogram of drop size distribution of the emulsion for different Pibsa-UREA concentrations

Table 3.20: Under sizes of the emulsion at different Pibsa-UREA concentrations in Mosspar with droplet size 12 μm

% Surfactant	$d_{0.1}$ (μm)	$d_{0.5}$ (μm)	$d_{0.9}$(μm)	D[3,2]
8	8.9	13.6	20.2	12.9
14	8.7	13.5	20.3	12.7

There is no need to demonstrate all the experimental results here, because all are essentially similar. All rheological properties and dependence of rheological properties on the surfactant concentration will be presented on the basis of the behaviour of samples with Pibsa-IMIDE in Mosspar. For the rheological data on emulsions with Pibsa-MEA, Pibsa-UREA and SMO/Pibsa-MEA, see Appendix A.

3.4.4.2 Viscoelastic properties

Figure 3.36 and Figure 3.37 show the influence of the surfactant concentration on the storage modulus as a function of strain amplitude, for two droplets sizes.

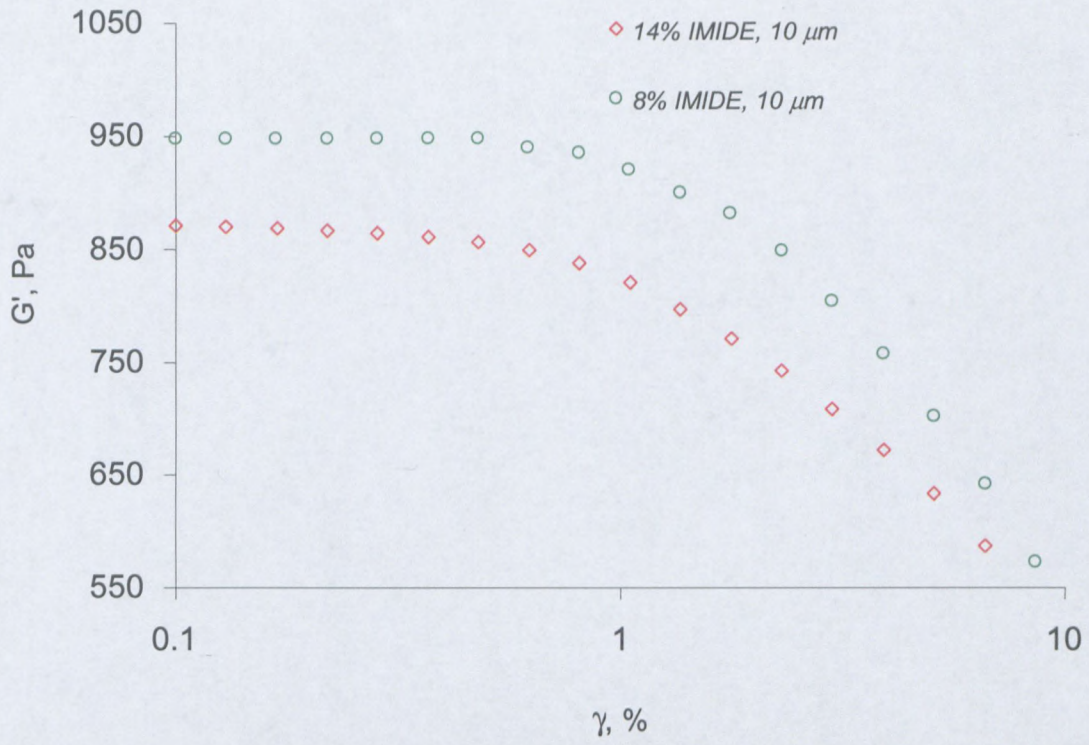

Figure 3.36: Strain amplitude dependencies of the storage modulus as a function of surfactant concentration in Mosspar (Pibsa-IMIDE, d = 10 μm)

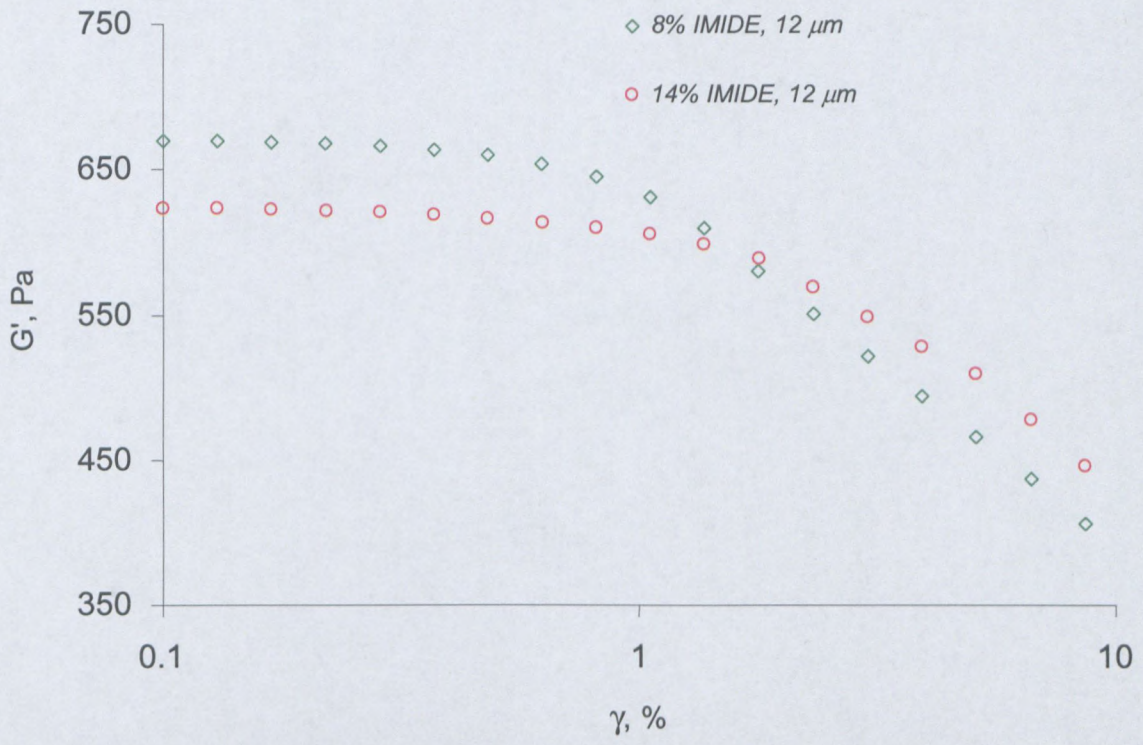

Figure 3.37: Strain amplitude dependencies of the storage modulus as a function of surfactant concentration in Mosspar (Pibsa-IMIDE, d = 12 μm)

The effects of the surfactant concentration on the storage modulus associated with the linear region, for all surfactant types, are listed in Table 3.21.

Table 3.21: Effect of surfactant type on viscoelastic properties of explosive emulsions

Surfactant type	d, μm	% Surfactant	G', Pa
Pibsa-MEA	10	8	1012
		14	884
	12	8	696.5
		14	630.5
Pibsa-IMIDE	10	8	948
		14	868.9
	12	8	669.5
		14	622.2
Pibsa-IMIDE	10	8	953
		14	877
	12	8	675
		14	630.3
Pibsa-UREA	10	8	911
		14	809.8
	12	8	656.4
		14	603
Pibsa-MEA/SMO	10	8	661
		14	550

The effect of the surfactant concentration on the viscoelastic properties is quite evident:

- For all Pibsa-based surfactants used in this study, the storage modulus of explosive emulsions was sensitive to the surfactant concentration. However, the effect was seen to decrease as the droplet size increased.
- The storage modulus was a decreasing function of surfactant concentration within our experimental window. This effect could not be accounted for on the basis of the interfacial tension or adhesive forces. In fact, the interfacial tension was not sensitive to the surfactant concentration (see Table 3.10). On the other hand, an increase in reverse micelle concentration was expected to increase the depletion osmotic pressure and thus improve elasticity because of the increase in adhesive forces between droplets (Babak *et al.*, 2002).

The above results emphasise that an increase in reverse micelle concentration does not affect the intrinsic elasticity of the droplet (the capillary pressure). It decreases only the magnitude of the additional elasticity. The interfacial elastic modulus cannot explain this observation (because, as said before, the dilatational elastic modulus was not sensitive to

the surfactant concentration). We consider this fact as rather important. It is reasonable to accept it as additional proof of the impact of the interaction potential between droplets on the bulk elasticity of explosive emulsions.

In explosive emulsions reverse micelles could act as stabilisers in preventing contact between the contents of different droplets. Indeed, the highly unstable emulsions are those in which the reverse micelle concentration is very small (White *et al.*, 2004). The stabilising forces could be attributable to both steric and electrostatic repulsive forces (Ganguly *et al.*, 1992). It is worth mentioning that Pibsa-based reverse micelles present in the oily phase of explosive emulsions possess electrical charges because of the presence of ammonium nitrate in the core (Reynolds *et al.*, 2000; 2001). According to these references we can assume that an increase in reverse micelle concentration could increase the repulsive (steric and electrostatic) forces in the system. This could reduce the impact of van der Waals attraction as additional source of elasticity, thus reducing the overall elasticity of the system.

3.4.4.3 Flow properties

Flow curves of the emulsions with different surfactant concentrations for two droplet sizes are shown in Figures 3.38 and 3.39

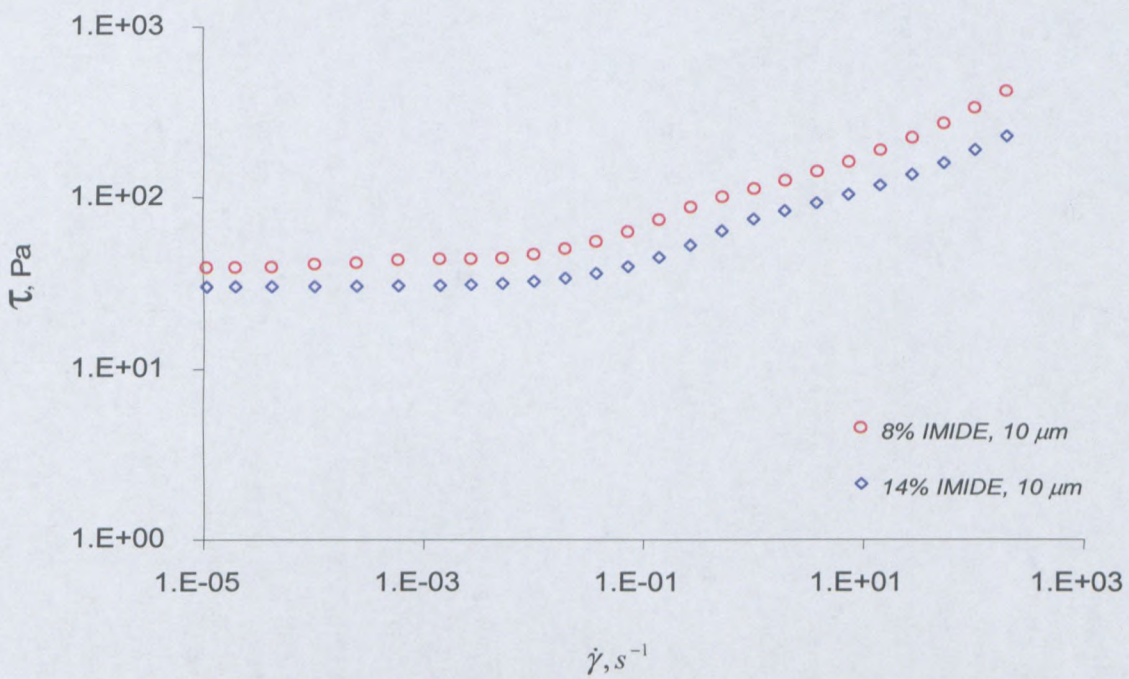

Figure 3.38: Flow curves of the emulsions with different surfactant concentrations (d = 10 μ m, Pibsa-IMIDE in Mosspar)

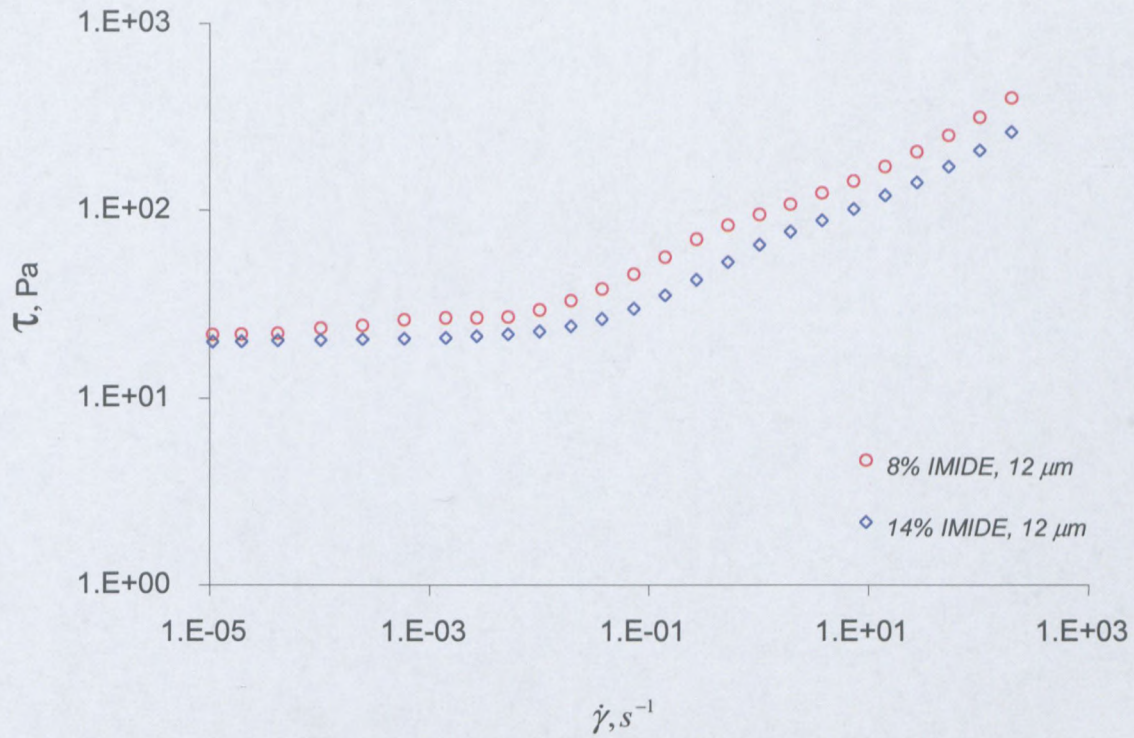

Figure 3.39: Flow curves of the emulsions with different surfactant concentrations (d = 10 μm, Pibsa-IMIDE in Mosspar)

The values of yield stress as a function of surfactant concentration are reported in Table 3.22.

Table 3.22: Yield stress values determined from FC for different surfactant concentrations

Surfactant type	d, μm	% Surfactant	τ_y, Pa
Pibsa-MEA	10	8	41.9
		14	34.5
	12	8	24.8
		14	20.5
Pibsa-IMIDE	10	8	37.4
		14	30.5
	12	8	21.9
		14	19.3
Pibsa-IMIDE	10	8	39.5
		14	31.2
	12	8	22.5
		14	20.1
Pibsa-UREA	10	8	35.6
		14	24.6
	12	8	21.9
		14	16
Pibsa-MEA/SMO	10	8	22.6
		14	18.2

It is clear that the type of surfactant affects the yield stress of explosive emulsions, following the same trend as the elastic modulus.

3.4.5 General conclusions regarding the effect of surfactant type and concentration

The sensitivity of the rheological properties of high-internal phase water-in-oil explosive emulsions to the type and concentration of the surfactant has been investigated in this study (see section 3.4.3 and section 3.4.4). It was found that the type of surfactant and surfactant concentration affect the rheological properties of explosive emulsions. In fact, both the elastic modulus and the yield stress decrease in the following order: MEA-IMIDE-UREA-MEA/SMO and also decrease as the surfactant concentration increases. However, the sensitivity of the rheological parameters to the type or concentration of surfactant becomes less pronounced as the droplet size increases.

In the linear regime, the dimensionless elastic modulus was found to depend on the type and concentration of surfactant. This was an indication of the existence of additional sources of elasticity in the system. Indeed, with other factors such as electrolyte concentration, phase ratio, surfactant concentration and the nature of the external phase being kept constant, IMIDE-based emulsions showed very high dimensionless elastic moduli compared to emulsions prepared with other Pibsa-based surfactants. It was found, moreover, that changing the surfactant type affects both the intrinsic elasticity of the droplets (by changing the interfacial tension) and the magnitude of the additional elasticity while an increase in surfactant concentration does not affect the intrinsic elasticity of the droplet (the capillary pressure). It decreases only the magnitude of the additional elasticity.

The structure of the emulsion explosive is directly related to its rheology. Because the dispersed phase volume fraction was much higher than the critical concentration for systems with uncompressed spheres, the polyhedral distortions occurred in the emulsion under investigation (see Figure 3.8).

Lissant *et al.* (1974) proposed that free droplets make contact with the film separating the droplets at a finite angle which is a function of the dispersed phase volume fraction and a function of molecular forces across the film. This forces the droplets into complex non-spherical shapes. Kirby (1983) has developed a semi-empirical theory for the geometry of emulsion explosives which describes this in terms of the radius of curvature of the pockets of

oil phase at the corners between droplets, the thickness of the film separating droplets, and the plateau angle.

It has been emphasised before in this study (see section 3.4.3) that the surfactant concentrations that were used were far above the CMC. In our emulsion, therefore, the major part of the surfactant was in the form of reverse micelles in the oil phase, and dissolved in the oil phase. Rather less occurred as a monolayer at a flat aqueous-oil interface. Furthermore, Pibsa-based reverse micelles present in the oily phase of explosive emulsions are expected to be spherical and to possess electrical charges because of the presence of ammonium nitrate in the core (Reynolds *et al.*, 2000; 2001).

The rheological properties of concentrated emulsions are governed by the different forces that occur in the system, which, in turn, depend on the thickness of the interdroplet layer (thin film between droplets), on type of surfactant and on surfactant concentration. In the particular case of the Pibsa-based emulsion explosives used in this study: on the one hand, because of the non-ionic character of surfactants, the dominant interaction energy between droplets could be ascribed to van der Waals attraction (Alvarez *et al.*, 2006; Bibette *et al.*, 1999; Baravian *et al.*, 2006; Quintero *et al.*, 2008). Moreover ion-fluctuation within the aqueous droplets could have given rise to an additional attractive potential energy in the thin film between droplets, similar to the van der Waals interaction between neutral atoms (Sheng *et al.*, 2004; Tsao *et al.*, 2002). Such electrostatic attraction is insensitive to the ion concentration and consists of contributions from various induced multipole-multipole interactions, including dipole-dipole, dipole-quadrupole, dipole-octupole, and quadrupole-quadrupole interactions (Sheng *et al.*, 2004). On the other hand, because of the polymeric nature of the surfactants and the presence of AN in their core (Reynolds *et al.*, 2000; 2001), reverse micelles might induce both steric and electrostatic repulsive forces (Ganguly *et al.*, 1992), whereas the separation of charges induced by surfactant-electrolyte interaction (Ashok *et al.*, 1991; Ganguly *et al.*, 1992) could give rise to electrostatic repulsion between adjacent droplets, similar to the repulsions between permanent dipoles.

In summary: above the CMC, the influence of the surfactant concentration on the rheological behaviour for our emulsions was qualitatively different from the effect of surfactant type. All changes observed could be understood by taking into account that changing of surfactant type gives rise to modification of both the interfacial properties (interfacial tension and interfacial elasticity) and the reverse micelle structure in the oily phase. It could also have affected the distribution of ions within the droplet (number of ions involved in the formation of hydrogen-

bonded species with the surfactant, ion-fluctuation and the magnitude of the dipole moment of the droplet). In contrast, the variation of surfactant concentration led only to changes in reverse micelle concentration, the quality of the monolayer and interfacial properties remaining the same. However it must be emphasised that in both cases the thickness of the interdroplet layer may have undergone slight changes due to the modification in molecular forces across the film (interactions between surfaces of adjacent droplets and/or interactions between reverse micelles in the thin film). Furthermore, because of their electrostatic charge, reverse micelles may well have affected the distribution of charges inside the droplet.

The rheological properties of the compressed emulsions under investigation depended sensitively on the intrinsic elasticity of the droplets, on the concentration of reverse micelles and seemed to depend also on the interfacial elastic modulus, the distribution of ions within the droplet (surfactant-electrolyte interactions, ion-fluctuation, dipole-dipole...) and the van der Waals attraction between adsorbed surfactants. The elasticity of droplets, and the degree of deformation, are controlled by their internal pressure (Laplace pressure) and the oil film network structure, whereas the strength of the interface could have been controlled mainly by the surfactant-AN interaction (binding affinity of the surfactant). On the other hand, the reverse micelle concentration, the distribution of ions within the droplet, the physical interaction between interface layers of different droplets and the van der Waals attraction could have controlled the pair potential energy in the thin film between droplets. Indeed, the dilatational elastic modulus, the ion-fluctuation attraction and the van der Waals attraction could have acted as sources of additional elasticity. However, any increase in electrostatic or steric repulsive forces in the system (increase in dipole moment of the droplet or increase in reverse micelle concentration) could have reduced the contribution of the van der Waals attraction to the overall elasticity. The balance repulsive forces-attractive forces could be one of the major factors which might determine the magnitude of the additional elasticity in the overall bulk elasticity of explosive emulsions. The strong deviation of the IMIDE-scaled elastic modulus in comparison with other surfactants could be an indication of the highest impact of attractive forces (ion-fluctuation and van der Waals forces) as additional sources of elasticity.

It can be concluded that, because the lipophilic tail group (non-polar region) is the same for all surfactants used in this study, the observed differences in rheological properties of explosive emulsions have to be attributed primarily to the different chemical structures of the surfactant head group and their possible influence on the surfactant-electrolyte interactions. Indeed the balance repulsive-attractive forces, the intrinsic elasticity or the interfacial elastic modulus are very sensitive to this factor.

The stability of emulsion explosives is connected with crystallisation of the aqueous phase. In fact, because of the presence of supersaturated drops, emulsions in this study were in an inherently metastable system. At temperatures lower than the crystallisation temperature of the AN-solution (fudge point = 60° C) we had to be concerned with crystal nucleation. As a result, the ageing of the emulsion under investigation had to be associated with the crystallisation process of AN droplets (metastable).

The above denotes that, during the ageing process, the two-phase samples would transform to multiphase dispersions, the substances consisting of two phases (droplets and crystals) dispersed within a continuum of a third phase. Being transformed into particle suspensions (crystals) in viscoelastic media (emulsion) the studied samples could exhibit interesting rheological properties (Pal, 2000b; Marcovich *et al.*, 2004; Harzallah & Dupuis, 2003).

It should be realised that crystals are not necessarily confined to their original droplet shape, but can break through the films separating droplets (Becher, 1988; Kharatiyan, 2005; Masalova *et al.*; 2006; Masalova & Malkin, 2007b). Therefore, the strength (elasticity) of the interface (Masalova *et al.*, 2005; White *et al.*, 2005), the reverse micelle concentration (White *et al.*,2004), the interfacial tension and the van der Waals attraction are important when investigating the emulsion stability (degree of crystallisation) with ageing.

The ageing could be considered as:

- Initiation of crystallisation of the dispersed phase of the emulsion
- Penetration of the crystallinity throughout the substance

The homogeneous nucleation process depends strongly on the spatial distribution of ions within the droplet. In fact, when increasing the AN concentration in an aqueous solution, there is a decrease in the coordination number and the hydration shell moves closer in at higher concentrations. With AN concentrations higher than 60 % by mass, there is evidence of direct interaction between NH_4^+ and NO_3^- (Walker *et al.*, 1989). Thus the stability against homogeneous nucleation depends mostly on the ability of additives (ions, molecules, surfactant head group) to increase the separation distance between NH_4^+ and NO_3^- ions (Ashok *et al.*, 1991; Ganguly *et al.*, 1992).

The penetration of the crystallisation process with time (kinetic of crystallisation) could depend on reverse micelle concentration as well as on the strength of the interface (Kharatiyan, 2005; White *et al.*, 2005). In fact, the strength of the interface could act as an

3.4.6.1 Droplet size measurements

The droplet size measurements of samples were performed every week until the crystallisation process initiation showed no significant changes in the sizes of droplets (Figure 3.40).

- **Particle Size Distribution (8 % Pibsa-IMIDE in Mosspar for droplet size 10 μm)**

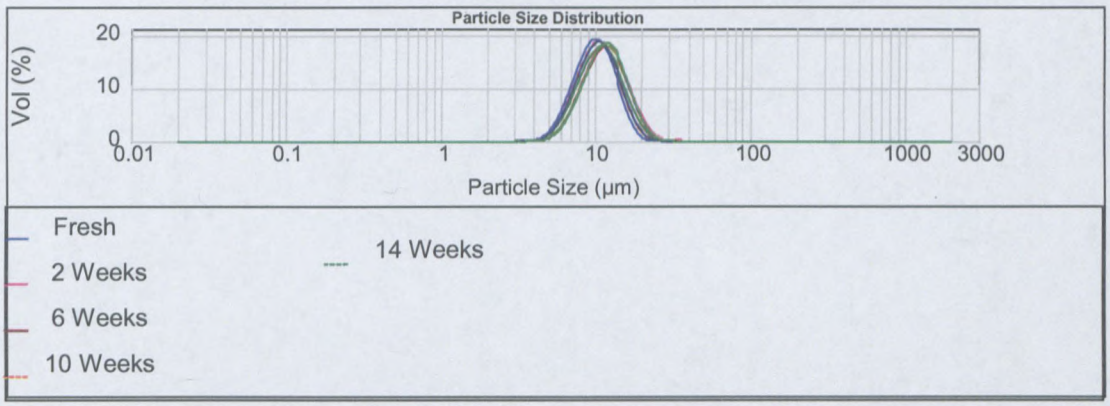

Figure 3.40: Histogram of typical droplet size distribution of the emulsion with time before the crystallisation of the dispersed phase took place.

Based on the above histogram, we may assume that no coalescence took place during the process of ageing of the samples under investigation, and all structural changes are related to the crystallisation of the dispersed phase. A similar result was found in earlier publications (Kharatiyan, 2005; Masalova *et al.*; 2006; Masalova & Malkin, 2007b). This could be related to the electrostatic and steric effects induced by the presence of reverse micelles and/or the presence of a net electrostatic charge inside the droplets caused by the surfactant-electrolyte interaction.

3.4.6.2 Optical analysis

A qualitative investigation of the crystallisation process was performed using an optical 'Leica' microscope equipped with a digital camera, at a magnification of 500 times. The aim of this exercise was to analyse the shape and size of crystals as a function of surfactant type.

The optical microscopy showed that ageing of the emulsion was associated with the crystallisation process of the dispersed phase. The observation of microscopic images also suggested that the crystals were a mixture of stone-like and needle-like shapes. It should be noted, also, that the droplets of emulsions are much smaller than the suspended crystals as can be seen clearly from the photomicrographs shown in Figures 3.41 to 3.43. This result

can be understood as follows: no matter which type of surfactant is used, when crystallisation starts, the crystals do not remain inside the droplet.

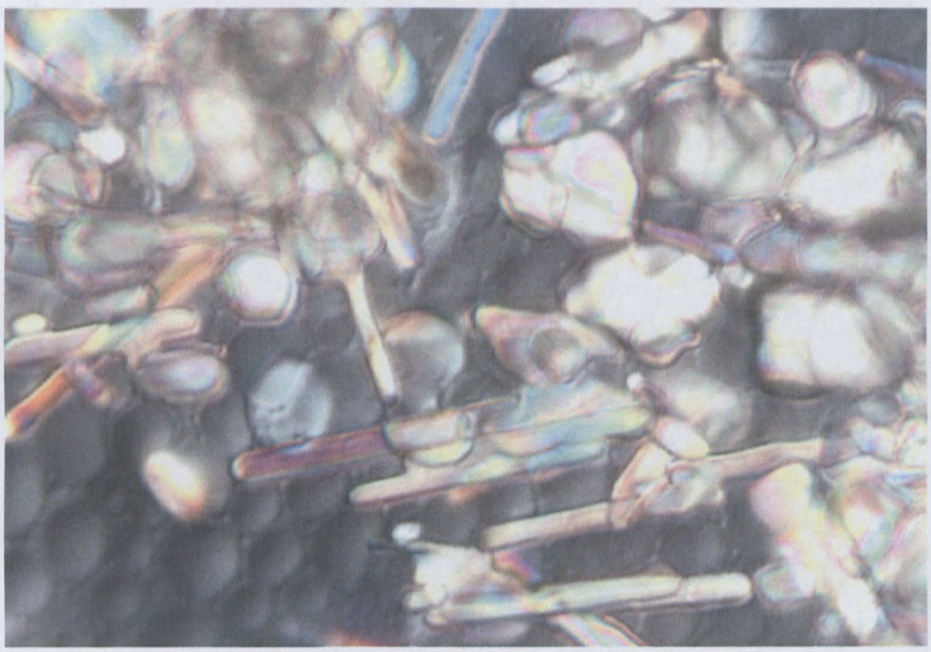

Figure 3.41: Microscopic image, magnification 500 x, age 17 weeks (8 % Pibsa-IMIDE in Shellsol, 10 μm)

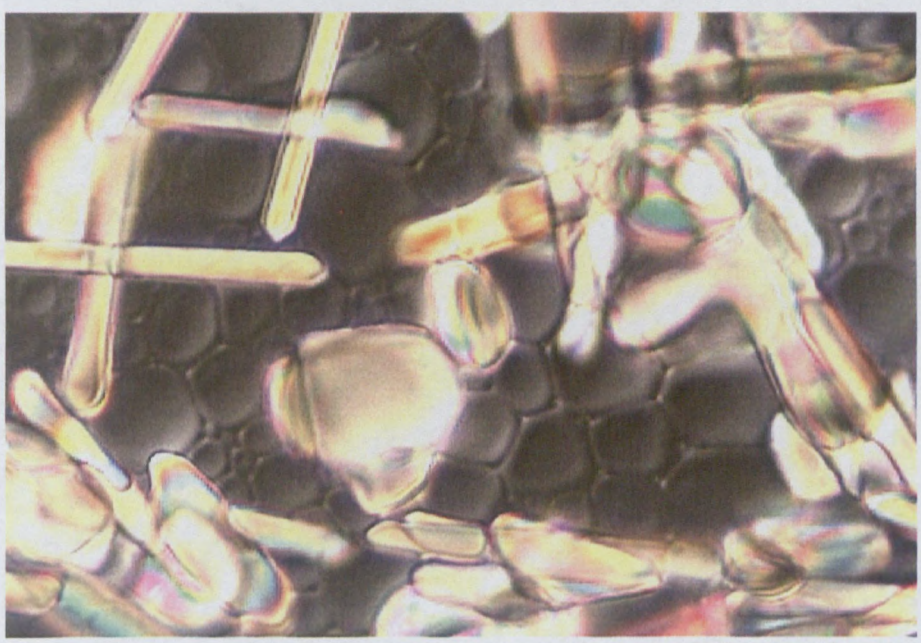

Figure 3.42: Microscopic image, magnification 500 x, age 17 weeks (8 % Pibsa-IMIDE in Mosspar, 10 μm)

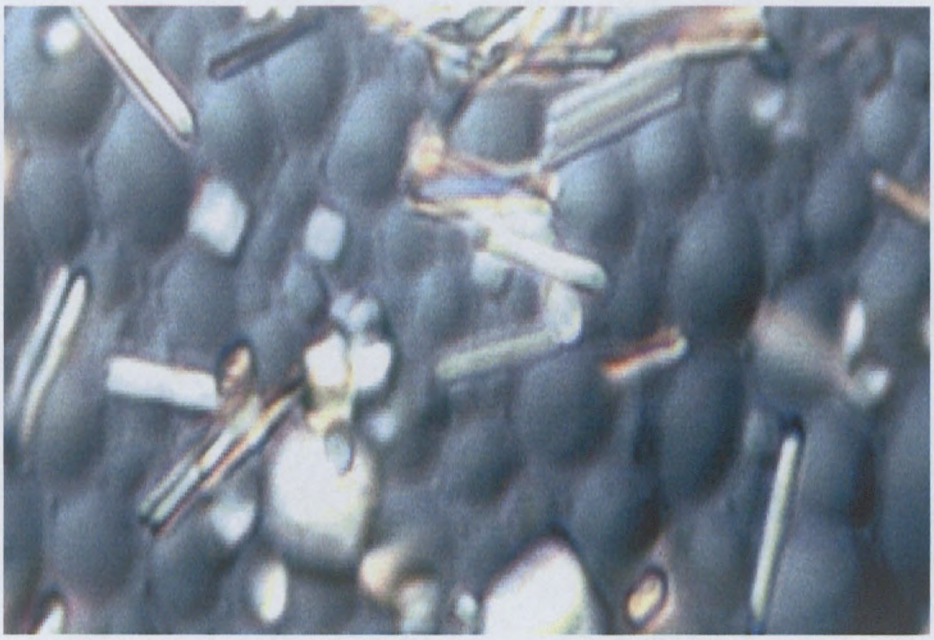

Figure 3.43: Microscopic image, magnification 500 x, age 17 weeks (8 % Pibsa-MEA/SMO in Mosspar, 10 μm)

3.4.6.3 X-ray diffraction

The X-ray analysis was performed weekly over a period of 36 weeks for all samples under investigation in order to quantitatively follow the structural changes in terms of the degree of crystallinity of emulsion with ageing. The X-ray diffraction analysis to determine the emulsions crystallinity was done on a Bruker D8 Advance powder diffractometer using Cu radiation. Conventional Bragg Brentano geometry was used with a Ni filter and a 2θ scan range of 10 to 60° at 0.02-step intervals and at a scan rate of 1 sec/step. The emulsion samples were placed into a standard top-loading polycarbonate sample holder and supported on a horizontal rotating sample stage. Structural information obtained from the literature of the various solid phases of ammonium nitrate was used to do Rietveld refinement of the complete diffraction pattern and to determine the degree of crystallinity, using the Topas 3.0. Once a sample had achieved full crystallisation, the degree of crystallinity for each sample as determined from the diffraction data and the subsequent Rietveld refinement could be normalised relative to the fully crystallised sample. This configuration allowed the analysis of uneven samples in particular slurries or emulsions without causing any shifts of the respective diffracted peaks. An external corundum standard was used to align the diffractometer, ensuring that similar diffracted intensity peaks were obtained for each batch of samples analysed.

X-ray studies were based on following the diffraction pattern of $NH_4 NO_3$ (AN) as the main solid component of a dispersed phase.

The relative crystallinity, X, was determined from the intensity differences of the fully crystalline and the amorphous phases of the room temperature AN emulsion. This was done by considering the super-cooled emulsion as amorphous (I_{am}). The fully crystalline phase (I_{cr}) is observed when the AN emulsion has completely broken down resulting in almost complete crystallisation of the material. This is achieved by observing the fact that a selected sample indicates very little or no change in its respective intensities of the diffraction pattern over time. The peak intensities chosen for this study were the 17 reference peaks for pure AN phase IV obtained from PDF (powder diffraction file release, 2002).

The *X* values were calculated from the dependence of (I_x - I_{am}) versus (I_{cr} - I_{am}) where I_x is the intensity of a sample with unknown crystallinity. The differences of (I_x - I_{am}) versus (I_{cr} - I_{am}) are shown graphically in Figure 3.44 for 17 reference peaks with the corresponding straight line that passes through the origin. It is important that all 17 points lie on the straight line where the slope of the straight line relates to the relative crystallinity. It is evident that, for an amorphous sample, the slope equals zero and, for a completely crystalline sample, the slope equals 1. In an example presented in Figure 3.44 X = 78% with a R^2 correlation of 0.99.

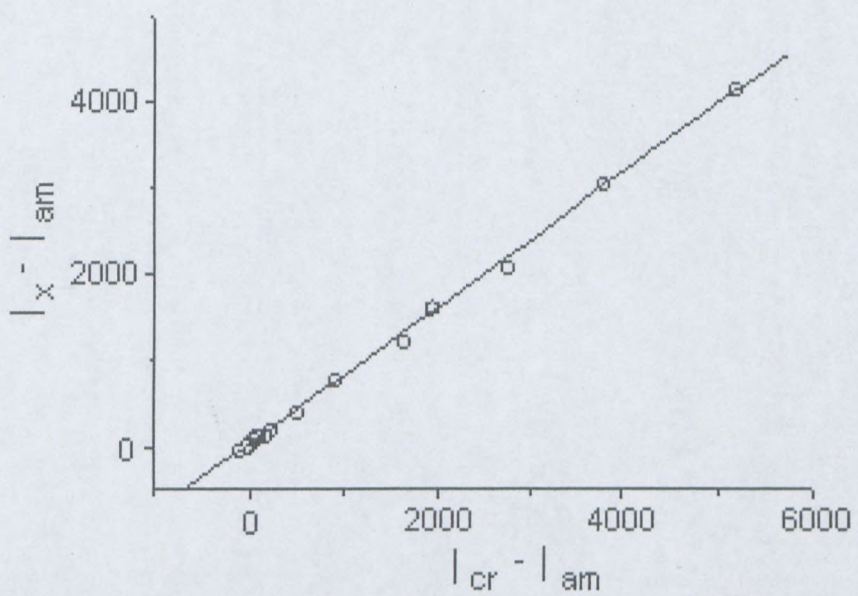

Figure 3.44: Calibration line for X-ray analysis for a sample aged 17 weeks and showing a crystallinity of 78 %.

X-ray diffraction patent analysis was devoted to evaluating the structural changes (degree of crystallinity of the dispersed phase, and phase transitions of ammonium nitrate solid) during the ageing period.

There is no need to demonstrate all the experimental results here because all the experimental diffractograms are essentially similar. Typical diffractograms of the AN emulsions studied are shown in Figure 3.45.

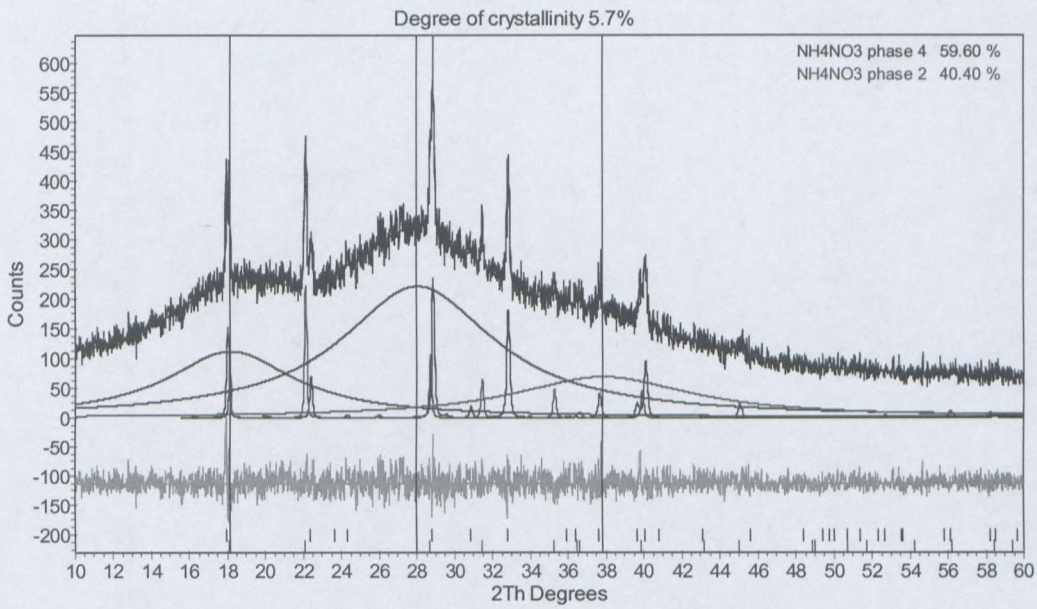

Figure 3.45: Staggered X-ray powder diffractograms of the AN emulsion

The kinetic of crystallisation and different phase transitions in the solid state could be extracted from the X-ray diffraction analysis and the results are presented in Tables 3.23, 3.24, 3.25, 3.26 and 3.27 respectively for all surfactant types in Mosspar and Shellsol for all surfactant concentrations.

Table 3.23: Degree of crystallinity and phase transitions for different surfactant types during ageing (Pibsa-IMIDE in Mosspar)

Surfactant Type	% Surfactant	d, μm	t, week	X_{Cr}, %	Phase transition, IV to II
Pibsa-IMIDE	8	10	0-8	0	
			9	2.5	85/15
			10	3.5	81/19
			13	6.5	88/12
			17	13.5	57/43
			19	19	82/18
			24	24	64/36
			27	41.5	55/45
			31	49	76/24
		12	0	0	-
			3	1	-
			6	2	-
			9	4.5	42/58
			10	15	29/71
			19	27	43/57
			24	61	87/13
			27	76	93/7
			31	100	100/0
			36	100	-
		15	0	0	-
			3	1.5	-
			6	2	-
			10	6	-
			13	11	80/20
			17	24	57/43
			19	32	72/28
			24	71	96/4
			27	94	100/0
			31	100	-
			36	100	-
	14	10	0-13	0	-
			17	5.5	38/62
			24	6	54/46
			27	12	70/30
			31	13	42/58
			36	17	24/76
		12	0-6	0	-
			7	4	-
			10	6.5	38/62
			13	8.5	36/64
			17	9.5	39/61
			19	11	36/64
			24	26	23/77
			27	31	39/61
			31	39	50/50
			36	42	65/35

Table 3.24: Degree of crystallinity and phase transitions for different surfactant types during ageing (Pibsa-IMIDE in Shellsol).

Surfactant Type	% Surfactant	d, μm	t, week	X_{Cr}, %	Phase transition, II to IV
Pibsa-IMIDE	8	10	0-4	0	
			6	1	-
			8	4.5	-
			10	5	-
			13	16	-
			17	36	24/76
			24	40	29/71
			27	45	37/63
			31	50	72/28
		12	0-4	0	-
			6	5.5	-
			8	11.5	-
			10	13	46/54
			13	37	67/33
			17	100	97/3
			17.5	100	-
		15	0	0	
			3	0.98	-
			4	12.20	31/69
			6	31.22	47/53
			10	73.17	90/10
			13	100	98/2
			17	100	100
	14	10	0-9	0	
			10	2	46/54
			13	4	67/33
			17	7	97/3
			19	7	-
			24	16	34/66
			27	23	54/46
			31	28	-
			36	30	-
		12	0-5	0	-
			6	3.8	61/39
			8	9.23	49/51
			10	15.38	18/82
			13	20.38	68/32
			17	41.92	63/37
			19	39.62	59/41
			24	65	79/21
			27	70	98/2
			31	100	100/0

Table 3.25: Degree of crystallinity and phase transitions for different surfactant types during ageing (SMO/Pibsa-MEA in Mosspar)

Surfactant Type	% Surfactant	d, μm	t, week	X_{Cr}, %	Phase transition, IV to II
SMO/Pibsa-MEA	8	10	0-5	0	
			6	1.5	-
			9	4.5	39/61
			10	5	42/58
			13	10.5	68/32
			17	21	11/89
			19	34.5	57/43
			24	41	85/14
			27	68.5	-
			31	89	56/44
			36	100	-
		12	0-9	0	-
			10	1.5	-
			13	1.5	-
			17	3.5	-
			19	3	-
			24	8.5	-
			27	7.5	-
			31	13	-
			36	16	-
		15	0-5	0	
			6	1.5	-
			10	3	-
			13	4	-
			17	5.5	-
			24	6.5	23/77
			27	7.5	40/60
			31	16	7/92
			36	23.5	20/80
	14	10	0	0	
			17	2.5	-
			24	7	-
			27	7	-
			31	12.5	-
			36	16	-

Table 3.26: Degree of crystallinity and phase transitions for different surfactant types during ageing (SMO in Mosspar).

Surfactant Type	% Surfactant	d, μm	t, week	X_{Cr}, %	Phase transition, IV to II
SMO	8	10	0	0	-
			3	7.1	-
			3.5	12.3	-
			4	20.7	-
			7	75.8	-
			8	100	-
			10	100	-
			13	100	-
	14	10	0	0	-
			3	5	-
			8	94.6	-
			10	100	-
			13	100	-
			17	100	-

Table 3.27: Degree of crystallinity and phase transitions for different surfactant types during ageing (Pibsa-MEA, and Pibsa-UREA in Mosspar).

Surfactant Type	% Surfactant	d, μm	t, week	X_{Cr}, %	Phase transition, IV to II
Pibsa-MEA	8	10	0-36	0	
		12	0-36	0	-
		15	0-36	0	
	14	10	0-36	0	-
		12	0-36	0	-
		15	0-36	0	-
Pibsa-UREA	8	10	0-36	0	-
		12	0-36	0	-
		15	0-35	1	33/67
			36	1.5	3/97
	14	10	0-36	0	-
		12	0-36	0	-
		15	0-36	0	-

3.4.6.4 Phase transition

The dispersed aqueous droplets in our emulsions consisted of a supersaturated aqueous solution of ammonium nitrate salt (at room temperature). The ammonium nitrate concentration was 80 % by mass while water comprised less than 20 % by mass. It is worth noting that this concentration of AN corresponded to ca. 1:1 molecular ratio of H_2O: NH_4NO_3 (Ashok & Neilson 1991).

Solid ammonium nitrate (NH_4NO_3) exists in five stable polymorphic forms (designated as phases I, II, III, IV, and V) below its melting point at around 170°C (Doxsee & Francis, 2000; Wu, Chan & Chan, 2007). (See Table 3.28).

Table 3.28:. Ambient Pressure Phases of AN

Phase designation	Phase designation range of stability (°C)	Crystal system	Space group
I	125.2-169.2	Cubic	Pm3m
II	84.2-125.2	Tetragonal	$P42_1m$
III	32.2-84.2	Orthorhombic	Pnma
IV	-18-32.2	Orthorhombic	Pmmn
V	Less than -18	Orthorhombic	Pccn

(Adapted from Doxsee & Francis, 2000:3493)

Hendricks *et al.* (1932) gave the transition temperatures as

$$V \overset{-18°C}{\leftrightarrow} IV \overset{32.2°C}{\leftrightarrow} III \overset{84.2°C}{\leftrightarrow} II \overset{152.2°C}{\leftrightarrow} I$$

They also observed a metastable transition IV ↔ II at ca 50°C. This has been confirmed by Shinnaka (1956).

Forms V, IV, II and I are structurally similar and the transitions between them can take place with only minor distortions of the crystals and there is a marked tendency for the crystallographic axes to be maintained (Brown & McLaren, 1961). The crystal structures of these modifications revert to the CsCl pattern of arrangement (Hendricks, Posnjak & Kracek, 1932). Conversely, phase III has a completely different, loose-packing mode of molecules in a crystal lattice that resemble NiAs (Wyckoff, 1964). Thus a considerable distorsion of the crystals occurs during the II↔IIII or IV↔III transitions because of the severe structural changes involved. Moreover, transitions involving phase III are kinetically sluggish in anhydrous ammonium nitrate, so that routine thermal analysis frequently displays only the IV↔II transition. The introduction of increasing amounts of water kinetically reintroduces the IV↔III phase change (Boeyens *et al.*, 1991).

From Table 3.24, Table 3.25, Table 3.26 and Table 3.27 it can be seen clearly that: the interconversion of phase II and phase IV during the crystallisation process of super-cooled

dispersed droplets is quite evident. However, phase II, which is metastable at room temperature, completely disappeared when the sample was fully crystallised. Moreover, it is possible to notice that the transition III↔IV is absent.

The IV↔II transition was not expected to occur in our emulsions because the storage temperature (ca. 20°C) was lower than the temperature corresponding to this transition (ca. 50°C) (Brown & McLaren, 1961; Doxee & Francis, 2000). It is worth mentioning that the main difference between phase II and phase IV is that, in phase IV, the O-H bond between NH_4^+ and NO_3^- ions is strong enough to produce an ordered structure (alignment of the NO_3^- ion planes parallel to the (010) plane, and orientational ordering of each NO_3^- ion within its own plane and spatial ordering of the NH_4^+ ions) whereas this bond is not strong enough to avoid a high degree of disorder in the structure in phase II. In effect, in phase II the NO_3^- ions are partially orientationally disordered and this involves the rupturing of O-H bonds. This might increase the probability of the NH_4^+ ion to move away from its lattice site and may explain the partial ordering of the NH_4^+ ions (Brown & McLaren, 1961). It must be emphasised that an energy barrier comes into operation at the II↔IV transition, locking the NO_3^- ions into a fixed orientation (Hendricks *et al.*, 1932; Brown & McLaren, 1961) and preventing the translational diffusion of the NH_4^+ ions. This is accompanied by a further distortion of the lattice from tetragonal to orthorhombic (see Figure 3.46) (Brown & McLaren, 1961).

According to the above references we can assume that the appearance of phase II (the phase in which the degree of disorder is higher, compared to phase IV) at room temperature could be primarily attributed to the presence of surfactant head groups and their impact on surfactant-AN interactions. Indeed, when there is not enough water in the system to induce drastic transformations (transformations involving phase III), all the transitions appear to be of the order-disorder type. When decreasing the temperature, the different structures arising from the development of different degrees of order in the orientation of the NO_3^- ions and/or in the position of the NH_4^+ ions (Brown & McLaren, 1961). On the other hand, by interacting with the NH_4^+, the surfactant head groups break the O-H bond by increasing the distance between NH_4^+ and NO_3^- (Ashok & Neilson, 1991; Ganguly *et al.*, 1992). Thus, by trying to maintain the O-H bond in a broken state, the AN-surfactant interaction and the repulsive forces between droplets could introduce an energy barrier which could delay the organisation of the system at room temperature (in delaying crystallisation or the appearance of more ordered structures) and at the same time promote the appearance of phase II, which is more disordered. This hypothesis can be supported by the fact that the appearance of phase II

was not observed in very unstable emulsions such as SMO-based emulsions. Indeed, the quasi-absence of steric effects, combined with the van der Waals attraction between surfactant layers (reinforced by the non-ionic nature of SMO), enhance the susceptibility to coalescence (Alvarez *et al.* 2006). The resulting increase of droplet size could weaken the AN-surfactant interaction.

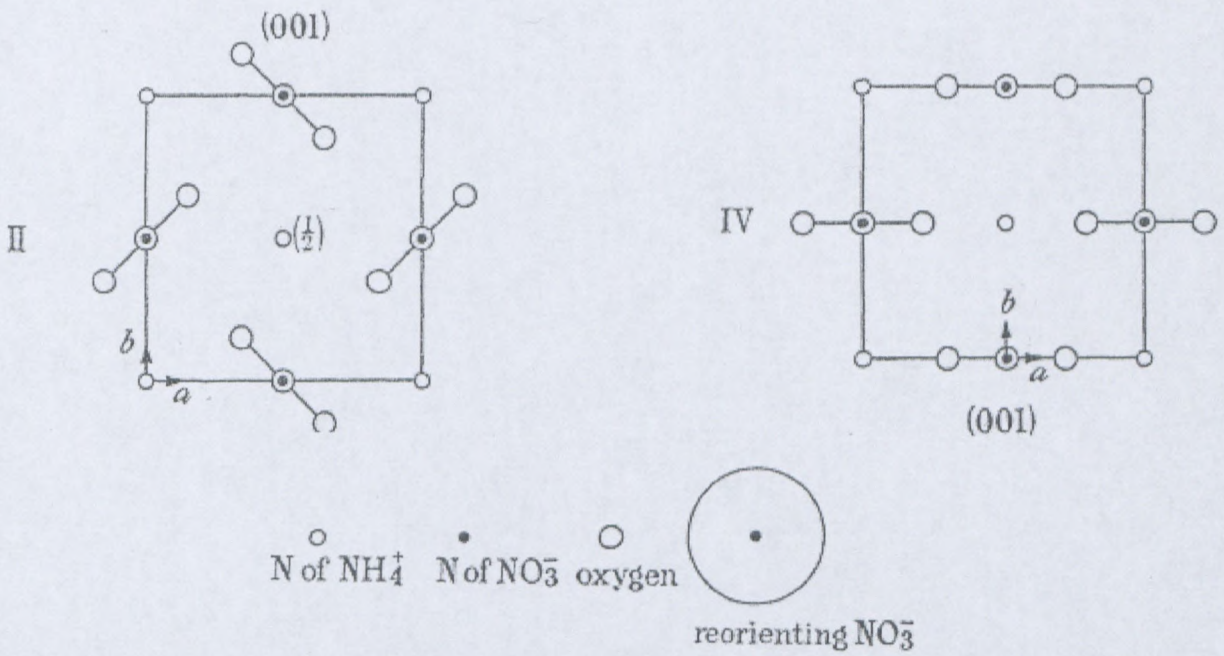

Figure 3.46: Projections of the structures of forms II and IV of ammonium nitrate (Adapted from Brown & McLaren, 1961:341)

Since there was less water in the system and the storage temperature (ca. 20°C) was less than the temperature corresponding to the transition II↔III (84.2°C) or III↔IV (32.2°C), the absence of phase III was expected. Indeed the structural changes involved in the IV↔III or II↔III transitions are drastic and it is for this reason that the presence of water is needed. These do not appear to be order-disorder transitions, but rather transitions involving a process of dissolution and crystallisation. The phase boundary between the two solid phases is, therefore, visualised as a region of almost complete disorder and its width is probably large compared with inter-ionic distances (Brown & McLaren, 1961; Oommen & Jain, 1999).

The projection onto (001) of the structures of form III of ammonium nitrate is shown below in Figure 3.47.

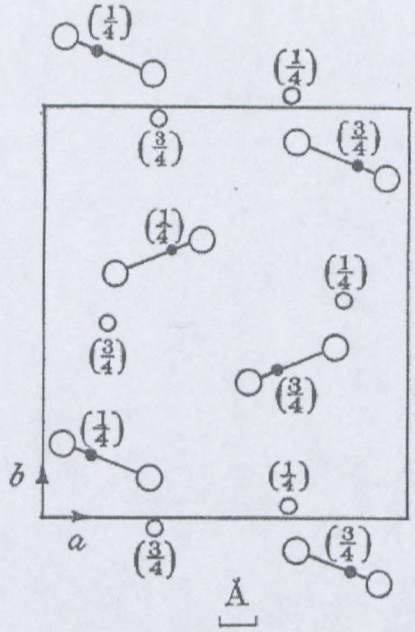

Figure 3.47: Projection onto (001) of the structures of form III of ammonium nitrate

(Adapted from Brown & McLaren, 1961:342)

Another feature of the complex phase behaviour of our emulsions was that solid AN exhibited interesting behaviour on thermal cycling. The transition behaviour on thermal cycling was found to depend on the heating temperature:

Our experimental results showed that, when a fully crystallised sample was heated up to 40°C, one obtained an amorphous structure after cooling at room temperature. The amorphous structure disappeared in the next cycle, during which the sample was heated up to 55°C and cooled down to room temperature. In this case, phase II appeared on heating and the II ↔IV transition was observed on cooling.

The appearance of the amorphous structure could not have been a consequence of the II↔IV transition since this transition involves minor structural changes and the boundary between the forms during the transformation therefore may be expected to have properties not markedly different from the stable forms (Brown & McLaren, 1961). The amorphous structure could have been a metastable product generated during the IV↔III transition, due to the simultaneous actions of water, AN-surfactant interaction and temperature. On the one hand, the IV↔III transition, on heating, undeniably takes place by the dissolution and re-crystallisation of the solid (Brown & McLaren, 1961; Boeyens *et al.*, 1991, Doxee & Francis,

2000) and its kinetic is well known to be a decreasing function of water content (Brown & McLaren, 1961; Boeyens *et al.*, 1991). Therefore the presence of water in our emulsion could have promoted the IV↔III transition, and its amount may not have been enough to markedly improve the kinetics of this transition. On the other hand, since the phase boundary between the two solid phases is visualised as a region of almost complete disorder (Brown & McLaren, 1961), the AN-surfactant interaction could maintain the sample in this state by delaying the initiation of recrystallisation.

3.4.6.5 Kinetics of crystallisation

Figures 3.48 and 3.49 respectively show the results of the kinetics of crystallisation for several surfactant types. The results give the quantitative measure of the crystallisation rate that can be satisfactorily described by the standard JMAK equation:

$$X_{Cr} = 1 - e^{-\left(\frac{t}{\theta}\right)}, \qquad \textbf{Equation 3.2}$$

where X_{Cr} is the degree of crystallinity, θ is the characteristic time-related constant of the process and n is an empirical factor called the Avrami coefficient. However, the choice of the constants is ambiguous due to the non-linear procedure of fitting, though the values in Table 3.27 are satisfactory for *θ* and n for different surfactants studied.

It is worth mentioning that the relative crystallinity for samples which are fully crystallised is between 20 and 25% of the total mass of the emulsion. This average value will be used as a basis to predict the kinetics of crystallisation of samples which are not yet fully crystallised.

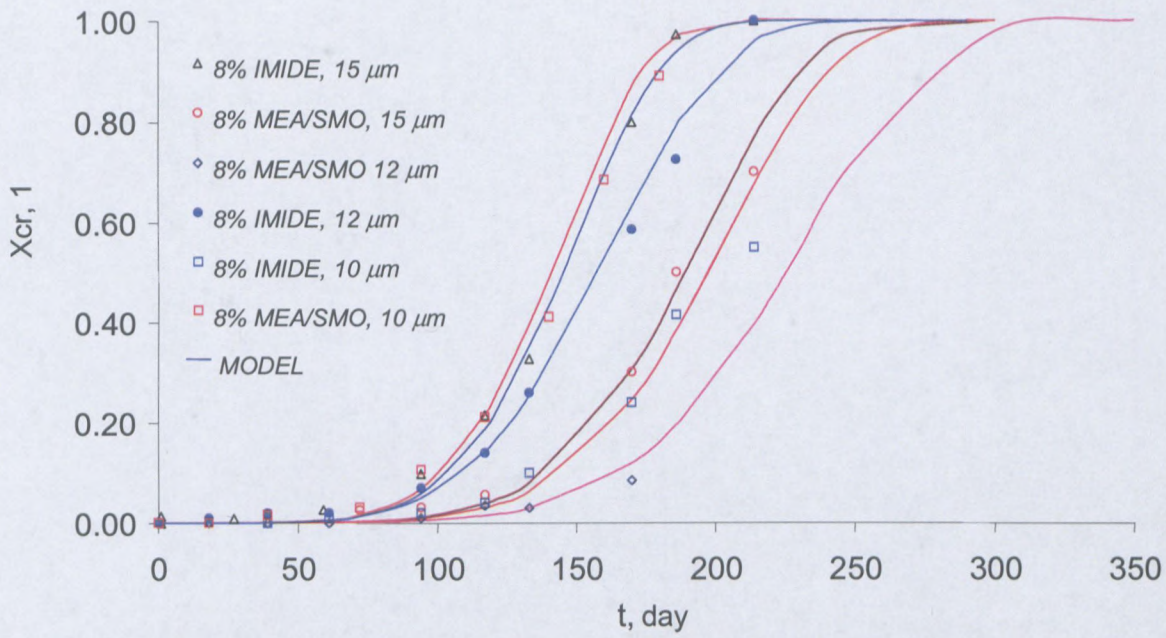

Figure 3.48: Change in relative crystallinity over time for different surfactant types (8% surfactant; d =10 μm)

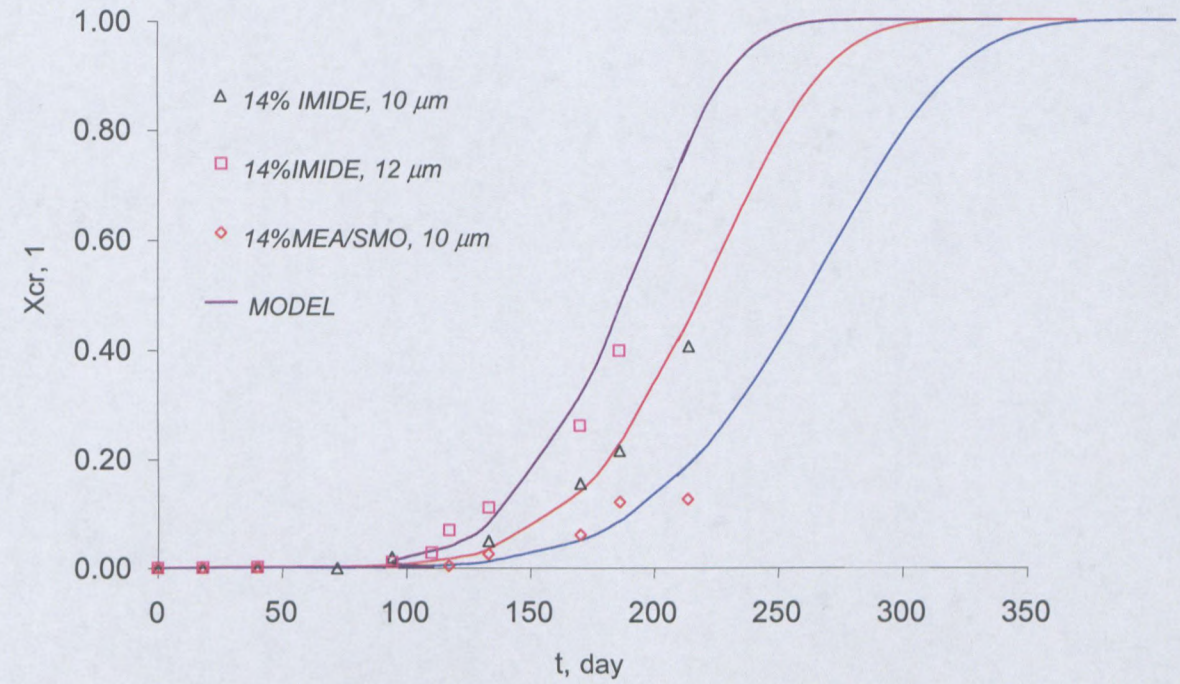

Figure 3.49: Change in relative crystallinity over time for different surfactant types (14% surfactant; d =10 μm)

Table 3.29: The JMAK equation constants for all surfactant types in Mosspar

% surfactant	d, μm	Surfactant type	Θ, week	n, 1
8	10	Pibsa - IMIDE	30	6
		SMO/Pibsa - MEA	22	6
		SMO	5	6
	12	Pibsa - IMIDE	24	6
		SMO/Pibsa - MEA	34	6
	15	Pibsa-IMIDE	22	6
		SMO/Pibsa - MEA	29	6
14	10	Pibsa - IMIDE	38	6
		SMO/Pibsa - MEA	40	6
		SMO	6	6
	12	Pibsa - IMIDE	28	6

It is interesting that the constant *n* in all cases can be assumed equal to 6 (Table 3. 29) as was obtained in earlier publications (Kharatiyan, 2005; Masalova *et al.*; 2006; Masalova & Malkin, 2007b).

This is an unusually high value (for the position of the Kholmogorov-Avrami kinetic models) because *n* should not be higher than 4 in all geometrical schemes of homogeneous crystallisation taking place on individual sites and treated within the frames of the Kholmogorov-Avrami growth of crystals (Walter *et al.*, 2000; Humphreys & Hatherly, 1996). Actually, it reflects the special character of the mechanism of crystallisation in our case, because – as mentioned above – crystals, in the observed cases, did not grow from different independent centres but by single crystals breaking through boundaries of droplets occupying several separate droplets. This mechanism of crystal growth is clearly seen in Figures 3. 41, 3.42 and 3.43.

The onset of crystallisation (~ 2 % crystallinity), the time of 10 %, 20 %, 30 %, 50 % and 100 % crystallinity for all surfactant types in Mosspar, different types of oils and for all surfactant concentrations was determined using Equation. 3.1 and this is listed in Table 3.30.

Table 3.30: Stages of crystallisation for different surfactant types

d, μm	% surfactant	Surfactant type	Crystallinity, week					
			2%	10%	20%	30%	50%	100%
10	8	Pibsa-IMIDE	16	21	23	25	28	39
		SMO/Pibsa-MEA	12	15	17	19	21	29
		SMO	2	3	4	4	4	6
		Pibsa-MEA	Still fresh					
		Pibsa-UREA	Still fresh					
12		Pibsa-IMIDE	13	17	19	20	23	31
		SMO/Pibsa-MEA	18	24	27	29	32	44
		Pibsa-MEA	Still fresh					
		Pibsa-UREA	Still fresh					
15		Pibsa-IMIDE	12	15	17	19	21	29
		SMO/Pibsa-MEA	15	20	22	24	27	37
		Pibsa-UREA	17	-	-	-	-	-
		Pibsa–MEA	Still fresh					
10	14	Pibsa-IMIDE	20	26	29	32	36	49
		SMO/Pibsa-MEA	21	27	31	34	38	52
		SMO	4	5	5	6	6	9
		Pibsa–MEA	Still fresh					
		Pibsa-UREA	Still fresh					
12		Pibsa-IMIDE	15	20	22	24	27	37
		Pibsa-MEA	Still fresh					
		Pibsa-UREA	Still fresh					
15		Pibsa-MEA	Still fresh					

As can be seen clearly from the above Table 3.30, Figure 3.48 and Figure 3.49,

- The stability of explosive emulsions was sensitive to the surfactant type according to the sequence MEA-UREA-MEA/SMO-IMIDE-SMO. The effect was so strong that it masked the effect of other important factors reported in the literature, such as droplet size (Kharatiyan, 2005; Masalova *et al.*; 2006; Masalova & Malkin, 2007b) or surfactant concentration (Ganguly *et al.*, 1992; White *et al.*, 2004). Indeed, after 36 weeks of ageing, MEA-based or UREA-based emulsions were still fresh for all droplet sizes and all surfactant concentrations while emulsions prepared with IMIDE, SMO or

the mixture MEA/SMO were almost fully crystallised (even those corresponding to the smallest droplets and/or the highest surfactant concentration).

- Among the three Pibsa-based surfactants. the effect of surfactant type on both the onset of crystallisation and the kinetic of crystallisation were observed to follow the same trend as the expected sequence of surfactant-ammonium nitrate interaction (MEA-UREA-IMIDE), opposite to the expected trend following the impact of the van der Waals attraction on the pair potential energy in the thin film separating adjacent droplets (IMIDE-UREA-MEA) (see section 3.4.3).
- SMO-based emulsions were the most unstable emulsions, despite the fact that the AN-surfactant interaction with SMO was expected to be higher than the one with IMIDE. The high instability of SMO originates from the quasi-absence of steric effects (because SMO is a low molecular weight surfactant) combined with the high van der Waals attraction created by the physical interaction between the surfactant layers (because SMO is a non-ionic surfactant). Therefore SMO-based emulsions are susceptible to coalescence (Alvarez *et al.*, 2006). The resulting increase of droplet size could have weakened the impact of AN-surfactant interaction within the droplet, enhancing the susceptibility of explosive emulsions to the crystallisation process.

The above observations might support the fact that the initiation of crystallisation could depend mostly on surfactant-electrolyte interaction and might play a major role in the overall process of crystallisation in the case of emulsions with dissolved electrolytes in the aqueous phase (Ashok *et al.,* 1991; Ganguly *et al.*, 1992). Indeed, the initiation of crystallisation depends mostly on the ability of additives (ions, molecules, or surfactant head group) to increase the separation distance between NH_4^+ and NO_3^- ions (Ashok *et al.,* 1991; Ganguly *et al.*, 1992). The separation of charges inside the droplet is expected to keep the emulsion in a super-cooled state by reducing the chemical kinetics of oversaturated ammonium nitrate. Moreover, this separation could generate repulsive forces in the thin film between droplets, which could reduce the van der Waals attraction and consequently improve the stability. On a qualitative level, a strong surfactant-ammonium nitrate interaction is expected to give rise to a more stable emulsion (Ganguly *et al.*, 1992).

- The effect of surfactant type on the kinetics of propagation of the crystallisation throughout the emulsion was observed to be following the same trend as our results on the dilatational elastic modulus (MEA-UREA-MEA/SMO-IMIDE-SMO). This observation might support the fact that the strength of the interface could act as an

inhibitor to the propagation of crystallisation (Kharatiyan, 2005; White *et al.*, 2005). The high instability of IMIDE-based emulsions compared to other Pibsa-based emulsions could be due to both its less intense surfactant-ammonium nitrate interaction and its low interfacial elasticity. It must be emphasised that the high impact of van der Waals attraction associated with this surfactant could play an important role as well. It might enhance the probability of contact between different contents of droplets (Alvarez *et al.*, 2006) and thus facilitate the propagation of crystallisation from one droplet to another.

- Table 3.30 shows considerable differences between W/O explosive emulsions prepared with MEA/SMO and those corresponding to MEA. The stability of the MEA-based emulsions is extremely high, independently of droplet size and surfactant concentration, compared to MEA/SMO-based emulsions. This could be due to the fact that the presence of SMO reduced the strength of the interface (see Table 3.10) and, possibly, the effectiveness of charge separation inside the droplet (Ganguly *et al.*, 1992). Indeed the surfactant-electrolyte interactions were more intense in the case of Pibsa-MEA compared to SMO. On the other hand, the presence of SMO could reduce the reverse micelle concentration, enhancing the probability of contact between contents of different droplets (White *et al.*, 2004).
- For a given surfactant type and a given surfactant concentration, bigger droplets were crystallising faster than the small ones. This could be attributable to the more effective charge separation inside small droplets, compared to the bigger ones, because of their differences in volume. Moreover, the smallest interdroplet layer associated with the smallest droplets could have given rise to a more effective packing of reverse micelles, reducing the probability of contact between contents of different droplets.

It can be concluded that:

- The degree of crystallinity increases with ageing.
- The rate of crystallisation is very sensitive to the surfactant head group, therefore the evolution of emulsion ageing can be controlled by varying the surfactant head group.
- The initiation of crystallisation could be strongly dependent on the interactions between the surfactant head group and the ammonium nitrate solution, while the propagation of crystallisation could depend on the physical interaction between interface layers of different droplets, on the strength of the interface and/or on reverse micelle type and concentration. Indeed, as pointed out before, because of the non-ionic nature of the surfactant used in this study, the dominant interaction between droplets could be the van der Waals attraction (Alvarez *et al.*, 2006). The strength of

- **Flow properties**

In order to investigate the effect of ageing on flow behaviour, all samples were tested weekly over a period of 36 weeks. The typical effect of ageing on flow behaviour of the emulsion with 8 % Pibsa-IMIDE in Mosspar for a droplet size of 10 μm is shown in Figure 3.50.

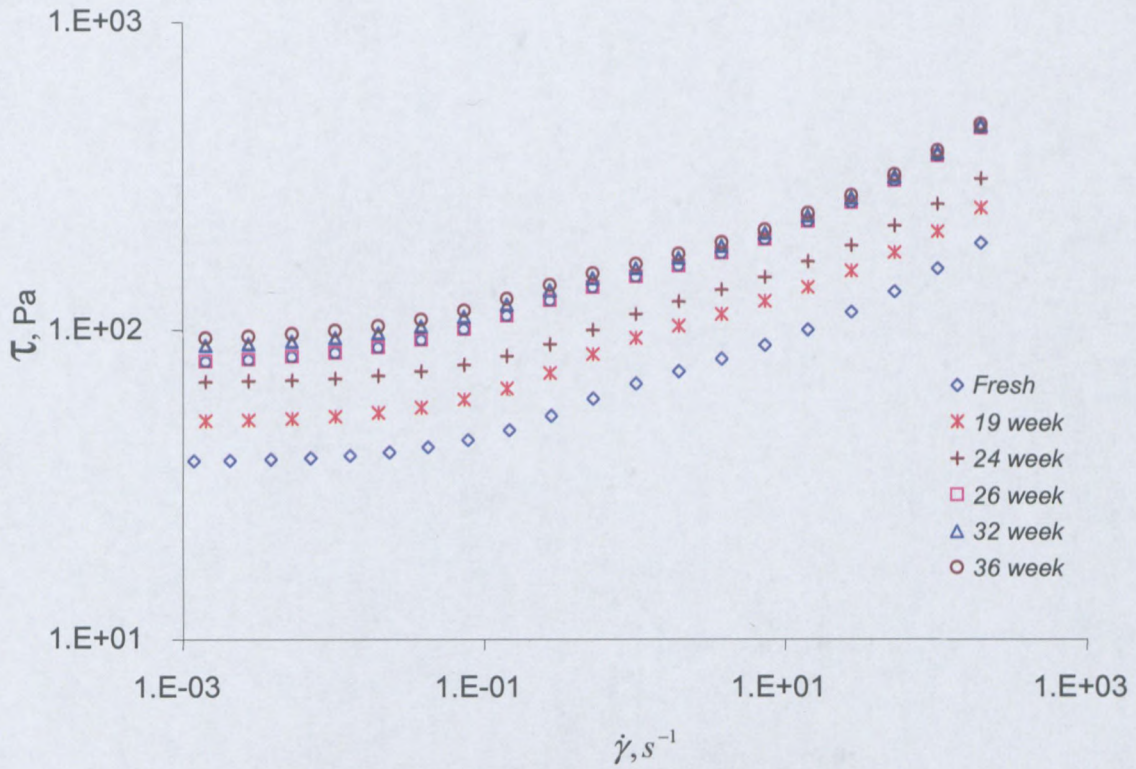

Figure 3.50: Flow curves of fresh and aged emulsions (8 % Pibsa-IMIDE for droplet size 10 μm).

It was found that the character of flow behaviour was not affected by storage, but all flow curves were shifted to higher values of shear stresses over the whole region of shear rates within the experimental window. In all cases, the increase in degree of crystallinity led to an increase in the viscosity, this increase being less marked at high shear rates. The same effect was observed in the ageing of explosive emulsions (Masalova *et al.*, 2006; Masalova & Malkin, 2007b; Kharatiyan, 2005) and by other rheologists, for suspensions of solid particles in a polymer solution (Harzallah & Dupuis, 2003).

The evolution with ageing of the yield stress for emulsions with all different surfactant types is presented in Table 3.31 and Table 3.32.

Table 3.31: Effect of ageing on the yield stress of emulsions with different PIBSA-based surfactants in Mosspar (8 % surfactant)

% Surfactant	d, μm	Surfactant type	t, week	τ_y, Pa
8	10	Pibsa-IMIDE	1 - 17	37.4
			19	49.1
			21	55
			24	66.3
			26	75.8
			28	80
			32	85
			36	90
		SMO/Pibsa-MEA	1 - 13	22.6
			15	42.1
			18	56
			23	64
			28	75.8
			30	76.8
		SMO	0 - 1	15.8
			3	45
			5	68
			7	66
	12	Pibsa-IMIDE	1 - 12	21.9
			14	31
			16	52
			22	67
			25	73
			28	74
			31	73
		SMO/Pibsa-MEA	1 - 17	17
			21	35
			23	40
			25	45
			28	55
			32	62
			36	70
	15	Pibsa-IMIDE	1 - 12	15.7
			14	20
			18	32
			21	40
			24	50.25
			26	60
			28	65
			30	67
		SMO/Pibsa-MEA	1 - 15	15
			17	20
			20	32.2
			24	38
			27	48
			30	55.7
			33	65.8
			36	66.5

Table 3.32: Effect of ageing on the yield stress of emulsions with different PIBSA-based surfactants in Mosspar (14 % surfactant)

% Surfactant	d, μm	Surfactant type	t, week	τ_y, Pa
14	10	Pibsa-IMIDE	1 - 20	31
			22	37.4
			24	45
			26	55
			28	63
			32	69.7
			36	77
		SMO/Pibsa-MEA	1 - 23	18.2
			25	23
			27	28
			29	37
			32	58
			36	65
		SMO	1 - 4	20.9
			5	30
			6	45
			7	60
			8	70
			9	71
	12	Pibsa-IMIDE	1 - 15	22
			17	25.4
			19	30
			21	39.7
			23	45.1
			25	59
			27	63
			30	68
			33	72
			36	74

Due to the fact that the physical meaning of a yield stress is related to the strength of interparticular interactions in the physical structure of multi-phase systems, this parameter will be considered as a factor of emulsion stability in the following discussions.

It was found that the yield stress value is sensitive to the structure evolution of our emulsion with storage. It is clearly shown in Figures 3.51, 3.52 and 3.53 that the yield stress increased with ageing for all surfactant types used in the investigation for all droplet sizes.

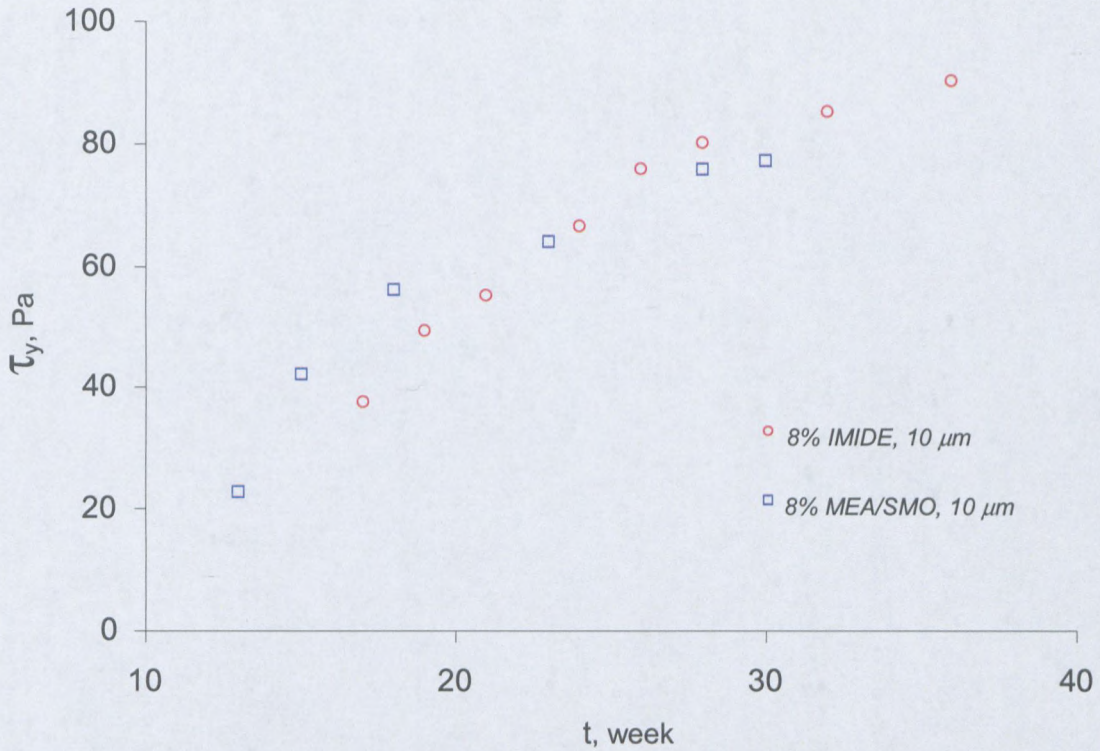

Figure 3.51: Yield stress vs ageing as function of surfactant type in Mosspar

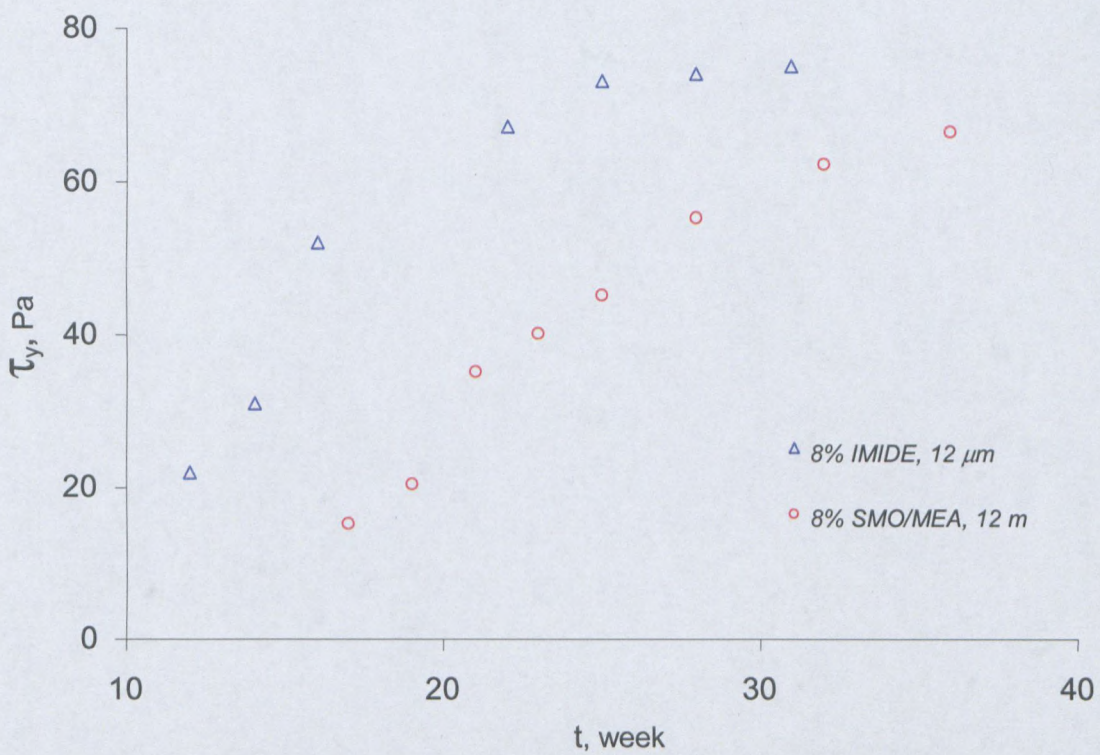

Figure 3.52: Yield stress vs ageing as function of surfactant type in Mosspar

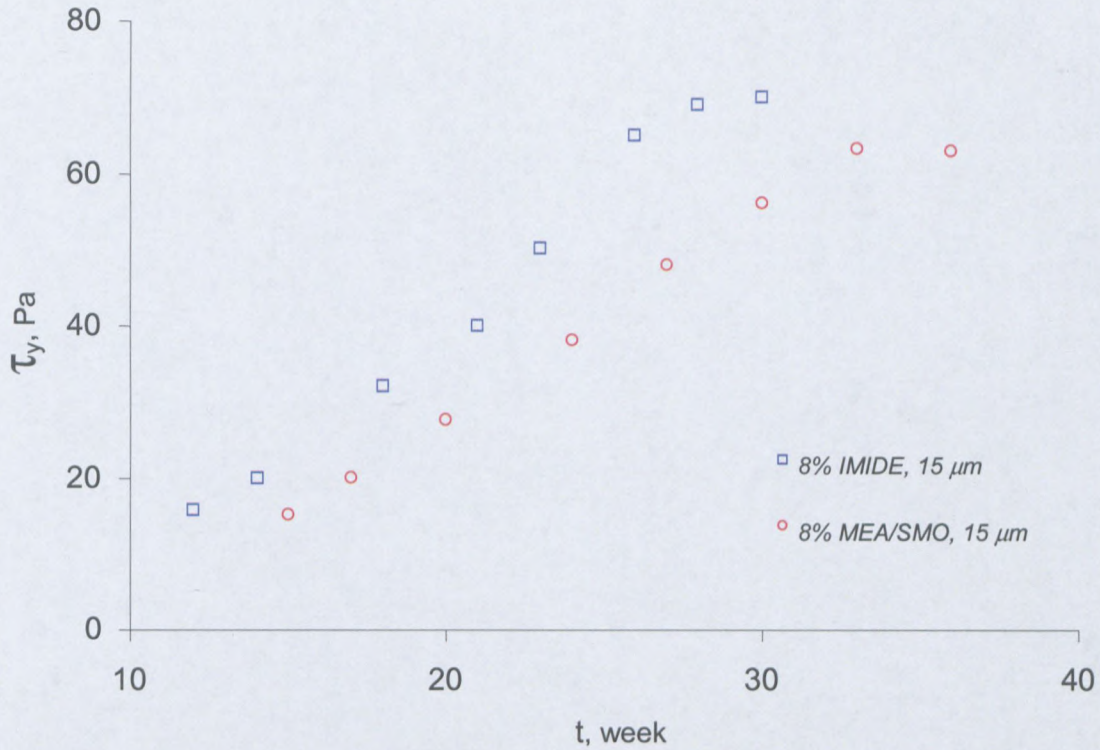

Figure 3.53: Yield stress vs ageing as function of surfactant type in Mosspar

The values of yield stress depend on the arrangement of crystals or, more precisely, of aggregate particles. The effect is enhanced by irregular shape of clusters which may cause a blocking of flow (Harzallah & Dupuis, 2003). At rest, crystals are distributed in irregularly shaped and non-uniformly sized aggregates. By increasing the concentration of crystals, the building of structures can take place and this can result in stronger resistance to the shear flow. The increase in the yield stress values with ageing point to an increase in the rigidity of the system and an increase in the strength of the solid particle (crystal) structure with ageing.

In conclusion:

- The yield stress value is sensitive to ageing (to the degree of crystallinity) of the emulsion.
- The highest yield stress value was obtained for fresh emulsions with the highest yield stress for both surfactant concentrations.
- For the same surfactant concentration, except for Pibsa-IMIDE, which was falling apart, the fresh emulsion with a lower value of yield stress reached the maximal value of yield stress (corresponding to 100 % crystallinity) in the shortest period of time.

- **Viscoelastic properties**

The ageing of the emulsions was investigated by measuring the storage modulus as a function of strain amplitude at constant frequency (1Hz). The experiments realised with the sample containing 8 % Pibsa-IMIDE in Mosspar-H for d = 10 μm are depicted in Figure 3.54.

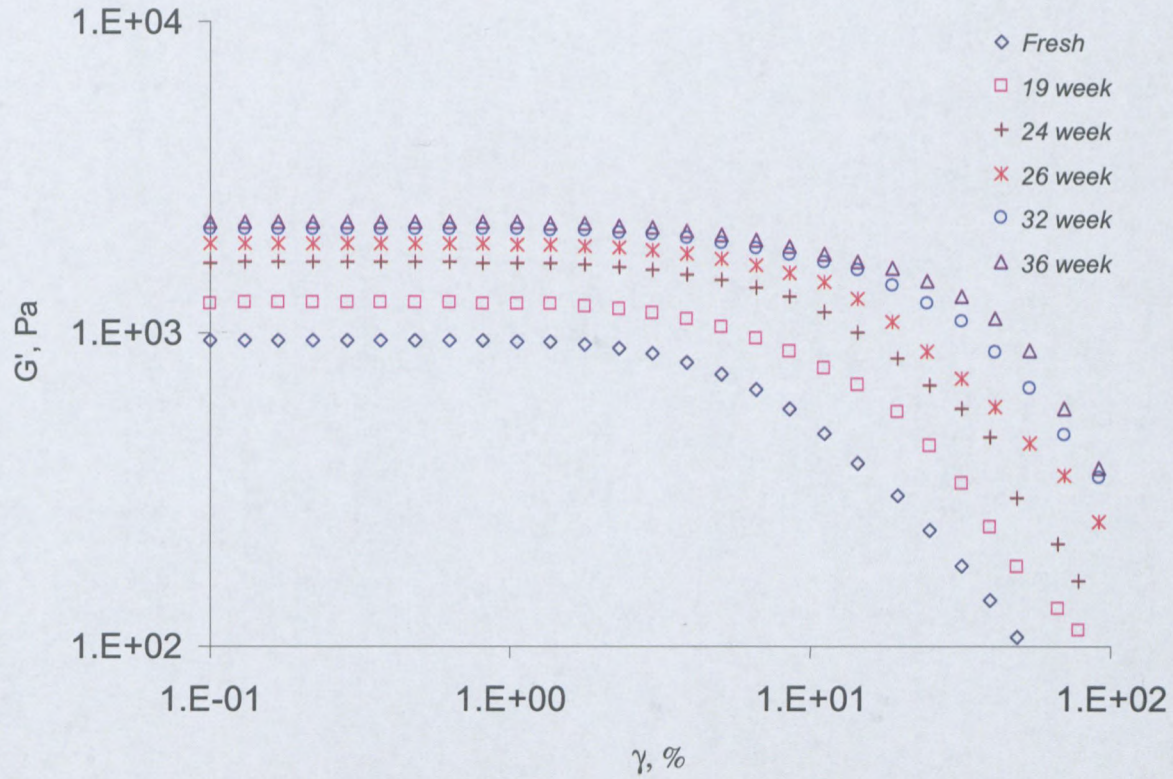

Figure 3.54: Storage modulus dependence on strain amplitude for fresh and aged samples (8% Pibsa-IMIDE in Mosspar for d = 10μm)

The evolutions with ageing of the storage modulus for emulsions with all different surfactant types are summarised in Table 3.33 and Table 3.34.

Table 3.33: Effect of PIBSA-based surfactant type on storage modulus over ageing (8 % surfactant)

% Surfactant	d, μm	Surfactant type	t, week	G', Pa
8	10	IMIDE	1 - 17	948
			19	1228
			21	1375
			24	1658
			26	1895
			28	2000
			32	2125
			36	2250
		MEA/SMO	1 - 13	661
			15	1053
			18	1400
			23	1600
			28	1895
			30	1870
		SMO	0 - 1	463
			3	1125
			5	1450
			7	1575
	12	IMIDE	1 - 12	670
			14	775
			16	1300
			22	1675
			25	1825
			28	1850
			31	1875
		MEA/SMO	1 - 17	511
			21	875
			23	1000
			25	1125
			28	1375
			32	1550
			36	1750
	15	IMIDE	1 - 12	433
			14	500
			18	800
			21	1000
			24	1256
			28	1625
			30	1675
		MEA/SMO	1 - 15	401
			17	500
			20	805
			24	950
			27	1200
			30	1393
			33	1645
			36	1663

Table 3.34: Effect of PIBSA-based surfactant type on storage modulus over ageing (14% surfactant)

% Surfactant	d, μm	Surfactant type	t, week	G', Pa
14	10	Pibsa-IMIDE	1 - 20	869
			22	1048
			24	1261
			26	1542
			28	1766
			32	1954
			36	2102
		SMO/Pibsa-MEA	1 - 23	550
			25	695
			27	846
			29	1118
			32	1451
			36	1662
		SMO	1 - 4	630.9
			5	750
			6	1125
			7	1500
			8	1750
			9	1775
	12	Pibsa-IMIDE	1 - 15	670
			17	635
			19	750
			21	993
			23	1128
			25	1475
			27	1575
			30	1700
			33	1800
			36	1850

The effect of ageing on the storage modulus for different surfactant types is illustrated in Figure 3.55, Figure 3.56 and Figure 3.57.

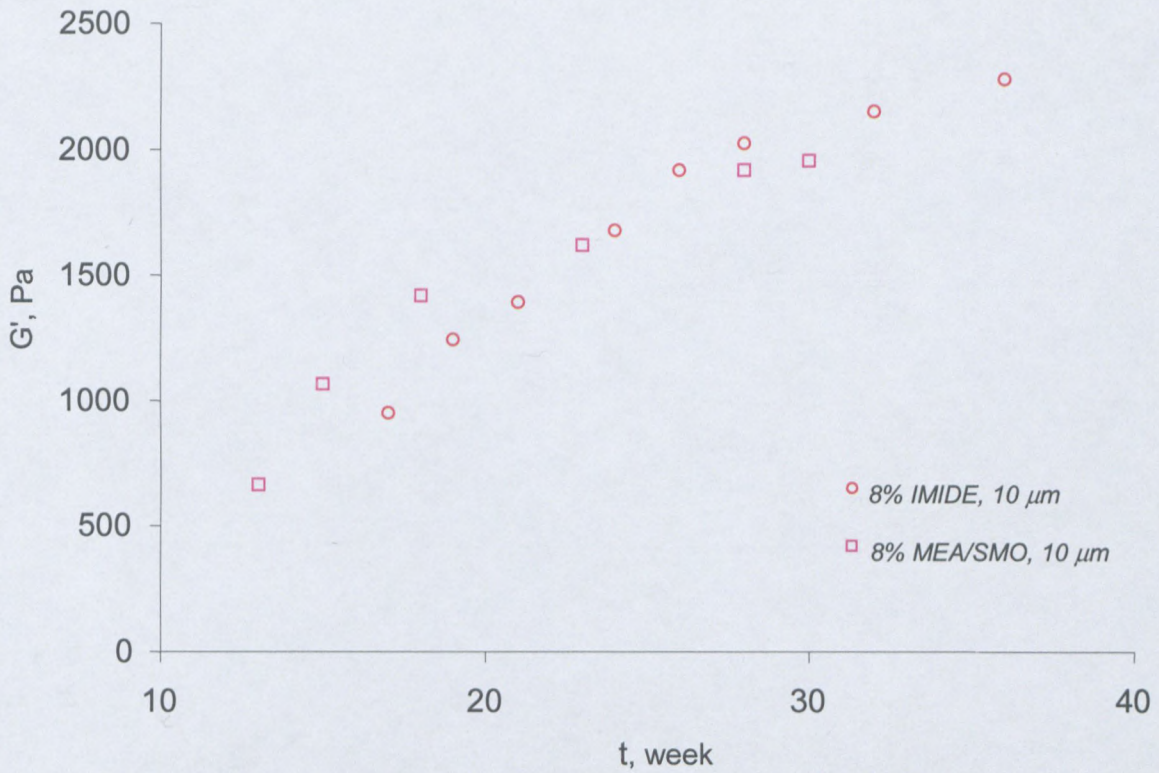

Figure 3.55: Storage modulus vs ageing as function of surfactant type in Mosspar

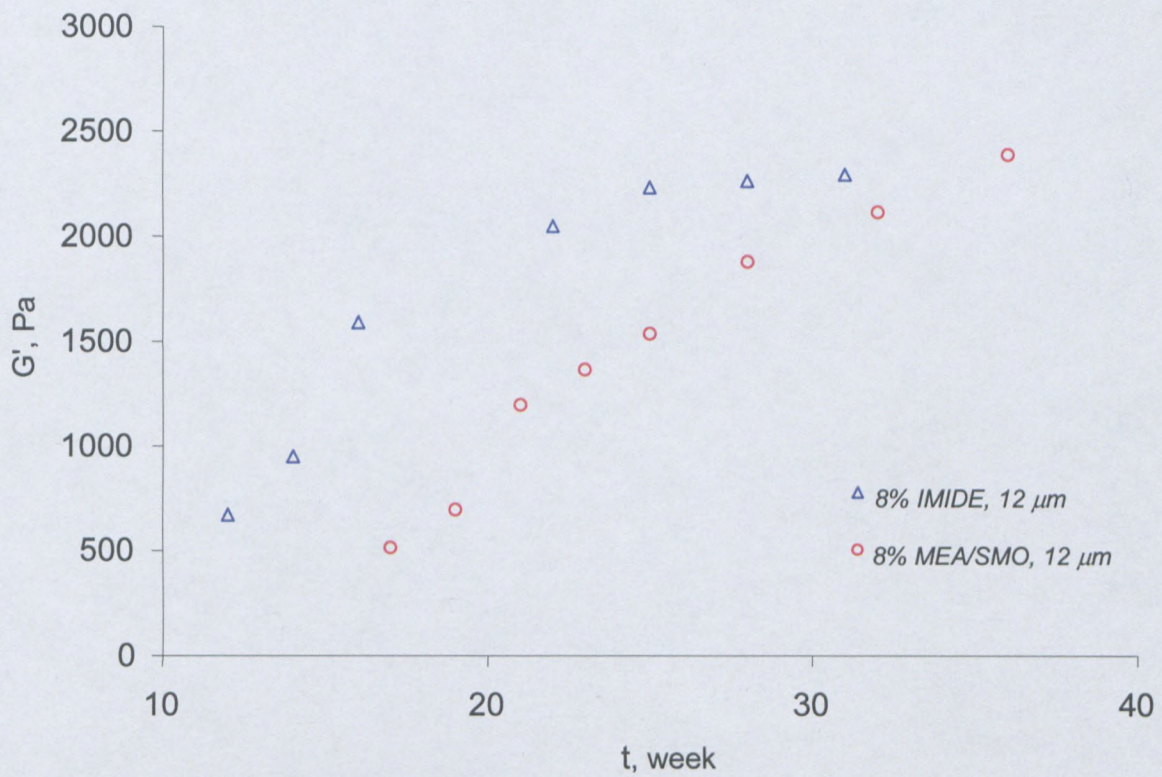

Figure 3.56: Storage modulus vs ageing as function of surfactant type in Mosspar

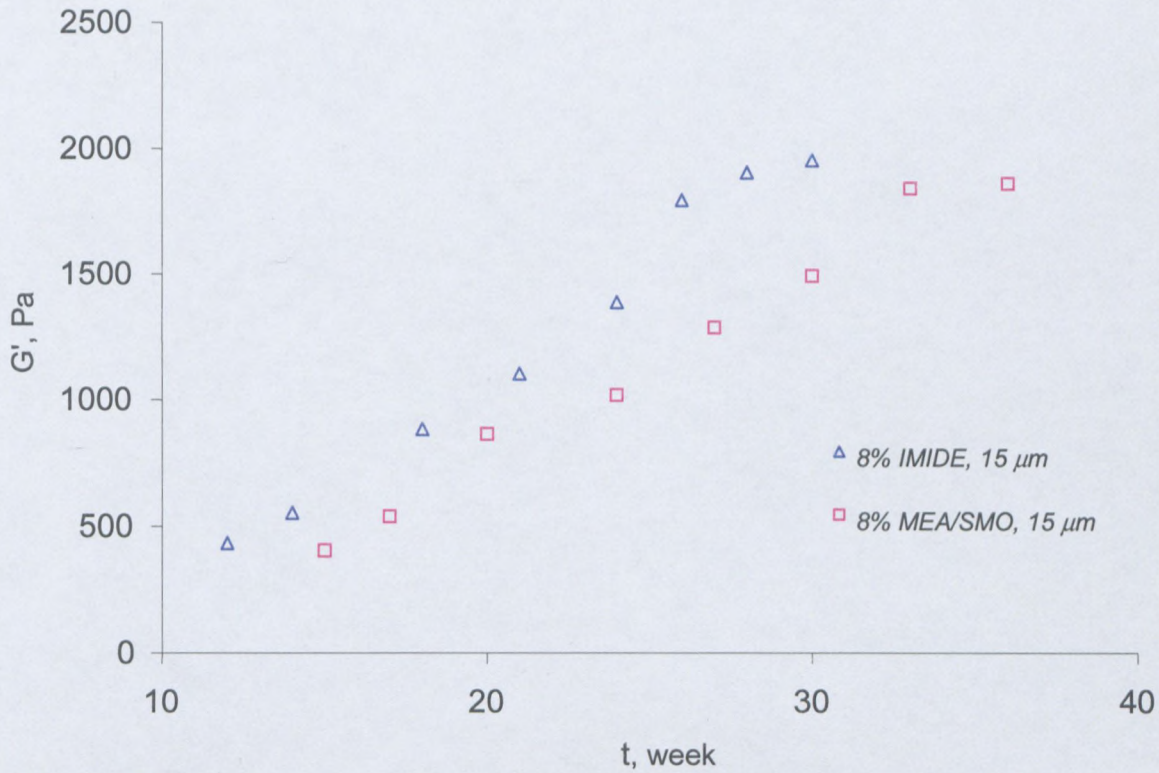

Figure 3.57: Yield stress vs ageing as function of surfactant type in Mosspar

It was found that ageing process affects the storage modulus in the same trend as the yield stress, i.e. the sample with the lowest initial storage modulus reached the highest storage modulus in the shortest time.

3.4.7 Effect of surfactant concentration on the stability of explosive emulsions with ageing

3.4.7.1 X-ray diffraction

The kinetics of the crystallisation process with ageing was investigated for samples with different surfactant concentrations by means of X-ray analysis. The results of measuring crystallinity over time as a function of surfactant concentration are presented in Figure 3.58, Figure 3.59 and Figure 3.60.

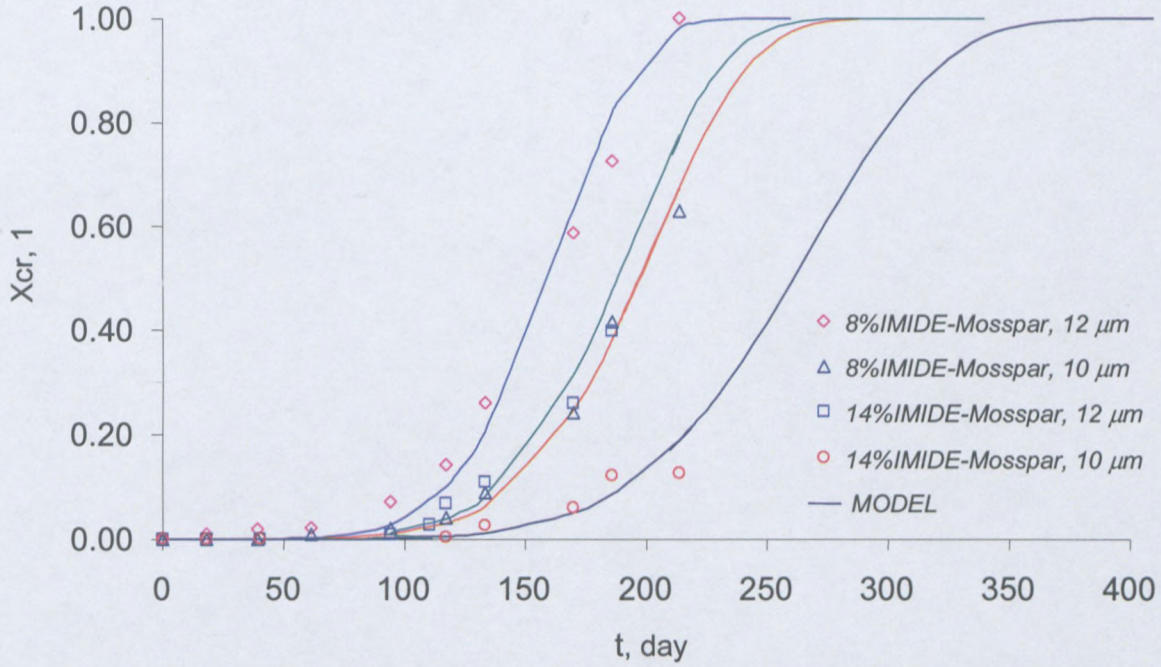

Figure 3.58: Change in relative crystallinity with time for different Pibsa-IMDE concentrations in Mosspar

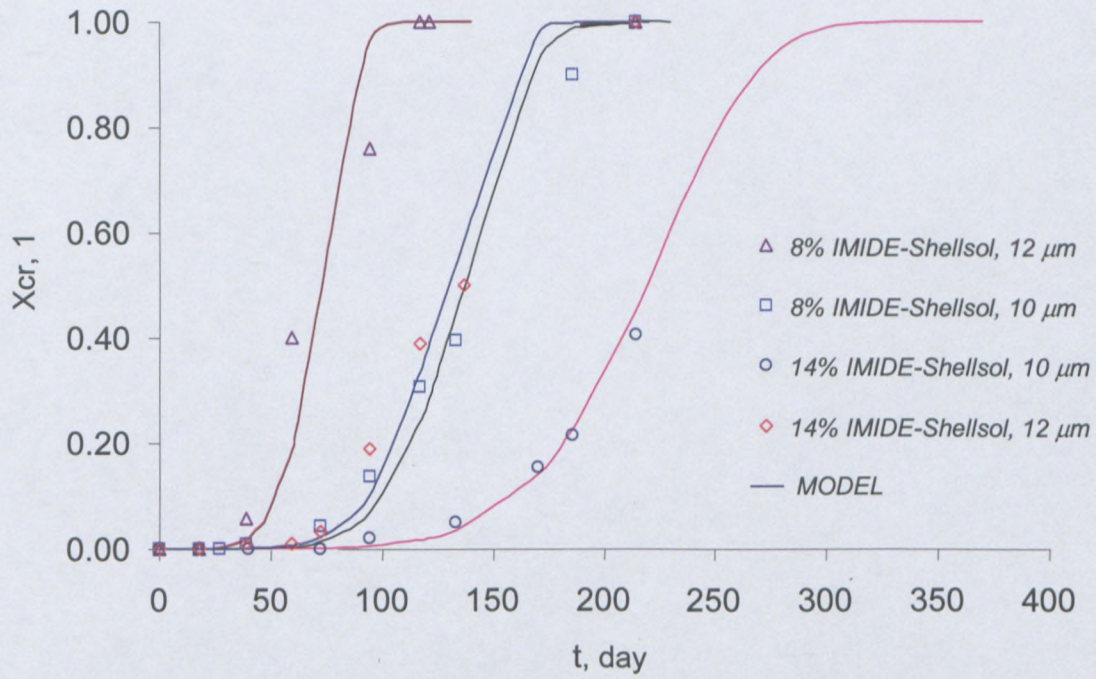

Figure 3.59: Change in relative crystallinity with time for different Pibsa-IMDE concentrations in Shellsol

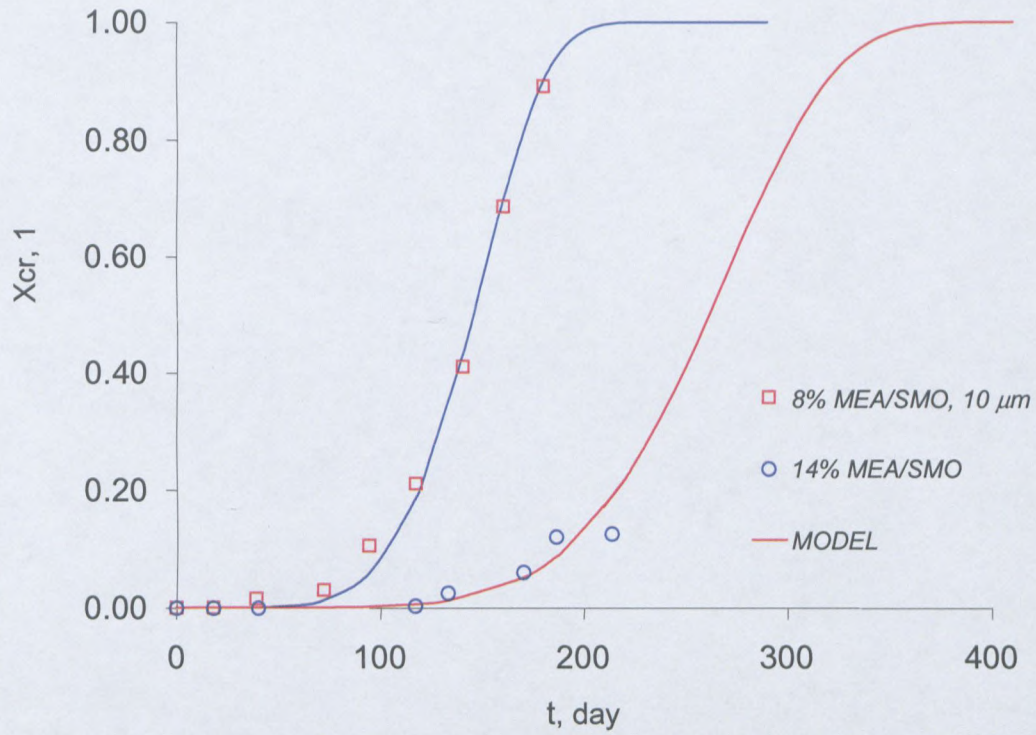

Figure 3.60: Change in relative crystallinity over time for different SMO/Pibsa-MEA concentrations

The values of the JMAK equation constants for samples with different surfactant concentrations are listed in Table 3.35.

Table 3.35: Effect of surfactant concentration on JMAK equation coefficients (Pibsa-IMIDE).

d, μm	Surfactant type	% surfactant	Θ, week	n, 1
Oil phase: Mosspar – H				
10	IMIDE	8	30	6
		14	38	6
	MEA/SMO	8	22	6
		14	40	6
	SMO	8	5	6
		14	6	6
12	IMIDE	8	24	6
		14	28	6
Oil phase: Shellsol				
10	IMIDE	8	21	6
		14	33	6
12	IMIDE	8	11	6
		14	19	6

The onset of crystallisation, the times of 50 % and 100 % crystallinity for different surfactant concentrations and for all droplet sizes were determined using Equation. 3.2 and these are listed in Table 3.36

Table 3.36: Stages of crystallisation for different surfactant concentrations in Mosspar

d, μm	Surfactant type	% Surfactant	Crystallinity, week					
			2 %	10 %	20 %	30 %	50 %	100 %
Oil phase: Mosspar-H								
10	IMIDE	8	16	21	23	25	28	39
		14	20	26	29	32	36	49
	SMO/MEA	8	12	15	17	19	21	29
		14	21	27	31	34	38	52
	SMO	8	2	3	4	4	4	6
		14	4	5	5	6	6	9
12	IMIDE	8	13	17	19	20	23	31
		14	15	20	22	24	27	37
Oil phase: Shellsol								
10	IMIDE	8	11	14	16	17	19	27
		14	17	23	26	28	31	43
12	IMIDE	8	6	8	9	9	10	14
		14	10	13	15	16	18	25

As can be seen from the above, in Figure 3.59, Figure 3.60, Table3.35 and Table 3.36,

- The degree of crystallinity was sensitive to the surfactant concentration. The effect was less pronounced compared to the effect of surfactant type or the effect of droplet size. Without a doubt, bigger droplet sizes associated with higher surfactant concentrations crystallised faster than small droplets associated with lower surfactant concentrations.
- The stability of explosive emulsions was improved by an increase in total surfactant concentration. This was attributable to the impact of reverse micelles. Indeed, as was mentioned before, the quality of the monolayer and the dilatational elastic modulus do not depend on surfactant concentration, while the reverse micelle concentration increases with increase in surfactant concentration (Reynolds *et al.*, 2000; 2001). The reverse micelles are expected to prevent contact between the contents of different

droplets, acting as a barrier to the propagation of crystallisation from one micron scale aqueous droplet through the rest of the emulsion (White *et al.*, 2004).

The inhibiting effect could be related to the repulsive forces (electrostatic and steric) exerted by reverse micelles between adjacent droplets (Ganguly *et al.*, 1992).

3.4.7.2 Rheological behaviour

The evolution of rheological data with ageing for this set of samples was similar to those previously shown in section 3.4.6. The relevant data can be found in appendix D, but the evolution of the main material characteristics as a function of surfactant concentration is presented in this section.

- **Flow properties**

Shear-rate stress measurements were carried out as a function of age for all surfactant concentrations over a period of 36 weeks. Flow curves were used to determine the values of yield stress (Table 3. 37, Table 3.38 and Table 3. 39). The evolution of yield stress values with ageing as a function of surfactant type is shown in Figure 3. 61

Table 3.37: Effect of IMIDE (Mosspar and Shellsol) concentration on yield stress with ageing

Surfactant type	Oil type	d, μm	% Surfactant	t, week	τ_y, Pa
Pibsa-IMIDE	Mosspar	10	8	1 - 17	37.4
				19	49.1
				21	55
				24	66.3
				26	75.8
				28	80
				32	85
				36	90
			14	1 - 20	31
				22	37.4
				24	45
				26	55
				28	63
				32	69.7
				36	77

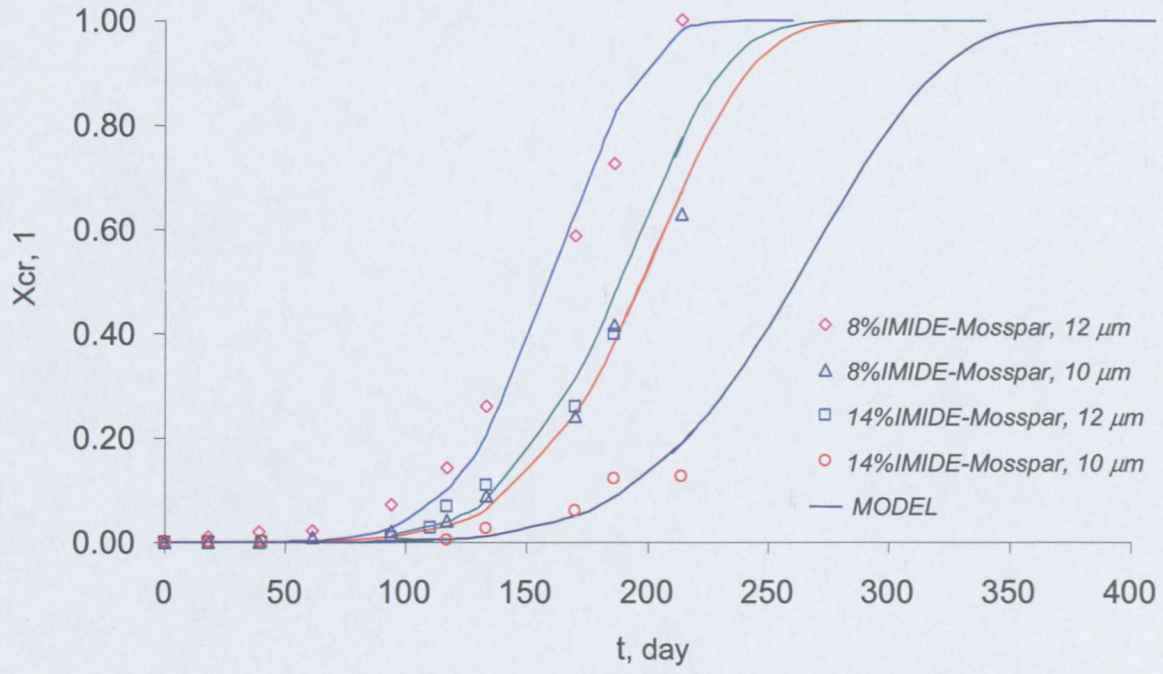

Figure 3.58: Change in relative crystallinity with time for different Pibsa-IMDE concentrations in Mosspar

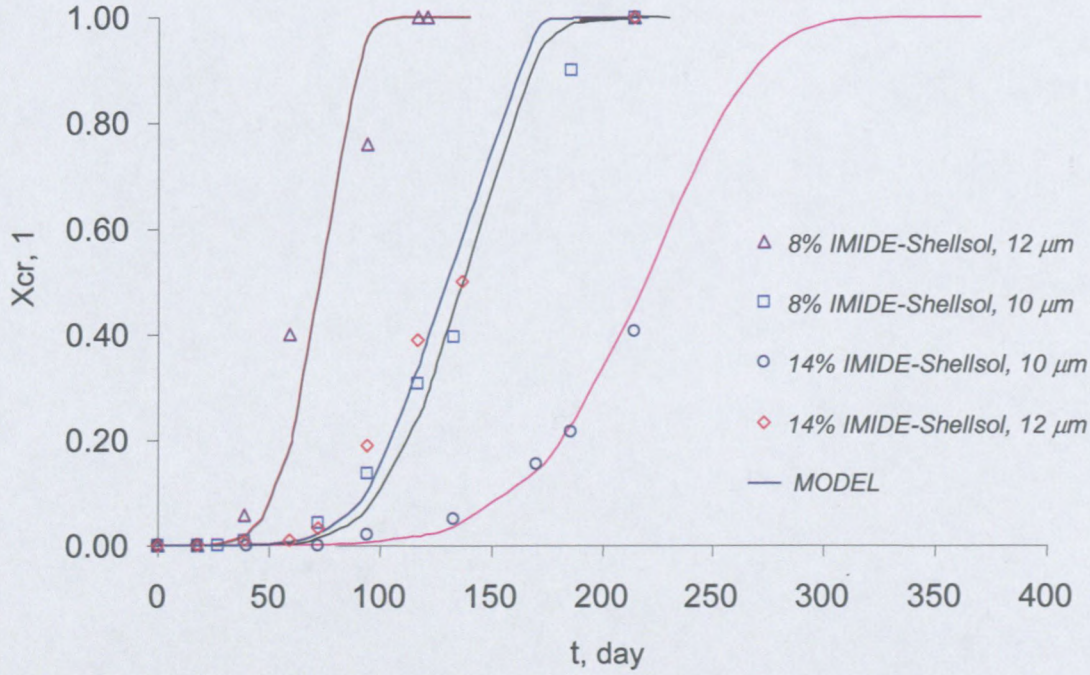

Figure 3.59: Change in relative crystallinity with time for different Pibsa-IMDE concentrations in Shellsol

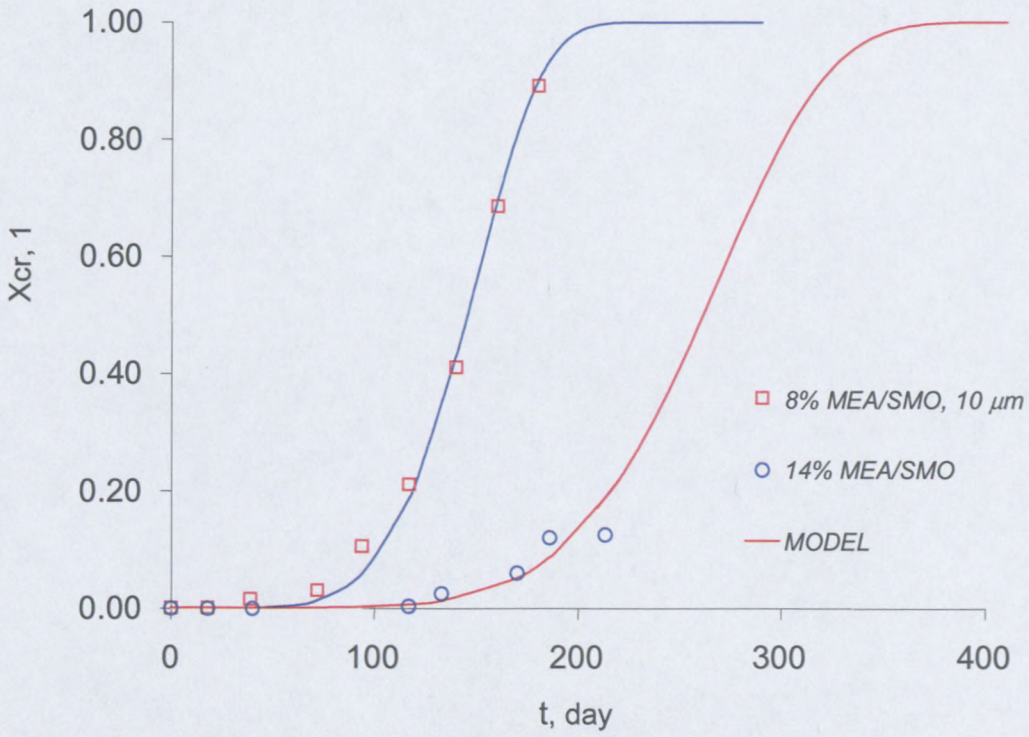

Figure 3.60: Change in relative crystallinity over time for different SMO/Pibsa-MEA concentrations

The values of the JMAK equation constants for samples with different surfactant concentrations are listed in Table 3.35.

Table 3.35: Effect of surfactant concentration on JMAK equation coefficients (Pibsa-IMIDE).

d, μm	Surfactant type	% surfactant	Θ, week	n, 1
Oil phase: Mosspar – H				
10	IMIDE	8	30	6
		14	38	6
	MEA/SMO	8	22	6
		14	40	6
	SMO	8	5	6
		14	6	6
12	IMIDE	8	24	6
		14	28	6
Oil phase: Shellsol				
10	IMIDE	8	21	6
		14	33	6
12	IMIDE	8	11	6
		14	19	6

The onset of crystallisation, the times of 50 % and 100 % crystallinity for different surfactant concentrations and for all droplet sizes were determined using Equation. 3.2 and these are listed in Table 3.36

Table 3.36: Stages of crystallisation for different surfactant concentrations in Mosspar

d, μm	Surfactant type	% Surfactant	Crystallinity, week					
			2 %	10 %	20 %	30 %	50 %	100 %
Oil phase: Mosspar-H								
10	IMIDE	8	16	21	23	25	28	39
		14	20	26	29	32	36	49
	SMO/MEA	8	12	15	17	19	21	29
		14	21	27	31	34	38	52
	SMO	8	2	3	4	4	4	6
		14	4	5	5	6	6	9
12	IMIDE	8	13	17	19	20	23	31
		14	15	20	22	24	27	37
Oil phase: Shellsol								
10	IMIDE	8	11	14	16	17	19	27
		14	17	23	26	28	31	43
12	IMIDE	8	6	8	9	9	10	14
		14	10	13	15	16	18	25

As can be seen from the above, in Figure 3.59, Figure 3.60, Table3.35 and Table 3.36,

- The degree of crystallinity was sensitive to the surfactant concentration. The effect was less pronounced compared to the effect of surfactant type or the effect of droplet size. Without a doubt, bigger droplet sizes associated with higher surfactant concentrations crystallised faster than small droplets associated with lower surfactant concentrations.
- The stability of explosive emulsions was improved by an increase in total surfactant concentration. This was attributable to the impact of reverse micelles. Indeed, as was mentioned before, the quality of the monolayer and the dilatational elastic modulus do not depend on surfactant concentration, while the reverse micelle concentration increases with increase in surfactant concentration (Reynolds *et al.*, 2000; 2001). The reverse micelles are expected to prevent contact between the contents of different

droplets, acting as a barrier to the propagation of crystallisation from one micron scale aqueous droplet through the rest of the emulsion (White *et al.*, 2004).

The inhibiting effect could be related to the repulsive forces (electrostatic and steric) exerted by reverse micelles between adjacent droplets (Ganguly *et al.*, 1992).

3.4.7.2 Rheological behaviour

The evolution of rheological data with ageing for this set of samples was similar to those previously shown in section 3.4.6. The relevant data can be found in appendix D, but the evolution of the main material characteristics as a function of surfactant concentration is presented in this section.

- **Flow properties**

Shear-rate stress measurements were carried out as a function of age for all surfactant concentrations over a period of 36 weeks. Flow curves were used to determine the values of yield stress (Table 3. 37, Table 3.38 and Table 3. 39). The evolution of yield stress values with ageing as a function of surfactant type is shown in Figure 3. 61

Table 3.37: Effect of IMIDE (Mosspar and Shellsol) concentration on yield stress with ageing

Surfactant type	Oil type	d, μm	% Surfactant	t, week	τ_y, Pa
Pibsa-IMIDE	Mosspar	10	8	1 - 17	37.4
				19	49.1
				21	55
				24	66.3
				26	75.8
				28	80
				32	85
				36	90
			14	1 - 20	31
				22	37.4
				24	45
				26	55
				28	63
				32	69.7
				36	77

Table 3.38: Effect of IMIDE (Mosspar and Shellsol) concentration on yield stress with ageing

Surfactant type	Oil type	d, μm	% Surfactant	t, week	τ_y, Pa
Pibsa-IMIDE	Mosspar	12	8	1 - 12	21.9
				14	31
				16	52
				22	67
				25	73
				28	74
				31	75
			14	1 - 15	22
				17	25.4
				19	30
				21	39.7
				23	45.1
				25	59
				27	63
				30	68
				33	74
				36	76
	Shellsol	10	8	0 - 12	39.5
				14	48.4
				16	56
				18	65
				20	74
				22	80
				24	88
				26	92
				28	94
			14	0 - 18	31.4
				20	38
				22	47
				26	58
				30	68
				32	72
				36	78

Table 3.39: Effect of IMIDE (Shellsol), SMO/MEA and SMO concentrations on yield stress with ageing

Surfactant type	Oil type	d, μm	% Surfactant	t, week	τ_y, Pa
Pibsa-IMIDE	Shellsol	12	8	0 - 7	22.8
				9	27
				10	39.5
				11	45.6
				12	54.2
				13	64.8
				14	74
				15	76
			14	0 - 11	22
				13	25
				15	32
				17	49
				21	60
				23	72
				25	74
SMO/Pibsa-MEA	Mosspar	10	8	1 - 13	22.6
				15	42.1
				18	56
				23	64
				28	75.8
				30	76.8
			14	1 - 23	18.2
				25	23
				27	28
				29	37
				32	58
				36	65
SMO	Mosspar	10	8	0 - 1	15.8
				2	30
				3	45
				5	68
				7	70
			14	1 - 4	20.9
				5	30
				6	45
				7	60
				8	70
				9	71

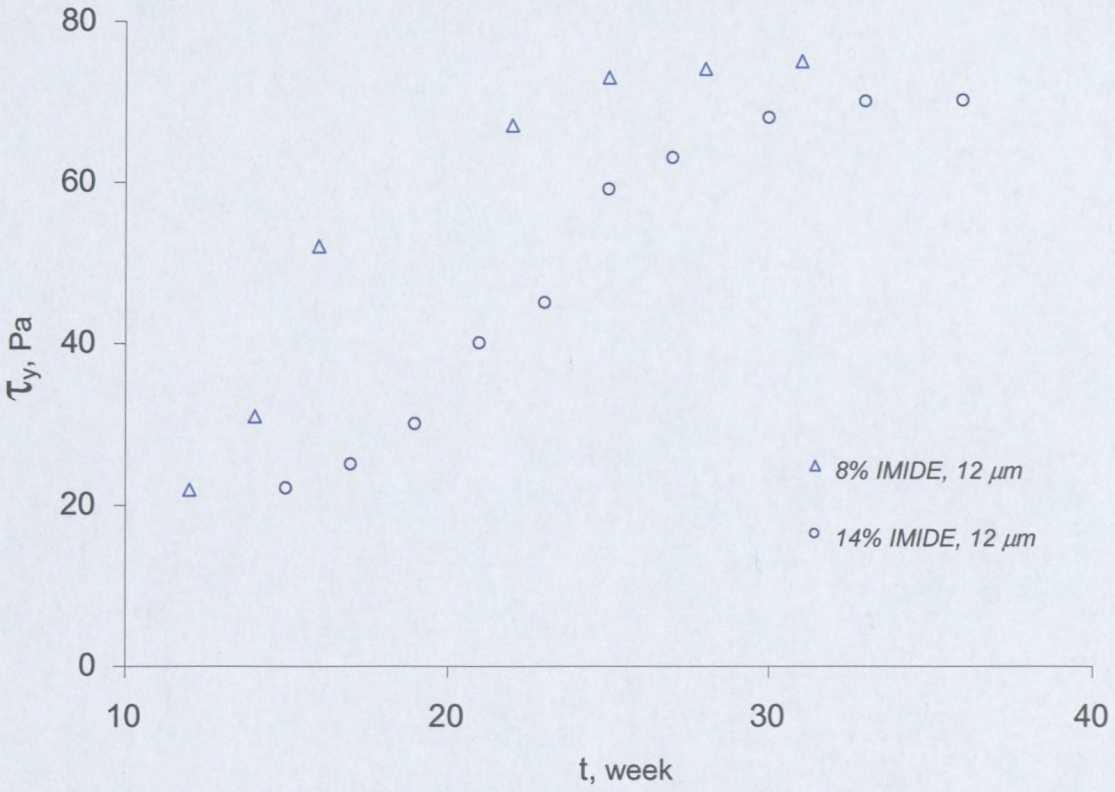

Figure 3.61: Yield stress vs ageing as a function of surfactant concentration in Mosspar

From the results shown in Figure 3.61 it can be seen that the yield stress increases with ageing. The yield stress as a function of time for different surfactant concentrations shows that for any of the emulsions studied, the shape of the curve of the yield stress as a function of time is similar. Furthermore, the lower the surfactant concentration, the higher the yield stress.

- **Viscoelastic properties**

  From the dynamic measurements, the storage and loss moduli were obtained as a function of amplitude of deformation (amplitude sweep) for samples with all surfactant concentrations during the ageing period. The values of storage moduli obtained from the above experiments with time for all samples are listed in Table 3.40 and Table 3.41. The evolutions of storage modulus with ageing as a function of surfactant concentration are presented in Figure 3. 62.

Table 3.40: Effect of IMIDE (Mosspar and Shellsol) concentration on storage modulus with ageing

Surfactant type	Oil type	d, μm	% Surfactant	t, week	G', Pa
Pibsa-IMIDE	Mosspar	10	8	1-17	948
				19	1228
				24	1658
				26	1895
				28	2000
				32	2125
				36	2250
			14	1 - 20	869
				22	1048
				24	1261
				26	1542
				28	1766
				32	1954
				36	2102
		12	8	1 - 12	670
				14	775
				16	1300
				22	1675
				25	1825
				28	1850
				31	1875
			14	1 - 15	670
				17	635
				21	993
				23	1128
				25	1475
				27	1575
				30	1700
				33	1800
				36	1850
	Shellsol	10	8	0 - 12	953
				14	1168
				16	1351
				18	1568
				20	1785
				22	1930
				24	2123
				26	2220
				28	2278
			14	0 - 18	869
				20	1048
				22	1261
				26	1542
				30	1766
				32	1954
				36	2102

Table 3.41: Effect of IMIDE (Shellsol), SMO/MEA and SMO concentration on storage modulus with ageing

Surfactant type	Oil type	d, μm	% Surfactant	t, week	G', Pa
Pibsa-IMIDE	Shellsol	12	8	0 - 7	672
				9	775
				10	988
				11	1140
				12	1355
				13	1620
				14	1850
				15	1900
			14	0 - 11	618
				13	702
				15	899
				17	1376
				21	1685
				23	2023
				25	1850
SMO/Pibsa-MEA	Mosspar	10	8	1 - 13	661
				15	1064
				18	1416
				23	1618
				28	1916
				30	1891
			14	1 - 23	550
				25	695
				27	846
				29	1118
				32	1451
				36	1662
SMO	Mosspar	10	8	0 - 1	463
				2	758
				3	1138
				5	1719
				7	1770
			14	1 - 4	463
				5	665
				6	997
				7	1329
				8	1551
				9	1573

Figure 3.62: Storage modulus vs ageing as a function of surfactant concentration in Mosspar

The results presented in Figure 3.62 clearly show that the storage modulus as a function of time increased for both surfactant concentrations.

3.4.8 Effect of oil type

The main goal of the discussion on the stability of explosive emulsions was the investigation of the surfactant nature and surfactant concentration with regard to the kinetic of the crystallisation of the internal phase providing the instability of explosive emulsions. Meanwhile, it is impossible not to pay attention to the influence of the continuous oil phase on the kinetic of crystallisation.

3.4.8.1 X-ray diffraction

The kinetic of the crystallisation process with ageing was investigated for samples with different oil types by X-ray analysis. The results of measuring crystallinity over time as a function of oil type for three different droplet sizes and two different surfactant concentrations are presented in Figure 3.63 and Figure 3.64.

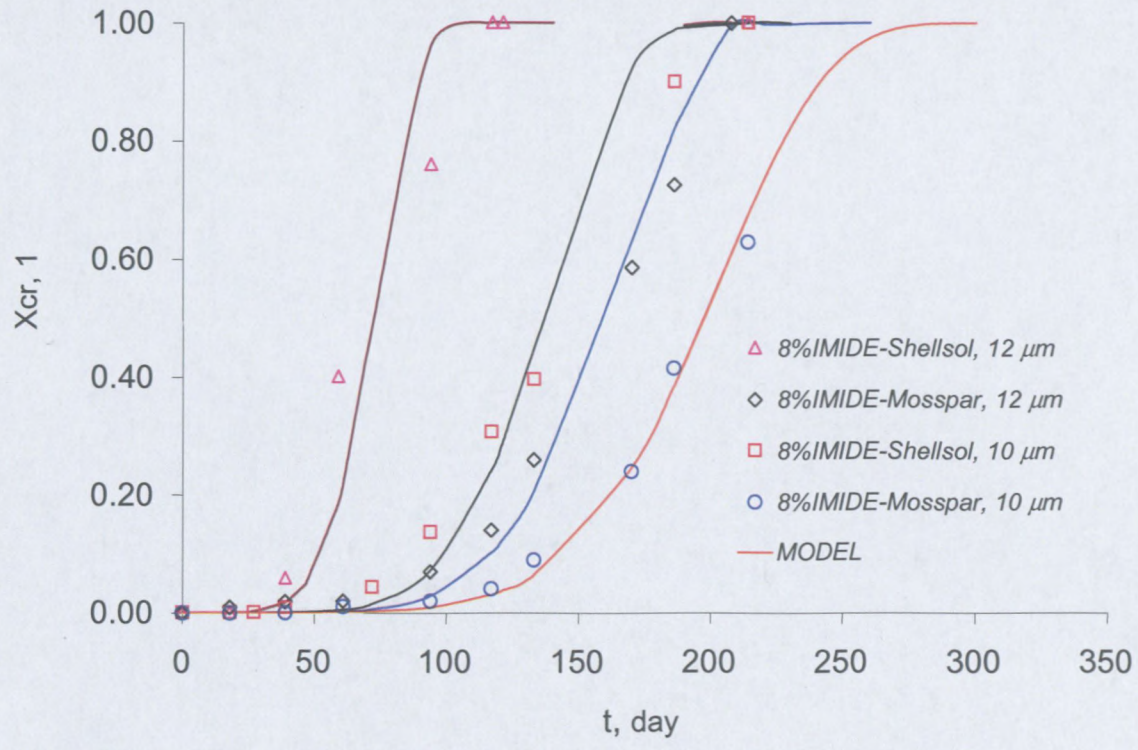

Figure 3.63: Change in relative crystallinity over time for two different oils (8 % Pibsa-IMIDE)

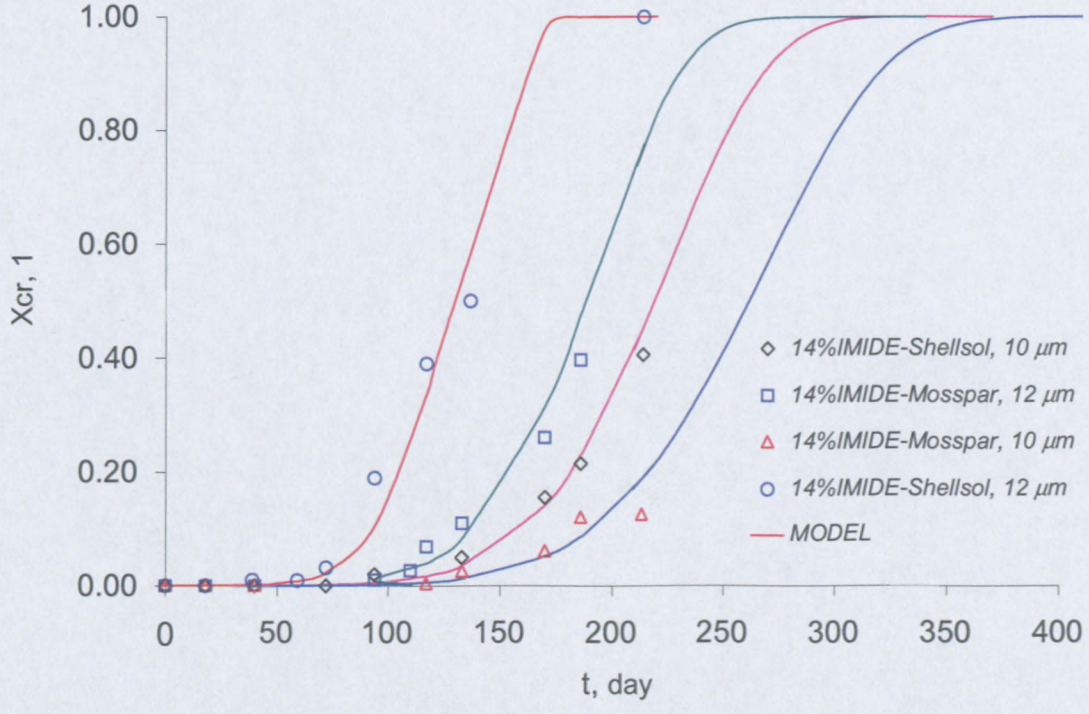

Figure 3.64: Change in relative crystallinity over time for two different oils (14 % Pibsa-IMIDE)

The values of the JMAK equation constants for Pibsa-IMIDE samples with different oils are listed in Table 3.42.

Table 3.42: Effect of oil type on JMAK equation coefficients (Pibsa-IMIDE)

d, μm	% Pibsa-IMIDE	Oil type	θ, week	n, 1
10	8	Mosspar-H	30	6
	8	Shellsol	21	6
	14	Mosspar-H	38	6
	14	Shellsol	33	6
12	8	Mosspar-H	24	6
	8	Shellsol	11	6
	14	Mosspar-H	28	6
	14	Shellsol	19	6
15	8	Mosspar-H	22	6
	8	Shellsol	7	6

The onset of crystallisation, the time of 10 %, 20 %, 30 %, 50 % and 100 % of crystallinity for different oil types and for all surfactant concentrations and droplet sizes were determined using Equation. 3.2. These findings are listed in Table 3.43.

Table 3.43: Stages of crystallisation for different oil types

d, μm	Oil type	% Surfactant	Crystallinity, week					
			2 %	10 %	20 %	30 %	50 %	100 %
10	Mosspar-H	8	16	21	23	25	28	39
	Shellsol	8	11	14	16	17	19	27
	Mosspar-H	14	20	26	29	32	36	49
	Shellsol	14	17	23	26	28	31	43
12	Mosspar-H	8	13	17	19	20	23	31
	Shellsol	8	6	8	9	9	10	14
	Mosspar-H	14	15	20	22	24	27	37
	Shellsol	14	10	13	15	16	18	25
15	Mosspar-H	8	12	15	17	19	21	29
	Shellsol	8	3	5	5	6	6	8

From Figure 3.63, Figure 3.64, Table 3.42 and Table 3.43, it is possible to conclude that the rate of crystallisation is sensitive to the oil type. The emulsions prepared with Mosspar were more stable than the ones prepared using Shellsol for all surfactant concentrations and droplet sizes. At a low surfactant concentration the effect was strong enough to dominate the effect of droplet size. Indeed, even bigger droplets associated with Mosspar-based emulsions were more stable than the smaller ones corresponding to Shellsol-based emulsions.

The effect of oil type on the stability of explosive emulsions can be accounted for on the basis of the compactability effect between the hydrocarbon chains of IMIDE and the hydrocarbon phase (oil phase):

- Chemical structure of IMIDE (see sub-section 3.2.12) and chemical composition of Mosspar and Shellsol (see Table 3.2) molecules suggest that the hydrocarbon chains of IMIDE can accommodate Mosspar (isoparaffinic solvent) molecules better than the Shellsol oil (mixture of paraffins, cycloparaffins and aromatics). Bearing in mind that a high degree of penetration of the oil molecules in the aliphatic layers of the surfactant films increases the cohesive interactions in the aliphatic layer, leading to a long-range ordered and more rigid interface (Gaicha, Leblanc, Villamagna & Chattopadhyay, 1995), it seems reasonable to assume that IMIDE in Mosspar gives rise to a more rigid interface compared to IMIDE in Shellsol.
- Many experimental and theoretical studies on amphiphilic bilayers and reverse micelles have suggested that oil penetration into the interfacial area increases the interfacial mixing entropy and stabilises the interfacial film (Magid & Martin, 1984; Friberg, Christenson, Bertrand & Larsen, 1984; Gaicha *et al.*, 1995). From these references we can assume that IMIDE in Mosspar forms stable reverse micelles compared to IMIDE in Shellsol.
- The nature of the hydrocarbon phase (oil phase) strongly influences the packing behaviour of the surfactant molecules (Ghaicha *et al.*, 1995). The differences in packing features are due to the differences in the penetration of the oil molecules in the aliphatic layers of the surfactant films (Ghaicha *et al.*, 1995). From this it can be assumed that the surfactant-AN nitrate interaction and/or the physical interaction between interface layers of different droplets associated with IMIDE in Mosspar are different from those associated with IMIDE in Shellsol.

3.4.8.2 Rheological behaviour

- **Flow properties**

Shear-rate stress measurements were carried out as a function of age for all oil types over a period of 36 weeks. Flow curves were used to determine the values of yield stress (Table 3.44, Table 3.45 and Table 3. 46). The evolution of yield stress values with ageing as a function of oil type is shown in Figure 3. 61

Table 3.44: Effect of oil type on yield stress with ageing

% Surfactant	d, μm	Oil type	t, week	τ_y, Pa
8	10	Mosspar	1 – 17	37.4
			19	49.1
			21	55
			24	66.3
			26	75.8
			28	80
			32	85
			36	90
		Shellsol	0 – 12	39.5
			14	48.4
			16	56
			18	65
			20	74
			22	80
			24	88
			26	92
			28	94

Table 3.45: Effect of oil type on yield stress with ageing

% Surfactant	d, μm	Oil type	t, week	τ_y, Pa
8	12	Mosspar	1 - 12	21.9
			14	31
			16	52
			22	67
			25	73
			28	74
			31	75
		Shellsol	0 – 7	22.8
			9	27
			10	39.5
			11	45.6
			12	54.2
			13	64.8
			14	74
			15	76
	15	Mosspar	1 – 12	15.7
			14	20
			18	32
			21	40
			24	50.25
			26	60
			28	65
			30	67
		Shellsol	0 – 4	16
			5	22.6
			6	37.9
			7	47
			8	58
			9	70

Table 3.46: Effect of oil type on yield stress with ageing

% Surfactant	d, μm	Oil type	t, week	τ_y, Pa
14	10	Mosspar	1 – 20	31
			22	37.4
			24	45
			26	55
			28	63
			32	69.7
			36	75
		Shellsol	0 – 18	31.4
			20	38
			22	47
			26	58
			30	68
			32	72
			36	78
	12	Mosspar	1 – 15	22
			17	25.4
			19	30
			21	39.7
			23	45.1
			25	59
			27	63
			30	68
			33	74
			36	76
		Shellsol	0 – 11	22
			13	25
			15	32
			17	49
			21	60
			23	72
			25	74

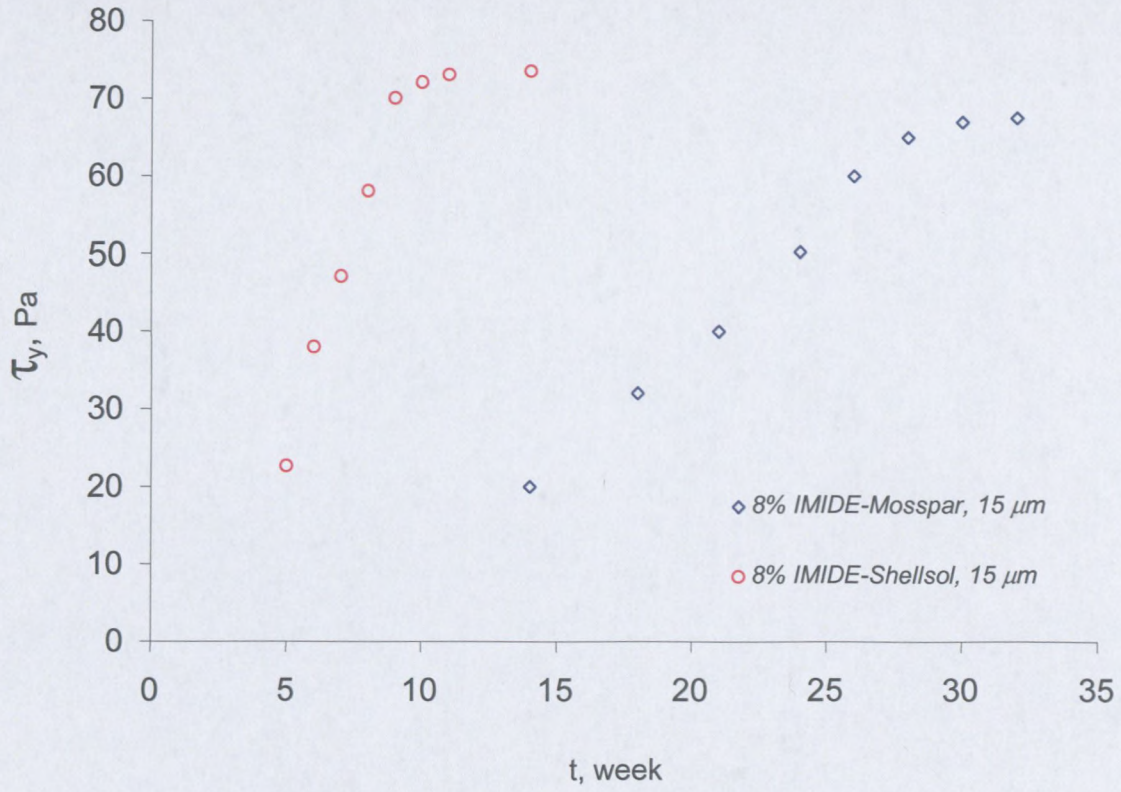

Figure 3.65: Yield stress vs ageing as a function of oil type (Pibsa-IMIDE)

From results presented in Figure 3.65 it can be seen that the yield stress as a function of time increases for both oil types.

- **Viscoelastic properties**

From the dynamic measurements, the storage and loss moduli were obtained as a function of amplitude of deformation (amplitude sweep) for samples with all surfactant concentrations during the ageing period. The values of storage moduli obtained from the above experiments with time for all samples are listed in Table 3.47 and Table 3.48. The evolutions of storage modulus with ageing as a function of surfactant concentration are presented in Figure 3. 66.

Table 3.47: Effect of oil type on storage modulus over ageing (8 % IMIDE)

% Surfactant	d, μm	Oil type	t, week	G', Pa
8	10	Mosspar	1 –17	948
			19	1228
			21	1375
			24	1658
			26	1895
			28	2000
			32	2125
			36	2250
		Shellsol	0 –12	953
			14	1168
			16	1351
			18	1568
			20	1785
			22	1930
			24	2123
			26	2220
			28	2278
	12	Mosspar	1 –12	670
			14	775
			16	1300
			22	1675
			25	1825
			28	1850
			31	1875
		Shellsol	0 –7	672
			9	775
			10	988
			11	1140
			12	1355
			13	1620
			14	1850
			15	1900
	15	Mosspar	1 – 12	433
			14	500
			18	800
			21	1000
			24	1256
			26	1500
			28	1625
			30	1675
		Shellsol	0 – 4	431
			5	609
			6	1021
			7	1266
			8	1562
			9	1886

Table 3.48: Effect of oil type on storage modulus over ageing (14 % IMIDE)

% Surfactant	d, μm	Oil type	t, week	G', Pa
14	10	Mosspar	1 – 20	869
			22	1048
			24	1261
			26	1542
			28	1766
			32	1954
			36	2102
		Shellsol	0 –18	887
			20	1073
			22	1328
			26	1638
			30	1921
			32	2034
			36	1950
	12	Mosspar	1 – 15	670
			17	635
			19	750
			21	993
			23	1128
			25	1475
			27	1575
			30	1700
			33	1800
			36	1850
		Shellsol	0 –11	618
			13	702
			15	899
			17	1376
			21	1685
			23	2023
			25	1850

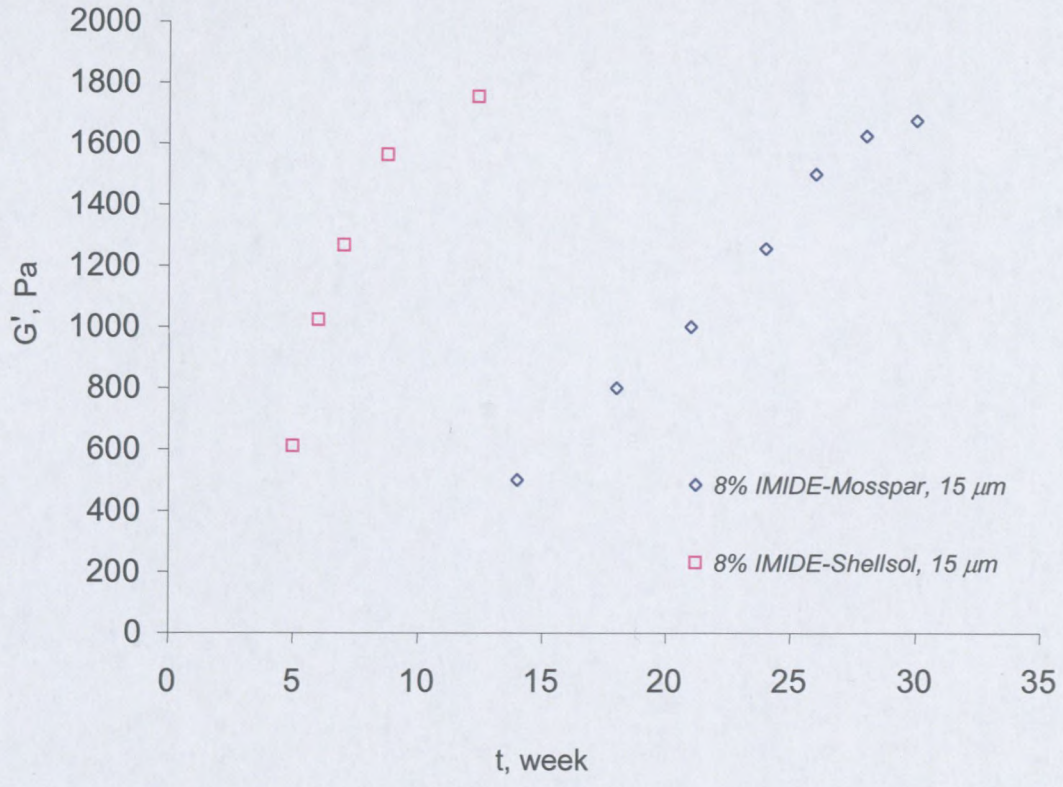

Figure 3.66: Yield stress vs ageing as a function of oil type (Pibsa-IMIDE)

Results presented in Figure 3.66 clearly show that the storage modulus as a function of time increases for both oil types.

3.4.9 Conclusion on stability of explosive emulsions with ageing

The stability (ageing) of water-in-oil explosive emulsions under investigation is connected to the crystallisation of the aqueous phase, which is a super-cooled ANFO-solution. This process leads to the increase of solid-like properties of the dispersion, which can be considered as the emulsion-to-suspension transition. Actually, an emulsion becomes a suspension of solidified droplets. In the process of ageing before crystallisation takes place, the size of droplets in Pibsa-based emulsions does not change. Any coalescence effects are therefore excluded. Ageing results in an increase of storage modulus over time. Viscosity measurements in the downward mode demonstrate plastic-like behaviour with an appearance of a strongly pronounced yield stress. This is a consequence of partial sol-to-gel transition. The rheological data provided information on the structural change during ageing which was consistent with the microscopic observation and the X-ray analysis. The stability of explosive emulsions is sensitive to the surfactant type, to the surfactant concentration and to the oil type with regard to the following trends:

- Surfactant type: (MEA, UREA)-MEA/SMO-IMIDE-SMO. As previously mentioned in this study, MEA-based and UREA-based emulsions were still fresh after 36 weeks of ageing
- Surfactant concentration: for the same type of surfactant, the emulsion with the lower surfactant concentration was less stable.
- Oil type: IMIDE-based emulsions prepared using Mosspar were more stable than the ones associated with Shellsol.

The following figures (for droplets with an average size of 10 μm) demonstrate the role of the surfactant nature:

Surfactant	*IMIDE*	*MEA/SMO*	*SMO*	*(MEA, UREA)*
for 8 % concentration of a surfactant:				
Characteristic time,θ, week	30	22	5	fresh (36 weeks' ageing)
for 14 % concentration of a surfactant:				
Characteristic time, θ, week	38	40	6	fresh (36 weeks' ageing)

The role of the droplet size is illustrated by the following figures (surfactant: *IMIDE*. Concentration of a surfactant 8 %):

Average droplet size, μm	10	12	15
Characteristic time, θ, week	30	24	22

The following figures demonstrate the superiority of the nature of the surfactant on the size of the droplet

Surfactant	*SMO*	*IMIDE*	*MEA/SMO*	*(MEA, UREA)*
for 8 % concentration of a surfactant:				
Characteristic time, θ, week	5 (10 μm)	24 (12 μm)	29 (15 μm)	fresh (15 μm)

The following figures (for droplets with an average size of 12 μm) demonstrate the superiority of the nature of the surfactant on the surfactant concentration:

Surfactant	*IMIDE*	*MEA/SMO*	*(MEA, UREA)*
for 8 % concentration of a surfactant:			

Characteristic time, θ, week	28 (14 % surf.)	34 (8 % surf.)	fresh (8 % surf.)

The role of the oil type is illustrated by the following figures (for droplets with an average size of 10 μm; surfactant: *Imide*. Concentration of the surfactant: 8 %):

Oil type	Mosspar	Shellsol
Characteristic time, θ, week	30	21

These data are rather representative. Firstly, they show that, above the CMC, the stability of W/O explosive emulsions is improved by the increase in total surfactant concentration but this factor does not play a key role. This is in contradiction with some earlier publications (White *et al.*, 2004; 2005). At least, the changes in characteristic times are less than the changes in the surfactant concentration in a continuous phase. This is explained by the fact that the surfactant molecules do not only form interfacial layers, but are partly dissolved in a continuous oil phase forming the reverse micelles (Reynolds *et al.*, 2000; 2001; White *et al.*, 2004; 2005). Secondly, the droplet size only slightly influences the kinetics of crystallisation, increasing the rate of crystallisation with the increase of the droplet size. Thirdly the oil type also slightly influences the kinetics of crystallisation, increasing the rate of crystallisation with the change in oil type from Mosspar to Shellsol. And finally, the above clearly shows that the nature of a surfactant plays a key role in the kinetics of the crystallisation. Indeed, its effect is sufficiently pronounced to obscure other important factors reported in the literature such as droplet size (Masalova *et al.*, 2006; Masalova & Malkin, 2007b) or surfactant concentration (White *et al.*, 2004; 2005). This is especially evident in the transition from oligomeric (PIBSA-based surfactants) to low-molecular-weight surfactants (SMO) or in the transition from surfactants with a head group rich in secondary amino groups (MEA, UREA) to those poor in secondary amino groups (IMIDE or SMO). It can be concluded that the surfactant type does play a key role in the stability of explosive emulsions. Moreover, the changes in the rate of crystallisation (the changes in the stability of the emulsion) are more strongly expressed than any possible changes in the interfacial tension. We consider the last fact as rather important. It seems reasonable to accept it as proof of an active role of a surfactant not only as a compound responsible for interfacial tension, but also creating physical interaction between interface layers of different droplets (because, as has been said, crystallisation develops by interaction of neighbouring droplets) and a droplet surface layer with the matter of a droplet.

On the basis of the results obtained in this study, it appears that:

- The initiation of crystallisation could be strongly dependent on the interactions between the surfactant head group and the ammonium nitrate solution, while the

propagation of crystallisation could depend on the reverse micelle type, the reverse micelle concentration and on the strength of the interface. Indeed the kinetic of crystallisation has been found to follow the same trend as the interfacial elastic modulus (see section 3.4.6). The strength of the interface could act as a mechanical barrier to the propagation of crystallisation throughout the emulsion, while the reverse micelle might act as both an electrical (due to its electrostatic charge) or steric barrier (due to the polymeric nature of the surfactant molecules) by reducing the large impact of the van der Waals attraction, reinforced by the non-ionic nature of the surfactant.

- The high instability of IMIDE-based emulsions compared to other Pibsa-based emulsions could be due to both its the less intense surfactant-ammonium nitrate interaction and its low interfacial elasticity. The high impact of van der Waals attraction associated with this surfactant could play an important role as well. It might enhance the probability of contact between different contents of droplets, thus facilitating the propagation of crystallisation from one droplet to another.

Based on conclusions made in this study it can be assumed that:

1. The propagation of the crystallisation throughout the emulsion could be governed by:
   - The presence of a mechanical barrier at the interface (strength of the interface).
   - The presence of any repulsive potential energy in the thin film between droplets induced either from the inside of the droplet (presence of a net charge in the droplet) or from the oily phase (reverses micelles). Indeed, an increase in the positive potential is expected to reduce the probability of contact between droplets by reducing the impact of the Van der Waals attraction.

2. The stability (delay of both initiation and propagation of crystallisation) of W/O explosive emulsions is governed by several factors, the important ones being:
   - the surfactant head group-ammonium nitrate interaction;
   - the strength of the interface;
   - The reverse micelle structure and the reverse micelle concentration; packing of reverse micelles in the interdroplet layer, reverse micelle-droplet interaction, reverse micelle-reverse micelle interaction.
   - The ammonium nitrate-surfactant head group interaction could play the most important role in the stability of explosive emulsions. Indeed, besides its strong influence on the onset of crystallisation, the ammonium nitrate-surfactant interactions might affect the strength of the interface through the binding energy of the surfactant

to the interface. Moreover, the structure of reverse micelles could depend strongly on this parameter (Reynolds *et al.*, 2000; 2001)

The two parameters, yield stress and storage modulus, characterise the microstructure of the dispersions, especially the tendency of emulsions to form the elastic network or the tendency of solid particles to form aggregates, and the resistance to the break-up of the network or aggregates. The evolution of the storage modulus follows the same pattern as the evolution of yield stress with ageing. That is why only one characteristic parameter namely the yield stress was chosen for the correlation with the kinetic of structural changes (degree of crystallinity) in the following analysis.

3.4.10 Using rheology in the estimation of degree of crystallinity of the emulsion dispersed phase

This effect has already been described for a single surfactant by Masalova *et al.* (2006); Masalova and Malkin (2007b) and Kharatiyan (2005). However the experimental data obtained in this work allows us to answer the question about the general character of the correlation between the yield stress (as the most evident rheological parameter of emulsions) and the relative degree of crystallinity assumed in Masalova *et al.* (2006); Masalova and Malkin (2007b) and Kharatiyan (2005) for different surfactants.

3.4.10.1 Correlation stability-rheology

In emulsion explosives, the yield stress is sensitive to the ageing (to the degree of crystallinity) of emulsions. The values of yield stress depend on the arrangement of crystals or, more precisely, of aggregate particles. The effect is enhanced by the irregular shape of clusters which may cause a blocking of flow (Harzallah & Dupuis, 2003). At rest, crystals are distributed in irregular shapes and non-uniform-sized aggregates. By increasing the concentration of crystals, the building of structures can take place and this can result in stronger resistance to the shear flow. The increase in the yield stress values with ageing points to an increase in the rigidity of the system and to an increase of the strength of solid particle (crystal) structure with ageing (Masalova *et al.*, 2006; Masalova & Malkin, 2007b; Kharatiyan, 2005). Empirical quantitative relations between the rheological parameters and characteristic parameters of relative crystallinity have been established by Masalova *et al.* (2006); Masalova and Malkin (2007b) and Kharatiyan (2005).

$$\Theta = 0.7\tau_y^{\,0} + 10 \qquad \text{Equation 3.3}$$

$$\tau_y^{\,max} = 52 + 1.5\tau_y^{\,0} \qquad \text{Equation 3.4}$$

$$Y = \frac{\tau_y^{\,t} - \tau_y^{\,0}}{\tau_y^{\,max} - \tau_y^{\,0}} = X_{CR}^{\,0.51} e^{0.46(1-X_{CR})} \qquad \text{Equation 3.5}$$

The authors found that the above relations were valid in their experimental window, no matter what the formulation of the emulsion (dispersed phase volume fraction) was or what the emulsion droplet size was. However, it is worth mentioning that the above correlations were established for a single surfactant and a constant surfactant concentration.

3.4.10.2 Correlation between Θ and $\tau_y^{\,0}$

The characteristic time of the Avrami-Kolmogorov Equation 3.2 for all emulsions used in this study was plotted against the yield stress of fresh samples and is shown in Figure 3.56.

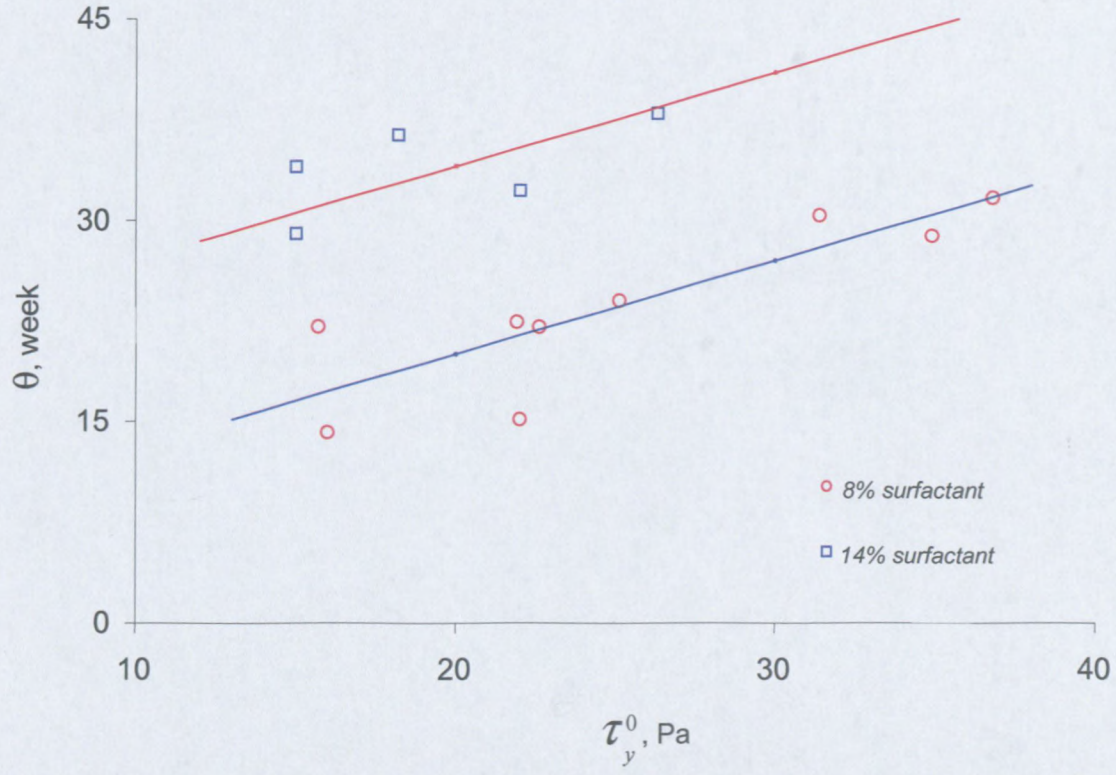

Figure 3.67: Relation between characteristic time and minimal value of the yield stress.

As can be seen from Figure 3.65, the relation between characteristic time and the yield stress of the emulsion at 0 % of crystallinity can be described by the following equations:

$\Theta = 0.7\,\tau_y^{\,0} + 6 \longrightarrow$ *8% surfactant concentration* **Equation 3.6**

$\Theta = 0.7\,\tau_y^{\,0} + 20 \longrightarrow$ *14% surfactant concentration* **Equation 3.7**

A general relation can be written as follows

$$\theta = 0.7\,\tau_y^{\,0} + C, \qquad \textbf{Equation 3.8}$$

where the constant, C, seems to be related to the initial micelle concentration, where θ is the characteristic time of the sample, as defined by the JMAK equation, and $\tau_y^{\,0}$ is the yield stress of the fresh sample. The above relations are valid for all droplet sizes and all surfactant types, except IMIDE. This is probably due to the fact that the dominant source of elasticity for other Pibsa-based surfactants is the interface, while the van der Waals attraction could be the main source of elasticity in the case of IMIDE. Indeed, the effect of interfacial elasticity on the bulk rheology follows the same trend with regard to its effect on emulsion stability. However, the van der Waals attraction decreases the emulsion stability while increasing the overall elasticity. Different surfactant concentrations affect only the intercept. The latter decreases as the surfactant concentration increases. Once again, this could be due to the fact that an increase in reverse micelle concentration could reduce the impact of the van der Waals attraction in the thin film separating adjacent droplets. This effect is expected to reduce elasticity while the stability is improved.

It can be concluded that the characteristic time is an increasing function of the yield stress of the fresh sample only if the main source of elasticity is the interface. If the impact of the van der Waals attraction on the overall elasticity is large, the opposite effect might be observed.

3.4.10.3 Correlation between $\tau_y^{\,max}$ and $\tau_y^{\,0}$

The yield stress of fully crystallised emulsion (maximal yield stress) is plotted against the yield stress of the fresh sample (minimal value of the yield stress) for all surfactant types, all surfactant concentrations and all droplet sizes (Figure 3.68).

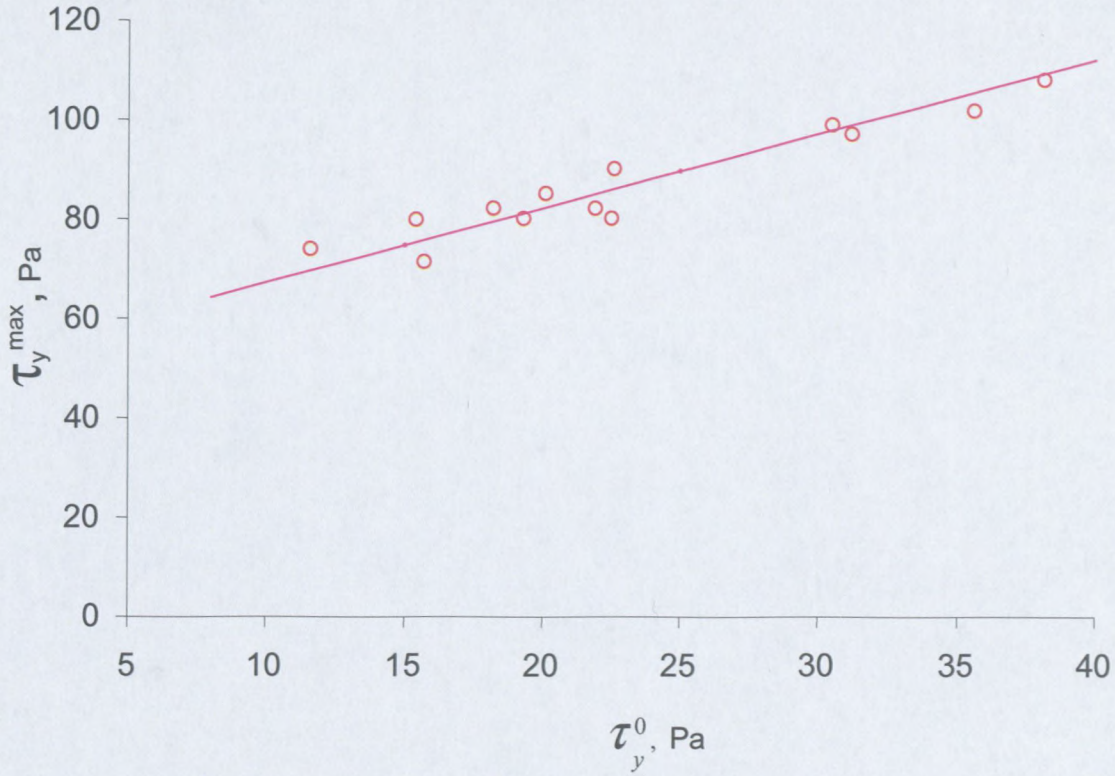

Figure 3.68: Maximal yield stress vs minimal yield stress

As can be seen from Figure 3.66, the relation between maximal and minimal yield stress (no matter what the surfactant type is, what the surfactant concentration is, or what droplet sizes are used) can be described by the following equation:

$$\tau_y^{max} = 52 + 1.5\tau_y^0, \qquad \textbf{Equation 3.9}$$

where τ_y^{max} is the maximal value of the yield stress (at 100 % of crystallinity), τ_y^0 is the minimal value of the yield stress (at 0 % of crystallinity).

It can be concluded that the above relation is valid, no matter what the emulsion formulation is, what the emulsion droplet size is, what the surfactant type is and what surfactant concentration is used.

3.4.10.4 Correlation between the relative growth of yield stress Y and X_{Cr}

The relative growth of the yield stress during ageing (Y) was calculated using the following equation:

$$Y = \frac{\tau_y^{\,t} - \tau_y^{\,0}}{\tau_y^{\,\max} - \tau_y^{\,0}} = \frac{\Delta\tau_y}{\tau_y^{\,\max} - \tau_y^{\,0}}, \qquad \text{Equation 3.10}$$

where $\tau_y^{\,0}$ is the yield stress of a fresh sample, $\tau_y^{\,\max}$ is the yield stress of a fully crystallised sample, and $\tau_y^{\,t}$ is the yield stress of a sample aged for t weeks. The evolution of the relative growth of yield stress with ageing as a function of relative crystallinity for all samples (all surfactant types, all surfactant concentrations, all droplet sizes and, both oil types) is presented in Figure 3.67.

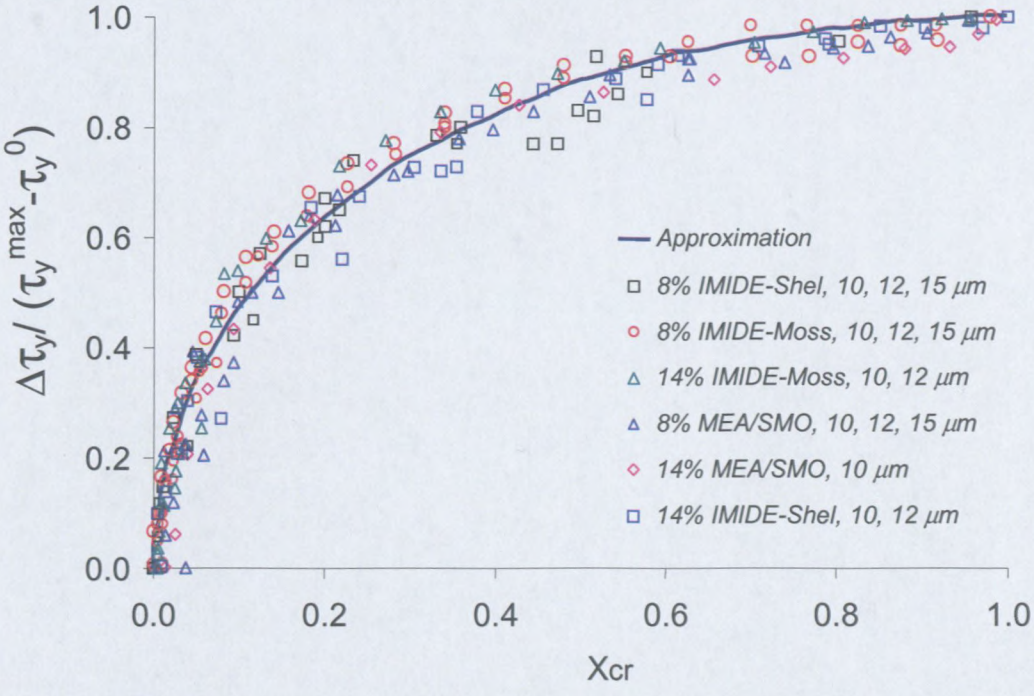

Figure 3.69: Relative growth of the yield stress vs relative crystallinity

The dependence of the relative yield stress on the relative crystallinity for all surfactant types, all surfactant concentrations, all droplet sizes and for both oil types can be described by the equation:

$$Y = \frac{\tau_y^{\,t} - \tau_y^{\,0}}{\tau_y^{\,\max} - \tau_y^{\,0}} = X_{CR}^{\,0.51} e^{0.46(1-X_{CR})}, \qquad \text{Equation 3.11}$$

where $\tau_y^{\,0}$ is the yield stress of the fresh sample, $\tau_y^{\,\max}$ is the yield stress of the fully crystallised sample, $\tau_y^{\,t}$ is the yield stress aged for a sample of t weeks, and X_{Cr} is the relative crystallinity.

One can see that this fitting equation is equivalent to one obtained by Masalova *et al*. (2006); Masalova and Malkin (2007b) and Kharatiyan (2005) for a single surfactant. This equation therefore is of general value for the description of the evolution of rheological properties for different explosive emulsions during their ageing.

This equation allows one to predict rheological behaviour on the basis of the kinetics of crystallisation and vice versa.

CHAPTER 4
SUMMARY AND CONCLUSION

The rheological properties of highly concentrated water-in-oil explosive emulsions (emulsions in which the dispersed droplets are super-cooled aqueous solutions of mainly ammonium nitrate salt in water and are deformed from the optimal spherical shape by the presence of neighbours); the effect of the surfactant type, the effect of the surfactant concentration on rheological properties of the emulsion; and the influence of emulsion formulation on its stability with ageing were investigated experimentally, and the results were used in the estimation of the sensitivity of the rheological parameter (namely yield stress) to the structural changes in the emulsion (crystallisation process) during ageing.

The relative crystallinity of the materials during ageing was analysed using a Brucker D8 X-ray powder diffractometer with Cu radiation.

The bulk rheological measurements were carried out using a rotational dynamic rheometer MCR 300 (Paar Physica). Samples of different surfactant types (*Pibsa-MEA*, *Pibsa-UREA*, *Pibsa-IMIDE*, *SMO* and *SMO/Pibsa-MEA*) and different surfactant concentrations were studied. The first three surfactants belong to the same type of chemical compounds, though with different end groups, and they can be treated as oligomers, while *SMO* is a monomeric surfactant. It is also worth mentioning that the droplet size distributions for all samples under investigation were Gaussian and, practically, did not depend on the nature or concentration of the used surfactant. The bulk rheological measurements included the following:

- Flow curves including yield stress;
- Strain amplitude dependence of the components of dynamic modules.

A system of parameters characterising the bulk rheological properties of the samples under investigation was obtained.

All the above bulk rheological factors are connected with the structure of the oil film network of the emulsions under investigation; different forces induced in the interdroplet layer (surfactant-surfactant interaction, ion-fluctuation within the droplets, surfactant-electrolyte interactions); as well as with the content of crystals (solid particles) of the ammonium nitrate solution of the super-cooled phase, which appears to increase during ageing. The dependence of the relative growth of the yield stress on relative crystallinity was found to be

uninfluenced by the type of surfactant, surfactant concentration and the size of droplets used for this study.

It has been shown that the total amount of surfactant used in this study is far in excess of the amount adsorbed at the oil/water interface, even for the lowest surfactant concentration. This was an indication that the majority of Pibsa-based surfactants is in the form of spherical reverse micelles in the oily phase, and dissolved in the oil phase. Rather fewer occur as a monolayer at a flat aqueous-oil interface (White *et al.*, 2004; Reynolds *et al.*, 2000; 2001). Moreover, it was found that different types of surfactant yield different interfacial properties. Indeed, both the interfacial tension and the dilatational elastic modulus were found to decrease according to the sequence MEA-UREA-MEA/SMO-IMIDE-SMO. The important finding in this study was the rather close values of the interfacial properties (interfacial tension and the interfacial elastic modulus) of all the Pibsa-based surfactants and their non-dependence on surfactant concentration.

The typical rheological behaviour was investigated and existence of the yield stress and strong non-Newtonian behaviour at high shear stresses were observed.

It was established that the surfactant type and surfactant concentration affect rheological properties of explosive emulsions. In fact, both the elastic modulus and the yield stress decrease in the following order: MEA-IMIDE-UREA-MEA/SMO, whereas they decrease as the surfactant concentration increases. However, the sensitivity of the rheological parameters to the type or concentration of surfactant was found to decrease as the droplet size increases. The changes in rheological parameters have been found to be much more strongly expressed than any changes in interfacial tension (e.g. an increase in surfactant concentration decreases the storage modulus and the yield stress, while the interfacial tension remains constant). This last fact was considered as rather important. It seemed reasonable to assume that it provided proof of an active role of a surfactant, not only as a compound responsible for the interfacial tension, but also as creating additional sources of elasticity.

The research indicated that, in the linear regime, the dimensionless elastic moduli do not collapse on a single master curve. Indeed, with other factors such as electrolyte concentration, phase ratio, surfactant concentration and the nature of the external phase being kept constant, IMIDE-based emulsions, for example, showed very high dimensionless elastic moduli compared to other Pibsa-based emulsions. Moreover, it was found that an increase in surfactant concentration does not affect the intrinsic elasticity of the droplets (the

capillary pressure). It decreases only the magnitude of the additional elasticity. Bearing in mind the rather close values of the interfacial elastic modulus of all the surfactants used and the non-dependence of this factor on the surfactant concentration, the above observations were indications that the interaction potential between droplets (physical interaction between interface layers of different droplets and a droplet surface layer with the matter of a droplet) does play a key role in generating additional sources of elasticity in the system.

The rheological properties of concentrated emulsions are governed by the different forces that occur in the system, which, in turn, depend on the thickness of the interdroplet layer (thin film between droplets), on surfactant type and on surfactant concentration. In the particular case of the Pibsa-based emulsion explosives used in this study, the dominant interaction energy between droplets could be due to van der Waals attraction because of the non-ionic character of surfactants (Alvarez *et al.*, 2006; Bibette *et al.*, 1999; Baravian *et al.*, 2006; Quintero *et al.*, 2008). Moreover, ion-fluctuation within the aqueous droplets could give rise to an additional attractive potential energy in the thin film between droplets, similar to the van der Waals interaction between neutral atoms (Sheng *et al.*, 2004; Tsao *et al.*, 2002). This electrostatic attraction is insensitive to the ion concentration and consists of contributions from various induced multipole-multipole interactions, including dipole-dipole, dipole-quadrupole, dipole-octupole, and quadrupole-quadrupole interactions (Sheng *et al.*, 2004). On the other hand, because of the polymeric nature of the surfactants and the presence of AN in their core (Reynolds *et al.*, 2000; 2001), reverse micelles might induce both steric and electrostatic repulsive forces (Ganguly *et al.*, 1992), whereas the separation of charges induced by surfactant-electrolyte interaction (Ashok *et al.*, 1991; Ganguly *et al.*, 1992) could give rise to electrostatic repulsions between adjacent droplets, similar to the repulsions between permanent dipoles.

In summary: above the CMC the influence of surfactant concentration on the rheological behaviour for our emulsions was qualitatively different from the effect of surfactant type. All changes observed may be understood by taking into account that changing of the surfactant type gives rise to a modification of interfacial properties (interfacial tension and interfacial elasticity) and could affect the pair potential energy in the thin film between adjacent droplets. In fact, because of the differences in their head groups, it seemed reasonable to assume that a change in surfactant type can affect the AN-surfactant interaction, the physical interaction between interfacial layers of different droplets, the interaction between reverse micelles and droplets and the distribution of ions within the droplets (number of ions involved in the

formation of hydrogen-bonded species with the surfactant, ion-fluctuation or the magnitude of the dipole moment of the droplet). On the other hand, the variation of surfactant concentration leads only to the changes in reverse micelle concentration, the quality of the monolayer with interfacial properties remaining the same. Therefore the surfactant concentration can affect only the potential energy in the thin film. It must, however, be emphasised that, in both cases, the thickness of the interdroplet layer may undergo slight changes due to modification in the molecular forces across the film (interactions between surfaces of adjacent droplets and/or interactions reverse micelle-droplet or reverse micelle-reverse micelle).

The rheological properties of the compressed emulsions under investigation depended sensitively on the intrinsic elasticity of the droplets and the pair potential energy in the thin film, and could depend on the interfacial elastic modulus. The elasticity of droplets and the degree of deformation are controlled by their internal pressure (Laplace pressure) and the oil film network structure, whereas, above the CMC, the strength of the interface could be controlled mainly by the surfactant-AN interaction. On the other hand, the reverse micelle concentration, the distribution of ions within the droplet and the van der Waals attraction could control the pair potential energy in the thin film between droplets. The dilatational elastic modulus, the ion-fluctuation and the van der Waals attraction (reinforced by the non-ionic nature of the surfactant) could indeed act as sources of additional elasticity. It is worth mentioning that any increase in electrostatic or steric repulsive forces in the system (e.g. an increase in reverse micelle concentration) could reduce the contribution of the van der Waals attraction to the overall elasticity. The balancing repulsive-attractive forces could be one of the major factors which might determine the magnitude of the additional elasticity in the explosive emulsions. As mentioned before, the tails of oligomeric surfactants used in this study are the same. Therefore the possible differences in the conformations, in the distribution of ions within the droplets, and in the reverse micelle structure will have depended mainly on the AN-surfactant interaction (because, as we have said, emulsions prepared with different surfactants were tested under the same environmental conditions). It seemed reasonable to assume that the balancing attractive-repulsive forces (the interaction potential between droplets) is controlled by the AN-surfactant interaction. A high level of surfactant-AN interaction is expected to increase repulsive forces in the system. The strong deviation of the IMIDE-scaled elastic modulus in comparison with other surfactants could be an indication of the highest impact of attractive forces (ion-fluctuation and van der Waals forces) due to the expected low magnitude of AN-surfactant interaction.

The stability of emulsion explosives was connected with the crystallisation of the aqueous phase, which was a super-cooled ANFO-solution. A qualitative investigation of the crystallisation process as a function of surfactant type was performed using an optical microscope. The results showed the crystals as a mixture of stone-like and needle-like forms, whereas the droplets of emulsions were much smaller than the suspended crystals. These results can be understood in that, no matter what type of surfactant was used, the crystals did not grow from different independent centres, but by single crystals breaking through the boundaries of the droplets to occupy several separate droplets. The quantitative measure of the crystallisation rate showed that the kinetics of crystallisation was sensitive to both the surfactant type and surfactant concentration:

- The experimental data showed that the stability of W/O explosive emulsions is improved above the CMC by an increase in total surfactant concentration, but this factor does not play a key role. At least, the changes in characteristic times were less than changes in the surfactant concentration in a continuous phase. This is explained by the fact that the surfactant molecules do not form interface layers only, but are partly dissolved in a continuous oil phase forming the reverse micelles (Reynolds *et al.*, 2000; 2001; White *et al.*, 2004; 2005).
- The droplet size only slightly influences the kinetics of crystallisation, in increasing the rate of crystallisation with the increase of the droplet size.
- The nature of a surfactant does influence the kinetics of crystallisation according to the following trend: MEA-UREA-MEA/SMO-IMIDE-SMO. It was clearly demonstrated that this parameter plays a key role in the kinetics of crystallisation (in the stability of explosive emulsions). Indeed, its effect has been found to be so pronounced as to obscure other important factors reported in the literature, such as droplet size (Masalova *et al.*, 2006; Masalova & Malkin, 2007b) or surfactant concentration (White *et al.*, 2004; 2005). This was especially evident in the transition from oligomeric (PIBSA-based surfactants) to low-molecular-weight surfactants (SMO), or in the transition from surfactants with a head group rich in secondary amino groups (MEA or UREA) to the ones poor in the latter groups (IMIDE or SMO). Moreover, the changes in the rate of crystallisation (the changes in the emulsion's stability) are more strongly expressed than any possible changes in the interfacial tension. We, again, consider this a rather important fact. It confirms the active role of a surfactant not only as a compound responsible for interfacial tension, but also as creating the physical interaction between interface layers of different droplets (because, as was said, crystallisation develops by the interaction of neighbouring droplets) and a droplet surface layer with the matter of a droplet.

- X-ray diffraction demonstrated the interconversion of phase II and phase IV during the crystallisation of Pibsa-based explosive emulsions at room temperature. The formation of a more disordered phase (Phase II) at room temperature in Pibsa-based emulsions was assumed to be an additional proof of the strong influence of both the surfactant-electrolyte interaction and the physical interaction between interface layers of different droplets on the stability of explosive emulsions. A strong surfactant-ammonium nitrate interaction and/or a strong repulsion between different droplets introduce an inhibiting force in the formation of organised phases (because the AN-surfactant introduces charge separation inside the droplet and a strong repulsive force between droplets can avoid a weakening of the surfactant-electrolyte interaction due to coalescence). Transitions involving phase III were absent, probably because of the low level of water in the system.

It has been found reasonable to assume that the initiation of crystallisation is strongly dependent on the AN-surfactant interaction and on the physical interaction between interface layers of different droplets. On the other hand, the propagation of crystallisation from one droplet to another could depend on the strength of the interface (mechanical barrier) and/or on micelle type and micelle concentration (electrical and/or steric barrier). Among the three Pibsa-based surfactants used in this study (same hydrophilic tail), the ammonium nitrate-surfactant head group interaction could play the most important role in the stability of explosive emulsions. Besides its strong influence on the onset of crystallisation (the higher the AN-surfactant interaction, the more stable the emulsion), the degree of ammonium nitrate-surfactant interaction could strongly influence the binding energy of the surfactant to the interface and thus the strength of the interface. The structure of reverse micelles could depend strongly on this parameter and the formation of phase II at room temperature could be promoted by this parameter. The results of ageing involving all the non-ionic surfactants suggested that the stability of explosive emulsions is governed by both the AN-surfactant interaction and the (steric and/or electric barrier) balancing repulsive forces-attractive forces (van der Waals attraction). Indeed, the length of the hydrophobic tail and the presence of secondary amines in the core can be considered as the two parameters that strongly influence surfactant ability in stabilising explosive emulsions.

It has been found that the length of the hydrophobic tail and the presence of secondary amines in the core are two parameters that strongly influence the surfactant ability in stabilising explosive emulsions.

The process of ageing leads to an increase in solid-like properties of the dispersion that can be considered as the emulsion-to-suspension transition. Actually, the emulsion becomes a suspension of solidified droplets. This transition is incomplete because these very concentrated dispersions store the possibility of flow. In the process of ageing, before the crystallisation takes place, the size of droplets does not change. Any effect of coalescence is therefore excluded. Ageing results in an increase in the storage modulus over time. Flow curves measured in the downward mode demonstrated plastic-like behaviour with a strongly pronounced yield stress. This also is a consequence of partial sol-to-gel transition. The kinetics of crystallisation corresponds to the evolution of plastic behaviour (characterised by the yield stress) of the emulsion.

It has been established that:

- For the same surfactant concentration, the rate of the crystallisation process (characteristic time of the crystallisation process) depended on the value of the yield stress of the fresh sample, no matter what the surfactant type and/or the oil type and/or what the droplet size used in our investigation. Except for IMIDE-based emulsions, it was found that the more stable emulsion formulations were those corresponding to the highest values of yield stress. This is probably due to the fact that the dominant source of elasticity for other Pibsa-based surfactants is the interface, while the van der Waals attraction could be the main source of elasticity in the case of IMIDE. The effect of interfacial elasticity on the bulk rheology was found to follow the same trend as on emulsion stability in contrast to the van der Waals attraction, which decreases emulsion stability while increasing the overall elasticity.
- There was a linear relationship between the maximal (of fully crystallised emulsion) and minimal (of fresh material) values of yield stress, no matter what the surfactant type and/or what the surfactant concentration and/or what the droplet size used in our investigation;
- The relative growth of the yield stress during ageing was related exponentially to the relative crystallinity, no matter what the surfactant type and/or what the surfactant concentration and/or what the emulsion droplet size used in our investigation. The fitting equation is equivalent to the one obtained in Masalova *et al.* (2006); Masalova and Malkin (2007b) and Kharatiyan (2005) for a single surfactant:

$$\tau_y^{max} = 52 + 1.5\tau_y^{0} \qquad \textbf{Equation 3.12}$$

$\Theta = 0.7\,\tau_y^{0} + C$ (C = 6 and 20 respectively for 8 % and 14 %) **Equation 3.13**

$$Y = \frac{\tau_y^{\,t} - \tau_y^{\,0}}{\tau_y^{\,\max} - \tau_y^{\,0}} = X_{CR}^{\,0.51} e^{0.46(1-X_{CR})}$$ **Equation 3.14**

It is possible to see that the degree of crystallinity in the ageing of emulsions really is a unique measure of the rheology of these emulsions. These equations therefore are of a general value for the description of the evolution of rheological properties for different explosive emulsions in their ageing.

These equations allow one to follow the structural changes by the structural characteristic, namely yield stress, and to predict the degree of crystallinity of the sample stored for some time by measuring the yield stress of fresh emulsion and the yield stress of stored emulsions; or to predict the time when the emulsion will reach a certain degree of crystallinity by measuring the yield stress of the fresh sample.

The following aspects were not covered in this thesis and should be investigated:

- The effect of the type and concentration of surfactant on the surfactant-electrolyte interaction;
- The effect of the type and concentration of surfactant on the initiation of crystallisation;
- The effect of the ammonium nitrate concentration on rheological properties and ageing of explosive emulsions; and
- The effect of the type and concentration of surfactant on the structural parameters of the micellar solution of the continuous phase (micellar concentration, size, electrical charge, etc.).

BIBLIOGRAPHY

Acrivos, A. & Lo, T.S. 1978. Deformation and break up of a single slender drop in an extensional flow. *J. Fluid Mech.*, 86:641–672.

Adam, N.K. 1941. *The Physics and Chemistry of Surfaces.* 3rd edition, London: Oxford University Press.

Adamson, A.W. 1997. *Physical chemistry of surfaces.* 6th edition. New York: Wiley-Interscience publication.

Alvarez, O., Mougel, J., Baravian, C., Caton, F., Marchal, P., Stébé, J.M. & Choplin, L. 2006. Aging of an unstable water-in-oil gel emulsion with a nonionic surfactant. *Rheol Acta* 45:555–560.

Aronson, M.P. & Petko, F.M. 1993. Highly concentrated water-in-oil emulsions: Influence of electrolyte on their properties and stability. *J. Colloid Interface Sci.*, 159:134–149.

Aronson, M.P. & Princen, H.M. 1980a. Contact angles associated with thin liquid films in emulsions. *Nature*, 286:370–372.

Aronson, M.P. & Princen, H.M. 1980b. Contact angles in oil-in-water emulsions stabilized by ionic surfactant. *Colloid Surf*, 4:173–184.

Ashok, K.A. & Neilson, G.W. 1991. *J. Chem. Soc. Faraday Trans.* 87:279–286.

Atkins, P.W. 1994. *Physical Chemistry*, 5th edition. Oxford: Oxford University Press.

Babak, V.G., Langenfeld, A., Fa, N. & Stebe, M.J. 2001. Rheological properties of highly concentrated fluorinated water-in-oil emulsions. *Prog. Colloid Polym. Sci.*, 118:216–220.

Babak, V.G. & Stebe, M.J. 2002. Highly concentrated emulsions: Physicochemical principles of formulation. *J. Dispersion Science and Technology.* 23:1–22.

Bampfield, H.A. & Cooper, J. 1988. In Becher (Ed.). *Encyclopedia of emulsion technology.* New York: Marcel Dekker. vol. 3.

Baravian, C., Mougel, J., Alvarez, O. 2006. Physical properties of non stable gel emulsions with non ionic surfactant. *Proceedings of the 4th Congress on Emulsion. Lyon,* France. *Abstract* 281.

Barnea, E. & Mazrahi, J. 1973. Generalized approach to the fluid dynamics of particulate systems. – 1. General correlation for fluidization and sedimentation in solid multiphase systems. *Chem. Eng. J. and Biochem. Eng. J.*, 5:171–189.

Barnes, H.A. 1989. Shear-thickening ("Dilatancy") in suspensions of nonaggregating solid particles dispersed in Newtonian liquids. *J. Rheol.*, 33:329–366.

Barnes, H.A. 1994. Rheology of Emulsions – a Review. Colloids Surf, 91:89–95.

Barnes, H.A. 1995. A review of the slip (wall depletion) of polymer solutions, emulsions and particle suspensions in viscometers: its cause, character, and cure. *J. Non-Newtonian Fluid Mech.*, 56:221–251.

Barry, B.W. 1975. Viscoelastic properties of concentrated emulsions. *Adv. Colloid Interface Sci.*, 5:37–75.

Barthes-Biesel, D. & Acrivos, A. 1973. The rheology of suspensions and its relations on phenomenological theories for non-Newtonian fluids. *Int. J. Multiphase Flow*, 1.

Becher, P. 1965. *Emulsions: theory and practice.* 2nd edition. New York: Reinhold.

Becher, P. 1983. *Encyclopedia of Emulsion Technology.* New York: Marcel Dekker. vol. 1

Becher, P. 1988. *Encyclopedia of Emulsion Technology.* New York: Marcel Dekker, Inc. and Basel, vol. 3.

Benali, L. 1993. Rheological and granulometrical studies of a cutting oil emulsion. I. The effect of oil concentration. *J. Colloid Interface Sci.*, 156:454–461.

Bengtsson, L.A., Frostemark, F. & Holmberg, B. 1994. Speciation, structural characteristics and proton dynamics in the systems NH_4NO_3. $1.5H_2O$ and NH_4NO_3 . $1.5H_2O$-(HNO_3, NH_4F, NH_3)-H_2O at 50 $^{\circ}C$. *J. Chem. Soc. Faraday Trans.*, 90(4):59–570.

Bengoechea, C., Cordobés, F. & Guerrero, A. 2006. Rheology and microstructure of gluten and soya-based o/w emulsions. *Rheol. Acta* 46:3–21.

Bentley, B.J. & Leal, L.G. 1986. Experimental investigation of drop deformation and break up in steady, two-dimensional linear flow. *J. Fluid Mech.*, 167:241–283.

Bergenstahl, G. 1997. Physiochemical aspects of an emulsifier functionality, in *Food Emulsifiers and Their Applications.* Eds. New York: Chapman & Hall.

Bibette, J. 1992. Stability of thin film in concentrated emulsions. *Langmuir*,8:3178–3182.

Bibette, J., Leal-Calderon, F., Poulin, P. 1999. Emulsions: basic principles. *Rep. Prog. Phys.*, 62:969–1033.

Bikerman, J.J. 1973. *Foams.* New York: Springer.

Binet, R., Cloutier, J.A.R., Edmonds, A.C.F., Holden, N.W. & McNickol, M.A. 1982. US Patent, 4, 357, 184.

Bird, R.B., Armstrong, R.C. & Hassager, O. 1987. *Dynamic Liquids.* New York: Willey.

Boeyens, J.C.A., Ferg, E., Levendis, D.C., Schoning, F.R.L. 1991. X-ray diffraction analysis of the ammonium nitrate IV-III-II and IV-II Phase changes under controlled humidity conditions. *S. Afr. J. Chem.*, 42- 44

Bousmina, M. 1999. Rheology of polymer blends: linear model for viscoelastic emulsions. *Rheol. Acta*, 38:73–83.

Bousmina, M. & Muller, M. 1993. Linear viscoelasticity in the melt of impact PMMA. Influence of concentration and aggregation of dispersed rubber particles. *J. Rheol.*, 37:663–679.

Bousmina, M., Bataille, P., Sapieha, S. & Schreiber, H.P. 1995. Comparing the effect of corona treatment and block copolymer addition on rheological properties of polystyrene/polyethylene blends. *J. Rheol.*, 39: 499–517.

Bower, C., Gallegos, C., Macley, M.R. & Madiedo, J.M. 1999. The rheological and microstructural characterization of the non-linear flow behaviour of concentrated oil-in-water emulsions. *Rheol. Acta*, 38: 145-159.

Brahimi, B., Ait-kadi, A., Ajji, A., Jerome, R. & Fayt, R. 1991. Rheological properties of copolymer modified polyethylene/polystyrene blends. *J. Rheol.*, 35:1069–1091.

Bressy, L., Hebraud, P., Schmitt, V. & Bibette, J. 2003. Rheology of emulsions stabilized by solid interface. *Langmuir,* 19:598–604.

Brown, R.N. & McLaren, A.C. 1961. On the Mechanism of the Thermal Transformations in Solid Ammonium Nitrate. *Proc. R. Soc.,* 266:329.

Buzza, D.M.A., Cates, M.E, 1994. Uniaxial elastic modulus of concentrated emulsions. *Langmuir*, 10:4503–4508.

Celli, A., Zanotto, E.D. & Avramov, I. 2003. Primary crystal nucleation and growth regime transition in isotactic polypropylene. *J. Macromolecular Sci.*, part B – Physics, 42:387–401.

Chabra, R.P. & Richardson, J.F. 1999. *Non-Newtonian flow in the process industries.* Oxford: Butterworth Heinemann.

Choi, S.J. & Schowalter, W.R. 1975. Rheological properties of nondilute suspensions of deformable particles. *Phys. Fluids*, 18:420.

Clarke, N. & Mc Leigh, T.C.B. 1998. Shear flow effects on phase separation of entangled polymer blends. *Rhys. Rev. E*, 57:3731–3734.

Clasen, C.H. & Mc Kinley, G.H. 2004. Gap-dependent micrometry of complex liquids. *J. non-Newt. Fluid Mech.*, 124:1–10.

Cross, M.M. 1965. Rheology of non-Newtonian fluids: a new flow equation for pseudoplastic systems. *J. Colloid Sci.*, 20:417–437.

Davis, H.T. 1994. Factors determining emulsion type: Hydrophile-lipophile balance and beyond. *Colloids and Surfaces A: Physicochemical and Engineering Aspects*, 91:9.

Defay, R. & Petre, G. 1979. Dynamic surface tension. In Matijevie (Ed.). *Surface & Colloid Sci.*, 3. New York: Wiley.

Delaby, I., Ernst, B., Germain, Y. & Muller, R. 1994. Droplet deformation in polymer blends during uniaxial elongation flow. Influence of viscosity ratio for large capillary number. *J. Rheol.*, 38:1705–1720.

Dickinson, E. 1992. *Introduction to Food Colloids.* Oxford: Oxford University Press.

Dickinson, E. 1989. Food colloids – an overview. *Colloids Surface*, 42:191–204.

Dickinson, E. & McClements, D.J. 1995. *Advances in Food Colloids*. London: Chapman & Hall.

Dimitrova, T.D. & Leal-Calderon, F. 2001. Bulk elasticity of concentrated protein-stabilized emulsions. *Langmuir*, 17(11):3235–3244.

Dimitrova, T.D. & Leal-Calderon, F. 2004. Rheological properties of highly concentrated protein-stabilized emulsions. *Advances in Colloid & Interface Science,* 108–109:49–61.

Doxsee, K.M. & Francis, P.E. 2000. Crystallization of ammonium nitrate from nonaqueous solvents. *Ind. Eng. Chem. Res.,* 39:3493–3498.

Edwards, D.A. & Wasan, D.T. 1988. Surface rheology. I. The planar fluid surface. *J. Rheology*, 32:429–455.

Edwards, D.A., Brenner, H., Wasan, D.T. 1991. *Interfacial Transport Process and Rheology*. Boston, MA: Butterworth-Heinemann, p. 558.

Einstein, A. 1906. Investigations on the theory of the Brownian movement. New York: Dover.

Escalante, J.I. & Hoffmann, H. 2000. Non-linear rheology and flow induced transition to a lamellar-to-vesicle phase in ternary systems of alkyldimethyl oxide/alcohol/water. *Rheol. Acta*, 39:209–214.

Ferg, E.E., Levendis, D. & Schoening, F.R.L. 1993. X-ray diffraction study of the orientational relation between the IV and III phases of ammonium nitrate. *Chem. Mater.*, 5:1293–1298.

Fernández, M., Muñoz, M.E. & Santamaria, A. 1998. Rheological analysis of highly pigmented inks: Flocculation at high temperatures. *J. Rheol.*, 42:239–253.

Ferry, J.D. 1980. Viscoelastic properties of polymers. New York: Wiley.

Finkle, P., Draper, H.P. & Hildebrand, J.H. 1923. The theory of emulsification. *J. Am. Chem. Soc.*, 45:2780–2788.

Fischer, E.K. & Harkins, W.D. 1932. Monomolecular films. The liquid-liquid interface and the stability of emulsions. *J. Phys. Chem.*, 36:98–110.

Franco, J.M., Berjano, M. & Gallegos, C. 1997. Linear viscoelasticity of salad dressing emulsions. *J. Agric. Food Chem.*, 45:713–719.

Franco, J.M., Guerrero, A. & Gallegos, C. 1995. Rheology and processing of salad dressing emulsions. *Rheol. Acta*, 34:513–524.

Frankel, N.A. & Acrivos, A. 1970. The constitutive equation for a dilute emulsion. *J. Fluid. Mech.*, 44:65–78.

Fredrich, CH., Gleinser, W., Korat, E., Maier, D. & Weese, J. 1995. Comparison of sphere size distribution obtained from rheology and transmission electron microscopy in PMMA/PS blends. *J. Rheol.*, 39:1411–1425.

Fredrickson, A.G. 1964. *Principles and Applications of Rheology*. New Jersey: Prentice-Hall.

Friberg, S.E., Christenson, H., Bertrand, G. & Larsen, P.W. 1984. *In reverse micelles: Biological and technological relevance of amphiphilic structures in apolar media*. New York: Plenum Press. p.105.

Gaicha, L., Leblanc, R.M., Villamagna, F.& Chattopadhyay, A.K. 1995. Monolayers of mixed surfactants at the oil-water interface, hydrophobic interactions, and stability of water-in-oil emulsions. *Langmuir*, 11:585–590.

Ganguly, S., Krishna, V.M., Bhasu, V.C.J., Mathews, E., Adiseshaiah, K.S. & Kumar, A.S. 1992. Surfactant-electrolyte interactions in concentrated water-in-oil emulsions: FT-IR spectroscopic and low-temperature differential scanning calorimetric studies. *Colloids and surfaces*, 65:243–256.

Gao, Y.L., Shen, J., Sun, J.F., Wang, G., Xing, D.W., Xian, H.Z. & Zhou, B.D. 2003. Crystallization behaviour of ZrAlNiCu bulk metallic glass with wide supercooled liquid region. *Materials Letters*, 57:1894–1898.

Germain, Y., Ernst, B., Genelot, O. & Dhamani, L. 1994. Rheological and morphological analysis of compatibilized PP/PA blends. *J. Rheol.*, 38:681–697.

Gibbs, J.W. 1931. Collected Works, vol. 1. New York: Longmans Green & Co.

Grace, H.P. 1982. Dispersion phenomena in high viscosity immiscible fluid systems and application of static mixers as dispersion device in such systems. *Chem. Eng. Commun.*, 14:225–277.

Graebling, D., Muller, R. 1990. Rheological behaviour of polydimethylsiloxane/ poly-oxyethylene blend in the melt. Emulsion model of two viscoelastic liquids. *J. Rheol.*, 34:193–205.

Graebling, D., Benkira, A., Gallot, Y. & Muller, R. 1994. Dynamic viscoelastic behaviour of polymer blends in the melt. Experimental results for PDMS-POE, PS/PMMA and PS/PEMA blends. *Eyr Polym. J.*, 30:301–308.

Graebling, D., Muller, R. & Palierne, J.F. 1993. Linear viscoelastic behaviour of some incompatible polymer blends in the melt. Interpretation of data with a model of emulsion of viscoelastic liquids. *Macromolecules*, 26:320–329.

Grassi, M., Lapasin, R. & Pricl, S. 1996. A study of the rheological behaviour of scleroglucan weak gel systems. *Carbohydrate Polymers*, 29:169–181.

Guerrero, A., Partal, P., Berjano, M. & Gallegos, C. 1996. Linear viscoelasticity of o/w sucrose palmitate emulsions. *Prog. Colloid Polym. Sci.*, 100:246–251.

Guerrero, A., Partal, P. & Gallegos, C. 1998. Linear viscoelastic properties of sucrose ester-stabilized oil-in-water emulsions. *J. Rheol.*, 42:1375–1388.

Hackley, V.A. & Ferraris, C.F. 2001. *Guide to Rheological Nomenclature: Measurements in Ceramic Particulate Systems.* National Institute of Standards and Technology, Special Publication 949.

Harkins, W.D. 1952. *The physical chemistry of surface films*. New York: Reinhold Publishing Corp. 83–91.

Harzallah, O.A. & Dupuis, D. 2003. Rheological properties of suspensions of TiO_2 particles in polymer solutions. I. Shear viscosity. *Rheol. Acta*, 42:10–19.

Hemar, Y., Hocquart, R. & Lequeux, F. 1995. Effect of interfacial rheology on foams viscoelasticity, an effective medium approach. *J. Phys. II France* 5:1567–1576.

Hemar, Y. & Horne, D.S. 2000. Dynamic rheological properties of highly concentrated protein-stabilized emulsions. *Langmuir*, 16:3050–3057.

Hendricks, S.B., Posnjak, E. & Kracek, F.C. 1932. Molecular rotation in the solid state. The variation of the crystal structure of ammonium nitrate with temperature. *J. Am. Chem. Soc.*, 54:2766.

Hiemenz, P.C. 1986. *Principles of Colloids and Surface Chemistry*. 2nd edition. New York: Marcel Dekker.

Hiemenz, P.C. & Rajagopalan, R. 1997. *Principles of colloid and surface chemistry*. New York: Marcel Dekker.

Hoffman, R.L. 1992. Factors affecting the viscosity of unimodal and multimodal colloidal dispersions. *J. Rheol.*, 36:947–965.

Hugelshofer, D., Windhab, E.J. & Wang, J. 2000. Rheological and structural changes during the mixing of suspensions and emulsions. *Applied Rheol.*, 10:22-30.

Humphrey, F.J. & Hatherly, M. 1996. *Recrystallization and related annealing phenomena*. New York: Pergamon.

Hunter, R.J. 1993. *Introduction to Modern Colloid Sc*ience. Oxford: Oxford University Press.

Ikeda, Y., Inoae, A., Tanabe, Y., Airki, T. 1983. US Patent, 4, 386, 977.

Israelachvili, J. N. 1992. *Intermolecular and Surface Forces.* London: Academic Press.

Jager-Lézer, N., Tranchant, J.-F., Alard, V., Vu, C., Tchoreloff, P.C., Grossiord, J.-L. 1998. Rheological analysis of highly concentrated w/o emulsions. *Rheol. Acta*, 37:129–138.

Janssen, J.J.M., Boon, A. & Agterof, W.G.M. 1994. Influence of dynamic interfacial properties on droplet breakup in simple shear flocs. *Fluid Mechanics & Transport Phenomena,* 40:1929–1939.

Jeffrey, D.J. & Acrivos, A. 1976. The rheological properties of suspensions of rigid particles. *AIChE J*, 22: 417–432.

Kabalnov, A.S. & Shchukin, E.D. 1992. Ostwald ripening theory: Applications to fluorocarbon emulsion stability. *Advances in Colloid and Interface Science*, 38:69–97.

Kabalnov, A.S. & Wennerstrom, H. 1996. Macroemulsion stability: The orientated wedge theory revisited. *Langmuir*, 12:276

Kakudo, M. & Kasai, N. 1972. *X-ray diffraction by polymers*. Tokyo: Kodansha scientific books.

Kanai, A. & Amari, T. 1995. Negative thixotropy in ferric-oxide suspensions, *Rheol. Acta*, 34:303–310.

Karbstein, H. & Schubert, H. 1995. Developments in the continuous mechanical production of oil-in-water macro-emulsions. *Chemical Engineering and Processing*, 34:205–211.

Khan, S.A. & Armstrong, R.G. 1986. Rheology of foam. I. Theory for dry foams. *J. non-Newt. Fluid Mech.*, 22:1-22.

Khan, S.A. & Armstrong, R.G. 1987. Rheology of foam. II. Effect of polydispersity and liquid viscosity for foams having gas fraction approaching unity. *J. Non-Newt. Fluid Mech.*, 25:61–92.

Kharatiyan, E. 2005. Time effects in evolution of structure and rheology of highly concentrated emulsions. Unpublished DTech thesis, Cape Peninsula University of Technology, Cape Town, South Africa.

Kim, Y-H., Koczo, K. & Wasan, D.T. 1997. Dynamic film and interfacial tensions in emulsion and foam systems. *J. Colloid and Int. Sci.*, 187:29–44.

Kirby, I.J. 1983. Internal ICI reports, 1980.

Kozicki, W. & Kaung, P.Q. 1993. Prediction of lower/upper limiting viscosities. Canadian *J. of Chem. Eng.*, 71:329–331.

Kraynik, A.M. & Hansen, M.G. 1986. Foam and emulsion rheology. A quasistatic model for large deformations of spatially-periodic cells. *J. Rheol*, 30:409–439.

Lacasse, M.D., Grest, G.S. & Levine, D. 1996. Deformation of Small Compressed Droplets. *Phys. Rev. E*, 54:5436–5446.

Lacroix, C., Bousmina, M., Carreau, P.J., Favis, B.D. & Michel, A. 1996. Properties of PETG/EVA blends: Viscoelastic, morphological and interfacial properties, Part I. *Polymer*, 37:2939–2947.

Langenfeld, A., Schmitt, V. & Stebe, M.J. 1999. Rheological behaviour of fluorinated highly concentrated reverse emulsions with temperature. *J. Colloid & Interface Sci.*, 218:522–528.

Lapasin, R., Grassi, M. & Coceani, N. 2001. Effect of polymer addition on the rheology of o/w microemulsions. *Rheol. Acta*, 40:185–192.

Larson, R.G. 1999. *The structure and rheology of complex fluids*. New York: Oxford University Press.

Laughlin, R.G. & Brown, G.H. 1978. *Advances in liquid crystals*. New York: Academic Press.

Leal-Calderon, F., Gerhardi, B., Espert, A., Brossard, F., Alard, V., Tranchant, J.F., Stora, T. & Bibette, J. 1996. Aggregation Phenomena in Water-in-Oil Emulsions. *Langmuir*, 12:872–874.

Lee, S.J. 2006. Emulsion rheology and properties of polymerized high internal phase emulsions. *Korea-Australia Rheol. J.* 18:183–189.

Lissant, K.J. 1966. The geometry of high-internal-phase-ratio emulsions. *J. Colloid Interface Sci.* 22:462–468.

Lissant, K.J. 1970. Concentrated emulsions. 2. Effect of the interdroplet film thickness on droplet size and distortion in mono- and bidisperse face centered cubic packings *J. Soc. Cosmet. Chem.*, 21:141.

Lissant, K.J. 1974. *Emulsion and Emulsion Technology*. Part 1, p. 103, New York: Dekker.

Lissant, K.J. & Mayhan, K.G. 1973. A study of medium and high internal phase ratio water/polymer emulsions. *J. Colloid Interface Sci.*, 42:201–208.

Lissant, K.J., Peace, B.W., Wu, S.H. & Mayhan, K.G. 1974. Structure of high-internal-phase-ratio emulsions. *J. Colloid Interface Sci.*, 47:416–423.

Loewenberg, M. & Hinch, E.J. 1996. Numerical simulation of a concentrated emulsion in shear flow. *J. Fluid Mech.*, 321:395–419.

Loewenberg, M. 1998. Numerical simulation of concentrated emulsion flows. *J. Fluid Eng., Transaction of the ASME*, 120:824–831.

Loncin, M. & Merson, R.L. 1979. *Food Engineering: Principles and Selected Applications.* New York: Academic Press.

Lucassen-Reyanders, E.H. & Kuijpers, K.A. 1992. The role of interfacial properties in emulsification. *Colloids & Surfaces,* 65:175–184.

Macosko, C.W. 1994. *Rheology: Principles, Measurements and Applications*, New York: VCH Publishers.

Madiedo, J.M. & Gallegos, C. 1997. Rheological characterization of oil-in-water emulsions by means of relaxation and retardation spectra. Recent Res. *Dev. Oil Chem.*, 1:79–90.

Malkin, A. Ya. 1994. *Rheology Fundamentals.* ChemTac Publishing, Canada.

Malkin, A. Ya. & Kulichikhin, S.G. 1996. Phase transitions in polymer systems in mechanical fields. *Vysokomol. Soedin. B (Polymers – in Russian)* 38:362–374.

Malkin, A. Ya., Kulichikhin, S.G. & Shambilova, G.K. 1991. Influence of deformation on the phase state of poly(vinyl acetate) solutions. *Vysokomol. Soedin, B (Polymers – in Russian)*, 33:228–231.

Malkin, A. Ya. & Masalova, I. 2007. Shear and normal stresses in flow of highly concentrated emulsions. *J. Non-Newtonian Fluid Mech.,* 147:65–68.

Malkin, A. Ya., Masalova, I., Slatter, P. & Wilson, K. 2004a. Effect of droplet size on the rheological properties of highly-concentrated w/o emulsions. *Rheol. Acta*, 43:584–591.

Malkin, A. Ya., Masalova, I., Pavlovski, D. & Slatter, P. 2004b. Is the choice of flow curve fitting equation crucial for the estimation of pumping characteristics? *Applied Rheol.*, 14/2:89–95.

Magid, L. J. & Martin, C. A. *In reverse micelles: Biological and technical relevance of amphiphilic structures in apolar media.* New York: Plenum Press. p.181.

Manca, S., Lapasin, R., Partal, P. & Gallegos, C. 2001. Influence of surfactant addition on the rheological properties of aqueous Welan matrices. *Rheol. Acta*, 40:128–134.

Marcovich, N.E., Reboredo, M.M., Kenny, J. & Aranguren, M.I. 2004. Rheology of particle suspensions in viscoelastic media. Wood flour-polypropylene melt. *Rheol. Acta*, 43:293–303.

Masalova, I., Malkin, A.Y. 2007a. Peculiarities of rheological properties and flow of highly concentrated emulsions: The role of concentration and droplet size. *Colloid Journal,* 69(2):185–197.

Masalova, I., Malkin, A.Y. 2007b. A new mechanism of aging of highly concentrated emulsions: correlation between crystallization and plasticity. *Colloid Journal,* 69(2):198–202.

Masalova, I., Malkin, A.Y. 2007c. Rheology of highly concentrated emulsions - Concentration and droplet size dependencies. *Appl. Rheol.*, 17(4):1–9.

Masalova, I., Malkin, A.Y. 2008. Master curves for elastic and plastic properties of highly concentrated emulsions. *Colloid Journal,* 70(3):327–336.

Masalova, I., Malkin, A. Ya, Ferg, E., Taylor, M., Kharatiyan, E. & Haldenwang, R. 2006. Evolution of rheological properties of highly concentrated emulsions with aging—Emulsion-to-suspension transition. *J. Rheol.,* 50(4):435–451.

Masalova, I., Malkin, A.Y., Slatter, P. & Wilson, K. 2003a. The rheological characterization and pipeline flow of high concentration water-in-oil emulsions. *J. Non-Newtonian Fluid Mech.*, 112:101–114.

Masalova, I., Malkin, A.Y. & Slatter, P. 2003b. Effect of droplet size on the rheological properties of super-concentrated emulsions. *Proc. First Annual Rheology Conference, Guimaraes (Portugal).*

Mason, T.G. 1999. New fundamental concepts in emulsion rheology. *Current Opinion in Colloid & Interface Sci.*, 4:231–238.

Mason, T.G., Bibette, J. & Weitz, D.A. 1995. Elasticity of compressed emulsions. *Phys. Rev. Lett.*, 75(10):2051–2054.

Mason, T.G., Bibette, J. & Weitz, D.A. 1996. Yielding and flow of monodisperse emulsions. *J. Colloid Int. Sci.*, 179:439–448.

Mason, T.G., Lacasse, M.-D., Grest, G.S., Levine, D., Bibette, J. , Weitz, D.A. 1997. Osmotic pressure and viscoelastic shear moduli of concentrated emulsions. *Phys. Rev.* E: 56(3):3150–3166.

Matsumoto, T., Segawa, Y., Warashina, Y. & Onogi, S. 1973. Nonlinear behaviour of viscoelastic materials. II. The method of analysis and temperature dependence of nonlinear viscoelastic functions. *Trans. Soc. Rheol.*, 17:47.

Mc Clements, D.J. 1999. *Food Emulsion: Principles, Practice, and Techniques.* New York: CRC Press LLC.

Mc Clements, D.J. 2005. *Food Emulsion: Principles, Practice, and Techniques.* New York: CRC Press LLC

Meeker, S.P., Bonnelaze, R.T. & Cloitre, M. 2004. Slip and flow in pastes of soft particles: Direct observation and rheology. *J. Rheol.*, 48:1295–1320.

Metzner, A.B. & Whitlock, M. 1958. Flow behaviour of concentrated suspensions. *Trans. Soc. Rheol.*, 2:239–254.

Mewis, J. & Macosko, C.W. 1994. Suspension rheology, in C.W. Macosko (Ed.). *Rheology: Principles, Measurements and Applications.* New York: VCH Publishers. Chap. 10.

Michaels, M.A. 2006. *Quantitative model for the prediction of hydrodynamic size of nonionic reverse micelles.* Master's thesis, Virginia Commonwealth University, Virginia, USA.

Michaels, A.S. & Bolger, J.C. 1962. The plastic flow behaviour of flocculated kaolin suspensions. *Ind. Eng. Chem. Fundam.*, 1:153–162.

Minale, M., Wissbrun, K.F. & Massouda, D.F. 2003. Two-fluid demixing theory predictions of stress-induced turbidity of polystyrene solutions in dioctyl phthalate. *J. Rheol.*, 47:1–17.

Mittal, K.L. 1975. (Ed.). Ch. 4 in *Colloidal Dispersions and Micellar Behaviour*, ACS Symposium Series, No. 9, p. 76.

Myers, D. 1992. *Surfactant science and technology.* 2nd edition, New York: VCH Publishers, Inc.

Nippon oils & Fats K.K. 1980. Japanese Patent, 55/75, 995.

Nixon, J. & Beerbower, A. 1969. *Amer. Chem. Soc. Div. Petrol. Chem. Prepr.*, 14(1), 49, 62.

Oldroyd, J.G. 1953. The elastic and viscous properties of emulsions and suspensions. *Proc. Roy. Soc.* A, 218:122.

Oldroyd, J.G. 1959. Complicated Rheological Properties. In C.C. Mill, (Ed.). *Rheology of Dispersed Systems.* London: Pergamon.

Oommen, C. & Jain, S.R. 1999. Ammonium nitrate: a promising rocket propellant oxidizer. *J. Hazardous materials*, 6(3):253–281.

Otsobo, Y. & Prud'homme, R.K. 1994a. Rheology of oil-in-water emulsions. *Rheol. Acta*, 33: 29–37.
Otsobo, Y. & Prud'homme, R.K. 1994b. Effect of drop size distribution on the flow behaviour of oil-in-water emulsions. *Rheologica Acta*, 33:303–306.

Pal, R. 1990. On the flow characteristics of highly concentrated oil-in-water emulsions, *Chem. Eng. J.*, 43:53–57.

Pal, R. 1996a. Rheology of emulsions containing polymeric liquids. In P. Becher (Ed.). *Encyclopedia of Emulsion Technology*. New York: Marcel Dekker. 93–293.

Pal, R. 1996b. Effect of droplet size on the rheology of emulsions. *AIChE J.*, 42:3181–3190.

Pal, R. 1997. Scaling of relative viscosity of emulsions, *J. Rheol.*, 41:141–150.

Pal, R. 1999. Anomalous wall effects in parallel plate torsional flow of highly concentrated emulsions. *ASME FED*, 249:137–150.

Pal, R. 2000a. Slippage during the flow of emulsions in rheometers. *Colloids Surf*, 162:55–66.

Pal, R. 2000b. Linear viscoelastic behaviour of multiphase dispersions. *J. Colloid Interface Sci.*, 232:50–63.

Pal, R. 2001. Novel viscosity equations for emulsions of two immiscible liquids. *J. Rheol.*, 45: 509–520.

Pal, R. 2006. Rheology of high internal phase ratio emulsions. *Food Hydrocolloid.* 20:997–1005.

Palierne, J.P. 1990. Linear rheology of viscoelastic emulsions with interfacial tension. *Rheol. Acta*, 29:204–214.

Partal, P., Guerrero, A., Berjano, M. & Gallegos, C. 1997. Influence of concentration and temperature on the flow behaviour of oil-in-water emulsions stabilized by sucrose palmitate. *JAOCS*, 74:1203–1212.

Perrin, P. 2000. Droplet-droplet interactions in both direct and inverse emulsions stabilized by a balanced amphiphilic polyelectrolyte. *Langmuir*, 16(3):881–884.

Pons, R., Erra, P., Solans, C., Ravey, J.C. & Stebe, M.J. 1992b. Viscoelastic properties of gel-emulsions their relationship with structure and equilibrium properties. *J. Phys. Chem.* 97:12320–12335.

Pons, R., Solans, C., Stébé, M.J., Erra, P. & Ravey, J.C. 1992a. Stability and rheological properties of gel emulsions. *Prog. Colloid Polym. Sci.,* 89:110–113.

Pons, R., Solans, C. & Tadros, T.F. 1995. Rheological behaviour of highly concentrated oil-in-water (o/w) emulsions. *Langmuir*, 11:1966–1971.

Ponton, A., Clement, P. & Grossiord, J.L. 2001. Corroboration of Princen's theory to cosmetic concentrated water-in-oil emulsions. *J. Rheol.* 45:521–526.

Powder Diffraction File Release-2002, Intern Centre for Diffraction Data. Pennsylvania USA.
Princen, H.M. 1979. Highly Concentrated Emulsions: I. Cylindrical Systems. *J. Colloid and Interface Sci.*, 71:55–66.

Princen, H.M. 1983. Rheology of foams and highly concentrated emulsions. I. Elastic properties and yield stress of a cylindrical modes system. J. *Colloid & Interface Sci.,* 91:160–175.

Princen, H.M. 1985. Rheology of foams and highly concentrated emulsions. II. Experimental study of the yield stress and wall effects for concentrated oil-in-water emulsions. *J. Colloid Interface Sci.*, 105:150–171.

Princen, H.M. 1988. Pressure/volume/surface area relationships in foams and highly concentrated emulsions: Role of volume fraction. *Langmuir*, 4:164–169.

Princen, H.M., Aronson, M.P. & Moser, J.C. 1980. Highly Concentrated Emulsions: II. Real Systems. The Effect of Film Thickness and Contact Angle on the Volume Fraction in Creamed emulsions. *J. Colloid and Interface Sci.*, 75:246–271.

Princen, H.M. & Kiss, A.D. 1986a. Rheology of foams and highly concentrated emulsions. III Static shear modulus. *J. Colloid & Interface Sci.*, 112:427–437.

Princen, H.M. & Kiss, A.D. 1986b. Rheology of foams and highly concentrated emulsions. IV. An experimental study of the shear viscosity and yield stress of concentrated emulsions. *J. Colloid & Interface Sci.,* 128:176–187.

Princen, H.M. & Kiss, A.D. 1989. Rheology of foams and highly concentrated emulsions. IV. An experimental study of the shear viscosity and yield stress of concentrated emulsions. *J. Colloid & Interface Sci.*, 128:176–187.

Quemada, D. 1985. Phenomenological rheology of concentrated dispersions. *J. Theoretical Appl. Mech., special number*: 289–301.

Quemada, D., Berli, C. 2002. Energy of interaction in colloids and its implications in rheological modeling. *Adv. Colloid Interface Sci.* 98:51–85.

Quintero, G.C., Noïk, C., Dalmazzone, C. & Grossiord, L.J. 2008. Modelling and characterisation of diluted and concentrated water-in-crude oil emulsions: comparison with classical behaviour. *Rheol. Acta,* 47:417–424.

Rallison, J.M. 1980. Note on the time-dependent deformation of a viscous drop which is almost spherical. *J. Fluid Mech.*, 98:625–633.

Rangel-Nafaile, C., Metzner, A.B. & Wissbrun, K.F. 1984. Analysis of stress-induced phase separations in polymer solutions. *Macromolecules*, 17:1187–1195.

Reinelt, D.A. & Kraynik, A.M. 1989. Viscous effects in the rheology of foams and concentrated emulsions. *J. Colloid Int. Sci.*, 132:491–503.

Reinelt, D.A. & Kraynik, A.M. 1990. On the shearing flow of foams and concentrated emulsions. *J. Fluid Mech.*, 215:431–455.

Reinelt, D.A. & Kraynik, A.M. 1993. Large elastic deformations of three-dimensional foams and highly concentrated water-in-oil emulsions (gel emulsions). *J. Colloid Interface Sci.*, 159: 460–470.

Reiner, M. & Blair, S.D.W. 1967. In F.R. Eirich (Ed.). *Rheology. Theory and Applications*. NY-London: Acad. Press, vol. 4, Ch. 9.

Reynolds, A.P., Gilbert, P.E. & White, W.J. 2000. High internal phase water-in-oil emulsions studied by small-angle-scattering. *J. Phys. Chem. B,* 104:7012–702.

Reynolds, P.A., Gilbert, P.E. & White, W.J. 2001. High Internal Phase Water-in-Oil Emulsions and related Microemulsions Studied by Small Angle Neutron Scattering. *J. Phys. Chem. B*, 105:6925–6932.

Reynolds, P.A., Mc Gillivray, D.J., Gilbert, P.E. Holt, S.A., Henderson, M.J. & White, W.J. 2003. Neutron and X-ray reflectivity from Polyisobutylene-Based amphiphiles at the air-water Interface. *Langmuir,* 19:752–761.

Reynolds, P.A., Zank, J., Jackson, A.J., Baranyai, K.J., Perriman, A.W., Barker, J.G. & White, W.J. 2006. Aggregation in a high internal phase emulsion observed by SANS and USANS. *Physica B* 385–386:776–779.

Richardson, E.G. 1933. Uber die Viskositat von Emulsionen. *Kolloid-Z.*, 65:32–37.

Richardson, E.G. 1950. The formation and flow of emulsions. *J. Colloid Sci.*, 5:404–413.

Rocca, S. & Stebe, M.J. 2000. Mixed concentrated water-in-oil emulsions (fluorinated/hydrogenated): formulation, properties, and structural studies. *J. Phys. Chem.* B, 104:10490–10497.

Rosen, M.J. 1978. *Surfactants and Interfacial Phenomena* New York: Wiley-Interscience Publishers.

Rumscheidt, F.D. & Mason, S.G. 1961a. Particle motions in sheared suspensions. XI. Internal circulation in fluid droplets (experimental). *J. Colloid Interface Sci.*, 16:210–237.

Rumscheidt, F.D. & Mason, S.G. 1961b. Particle motions in sheared suspensions. XII. Deformation and burst of fluid drops in shear and hyperbolic flow. *J. Colloid Interface Sci.*, 16:238–261.

Sánchez, M.C., Berjano, M., Brito, E., Guerrero, A., Gallegos, C. 1998. Evolution of the microstructure and rheology of o/w emulsions during the emulsification process. *Can. J. Chem. Eng.*, 76:479–485.

Saint-Jalmes, A. & Durian, D.J. 1999. Vanishing elasticity for wet foams: Equivalence with emulsions and role of polydispersity. *J. Rheol.*, 43:1411–1422.

Saleeb, F.Z. & Kitchener, J.A. 1964. Fourth Int. Congress on Surface Activity, Brussels.
Schlaepfer, A.U.M. 1918. *J. Chem. Soc.*, 113:522.

Schubert, H. & Armbtuster, H. 1992. Principles of formation and stability of emulsions. *International Chemical Engineering*, 32:14.

Shen, Y. & Duhamel, J. 2008. Micellisation and adsorption of a series of succinimide dispersants. Langmuir, 24: 10665–10673.

Schulman, J.H. & Cockbain, E.G. 1940. *Trans. Faraday Soc.*, 36:651.

Sheng, Y.J. & Tsao, H.K. 2004. Electrostatic attraction between neutral microdroplets by ion fluctuations . *Phys. Rev.* E 69, 060401.

Sherman, P. (Ed.). 1968. *Emulsion Science*. London: Academic Press.

Sherman, P. 1970. *Industrial Rheology with Particular Reference to Foods, Pharmaceuticals and Cosmetics*. London: Academic Press.

Shinnaka, Y. 1956. On the metastable transition and crystal structure of ammonium nitrate. *J. Phys. Soc. Japan*, 11:393.

Shinoda, K. & Friberg, S. 1986. *Emulsions and Solubilization*. New York: John Wiley & Sons.

Shinoda, K. & Kunieda, H. 1983. Phase properties of emulsions: PIT and HLB. In P. Becher (Ed.). *Encyclopedia of Emulsion Technology* Vol.1. New York: Marcel Dekker.

Slatter, P.T. 1999. The role of rheology in the pipelining of mineral slurries. *Min. Pro. Ext. Met. Rev.*, 20:281–300.

Slatter, P.T. 2002. Non-Newtonian Laminar Pipe Flow – A place in the sun at last! Invited keynote address – *11th International Conference on transport and sedimentation of solid Particles – Ghent*. 33–40.

Slatter, P.T. & Wasp, E.J. 2002. Yield stress – How low can you go? *11th International Conference on transport and sedimentation of solid Particles – Ghent*, 173–182.

Soltero, J.F.A., Robles-Vasquez, O., Puig. J.E. & Manero, O. 1995. Note: Thixotropic-antithixotropic behavior of surfactant-based lamellar liquid crystals under shear flows. *J. Rheol.*, 39:235–240.

Stone, H.A. 1994. Dynamics of drop deformation and breakup in viscous fluids. *Annual Review of Fluid Mechanics*, 26:65–102.

Schwartz, L.W. & Princen, H.M. 1987. A theory of extensional viscosity for flowing foams and concentrated emulsions. *J. Colloid Interface Sci.*, 118(1):201–211.

Tadros, T.F. 1994. Fundamental principles of emulsion rheology and their applications. *Colloids and Surface A, Physical and Engineering aspects*, 91:39–55.

Tanner, R. 2000. *Engineering rheology*, 2nd Edition. New York: Oxford University Press.

Tsao, H.K., Sheng, Y.J. & Chen, S.B. 2002. Electrostatic interaction between two aqueous microdroplets in an apolar medium. *Phys. Rev. E* 65, 061403.

Taylor, G.I. 1932. The Viscosity of a Fluid Containing Small Drops of Another Fluid *Proc. R. Soc. Lond. A,* 138:41–48.

Taylor, G.I. 1934. The Formation of Emulsions in Definable Fields of Flow. *Proc. R. Soc. Lond. A*, 146:501–523.

Taylor, G.I. 1964. Polymers melt devolatilization. *Proceedings of the 11th International Congress on Applied Mechanics*–Munich, 790–796.

Thomas, C.S. & Halou, O.M. 2003. Explosive emulsion compositions containing modified copolymers of isoprene, butadiene, and/or styrene. US patent. Pub. No. WO/2003/002487

Torza, S., Cox, R.G. & Mason, S.G. 1972. Particle motions in sheared suspensions. XXVII. Transient and steady deformations and bust of liquid drops. *J. Colloid Interface Sci.*, 38:395–411.

Tumkurkar, U., Anand, A., Bhat, H.L., Bhat, S.V., Rudowiaz, C.Z., Yu, K.N. & Hiraoka, H. (Eds.). Modern Applications of EPR/ESR from Biophysics to Material Science. *Proc. of the First Asia-Pacific EPR/ESR Symposium*, Hong Kong, January 1997. Singapore: Springer-Verlag. 453–458.

Tung, M.A. & Paulson, A.T. 1995. Rheological concepts for probing ingredient interactions in food systems, in A. Gaonkar (Ed.). *Ingredient Interactions: Effect on Food Quality.* New York: Marcel Dekker.

Utracki, L.A. 1980. *CIL Internal Report.*

Van Driel, C.A., Van der Heijden, A.E.D.M., De Boer, S. & Van Rosmalen, G.M. 1994. The III–IV phase transition in ammonium nitrate: mechanisms. *J. Crystal growth*, 141(4):404–418.

Viper, AB, Krein, SE, and Bauman, VN. 1968. Effect of Additive Concentration on Solubilizing Ability. *Neftekhimiya*, 8 (6): 922-926.

Walker, P.A.M., Lawrence, D.G., Neilson, G.W. & Cooper, J. 1989. The structure of concentrated aqueous ammonium nitrate solutions. *J. Chem. Soc., Faraday Trans. 1*, 85: 1365–1372.

Walter, D., Gross, M.E., Evans-Lutterodt, K., Brown, W.L., Oh, M., Merchant, S. & Naresh, P. 2000. Room temperature recrystallization of electroplated copper thin film: methods and mechanisms. *Material Research Society Proceedings, 612, MRS Pittsburg, PA.*

Weaire, D. & Fu, T.L. 1988. The mechanical behaviour of foams and emulsions. *J. Rheol.*, 32:271–283.

Webber, R.M. 1999. Relation between Laplace pressure and the rheology of high internal phase emulsions. *AIChE*:226–232.

Wieringa, J.A., Van Dieren, F., Janssen, J.J.M. & Agterof, W.G.M. 1996. Droplet breakup mechanisms during emulsification in colloid mills at high dispersed phase volume fraction. *Chem. Eng. Research and Design*, 74:554–562.

Van der Werff, J.C. & De Kruif, C.G. 1989. Hard-sphere colloidal dispersions: The scaling of rheological properties with particle size, volume fraction, and shear rate. *J. Rheol.*, 33:421–454.

White, W.J., Henderson, J.M. & Perriman, A. 2004. The crystallization of supersaturated emulsions. *Isis experimental report.* 14591.

White, W.J., Reynolds, P.A., Hawley, A. & Perriman, A. 2005. Interfacial structure of block copolymers at the oil/water interface. *Isis experimental report.* 15255.

Williams, A., Janssen, J.J.M. & Prins, A. 1997. Behaviour of droplets in simple shear flow in the presence of protein emulsifier. *Colloids and Surfaces A*, 125:189–200.

Windhab, E.J., Dressler, M., Feigl, K., Fischer, P. & Megias-Alguacil, D. 2005. Emulsion processing – from single-drop deformation to design of complex process and products. *Chemical Engineering Sci.*, 60:2101–2113.

Wolf, B.A. 1984. Thermodynamic theory of flowing polymer solutions and its application to phase separation. *Macromolecules*, 17:615–618.

Wu, H.B., Chan, M.N. & Chan, C.K. 2007. FTIR characterization of polymorphic transformation of ammonium nitrate. *J. Aerosol Sci. & Tech.* 41(4):581–588.

Wu, S. 1989. Chain structure and entanglements. *J. Polym. Sci.*, 27:723–741.

Wyckoff, R.W.G. 1964. *Crystal Structures* Vol.2. New York: Interscience.

Yanase, H., Moldenears, P., Mewis, J., Abetz, V., Van Egmont, J. & Fuller, G.G. 1991. Structure and dynamics of a polymer solution subject to flow-induced phase separation. *Rheol. Acta*, 30:89–97.

Yorke, W.J., Binet, R., Lee, M.C. & Bamfield, H.A. 1983. US Patent, 4, 404, 050.

Yu, W. & Bousmina, M. 2003. Ellipsoidal model for droplet deformation in emulsions. *J. Rheol.*, 47:1011–1039.

Yu, W., Bousmina, M., Grmela, M., Palierne, J.F. & Zhow, C. 2002a. Quantitative relationship between rheology and morphology of emulsions. *J. Rheol*, 46:1381–1399.

Yu, W., Bousmina, M., Grmela, M., Zhow, C. 2002b. Modeling of oscillatory shear flow of emulsions under small and large deformation fields. *J. Rheol,* 46:1401–1418.

Yuhua, Y., Pal, R. & Masliyah, J. 1991. Rheology of oil in water emulsions with added kaoline clay. *Ind. Eng. Chem. Research*, 30:1931–1936.

APPENDICES

APPENDIX A: Effect of surfactant concentration on rheological properties of explosive emulsions

○ Viscoelastic properties

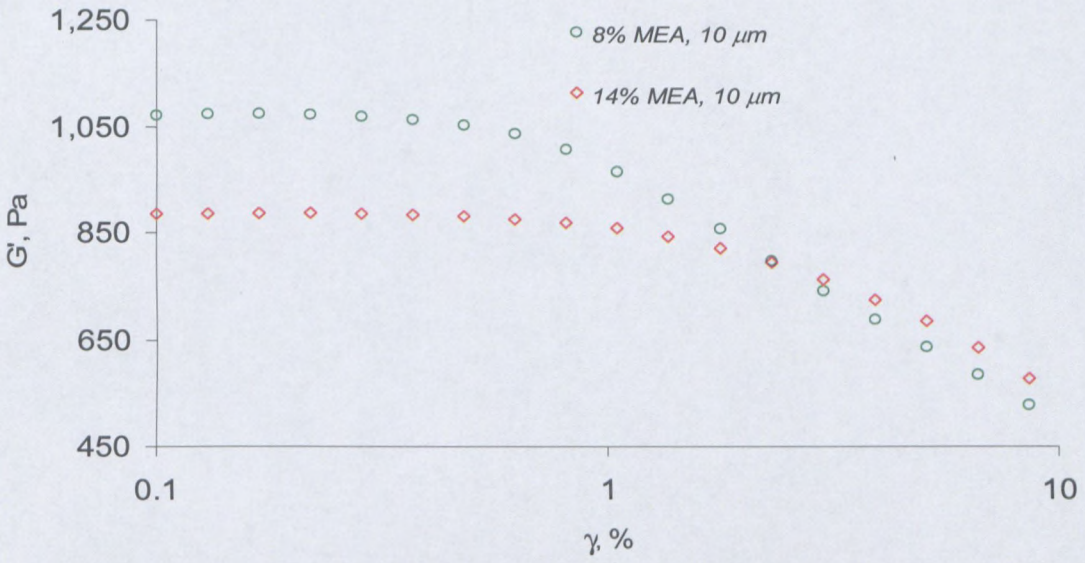

Figure A.1: Effect of surfactant concentration on storage modulus of explosive emulsions (MEA, d = 10 μm)

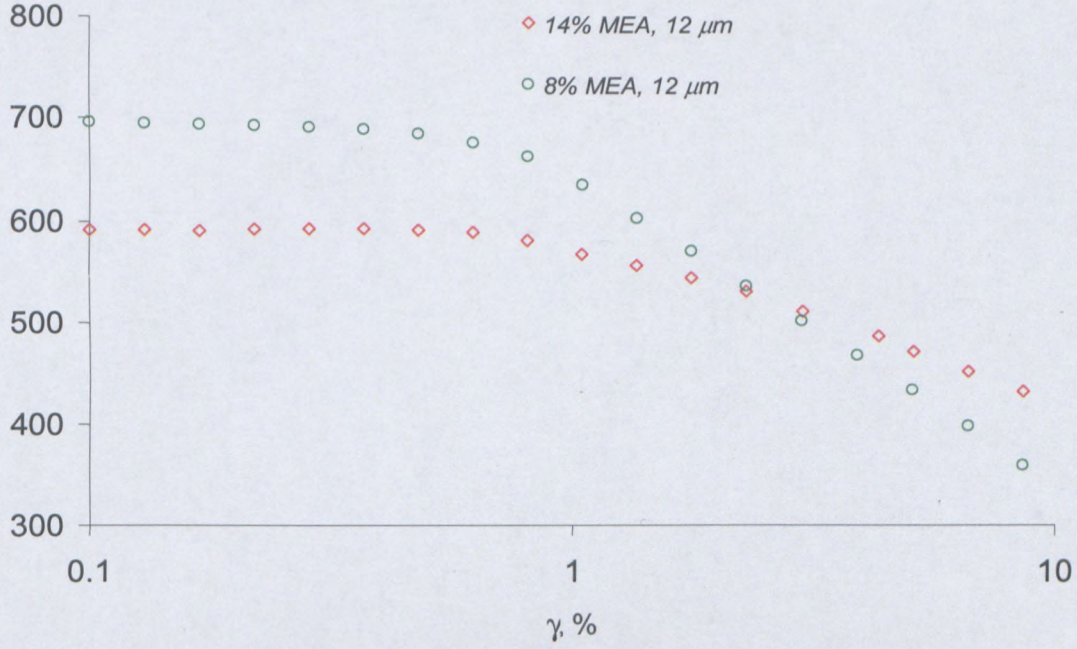

Figure A.2: Effect of surfactant concentration on storage modulus of explosive emulsions (MEA, d = 12 μm)

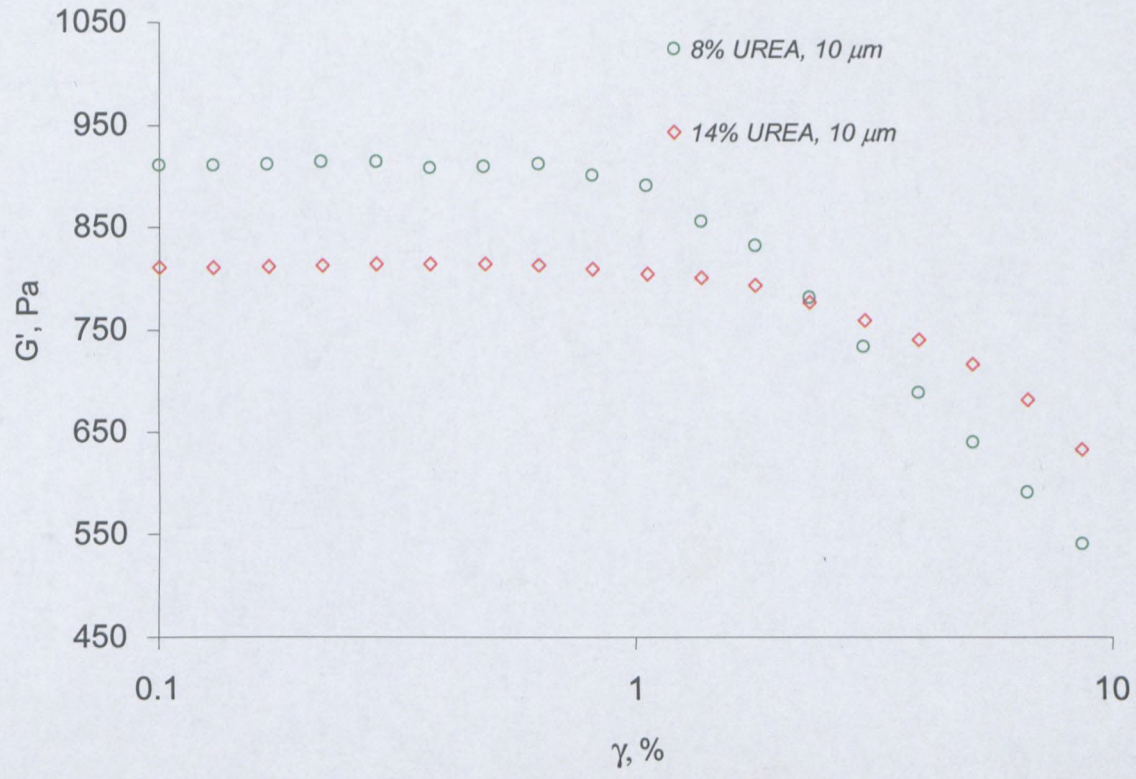

Figure A.3: Effect of surfactant concentration on storage modulus of explosive emulsions (UREA, d = 10 μm)

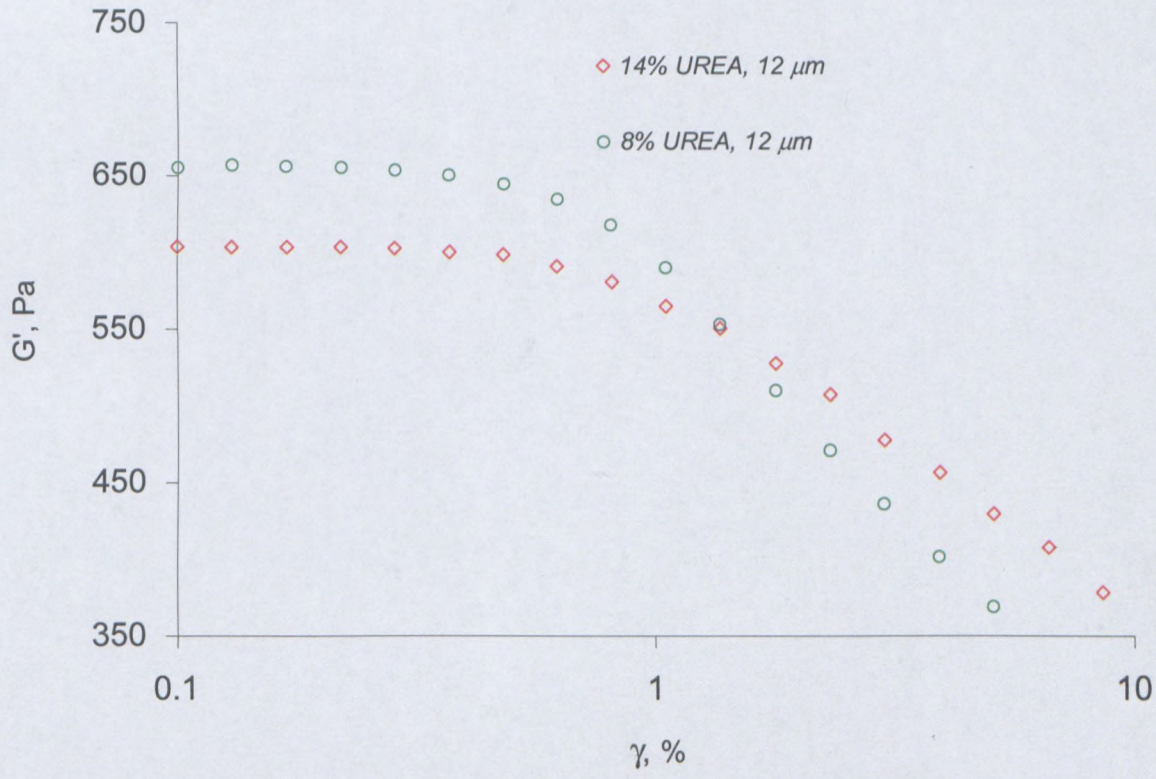

Figure A. 4: Effect of surfactant concentration on storage modulus of explosive emulsions (UREA, d = 12 μm)

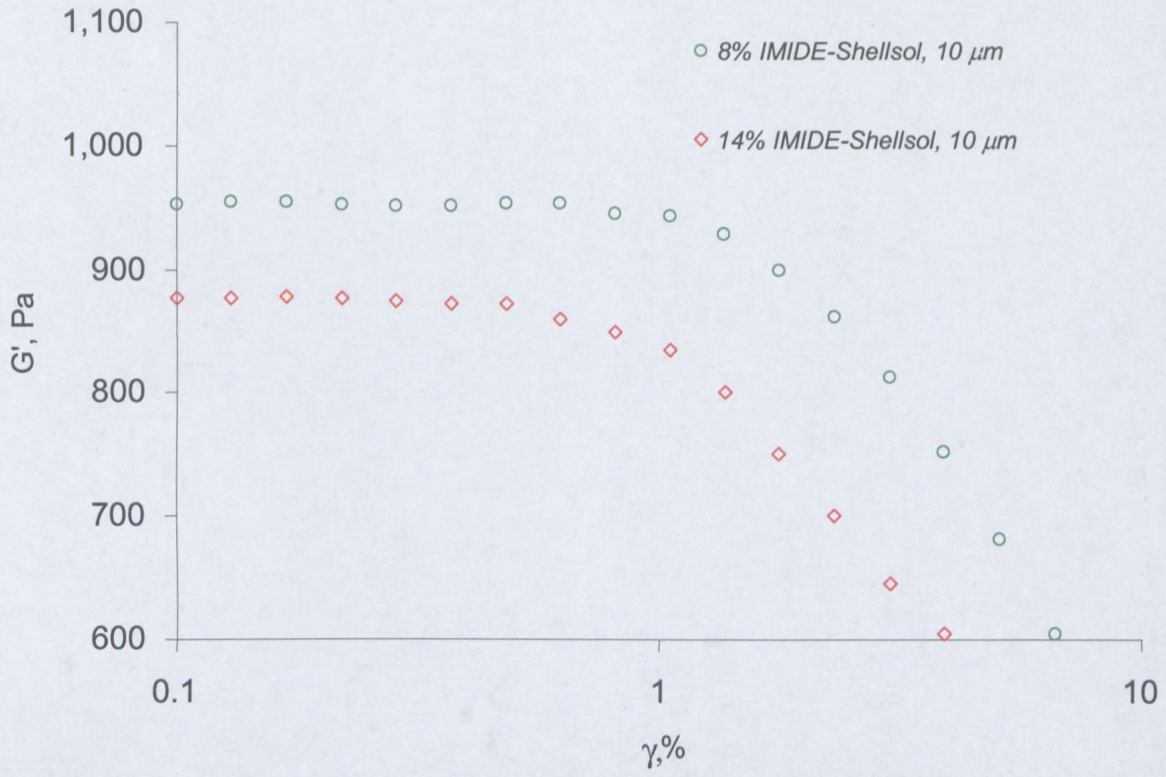

Figure A.5: Effect of surfactant concentration on storage modulus of explosive emulsions (IMIDE in Shellsol, d = 10 μm)

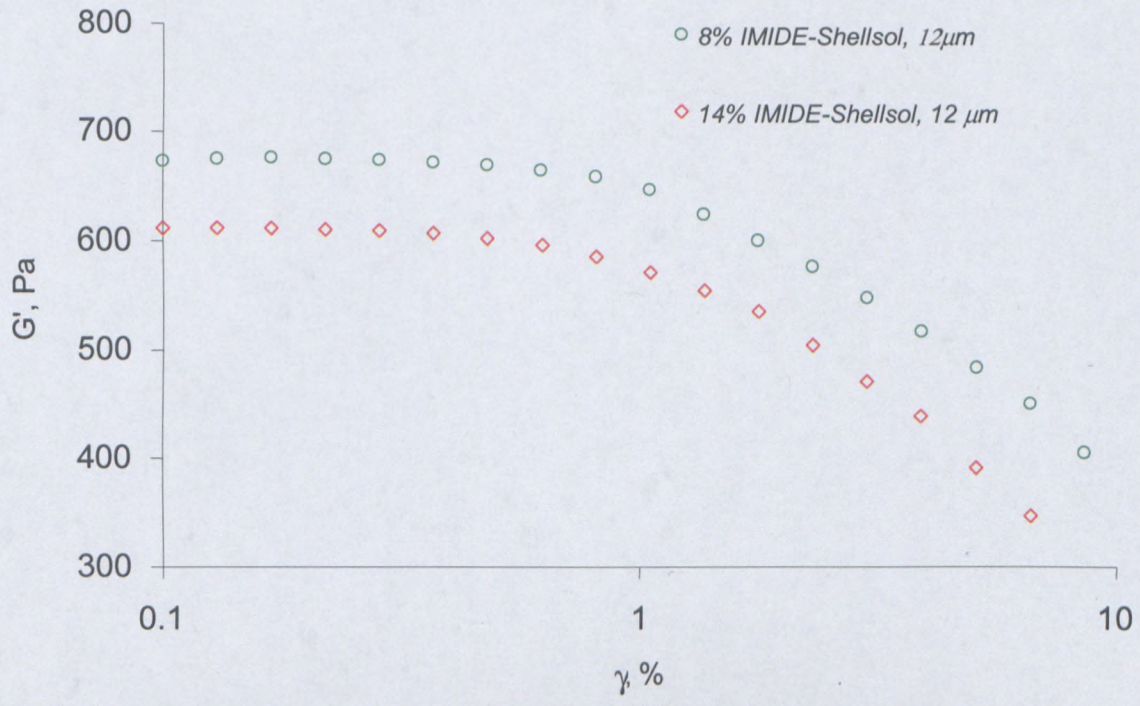

Figure A.6: Effect of surfactant concentration on storage modulus of explosive emulsions (IMIDE in Shellsol, d = 12 μm)

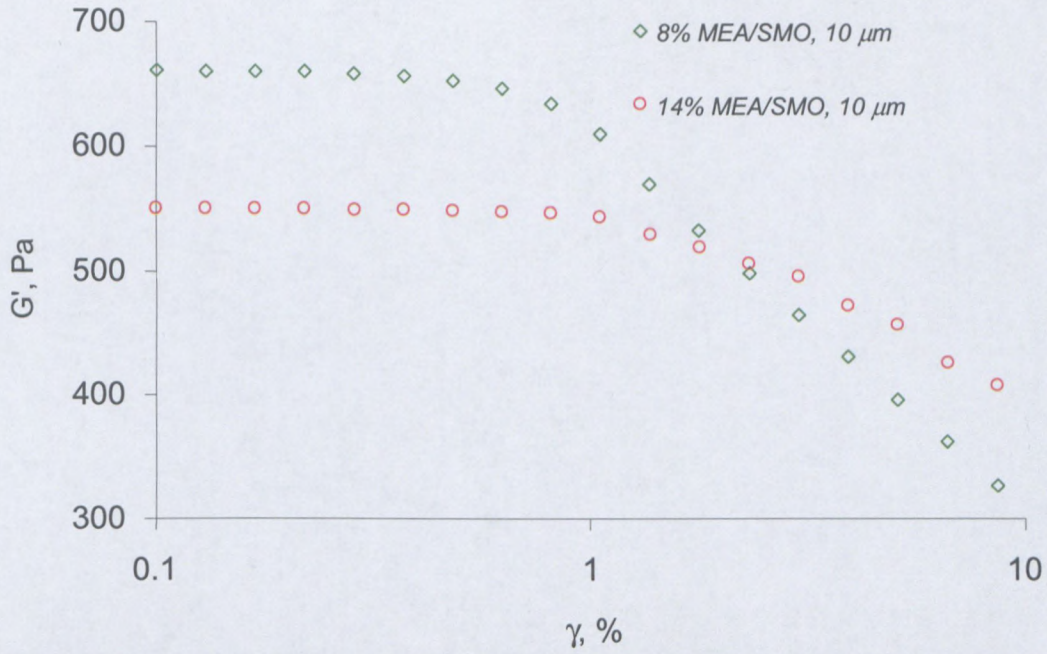

Figure A.7: Effect of surfactant concentration on storage modulus of explosive emulsions (MEA/SMO, d = 10 μm)

- Flow properties

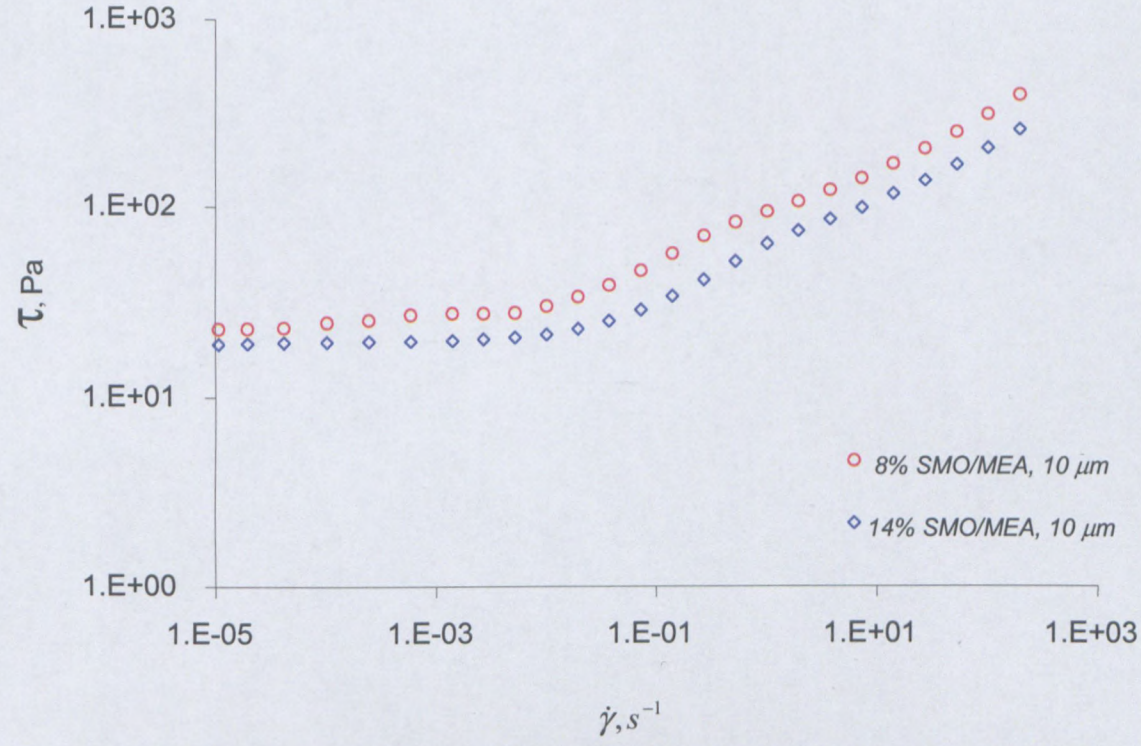

Figure A.8: Flow curves of the emulsions with different surfactant concentrations (d = 10 μm, MEA/SMO)

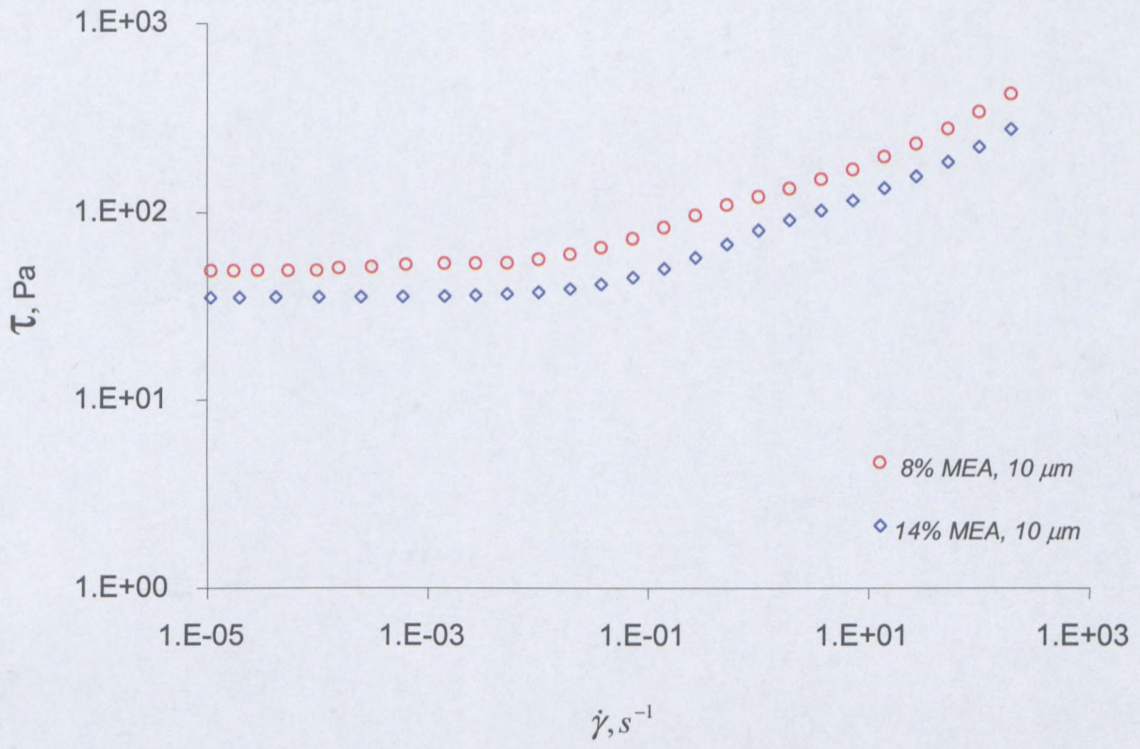

Figure A.9: Flow curves of the emulsions with different surfactant concentrations (d = 10 μm, MEA)

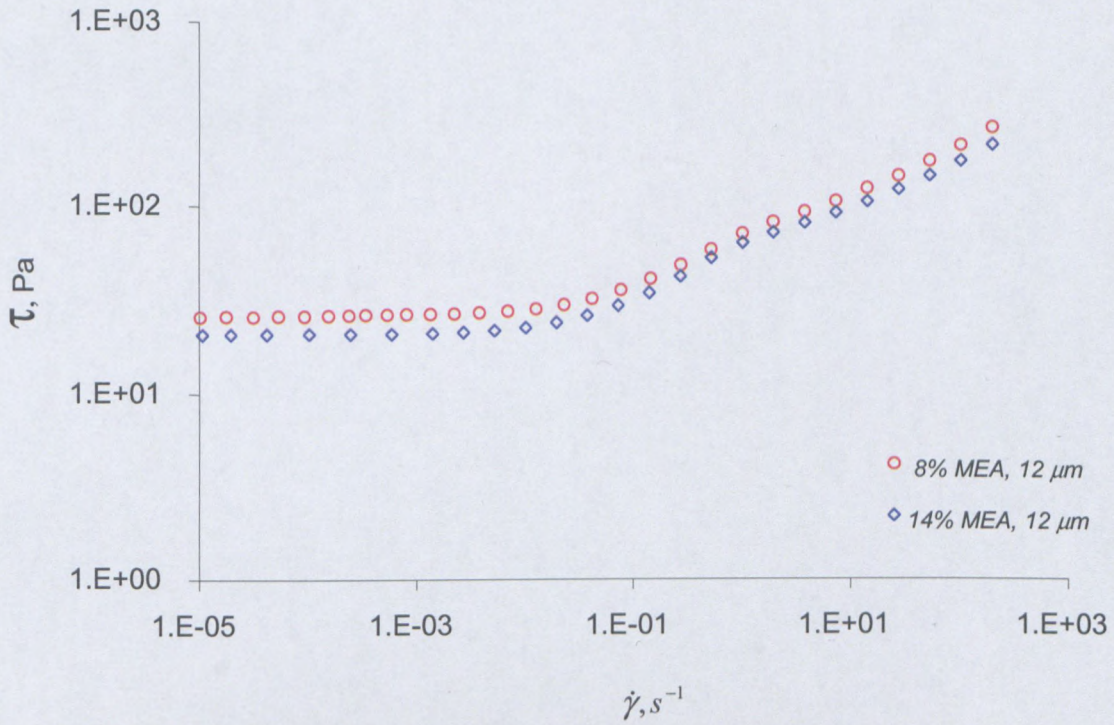

Figure A.10: Flow curves of the emulsions with different surfactant concentrations (d = 12 μm, MEA)

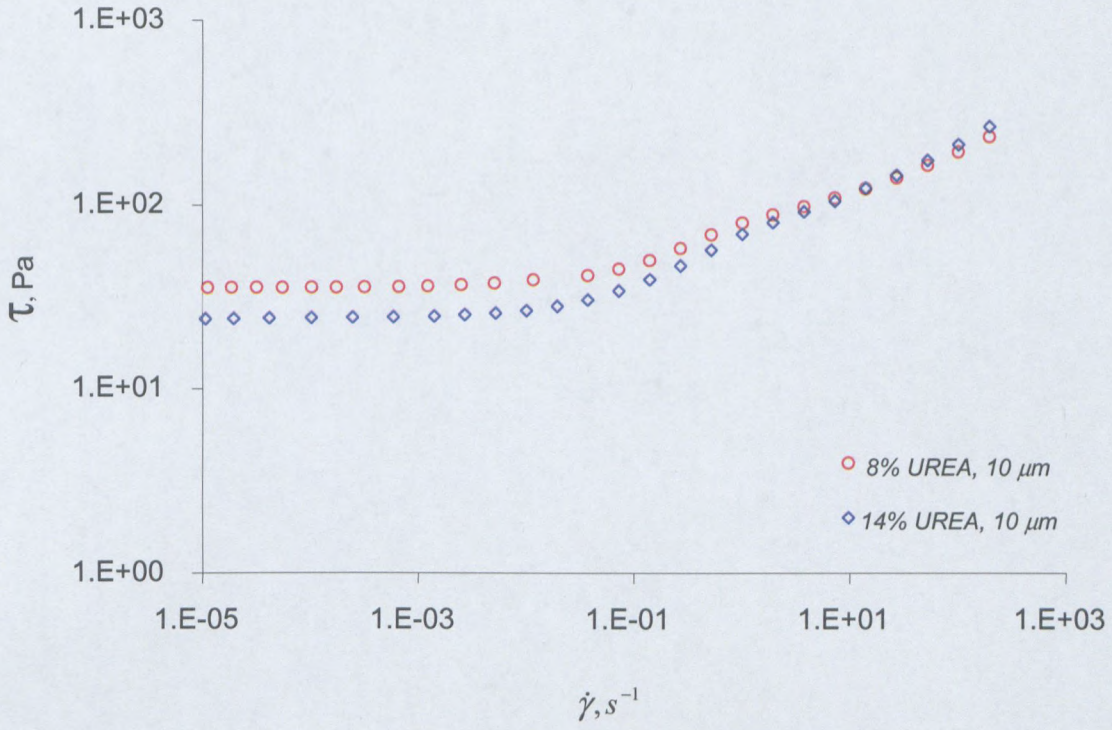

Figure A.11: Flow curves of the emulsions with different surfactant concentrations (d = 10 μm, UREA)

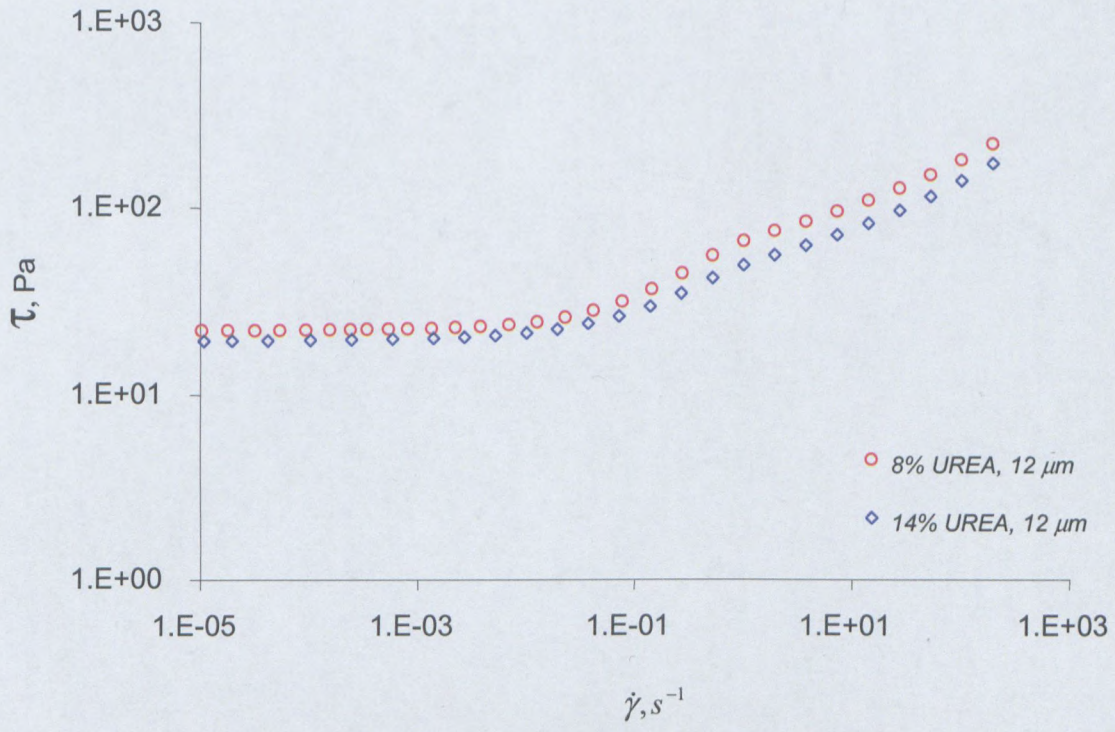

Figure A.12: Flow curves of the emulsions with different surfactant concentrations (d = 12 μm, UREA)

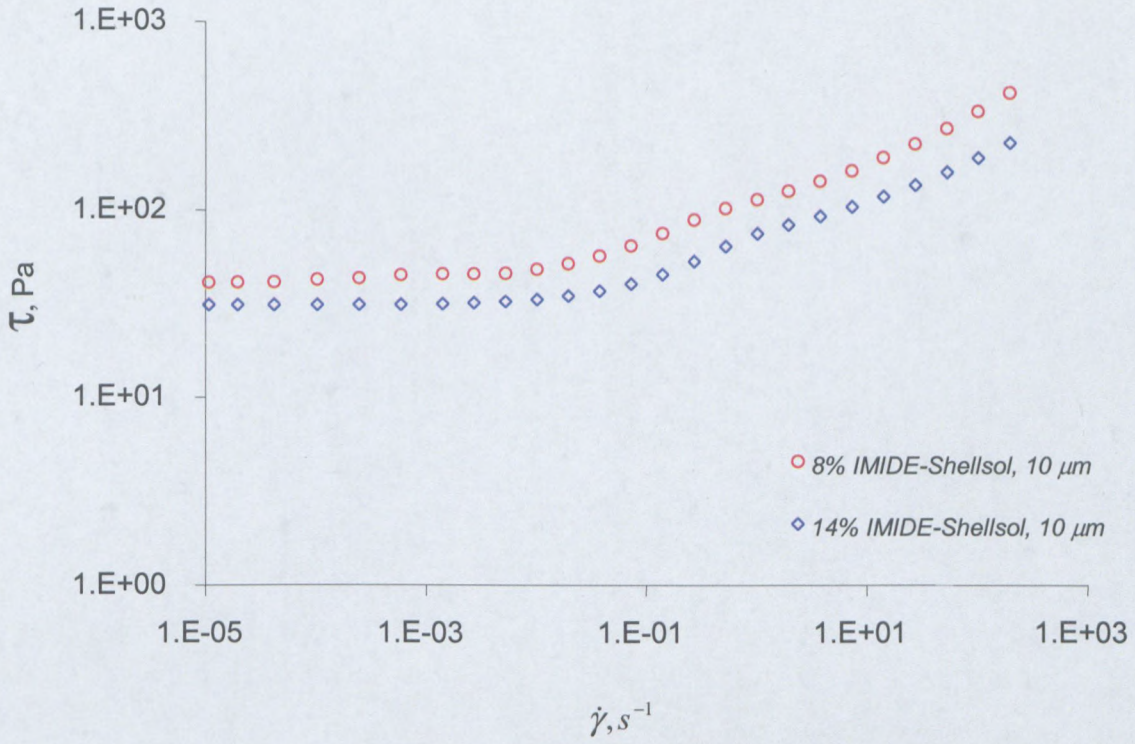

Figure A.13: Flow curves of the emulsions with different surfactant concentrations (d = 10 μm, IMIDE in Shellsol)

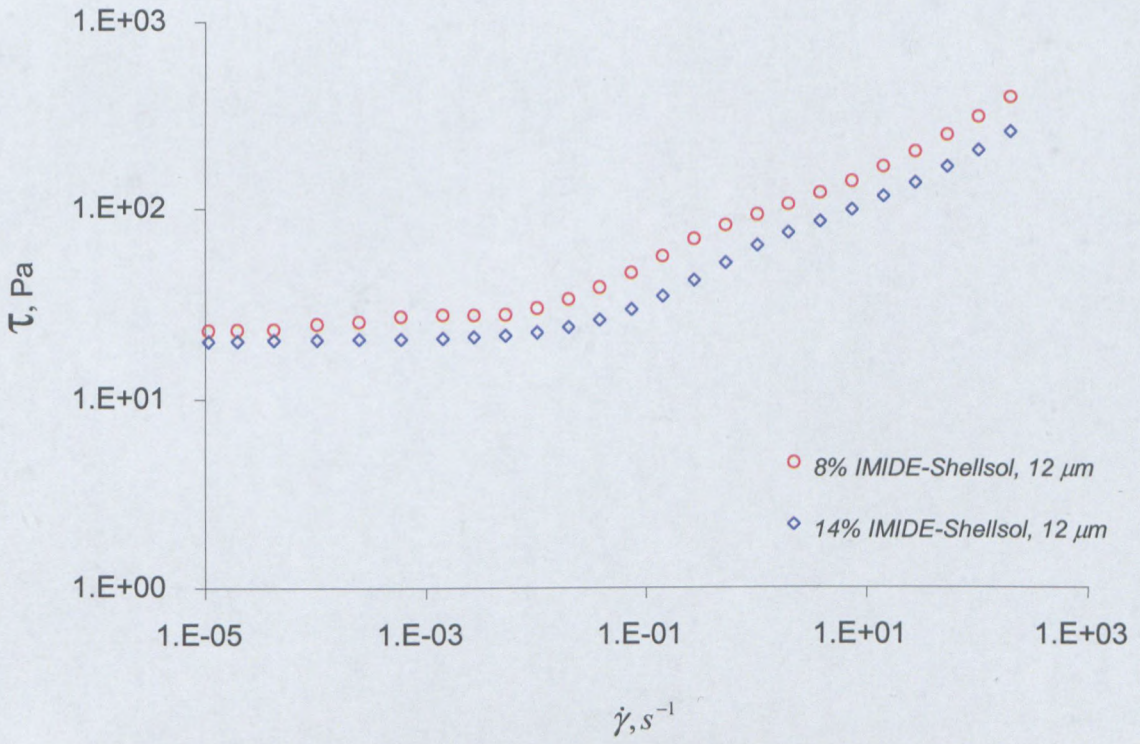

Figure A.14: Flow curves of the emulsions with different surfactant concentrations (d = 12 μm, IMIDE in Shellsol)

APPENDIX B: Effect of type and concentration of surfactants on interfacial properties of explosive emulsions and determination of CMC

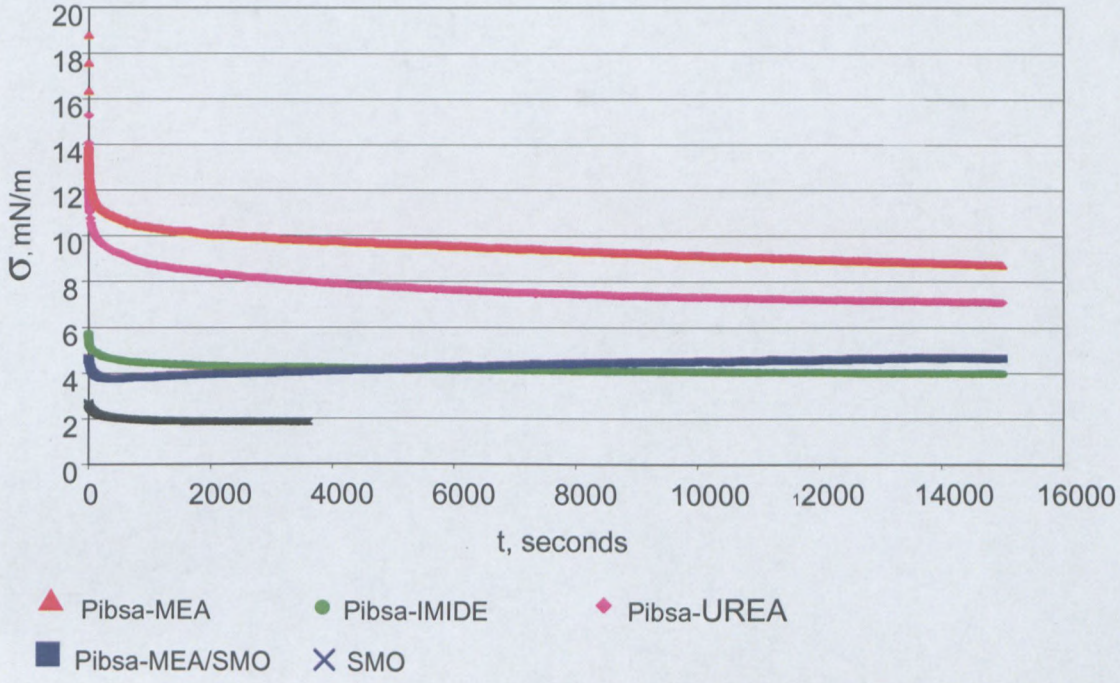

Figure B.1: Interfacial tension for 8 % surfactant / Mosspar/ 40 % Ammonium nitrate

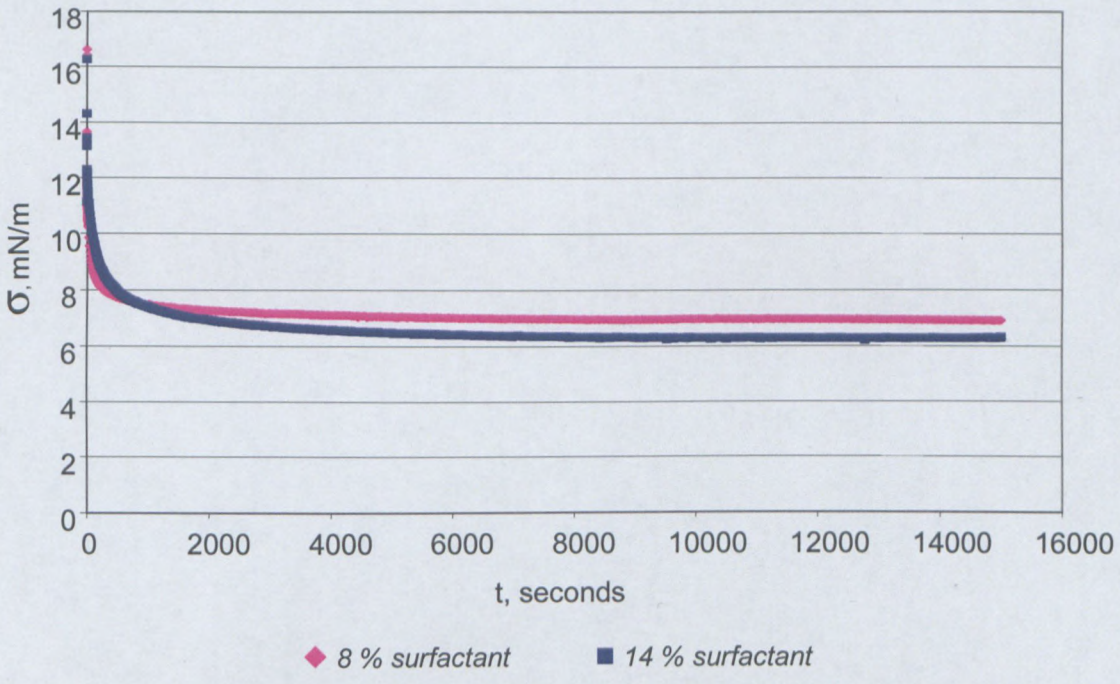

Figure B.2: Interfacial tension for Pibsa-MEA / Mosspar/40 % ammonium nitrate

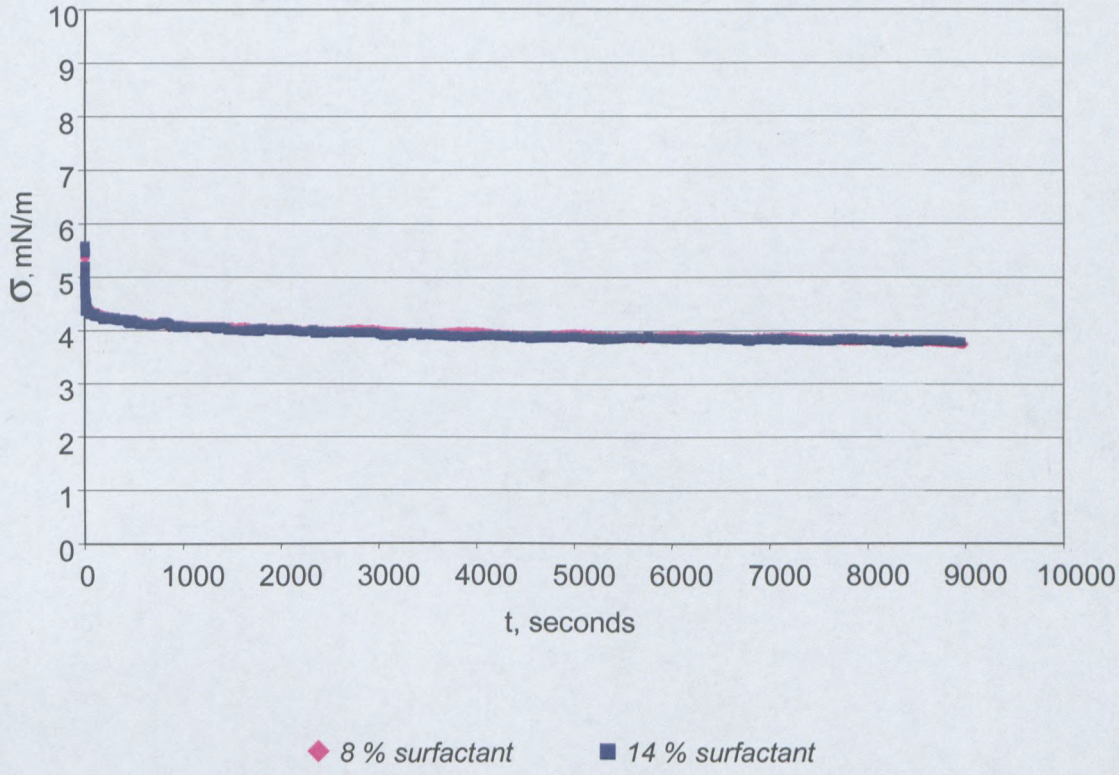

Figure B.3: Interfacial tension, Pibsa-Imide / Mosspar / 40 % ammonium nitrate

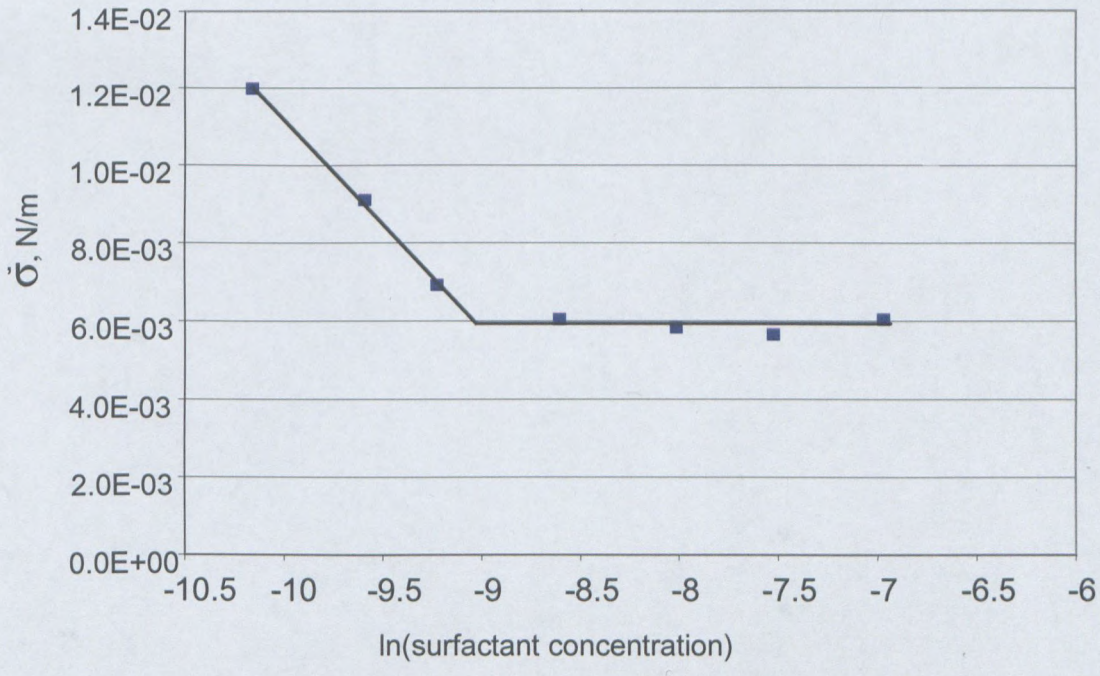

Figure B.4: interfacial tension against ln(surfactant concentration) for the system SMO / Mosspar / 40 % ammonium nitrate

APENDIX C: Effect of surfactant type on the stability of explosive emulsions

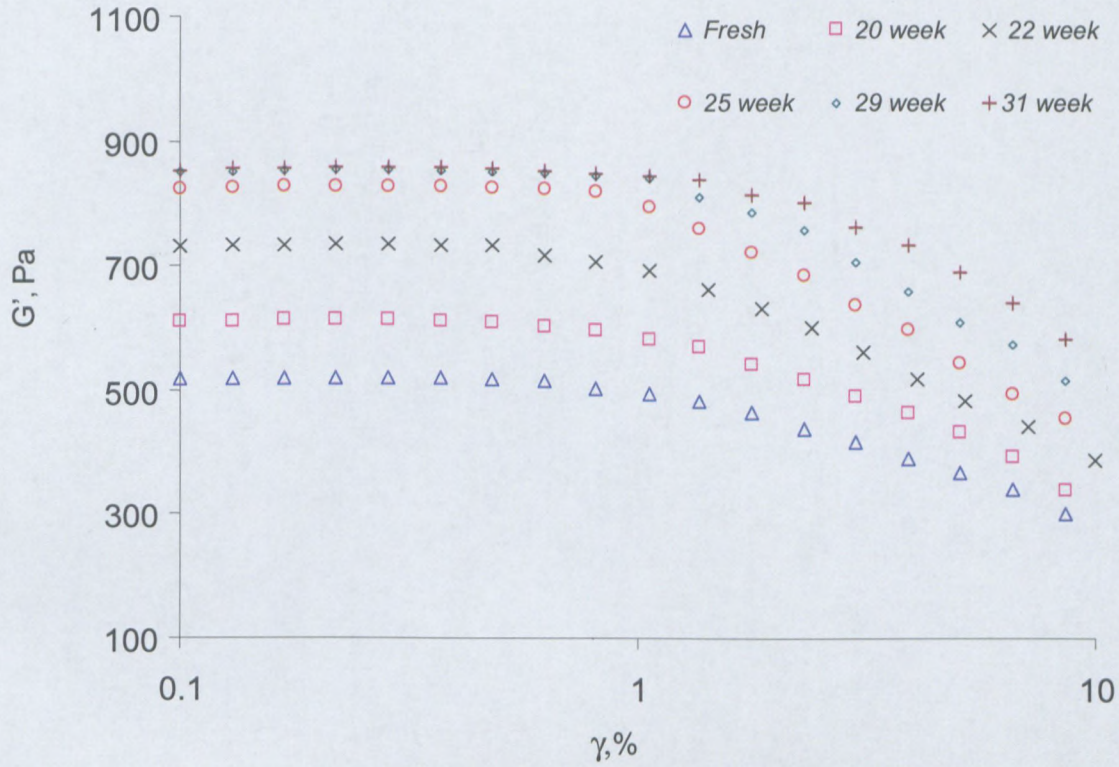

Figure C.1: Storage modulus dependence on strain amplitude for fresh and aged samples (8 % SMO/Pibsa-MEA in Mosspar for d = 10 μm)

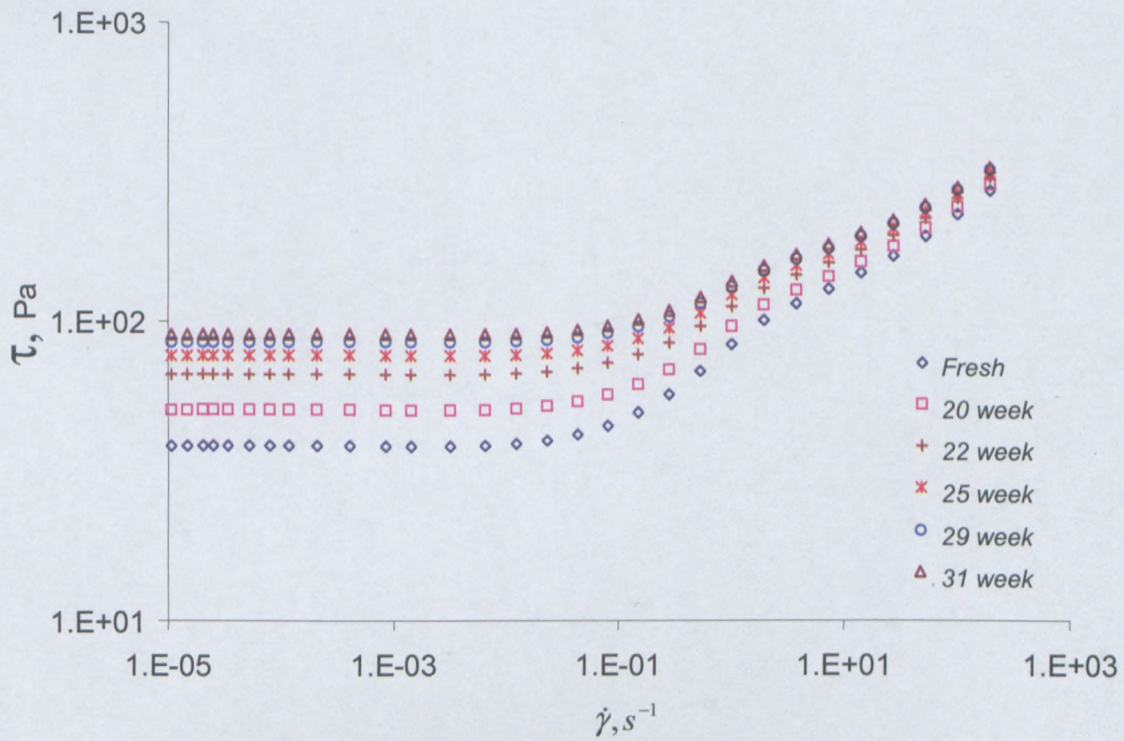

Figure C.2: Flow curves of fresh and aged emulsions (8 % SMO / Pibsa-MEA for droplet size 10 μm).

APENDIX D: Effect of surfactant concentration on the stability of explosive emulsions

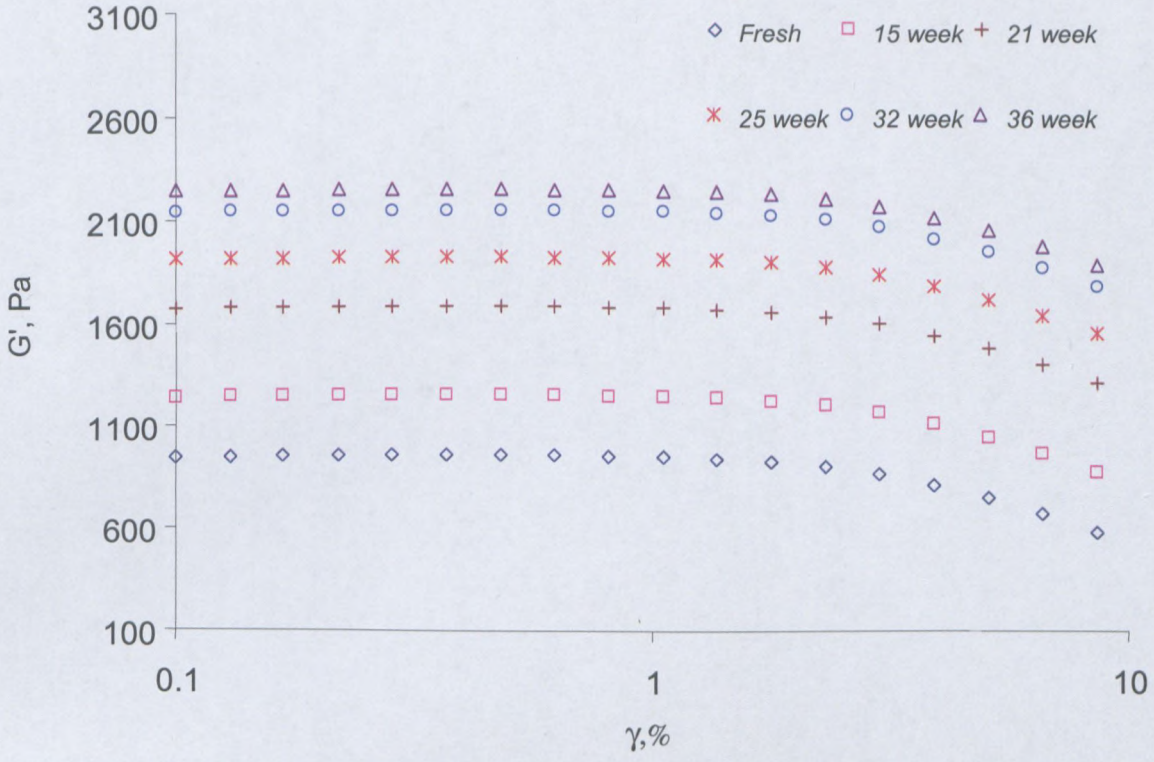

Figure C.3: Storage modulus dependence on strain amplitude for fresh and aged samples (14 % Pibsa-IMIDE in Mosspar for d = 10 μm)

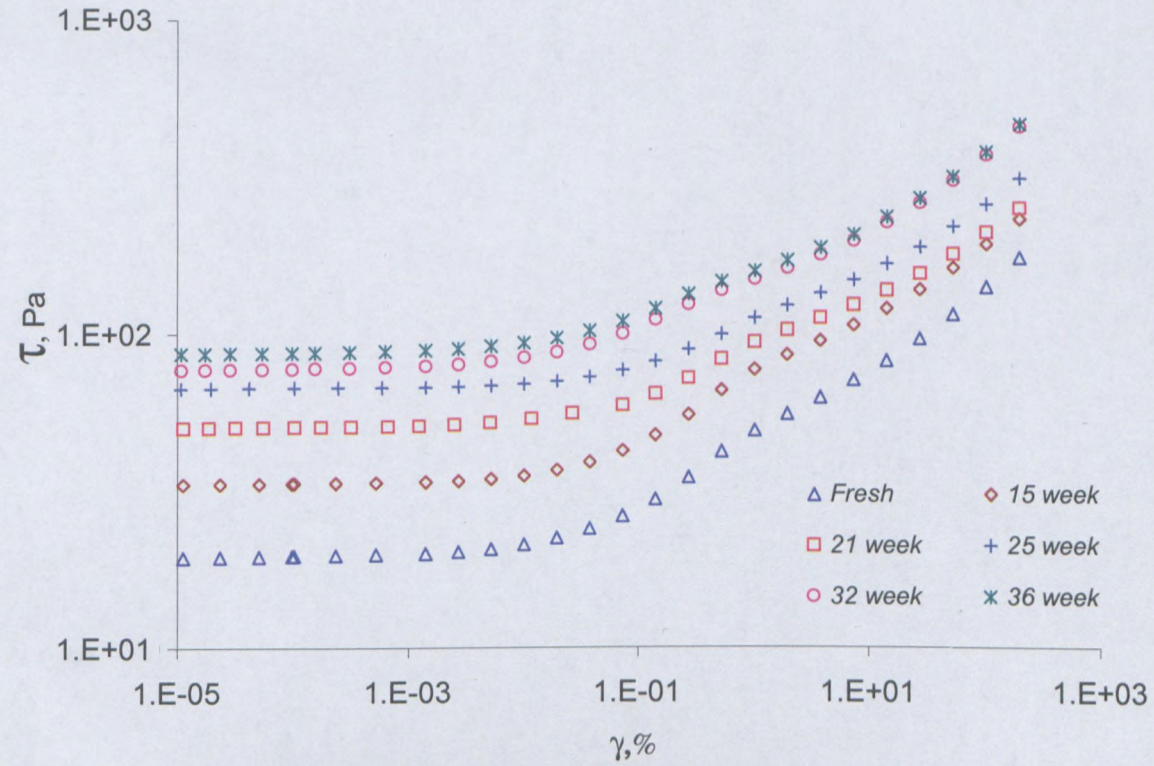

Figure C.4: Flow curves of fresh and aged emulsions (14 % Pibsa-IMIDE for droplet size d = 10 μm).

APPENDIX E: Effect of oil type on the stability of explosive emulsions

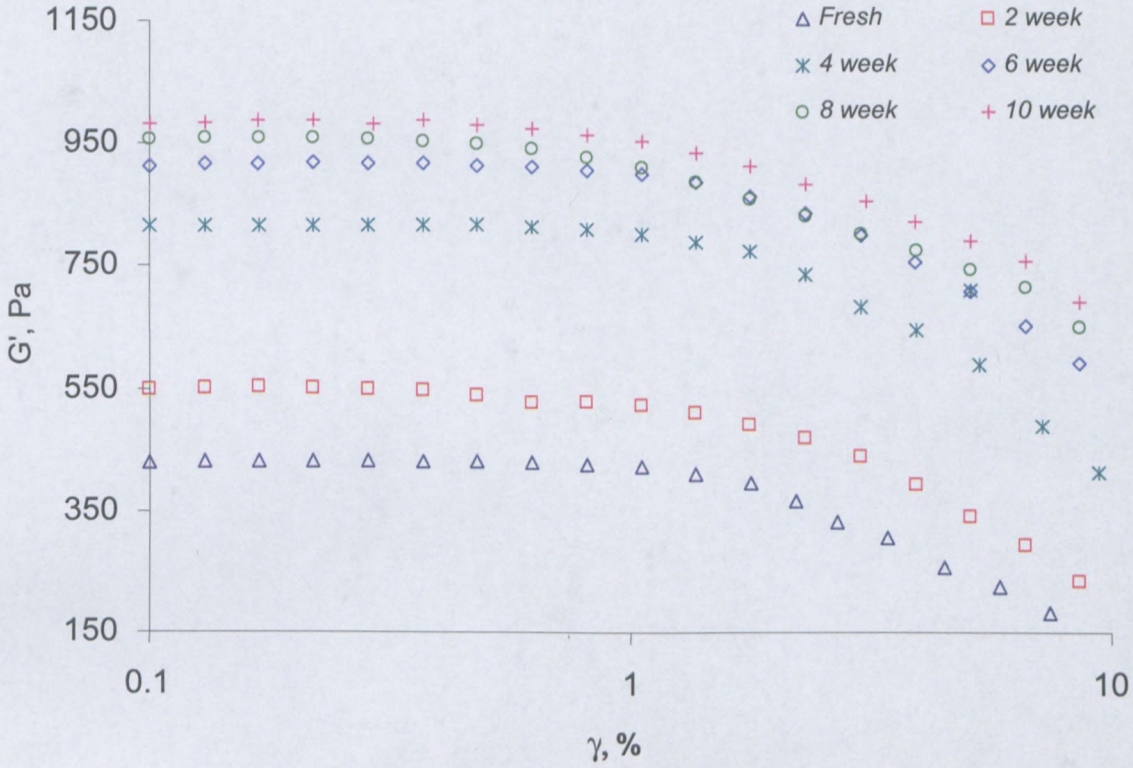

Figure C.5: Storage modulus dependence on strain amplitude for fresh and aged samples (14 % Pibsa-IMIDE in Mosspar for d = 10 μm)

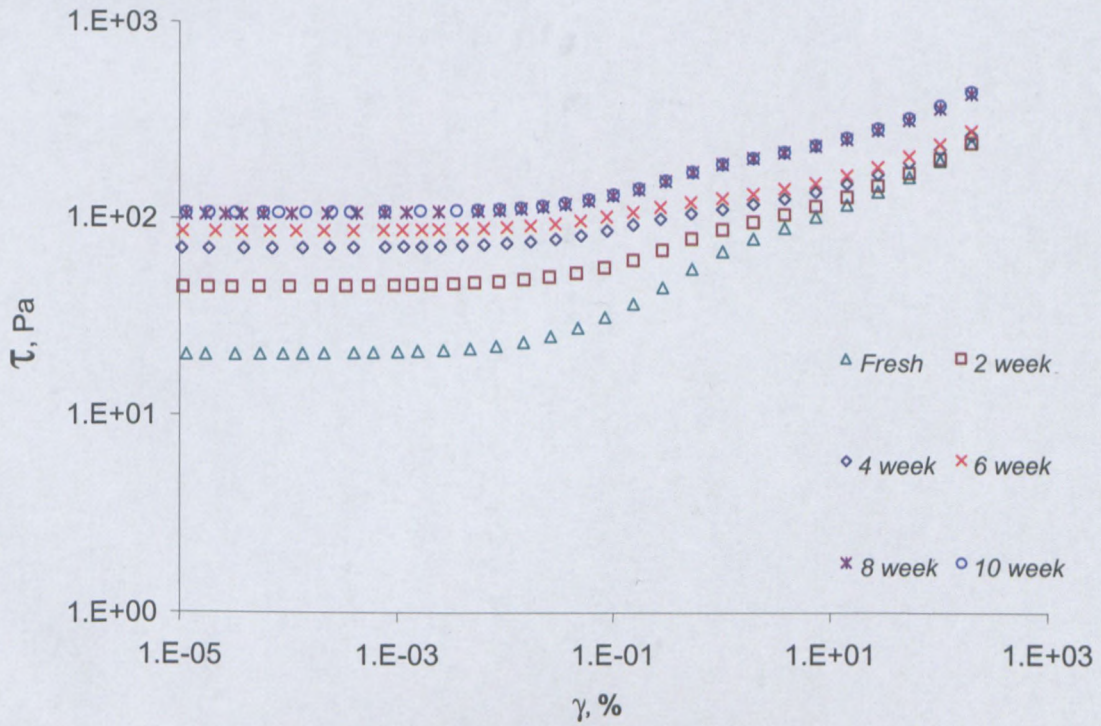

Figure C.6: Flow curves of fresh and aged emulsions (8 % Pibsa-IMIDE for droplet size 10 μm).